

Summer 8-31-2015

Thermochemistry and kinetics: hydrogen atom addition reactions with alkenes, oxidation of cyclopentadienone, trifluoroethene and transport properties

Suriyakit Yommee
New Jersey Institute of Technology

Follow this and additional works at: <https://digitalcommons.njit.edu/dissertations>

 Part of the [Environmental Sciences Commons](#)

Recommended Citation

Yommee, Suriyakit, "Thermochemistry and kinetics: hydrogen atom addition reactions with alkenes, oxidation of cyclopentadienone, trifluoroethene and transport properties" (2015). *Dissertations*. 127.
<https://digitalcommons.njit.edu/dissertations/127>

This Dissertation is brought to you for free and open access by the Electronic Theses and Dissertations at Digital Commons @ NJIT. It has been accepted for inclusion in Dissertations by an authorized administrator of Digital Commons @ NJIT. For more information, please contact digitalcommons@njit.edu.

Copyright Warning & Restrictions

The copyright law of the United States (Title 17, United States Code) governs the making of photocopies or other reproductions of copyrighted material.

Under certain conditions specified in the law, libraries and archives are authorized to furnish a photocopy or other reproduction. One of these specified conditions is that the photocopy or reproduction is not to be “used for any purpose other than private study, scholarship, or research.” If a user makes a request for, or later uses, a photocopy or reproduction for purposes in excess of “fair use” that user may be liable for copyright infringement,

This institution reserves the right to refuse to accept a copying order if, in its judgment, fulfillment of the order would involve violation of copyright law.

Please Note: The author retains the copyright while the New Jersey Institute of Technology reserves the right to distribute this thesis or dissertation

Printing note: If you do not wish to print this page, then select “Pages from: first page # to: last page #” on the print dialog screen

The Van Houten library has removed some of the personal information and all signatures from the approval page and biographical sketches of theses and dissertations in order to protect the identity of NJIT graduates and faculty.

ABSTRACT

THERMOCHEMISTRY AND KINETICS: HYDROGEN ATOM ADDITION REACTIONS WITH ALKENES, OXIDATION OF CYCLOPENTADIENONE, TRIFLUOROETHENE AND TRANSPORT PROPERTIES

by
Suriyakit Yommee

Thermochemical and transport properties and reaction kinetic parameters are important to understand and to model atmospheric chemistry, combustion and other thermal systems. These processes are all important to the environment. Thermochemical properties kinetic parameters and models for several atmospheric and combustion related chemical systems are determined using computational chemistry coupled with fundamentals of thermodynamics and statistical mechanics. Transport properties of hydrocarbon and oxygenated hydrocarbons which are important to the calculation of fluid dynamics of gas phase flow reactions and mixing needed for evaluation in the combustion and thermal (flow) fluid dynamic modeling. Transport properties of radicals cannot be measured so computational chemistry is method of choice. The dissertation determine dipole moment, polarizability and molecular diameters of hydrocarbon and oxygenated hydrocarbons needed for calculation of multicomponent viscosities, thermal conductivities, and thermal diffusion coefficients.

Cyclopentadienone with cyclic five-member ring aromatic structure is an important intermediate in combustion systems. Thermochemical and kinetic parameters for the initial reactions of cyclopentadienone radicals with O₂ and the thermochemical properties for cyclopentadienone - hydroperoxides, alcohols, alkenyl , alkoxy and peroxy radicals are determined by use of computational chemistry via Density Functional Theory (DFT) and the composite, Complete Basis Set (CBS) methods. Enthalpies of formation

($\Delta_f H^\circ_{298}$) with the isodesmic reaction schemes with several work reactions for each species are used for standard enthalpies. Entropy and heat capacity, $S^\circ(T)$ and $C_p^\circ(T)$ ($50\text{ K} \leq T \leq 5000\text{ K}$) are also determined. Chemical activation kinetics using quantum RRK analysis for $k(E)$ and master equation for fall-off are used for kinetic parameters and to show significance of chain branching as a function of temperature and pressure. The cyclopentadienone vinylic carbon radicals of with molecular oxygen appear to undergo chain branching via reaction with O_2 , to a higher extent to that of vinyl and phenyl radicals.

Reaction kinetics of hydrogen atom addition to primary (P), secondary (S), tertiary (T) vinylic (olefin) carbons to form an alkyl radical is investigated using Density Functional Theory (DFT) and ab initio composite level methods. Results from calculations at different levels are compared with the experimental literature data for hydrogen atom addition to Ethylene, Propene, 1-Butene, E-2-Butene, Z-2-Butene, and Isobutene. Activation energy and rate constants for forward and reverse paths are investigated and compared with available experimental data. One goal of the study is to determine accurate calculation method for use on large molecules.

Chlorofluorocarbons are widely present in the environment. Thermochemical and kinetic properties work will aid in the understanding the chlorofluorocarbons reactions in combustion and atmospheric environments. Trifluoroethene ($CF_2=CHF$) reaction in atmospheric and combustion environment initiated via OH radical system is investigated. The HF generated channel is currently not reported in any kinetic study. It is important as the toxic gas that can cause severe respiratory damage in humans.

**THERMOCHEMISTRY AND KINETICS: HYDROGEN ATOM ADDITION
REACTIONS WITH ALKENES, OXIDATION OF CYCLOPENTADIENONE,
TRIFLUOROETHENE AND TRANSPORT PROPERTIES**

**by
Suriyakit Yommee**

**A Dissertation
Submitted to the Faculty of
New Jersey Institute of Technology
in Partial Fulfillment of the Requirements for the Degree of
Doctor of Philosophy in Environmental Science**

Department of Chemistry and Environmental Science

August 2015

Copyright © 2015 by Suriyakit Yommee

ALL RIGHTS RESERVED

APPROVAL PAGE

THERMOCHEMISTRY AND KINETICS: HYDROGEN ATOM ADDITION REACTIONS WITH ALKENES, OXIDATION OF CYCLOPENTADIENONE, TRIFLUOROETHENE AND TRANSPORT PROPERTIES

Suriyakit Yommee

Dr. Joseph W. Bozzelli, Dissertation Advisor Distinguished Professor of Chemistry and Environmental Science, NJIT	Date
--	------

Dr. Tamara Gund, Committee Member Professor of Chemistry and Environmental Science, NJIT	Date
---	------

Dr. Nancy L. Jackson, Committee Member Professor of Chemistry and Environmental Science, NJIT	Date
--	------

Dr. Alexei Khalizov, Committee Member Assistant Professor of Chemistry and Environmental Science, NJIT	Date
---	------

Dr. Yogesh V. Joshi, Committee Member Senior Researcher, Exxon Mobile, NJ	Date
--	------

BIOGRAPHICAL SKETCH

Author: Suriyakit Yommee
Degree: Doctor of Philosophy
Date: May 2015

Undergraduate and Graduate Education:

- Doctor of Philosophy in Environmental Science,
New Jersey Institute of Technology, Newark, NJ, 2015
- Master of Science in Environmental Technology,
King Mongkut's University of Technology Thonburi, Bangkok, Thailand, 2003
- Bachelor of Science in Environmental Science,
Thammasat University, Bangkok, Thailand, 1997

Major: Environmental Science

Publications:

Yommee, S.; Bozzelli, J.W. Cyclopentadienone Oxidation Reaction Kinetics and Thermochemistry for the Alcohols, Hydroperoxides, Vinylic, Alkoxy and Alkylperoxy Radicals, submitted.

Oral Presentations:

Suriyakit Yommee and Joseph W. Bozzelli, "Reaction Kinetics of Hydrogen addition Reaction with Ethylene, Propene, 1-Butene, E_{nd} -2-Butene, Z-2-Butene, and Isobutene: Comparison with Experiment," 32nd Regional Meeting on Kinetics and Dynamics, Hartford, CT, January 2014.

Suriyakit Yommee and Joseph W. Bozzelli, "Thermochemical Properties for Cyclopentadienone Alcohols, Hydroperoxides, Alkenyl, Alkoxy and Alkylperoxy Radicals $R \cdot + O_2$ Kinetics," 33rd Regional Meeting on Kinetics and Dynamics, Amherst, MA, January 2015.

Poster Presentation:

Suriyakit Yommee and Joseph W. Bozzelli, "Calculation of Reaction Kinetic Parameters for Hydrogen Addition to Olefin Primary, Secondary and Tertiary Sites, and Reverse Elimination: Comparison with Experiments," 23rd International Symposium on Gas Kinetics and Related Phenomena, Hungary, July 2014.

Mom, Dad, Brother, My Love (Namoun) and her mom
I Love You!!!

Life Can Live, Because of You

ขอบคุณทุกความห่วงใยและกำลังใจที่มีให้กันตลอดมา

ACKNOWLEDGMENT

I would like to express my sincerely grateful to my advisor, Prof. Joseph W. Bozzelli, for his advice, patience, and ethical point of view on academic and also his kindness for all of students in research group. My sincerely expression extended to Prof. Tamara Gund, Prof. Nancy L. Jacson, Asst. Prof. Alexei Khalizov, and Dr. Yogesh V. Joshi for serving on my committee.

I would like to gratefully thank the Ministry of Science and Technology (Thailand) and Thammasat University (Thailand) for funding my studies at New Jersey Institute of Technology.

I would also thank all the members in the Computational Chemistry Research Group: Suarwee Snitsiriwat, Itasaso Auzmendi Murua, Heng Wang, Jason Hudzik and Dr. Alvaro Castillo for all their help and friendship during several years at New Jersey Institute of Technology.

TABLE OF CONTENTS

Chapter	Page
1 INTRODUCTION.....	1
2 COMPUTATIONAL METHODS.....	6
2.1 Thermochemical Properties.....	6
2.1.1 Computational Chemistry	6
2.1.2 Theoretical Methods	8
2.1.3 Calculation Methods.....	9
2.1.4 Internal Rotational Potential.....	10
2.1.5 Work Reactions and Enthalpy of Formation ($\Delta_f H^\circ_{298}$).....	11
2.1.6 Bond Dissociation Enthalpies (BDE).....	13
2.1.7 Entropy and Heat Capacity.....	13
2.1.8 Hindered Internal Rotors.....	16
2.2 Kinetic Analysis	18
2.2.1 Canonical Transition State Theory (CTST).....	18
2.2.2 Variational Transition State Theory (VTST).....	19
2.2.3 Chemical Activation Reaction	20
2.2.4 Quantum Rice-Ramsperger-Kassel (QRRK).....	20
3 DIPOLE MOMENTS, POLARIZABILITY AND LENNARD JONES DIAMETERS OF OXY-HYDROCARBONS: ALCOHOLS, ETHERS, ALDEHYDES, KETONES, AND RADICALS CORRESPONDING TO LOSS OF H ATOMS, FOR ESTIMATION OF TRANSPORT PROPERTIES: A THEORETICAL STUDY.....	22
3.1 Overview.....	22
3.1 Dipole Moments.....	25

TABLE OF CONTENTS (Continued)

Chapter	Page
3.2.1 Results Alcohols	26
3.2.2 Results Aldehydes.....	30
3.2.3 Results Ethers.....	33
3.2.4 Results Ketones.....	36
3.3 Polarizability	39
3.3.1 Results Alcohols	40
3.3.2 Results Aldehydes.....	43
3.3.3 Results Ethers.....	46
3.3.4 Results Ketones.....	49
3.4 Lennard Jones Diameters (σ).....	52
3.4.1 Results Alcohols.....	53
3.4.2 Results Aldehydes.....	56
3.4.3 Results Ether s.....	58
3.4.4 Results Ketones	62
3.5 Summary.....	64
4 CYCLOPENTADIENONE OXIDATION REACTION KINETICS AND THERMOCHEMISTRY FOR THE ALCOHOLS, HYDROPEROXIDES, VINYLIC, ALKOXY AND ALKYLPEROXY RADICALS	66
4.1 Overview.....	66
4.2 Thermochemical Properties.....	71
4.2.1 Uncertainty and Confidence Limits.....	71

TABLE OF CONTENTS

(Continued)

Chapter	Page
4.2.2 Standard Enthalpies of Formation ($\Delta_f H^\circ_{298}$).....	72
4.2.3 Internal Rotation Potentials.....	84
4.2.4 Entropy and Heat Capacity.....	85
4.3 Bond Dissociation Enthalpies (BDE).....	87
4.4 Kinetic Properties.....	93
4.4.1 Ring Opening Reactions of Cyclopentdienone Vinyl Radicals.....	93
4.4.2 $R \cdot + O_2$ Potential Energy Surface and Chemical Activation Reactions	95
4.4.3 Unimolecular Dissociation Reaction.....	107
4.5 Summary.....	111
5 KINETICS OF HYDROGEN ADDITION REACTION AT PRIMARY, SECONDARY AND TERTIARY SITES IN SMALL OLEFINS: COMPARISONS WITH EXPERIMENTAL DATA.....	113
5.1 Overview.....	113
5.2 Thermochemical Properties.....	115
5.2.1 Standard Enthalpy of Formation and Transition State.....	115
5.2.2 Entropy and Heat Capacities Data	117
5.3 kinetics.....	117
5.3.1 Activation Energy (E_a).....	118
5.3.2 Rate Constant (k).....	121
5.3.3 Hydrogen Addition to Butene and Further Interaction.....	123
5.3.4 Hydrogen Addition to Isobutene and Further Interaction.....	126
5.4 Summary	127

TABLE OF CONTENTS

(Continued)

Chapter	Page
6 THERMOCHEMICAL AND KINETICS OF THE CHEMICAL ACTIVATION REACTIONS OF OH RADICAL ADDITION (INITIATION) WITH TRIFLUOROETHENE (1,1,2 TRIFLUOROETHENE).....	129
6.1 Overview	129
6.2 Thermochemical Properties.....	130
6.3 Reactions and Kinetics.....	134
6.3.1 C ₂ F ₃ H + OH Reaction System	135
6.3.2 Chemical Activation Results for Kinetics of CF ₂ CHF + OH → (HO)CF ₂ C•HF to Products System.....	138
6.3.3 Unimolecular Dissociation of the (HO)CF ₂ C•HF stabilization adduct...	142
6.3.4 Chemical Activation Results for Kinetics of C ₂ F ₃ H + OH → C•F ₂ -CHF(OH) to Products System.....	144
6.3.5 Unimolecular Dissociation of the C•F ₂ CHFOH stabilization adduct.....	148
6.4 Summary.....	149
APPENDIX A ERROR ANALYSIS: UNCERTAINTY.....	150
APPENDIX B RESULTING RATE CONSTANTS IN QRRK CALCULATION OF CYCLO-PENTADIENONE-2-YL AND CYCLO-PENTADIENONE-3-YL RADICAL SYSTEM.....	152
APPENDIX C POTENTIAL ENERGY PROFILES FOR INTERNAL ROTATIONS OF CYCLO-PENTADIENONE-2-YL AND CYCLO-PENTADIENONE-3-YL RADICAL SYSTEM.....	158
APPENDIX D GEOMETRY COORDINATES AT CBS-QB3 COMPOSITE, VIZ B3LYP/CBSB7 LEVEL	163

TABLE OF CONTENTS
(Continued)

Chapter	Page
APPENDIX E INPUT FILE FOR MODIFIED COMPUTATIONAL METHOD M062X/6-311+G(D,P)//CBS-QB3.....	186
APPENDIX F RESULTING RATE CONSTANTS IN QRRK CALCULATION OF OH RADICAL ADDITION (INITIATION) WITH TRIFLUOROETHENE (1,1,2 TRIFLUOROETHENE)	187

LIST OF TABLES

Table	Page
3.1 Calculated Dipole Moment of Alcohols with Comparison to Literature.....	27
3.2 Calculated Dipole Moment of Alcohol Primary Radical Species	28
3.3 Calculated Dipole Moment of Alcohol Secondary Radical Species	28
3.4 Equations to estimate Dipole Moment for Alcohols and Alcohols Radicals.....	29
3.5 Calculated Dipole Moment of Aldehydes with Comparison to Literature	30
3.6 Calculated Dipole Moment of Aldehyde Primary Radical Species.....	31
3.7 Calculated Dipole Moment of Aldehyde Secondary Radical Species	31
3.8 Equations to estimate Dipole Moment for Aldehydes and Aldehydes Radicals...	32
3.9 Calculated Dipole Moment of Ethers with Comparison to Literature	33
3.10 Calculated Dipole Moment of Ether Primary Radical Species.....	34
3.11 Calculated Dipole Moment of Ether Secondary Radical Species.....	34
3.12 Equations to Estimate Dipole Moment for Ethers and Ethers Radicals.....	35
3.13 Calculated Dipole Moment of Ketones with Comparison to Literature	36
3.14 Calculated Dipole Moment of Ketone Primary Radical Species.....	37
3.15 Calculated Dipole Moment of Ketone Secondary Radical Species.....	37
3.16 Equations to Estimate Dipole Moment for Ketones and Ketones Radicals.....	38
3.17 Calculated Polarizability for Alcohols with Comparison to Literature	40
3.18 Calculated Polarizability for Alcohol Primary Radical Species.....	40
3.19 Calculated Polarizability for Alcohol Secondary Radical Species.....	42
3.20 Equations to Estimate Polarizability for Alcohols and Alcohols Radicals.....	43

LIST OF TABLES (Continued)

Table	Page
3.21 Calculated Polarizability for Aldehydes with Comparison to Literature	43
3.22 Calculated Polarizability for Aldehydes Primary Radicals Species.....	43
3.23 Calculated Polarizability for Aldehydes Secondary Radicals Species.....	45
3.24 Equations to Estimate Polarizability for Aldehydes and Aldehydes Radicals.....	46
3.25 Calculated Polarizability for Ethers with Comparison to Literature	46
3.26 Calculated Polarizability for Ethers Primary Radicals Species.....	46
3.27 Calculated Polarizability for Ethers Secondary Radicals Species.....	48
3.28 Equations to Estimate Polarizability for Ethers and Ethers Radicals Species.....	49
3.29 Calculated Polarizability for Ketones with Comparison to Literature	49
3.30 Calculated Polarizability for Ketone Primary Radicals Species.....	49
3.31 Calculated Polarizability for Ketone Secondary Radicals Species.....	51
3.32 Equations to Estimate Polarizability for Ketones and Ketones Radicals	52
3.33 Calculated L J Diameters for Alcohols with Comparison to Literature	53
3.34 Calculated L J Diameters for Alcohol Primary Radicals Species.....	54
3.35 Calculated L J Diameters for Alcohol Secondary Radicals Species.....	54
3.36 Equations to Estimate L J Diameters for Alcohols and Alcohols Radicals.....	55
3.37 Calculated L J Diameters for Aldehydes with Comparison to Literature.....	56
3.38 Calculated L J Diameters for Aldehyde Primary Radicals Species.....	57
3.39 Calculated L J Diameters for Aldehyde Secondary Radicals Species.....	57
3.40 Equations to Estimate L J Diameters for Aldehydes and Aldehydes Radicals.....	58

LIST OF TABLES (Continued)

Table	Page
3.41 Calculated L J Diameters for Ethers with Comparison to Literature	59
3.42 Calculated L J Diameters for Ether Primary Radicals Species.....	60
3.43 Calculated L J Diameters for Ether Secondary Radicals Species.....	60
3.44 Equations to Estimate L J Diameters for Ethers and Ethers Radicals.....	61
3.45 Calculated L J Diameters for Ketones with Comparison to Literature	62
3.46 Calculated L J Diameters for Ketone Primary Radicals Species.....	62
3.47 Calculated L J Diameters for Ketone Secondary Radicals Species.....	64
3.48 Equations to Estimate L J Diameters for Ketones and Ketones Radicals	64
4.1 Comparison of Experiment $\Delta_f H_{298}^{\circ}$ with Values from CBS-QB3 and B3LYP/6-31G(d,p) Calculation (kcal mol ⁻¹).....	72
4.2 Confidence Limits (95%) for Each of the Work Reaction Sets.....	72
4.3 Standard Enthalpies of Formation at 298.15 K of Reference Species Used in Work Reactions.....	76
4.4 Name and Nomenclature of Radical Species.....	78
4.5 Evaluated Enthalpies of Formation at 298 K of Target Molecules.....	79
4.6 Enthalpies of Formation at 298 K and Bond Dissociation Enthalpy (BDE) for Radicals.....	80
4.7 Ideal Gas-Phase Thermochemical Properties ^a vs. Temperature (^o K).....	86
4.8 Comparison of C—H, O—H, and OO—H Bond Dissociation Enthalpies.....	89
4.9 Comparison of R—OH, R—OOH, RO—OH, RO--O Bond Dissociation Enthalpies (kcal mol ⁻¹).....	92
4.10 High Pressure-Limit Rate Parameters for Ring Opening Reactions.....	93

LIST OF TABLES (Continued)

Table	Page
4.11 Ring Opening Reactions of Cyclo-Pentadienone-2-yl and Cyclo-Pentadienone-3-yl Radicals. Enthalpies of Reactants, Transition State Structures and Products.....	94
4.12 High Pressure-Limit Rate Parameters for Cyclo-Pentadienone-2-yl Radical Reactions.....	98
4.13 High Pressure-Limit Rate Parameters for Cyclo-Pentadienone-3-yl Radical Reactions.....	101
4.14 High Pressure-Limit Elementary Rate Parameter for Important Paths in Cyclo-Pentadienone-2-yl and Cyclo-Pentadienone-3-yl Peroxy Radical System versus Pressure.....	110
5.1 The Mechanism of Hydrogen Additional Reaction in This Study.....	116
5.2 Standard Enthalpies of Formation at 298.15 K of Reference Species	116
5.3 Thermodynamic Properties vs Temperature	117
5.4 Activation Energy (E_a) of Hydrogen Additional Reactions	120
5.5 Activation Energy (E_a) of Hydrogen Elimination Reactions.....	121
5.6 High Pressure-Limit Rate Parameter for Hydrogen Additional Reaction	123
5.7 High Pressure-Limit Rate Parameter for Hydrogen Elimination Reactions.....	124
5.8 High Pressure-Limit Rate Parameters for Hydrogen Additional to Butene.....	125
5.9 High Pressure-Limit Rate Parameters for Hydrogen Additional to Iso-butene....	126
6.1 Standard Enthalpies of Formation at 298 K for Reference Species.....	132
6.2 Evaluated Enthalpies of Formation at 298 K for Trifluoroethene + OH Reaction System Intermediates and Products.....	133
6.3 High Pressure-Limit Elementary Rate Parameter for Reactions in the Trifluoroethene + OH Reaction System	134

LIST OF FIGURES

Figure	Page
3.1 Trends in dipole moment versus carbon number for alcohols and extending equations	27
3.2 Dipole moment of alcohol primary radical species and extending equations.....	28
3.3 Dipole moment of alcohol secondary radical species and trends with carbon number.....	29
3.4 Dipole moment of aldehyde versus carbon number.....	30
3.5 Dipole moment of aldehyde primary radical species vs. carbon number.....	31
3.6 Dipole moment of aldehyde secondary radical species vs. carbon number.....	32
3.7 Dipole moment of ether vs. carbon number	33
3.8 Dipole moment of ether primary radical species vs carbon number.....	34
3.9 Dipole moment of ether secondary radical species vs. carbon number.....	35
3.10 Dipole moment of ketone vs. carbon number.....	36
3.11 Dipole moment of ketone primary radical species vs. carbon number	37
3.12 Dipole moment of ketone secondary radical species vs. carbon number	38
3.13 Polarizability of alcohol group vs. carbon number	41
3.14 Polarizability of alcohol primary radical species vs. carbon number	41
3.15 Polarizability of alcohol secondary radical species vs. carbon number	42
3.16 Polarizability of aldehydes group vs. carbon number	44
3.17 Polarizability of aldehydes primary radicals species vs. carbon number	44
3.18 Polarizability of aldehydes secondary radicals species vs. carbon number.....	45

LIST OF FIGURES (Continued)

Figure	Page
3.19 Polarizability of ethers group vs. carbon number	47
3.20 Polarizability of ethers primary radicals species vs. carbon number	47
3.21 Polarizability of ethers secondary radicals species vs. carbon number	48
3.22 Polarizability of ketone group vs. carbon number	50
3.23 Polarizability of ketone primary radicals vs. carbon number	50
3.24 Polarizability of ketone secondary radicals species vs. carbon number	51
3.25 L J diameters for alcohol group vs. carbon number	53
3.26 L J diameters for alcohol primary radicals vs. carbon number	54
3.27 L J diameters for alcohol secondary radicals vs. carbon number	55
3.28 L J diameters for aldehydes vs. carbon number	56
3.29 L J diameters for aldehyde primary radicals vs. carbon number	57
3.30 L J diameters for aldehyde secondary radicals vs. carbon number.....	58
3.31 L J diameters for ether group vs. carbon number.....	59
3.32 L J diameters for ether primary radicals vs. carbon number	60
3.33 L J diameters for ether secondary radicals species vs. carbon number.....	61
3.34 L J diameters for ketone group vs. carbon number	62
3.35 L J diameters for ketone primary radicals vs. carbon number.....	63
3.36 L J diameters for ketone secondary radicals vs. carbon number	63
4.1 Nomenclature for radical and functional group sites.....	70
4.2 Structure and abbreviated nomenclature of the target molecules.....	75

LIST OF FIGURES (Continued)

Figure	Page
4.3 Structure and abbreviated nomenclature of the cyclopentadienone radical corresponding to the loss of a hydrogen atom from the parent molecules.....	77
4.4 Reactions of cyclo-pentadienone-2-yl (TS=Transition State).....	97
4.5 Reactions of cyclo-pentadienone-3-yl (TS=Transition State).....	97
4.6 Rate constants (log k) vs temperature (1000/T) at 1 atm for of cyclo-pentadienone-2-yl system.....	99
4.7 Rate constants (log k) vs temperature (1000/T) at 50 atm of cyclo-pentadienone-2-yl system.....	99
4.8 Rate constants (log k) vs pressure (log P) at 298 K of cyclo-pentadienone-2-yl system.....	100
4.9 Rate constants (log k) vs pressure (log P) at 1000 K of cyclo-pentadienone-2-yl system.....	100
4.10 Rate constants (log k) vs temperature (1000/T) at 1 atm of cyclo-pentadienone-3-yl system.....	102
4.11 Rate constants (log k) vs temperature (1000/T) at 50 atm of cyclo-pentadienone-3-yl system.....	102
4.12 Rate constants (log k) vs pressure (log P) at 298 K of cyclo-pentadienone-3-yl system.....	103
4.13 Rate constants (log k) vs pressure (log P) at 1000 K of cyclo-pentadienone-3-yl system.....	103
4.14 Rate constants (log k) vs. temperature (1000/T) at 1 atm for cyclo-pentadienone-2-yl dissociation.....	105
4.15 Rate constants (log k) vs. temperature (1000/T) at 50 atm for cyclo-pentadienone-2-yl dissociation.....	105
4.16 Rate constants (log k) vs. pressure (log P) at 298 K for cyclo-pentadienone -2-yl dissociation.....	106

LIST OF FIGURES (Continued)

Figure	Page
4.17 Rate constants (log k) vs. pressure (log P) at 1000 K for cyclo-pentadienone-2-yl dissociation.....	106
4.18 Rate constants (log k) vs. temperature (1000/T) at 1 atm for cyclo-pentadienone-3-yl dissociation.....	108
4.19 Rate constants (log k) vs. temperature (1000/T) at 50 atm for cyclo-pentadienone-3-yl dissociation.....	108
4.20 Rate constants (log k) vs. pressure (log P) at 298 K for cyclo-pentadienone-3-yl dissociation.....	109
4.21 Rate constants (log k) vs. pressure (log P) at 1000 K for cyclo-pentadienone-3-yl dissociation.....	109
5.1 Rate constants (log k) vs. 1000/T at 1 atm. for $c=cc + h$	125
5.2 Rate constants (log k) vs. 1000/T at 1 atm. for $c=cc2 + h$	127
6.1 Geometry of lowest energy conformer of target molecules in trifluoroethene + OH system.....	131
6.2a Potential energy diagrams for the $C_2F_3H + OH \rightarrow C(OH)F_2C\cdot HF \rightarrow$ products system.....	136
6.2b Potential energy diagrams for the $C_2F_3H + OH \rightarrow C\cdot F_2CHF(OH) \rightarrow$ products system.....	137
6.3a Rate constants versus 1000/T (K) at 1.0 atm for the chemical activation reaction of $C_2F_3H + OH \rightarrow (HO)CF_2C\cdot HF^* \rightarrow$ products system.....	140
6.3b Rate constants versus 1000/T (K) at 100.0 atm for the chemical activation reaction of $C_2F_3H + OH \rightarrow (HO)CF_2C\cdot HF^* \rightarrow$ products system	140
6.4a Rate constants versus log pressure (atm) at 298 K for chemical activation reactions of $C_2F_3H + OH \rightarrow (HO)CF_2C\cdot HF^* \rightarrow$ products system.....	141
6.4b Rate constants versus log pressure (atm) at 1000 K for chemical activation reaction of $C_2F_3H + OH \rightarrow (HO)CF_2C\cdot HF^* \rightarrow$ products system.....	141
6.5a Rate constants versus log pressure (atm) at 298 K for the chemical dissociation reaction of $(HO)CF_2C\cdot HF^* \rightarrow C_2F_3H + OH$, and \rightarrow products system.....	142

LIST OF FIGURES (Continued)

Figure	Page
6.5b Rate constants versus log pressure (atm) at 500 K for the chemical dissociation reaction of $(\text{HO})\text{CF}_2\text{C}\cdot\text{HF}^* \rightarrow \text{C}_2\text{F}_3\text{H} + \text{OH}$, and \rightarrow products system.....	143
6.6 Rate constants versus $1000/T$ at 1.0 atm for the chemical dissociation reaction of $(\text{HO})\text{CF}_2\text{C}\cdot\text{HF}^* \rightarrow \text{C}_2\text{F}_3\text{H} + \text{OH}$, and \rightarrow products system	143
6.7a Rate constants versus $1000/T$ (K) at 1.0 atm for the chemical activation reaction of $\text{C}_2\text{F}_3\text{H} + \text{OH} \rightarrow \text{C}\cdot\text{F}_2\text{CHF}(\text{OH})^* \rightarrow$ products system.....	144
6.7b Rate constants versus $1000/T$ (K) at 100.0 atm for the chemical activation reaction of $\text{C}_2\text{F}_3\text{H} + \text{OH} \rightarrow \text{C}\cdot\text{F}_2\text{CHF}(\text{OH})^* \rightarrow$ products system.....	145
6.8a Rate constants versus log pressure (atm) at 298 K for the chemical activation reaction of $\text{C}_2\text{F}_3\text{H} + \text{OH} \rightarrow \text{C}\cdot\text{F}_2\text{CHF}(\text{OH})^* \rightarrow$ products system.....	145
6.8b Rate constants versus log pressure (atm) at 1000 K for the chemical activation reaction of $\text{C}_2\text{F}_3\text{H} + \text{OH} \rightarrow \text{C}\cdot\text{F}_2\text{CHF}(\text{OH})^* \rightarrow$ products system.....	146
6.9 Rate constants versus $1000/T$ at 1.0 atm for the chemical dissociation reaction of $\text{C}\cdot\text{F}_2\text{CHF}(\text{OH})^* \rightarrow \text{C}_2\text{F}_3\text{H} + \text{OH}$, and \rightarrow products system	147
6.10aRate constants versus log pressure (atm) at 298 K for the chemical dissociation reaction of $\text{C}\cdot\text{F}_2\text{CHF}(\text{OH})^* \rightarrow \text{C}_2\text{F}_3\text{H} + \text{OH}$, and \rightarrow products system.....	147
6.10bRate constants versus log pressure (atm) at 1000 K for the chemical dissociation reaction of $\text{C}\cdot\text{F}_2\text{CHF}(\text{OH})^* \rightarrow \text{C}_2\text{F}_3\text{H} + \text{OH}$, and \rightarrow products system	148

CHAPTER 1

INTRODUCTION

Transport properties are needed for evaluation of gas phase flow studies where multicomponent viscosities, thermal conductivities, diffusion and thermal diffusion coefficients are required in combustion and other thermal flow fluid dynamics modeling. While there are a number of estimation methods for known stable organic molecules that are fuels in combustion systems, there are none that we know of for the radicals, which make up the majority of species in combustion reactions. As computational fluid dynamic (CFD) modeling is becoming more and more available, there are needs to include reasonably accurate transport properties for both the molecules and the corresponding radical intermediates. This study uses computational chemistry to calculate dipole moments, polarizability and molecular diameters, which can be related to Lennard Jones diameters for hydrocarbons and corresponding radicals. Mopac¹ semiempirical and the B3LYP/6-31G (d,p)²⁻³ Density Functional Method are used to calculate the dipole moments, polarizability and molecular diameters of hydrocarbons, olefins, alkynes and related radicals. Linear relationships are estimated as a function of carbon number and reported for use in estimation of large species hydrocarbon and oxygenated hydrocarbons systems along with corresponding radicals are calculated up to twelve carbons.

Kinetic models using reaction mechanisms comprised of many elementary chemical reaction steps, along with fundamental thermochemical and kinetic principles, are presently widely used and in constant process of further development by researchers

attempting to optimize or more fully understand a number of chemical complex systems. These systems include combustion, flame inhibition, ignition times, atmospheric pollutant reactions and smog formation, stratospheric ozone depletion, municipal and hazardous wastes incineration, global warming, chemical vapor deposition, semiconductor etching, rocket propulsion and other related fields.

The objective of this dissertation is to apply well-known density functional theory and composite computational methods to calculate thermochemical properties and kinetics of hydrocarbons, oxygenates, and fluorocarbon species. Calculating accurate and reliable thermochemical properties, including enthalpies of formation ($\Delta_f H^\circ_{298}$), entropies ($S^\circ(T)$), heat capacities ($C_p^\circ(T)$), and bond dissociation energies (BDEs), will aid in the creation of chemical kinetic models while serving as representative species for estimation of larger proportion on related compounds. Calculated values are compared to literature experimental and calculation data, where available for evaluation of accuracy of the calculation.

Thermochemical properties, standard enthalpies, entropies, and heat capacity as function of temperature for cyclopentadienone and cyclopentadiene-peroxides, alcohols, alkyl and alkylperoxy and vinylic radicals along with corresponding bond energies are determined by use of computational chemistry. CBS-QB3⁴ composite methods and B3LYP density function theory have been used to determine the enthalpies of formation ($\Delta_f H^\circ_{298}$) using isodesmic reaction schemes with several work reactions for each species. Entropy and heat capacities, $S^\circ(T)$ and $C_p^\circ(T)$ ($50\text{ K} \leq T \leq 5000\text{ K}$), were determined using geometric parameters, internal rotor potentials, and vibration frequencies from mass electronic degeneracy B3LYP/6-31G (d,p)²⁻³ calculations. The standard enthalpy of

formation was reported for parent molecules as cyclopentadienone, and cyclopentadienone corresponding alcohols, and hydroperoxides, and radicals of cyclopentadienone: vinyl, alkoxy, peroxy corresponding to loss of a hydrogen atom from the carbon and oxygen sites. The estimation of the cyclopentadienone entropy and heat capacity values also are reported in this study for all parent and radical molecules. The reactions of the cyclopentadienone vinylic carbon radicals with molecular oxygen appear to undergo significant chain branching via reaction with O_2 . Canonical transition state theory was used to study ring opening reactions for Cyclo-pentadienone-2-yl [$y(c_5h_3do)j_2$] and Cyclo-pentadienone-3-yl [$y(c_5h_3do)j_3$] radicals. The M062X⁵ and ω B97X⁶ hybrid density functional theory methods were used in conjugation with 6-311+G(d,p) basis set, and by the composite CBS-QB3⁴ level of theory. The thermochemical analysis shows The $R^\bullet + O_2$ well depths are deep, on the order of 50 kcal mol^{-1} and the $R^\bullet + O_2$ reactions to $RO + O$ (chain branching products) for cyclopentadienone-2-yl and cyclopentadienone-3-yl have unusually low reaction (ΔH_{rxn}) enthalpies, some 20 or so kcal mol^{-1} below the entrance channels. Chemical activation kinetics using quantum RRK analysis for $k(E)$ and master equation for fall-off are used to show significance of chain branching as a function of temperature and pressure.

Hydrogen atoms are major active radicals in the atmosphere and in fuel combustion systems and olefins also indicated as an important substance for the formation of aromatics in the combustion system. The reaction kinetics of hydrogen atom addition to primary (P), secondary (S), tertiary (T) vinylic (olefin) carbons to form an alkyl radical is investigated using computational chemistry with Density Functional Theory (DFT) and ab initio composite level methods. Truhlar⁵ group functional M062X

with the 6-31g(d,p) and M062X/6-311+g(d,P) basis set were the DFT methods. The composite *ab initio* complete basis set methods were CBS-QB3- and CBS-APNO⁷. These addition barriers are relatively low, typically one to several kcal mol⁻¹, a second CBS-QB3 method was modified to incorporate the M06-2x calculated energies and structures for the barriers in the subsequent CBS energy calculation (CBS-QB3/M062x). Results from calculations at different levels are compared with the experimental and evaluated (reviewed) data for hydrogen atom addition to primary, secondary, tertiary of ethylene, propene, 1-butene, E-2-butene, Z-2-butene, isobutene, and tetramethylethylene. Activation energies and rate constants for forward and reverse paths are calculated and compared with literature. One objective of this study is to use the data from experimental on H atom addition to small olefins to identify a calculation method that reproduces the experimental results and can be recommended for use in calculating energy barriers and structure for systems where data is not available. The M06-2x modified CBS-QB3 method and the CBS-APNO show the closet agreement to the experimental data with CBS-QB3 next. In general, the DFT level calculations result in higher barriers.

Fluoro halocarbons are widely used as refrigerents and heat transfer fluids; they are routinely found in environmental waters and in the atmosphere, where concerns exist for their influence on global warming the general population health. The study is focused on CF₂=CHF (Trifluoroethylene), that is halocarbon (CFCs and HCFCs) and would be considered as the potential substance concerning with the ozone depletion in atmospheric chemistry, this compound used as a monomer in the preparation process of fluorocarbon polymer industry. Knowledge of the fundamental thermochemistry kinetics and reaction paths leads to understanding in its reaction in atmospheric chemistry and its combustion

properties. The initiate reaction involves with the OH addition with subsequent, H transfer, F (Fluoride transfer), HF (Hydrogen Fluoride) elimination, F atom elimination, H atom elimination, and isomerization reactions. The thermochemistry and kinetic studies for reactions of the $\text{CF}_2=\text{CHF} + \text{OH}$ adduct formation and further unimolecular reactions have been studied. The reaction kinetic analysis has included both the chemical activated and the stabilized intermediates. Thermochemical properties and reaction kinetics for the reaction systems as function of both temperature and pressure and reaction mechanisms for combustion are developed.

CHAPTER 2

COMPUTATIONAL METHODS

Computational chemistry calculations for thermochemical and kinetic properties are presented including background and calculation procedures for gas phase combustion and atmospheric chemistry modeling.

2.1 Thermochemical Properties

Atmospheric and Combustion modeling requires accurate thermochemical property data, specifically enthalpies (heats) of formation ($\Delta_f H^\circ_{298}$), standard entropy (S°) and heat capacities (C_p) as a function of temperature for reactants, intermediates, final products and reaction transition states. These data are used in conventional transition state theory for determination of the forward and reverse rate constants and evaluations of stability and reactivity.

2.1.1 Computational Chemistry

Computational chemistry uses quantum mechanics calculations to obtain thermochemical properties, structures and electrical properties for stable and reactive molecules and ions. This electronic structure theory (quantum mechanics) is used to calculate molecular properties such as the energy of the molecular structure (spatial arrangement of atom or nuclei and electrons), energies and structure of transition states, molecular geometries, vibrational frequencies, rotational frequencies and moments of inertia. Quantum mechanical energies are based on 0 K electronic structures, which give quantized values of the energy and partition functions. To find other properties, and properties at other

temperatures, statistical mechanics need to be applied to the structure, vibrations of the molecules.

Schrödinger derived a wave equation and applied it to a number of problems (the hydrogen atom, the harmonic oscillator, the rigid rotator, the diatomic molecule, the hydrogen atom in an electric field)⁸. The wave equation enables to determine certain functions (Ψ) of the coordinates of a system and the time (Ψ = Schrödinger wave functions or probability amplitude functions). The wave function is a function of the particle's coordinates, and from that input, the state of the system can be deduced. Schrödinger time independent form:

$$\hat{H}\Psi = E\Psi \quad (2.1)$$

Here \hat{H} is the *Hamiltonian*, a differential operator representing the total energy. E is the numerical value of the energy of the state, i.e., the energy relative to a state in which the constituent particles (nuclei and electrons) are infinitely separated and at rest. Ψ is a many-electron wave function, and it depends on the Cartesian coordinates of all particles and also on the spin coordinates. The square of the wave function, Ψ^2 , is the probability distribution of the particles within the molecule. Approximate solutions to the Schrödinger equation are calculated using a simpler Hamiltonian with parameters fit to experimental data. Higher level calculations are currently available, but semi-empirical methods are still practical for the analysis of very large molecules.

The many-electron Schrodinger equation cannot be solved exactly, and approximations need to be introduced to provide practical methods. The Schrödinger's equation can be solved exactly only for one electron atoms. The approximation of

separating electronic and nuclear motions is Born-Oppenheimer approximation that is also basic to quantum chemistry.

The Hartree-Fock (HF) approximation is used to calculate an electron – proton structure; it treats electron interactions between individual electrons by interactions between a particular electron and the average field created by all the other electrons. The HF model does not include a full treatment of the effects of instantaneous electron corrections (electron – electron interactions), and thus leads to overestimation of the electron-electron repulsion energy and total energy⁹. There is a need for Electron correlation corrections for coupling or correction of electron motions. Lack of this in the HF method leads to a lessening of the electron-repulsion energy and also leads to a lowering of the total energy (it omits electron – electron repulsion). The correction energy is described by the difference between the Hartree-Fock energy and the experimental energy. There are several theoretical methods developed with electron correction. These are higher level theoretical methods and the calculation are highly time consuming - both time and computer resources in different scales independently.

2.1.2 Theoretical Methods

Theoretical methods are approached in several methods for determination and calculation for electronic structure, frequencies, and energies of target molecules.

- *Ab initio methods* (from first principles): There are Hartree-Fock (Hartree-Fock, Restricted Open-Shell Hartree-Fock, Unrestricted Hartree-Fock), Post-Hartree-Fock (Moller-Plesset incorrect spelling-fix) perturbation theory¹⁰, Configuration Interaction, Coupled Cluster, Quadratic Configuration Interaction), and Multireference Methods. This theory is concerned with predicting the properties of atomic and molecular systems. It is based upon the fundamental laws of

quantum mechanics and uses a variety of mathematical transformation and approximation techniques to solve the fundamental equations

- *Semi-empirical methods*: are based on the Hartree Forck (HF) form, but use many parameters derived from experimental data to simplify the computation. They solve an approximate form of the Schrödinger's equation that depends on having appropriate parameters available for the type of chemical system in question. They are highly useful for the treatment of large molecules, where even the HF method without parametrization is too expensive. Examples semi – empirical methods are AM1, PM3 and MINDO/3.
- *Density Functional Theory (DFT) methods*: derives the properties of a many-electron system by using more functions in calculation. A variety of functionals have been defined, generally distinguished by the way that they treat exchange and correlation components. Some examples are B2PLYP, B3LYP and M06-2X.
- *Quantum Chemistry Composite methods*: combine methods with a high level of theory and a small basis set with methods that employ lower levels of theory with larger basis sets. Some examples are: G1, G2, G3, G3MP2B3 and CBS-QB3.

2.1.3 Calculation Methods

- *B3LYP*: combines the three parameter Becke exchange functional, B3, with Lee-Yang- Parr's correlation functional, LYP², it is based on the Density Functional Theory.
- *BMK*: Boese and Martin's¹¹ τ -dependent hybrid Density Functional Theory based method. The method is rated highly in evaluations for both thermochemistry and barrier accuracy.
- *ω B97X*: long-range corrected (LC) hybrid functional developed by Chai et al.¹², which includes the short-range (SR) Hartree-Forck (HF) exchange.

- *B2PLYP*: based on a mixing of standard generalized gradient approximations (GGAs) for exchange by Becke (B) and for correlation by Lee, Yang, and Parr (LYP) with Hartree-Fock (HF) exchange and a perturbative second-order correlation part (PT2) that is obtained from the Kohn-Sham orbitals and eigenvalues¹³.
- *M06-2X*: hybrid meta exchange correlation functional, it is a high nonlocality functional with double the amount of nonlocal exchange (2X), and it is parametrized only for nonmetals⁵.
- *CBS-QB3 (Complete Basis Set)*: There are multilevel chemistry model that predicts molecular energies with high accuracy and relatively low computational cost. Geometry optimization structure and frequencies is perform by B3LYP/CBSB7, and followed by a single point energy calculation at the CCSD(T)/6-31G+(d') with CBS extrapolation. Next steps are energy calculations by MP4SDQ/CBSB4, MP4/CBSB, and MP2/CBSB3, respectively and along with additive correction at the CCSD(T) calculation.
- *CBS-APNO (Complete Basis Set)*: It is based on HF/6-311G(d,p) calculations for the geometry optimization and frequencies, followed by a single point energy calculation at the QCISD/6-311G(d,p) and QCISD(T)/6-311++G(2df,p) following with MP2 level of theory. It includes a total energy extrapolation to the infinite basis-set limit using pair natural-orbital energies at the MP2/CBS-APNO level.

All quantum chemical calculations have been performed within the Gaussian 03¹⁴ and 09¹⁵ suit of program.

2.1.4 Internal (intramolecular) Molecular Rotation Potentials

Rotation of the C—C, C—H, C—OH, and O—OH bonds in the target molecules is needed to determine the lowest energy conformer and the potentials of the internal rotor

are needed to determine energy contributions and also the entropy and heat capacity values versus temperature.

Energy profiles for intramolecular internal rotations were calculated in this study to determine energies of the rotational conformers and inter-conversion barriers along with contributions to entropy and heat capacity for the low barrier (below 4.5 kcal mol⁻¹) rotors. The total energies as a function of the dihedral angles were computed at the B3LYP/6-31G(d,p) level of theory by scanning the torsion angles between 0° and 360° in steps of 10°, while all remaining coordinates were fully optimized. All potentials were rescanned when a lower energy conformer is found, relative to the initial low energy conformer. The total energy corresponding to the most stable molecular conformer was arbitrarily set to zero and used as a reference point to plot the potential barriers. The resulting potential energy barriers for internal rotations in the hydroperoxides, alcohols and peroxy radicals are shown in Appendix C along with data for the potentials.

Vibration frequencies calculated by the Gaussian code are examined by viewing the vibration mode movement; the contributions from frequencies corresponding to internal rotations are excluded from the entropy and heat capacity and replaced with a more accurate estimate of S and Cp(T) from the internal rotor contributions.

2.1.5 Work Reactions and Enthalpy of Formation ($\Delta_f H^\circ_{298}$)

Standard enthalpies of formation are evaluated using calculated energies, zero point vibration energy (ZPVE), plus thermal contributions (to 298K) at the B3LYP/6-31 g(d,p) and CBS-QB3 levels of theory plus use of work reactions¹⁶⁻¹⁷. The calculated total energy at B3LYP/6-31G(d,p) is corrected by the ZPVE, which is scaled by 0.9806 for this

calculation method, as recommended by Scott and Radom¹⁸. The CBS-QB3 composite method starts with a geometry from B3LYP/CBSB7 calculation method.

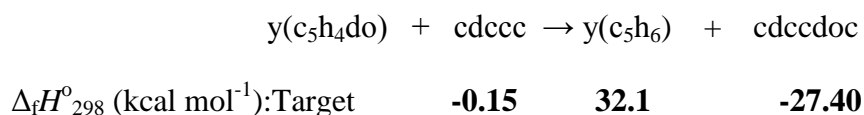
To more accurately evaluate the standard enthalpy of formation ($\Delta_f H^\circ_{298}$), a variety of homodesmotic and isodesmotic work reactions have been used to calculate the standard enthalpy of formation for both parent molecules and radicals at each level of theory. An isodesmotic reaction is a hypothetical reaction where the number and type of bonds is conserved on each side of the work reaction, and a homodesmotic reaction conserves number and type of bonds, but also conserves hybridization¹⁹.

The work reactions in this work have used to calculate the $\Delta_f H^\circ_{298}$ of the target molecule as following:

$$\Delta_{\text{rxn}} H^\circ_{298} = \sum \Delta H_f (\text{Product}) - \sum \Delta H_f (\text{Reactant}) \quad (2.2)$$

Where the two products and one reactant are the reference molecules that are known, and the three evaluated $\Delta_f H^\circ_{298}$ reference species from the literature thermodynamic properties have been use.

As an example the following equation is used to estimate $\Delta_f H^\circ_{298}$ for y(c₅h₄do)



The standard enthalpy of formation for each species in the reaction is calculated, and the heat of reaction, $\Delta_{\text{rxn}} H^\circ_{298}$, is then calculated from the set of data on the four molecules in the reaction. Literature values for enthalpies of formation of the three reference compounds (values above in bold) are used with the $\Delta_{\text{rxn}} H^\circ_{298}$ to obtained the enthalpy of formation on the target molecule, y(C₅h₄dO). The values in brackets correspond to B3LYP/6-31 g(d,p) calculated values (1 Hartree = 627.51 kcal/mol⁻¹)¹⁵.

$$\Delta_{\text{rxn}} H^\circ_{298} = [(-194.012906)+(-231.147354)] - [(-268.030211)+(-157.117923)] \times 627.51$$

$$= -7.61 \text{ kcal mol}^{-1}$$

Using the calculated $\Delta_{\text{rxn}}H^{\circ}_{298}$ and reference species to find $\Delta_f H^{\circ}_{298}$ of the target molecule in kcal mol^{-1}

$$-7.61 \text{ kcal mol}^{-1} = (-27.40) + (32.1) - (-0.15) - \Delta_f H^{\circ}_{298} \text{ y(C}_5\text{h}_4\text{dO)}$$

$$\Delta_f H^{\circ}_{298} \text{ y(C}_5\text{h}_4\text{dO)} = 12.46 \text{ kcal mol}^{-1}$$

2.1.6 Bond Dissociation Enthalpies (BDE)

The C—H bond dissociation Enthalpies are reported from the calculated $\Delta_f H^{\circ}_{298}$ of the parent molecule and the radical corresponding to loss of hydrogen atom at each carbon or oxygen site. The enthalpies of the parent molecule and product species are both calculated in this study and used with the value of $52.10 \text{ kcal mol}^{-1}$ for the H atom²⁰ to determine the corresponding BDE. The RO—OH bond dissociation enthalpies are from the calculated $\Delta_f H^{\circ}_{298}$ of parent hydroperoxide molecule and their alkoxy radical corresponding to loss of $\cdot\text{OH}$, where the enthalpies of parent molecule and radicals are calculated in this study in conjunction with the value of $8.95^{21} \text{ kcal mol}^{-1}$ for $\cdot\text{OH}$ at 298.15 K. The hydroperoxide carbon bond, the RC—OOH bond dissociation enthalpies are reported from the calculated $\Delta_f H^{\circ}_{298}$ of parent hydroperoxide molecule corresponding to loss of $\cdot\text{OOH}$ ($\Delta_f H^{\circ}_{298}$ of $2.94 \text{ kcal mol}^{-1}$)²² used in the calculation. The RO—O bond dissociated enthalpies were calculate with the value of $59.55 \text{ kcal mol}^{-1}$ for $\cdot\text{O}$ at temperature 298.15 K²⁰.

2.1.7 Entropy and Heat Capacity

Entropy and heat capacity values as a function of temperature are determined from the calculated structures, moments of inertia, vibration frequencies, internal rotor potentials,

symmetry, electron degeneracy, number of optical isomers and the known mass of each molecule. The calculations use standard formulas from statistical mechanics for the contributions of translation, vibrations and external rotation (TVR) using the SMCPs (Statistical Mechanics – Heat Capacity, Cp, and Entropy, S) program²³. This program utilizes the rigid-rotor-harmonic oscillator approximation from the frequencies along with moments of inertia from the optimized B3LYP/6-31G(d,p) level.

The entropy and heat capacity are derived from statistical mechanics principals²⁴.

The molar partition function (Q) for an assembly of identical molecules is:

$$Q = \sum_i p_i e^{-E_i/RT} \quad (2.3)$$

where Q is the partition function, p_i is the degeneracy, E_i is the energy of the i^{th} quantum level, R is universal gas constant, and T is temperature. Thermodynamic properties, as related to partition function.

$$Q = Q_{trans} \times Q_{rot} \times Q_{vib} \times Q_{elec} \quad (2.4)$$

Each of the thermodynamic properties²⁴ depends on the logarithm or logarithmic derivative of the partition function and will thus receive additive contributions from each of the degrees of freedom. The entropy calculation accounts for the contribution from the translations (S_{tran}), vibrations (S_{vib}), internal rotors ($S_{int,rot}$), hindered rotors ($S_{hind,rot}$), electronic contributions (S_{elec}), and the contribution of the optical isomers ($S_{opt,iso}$). The heat of capacity calculation accounts for the contribution from the translations ($C_{v,tran}$), vibrations ($C_{v,vib}$), internal rotors ($C_{v,rot}$), hindered rotors ($C_{v,hind,rot}$), and the electronic contributions ($C_{v,elec}$). The equations for entropy and heat capacity used in SMCPs come from standard statistical mechanics allowing for macroscopic thermochemical properties

to be calculated based on molecular energies from electronic structure calculations.

Equations are summed from the individual contributions where entropy is calculated as,

$$S = S_{tran} + S_{vib} + S_{int,rot} + S_{hind,rot} + S_{elec} + S_{opt,iso} \quad (2.5)$$

$$S_{tran} = 37.0 + \frac{3}{2}R \ln \left(\frac{M_w}{40} \right) + \frac{3}{2}R \ln \left\{ \frac{T}{298} \right\} \quad (2.6)$$

$$S_{vib} = R \ln \left(\frac{kT}{h\nu} \right) + R \quad (2.7)$$

$$S_{rot}^{linear} = 6.9 + R \ln \left(\frac{I}{\sigma_e} \right) + R \ln \left(\frac{T}{298} \right) \quad (2.8)$$

$$S_{rot}^{non-linear} = 11.5 + \frac{R}{2} \ln \left(\frac{I_m^3}{\sigma_e} \right) + \frac{3}{2}R \ln \left(\frac{T}{298} \right) \quad (2.9)$$

$$S_{rot}^{1D} = 4.6 + R \ln \left(\frac{I_r^{1/2}}{\sigma_i} \right) + \frac{R}{2} \ln \left(\frac{T}{298} \right) \quad (2.10)$$

$$S_{elec} \sim 0 \quad (2.11)$$

$$S_{opt,iso} = -R \ln(n) \quad (2.12)$$

The molar heat capacity at constant volume and at constant pressure with assumption of ideal gas behavior, are expressed as follow:

$$C_p = C_{v,tran} + C_{v,vib} + C_{v,rot} + C_{v,hind,rot} + C_{v,elec} + R \quad (2.13)$$

$$C_{v,tran} = \frac{3}{2}R \quad (2.14)$$

$$C_{v,vib} = R \sum_i \left[\frac{x_i^2 e^{x_i}}{(e^{x_i} - 1)^2} \right], \quad x_i = \frac{h\nu_i}{k_B T} \quad (2.15)$$

$$C_{v,rot}^{linear} = R \quad (2.16)$$

$$C_{v,rot}^{non-linear} = \frac{3}{2}R \quad (2.17)$$

$$C_{v,rot}^{1D} = \frac{R}{2} \quad (2.18)$$

$$C_{elec} \sim 0 \quad (2.19)$$

where R is the universal gas constant, Mw is the molecular weight, T is the temperature, P is the pressure, k_B is Boltzman's constant, h is Planck's constant, n is the number of optical isomers, I is the moment of inertia for a linear molecule about its center of mass, I_m^3 is the product of the three principal moments of inertia for a nonlinear molecule about the center of gravity, I_r is the reduced moment of inertia for the internal rotation, ν is the vibrational frequency (the moments of inertia and the frequencies are obtained from electronic structure theory calculations), σ_e is the external symmetry number of the molecule, and σ_r is the symmetry of the internal rotation.

2.1.8 Hindered Internal Rotors

Hindered internal rotors have a significant contribution to the thermodynamic properties for molecular species. The, S and $Cp(T)$ for each rotor need to be separately calculated and incorporated for estimation the hinder rotor contributions and not by using the vibration frequency for the torsion.

Two different programs were used in this study for the determination of the influence of the hindered rotors for comparison: Vibir²⁵ and Rotator²⁶.

Vibir: This method is best suited for rotations where the potential energy as a function of the angle, $V(\phi)$, can be expressed as:

$$V(\theta, V_o) = \sum_m \frac{V_m}{2} (1 - \cos(\sigma_m \theta_m)) \quad (2.20)$$

where V_m is the height of the potential barriers and m is the foldness of the potential energy graphs for each bond rotation. Reduced moments of inertia are calculated based on the optimized geometries using the mass and radius of rotation for the rotational groups. There are no adjustments for coupling of internal rotor motion with vibration and VIBIR assumes that the rotational groups are symmetrical, which is accurate for primary and terminal methyl group rotation, for example. Other types of rotational barriers are also estimated using averages of the calculated barrier heights.

Rotator: The program ROTATOR uses the potential to solve the 1-D Schrödinger equation in θ to calculate the energy levels, and the partition function of the hindered rotor. The program calculates the Hamiltonian matrix in the basis of the wave function of free internal rotation and performs the subsequent calculation of energy levels by diagonalization of the Hamiltonian matrix. From the obtained partition functions, the contribution to entropy and heat capacity are determined according to standard expressions of statistical thermodynamics. Entropy and heat capacity values obtained from SMCPS and ROTATOR are summed with the TVR contributions above, and used to calculate the entropy and heat capacity of the calculated species versus temperature. Entropy, S_{298}^o , and heat capacities, $C_p(T)$. A relaxed rotational scan is done with dihedral angle increments of 10° using B3LYP/6-31G(d,p) and the potential obtained is fitted to a truncated Fourier series expansion for the calculation of the contribution of the hindered rotor to the entropy and heat capacity²⁷.

$$V(\theta) = a_o + \sum_{n=1}^{10} a_n \cos(n\theta) + \sum_{n=1}^{10} b_n \sin(n\theta) \quad (2.21)$$

$$a_o = \frac{\sum_{i=1}^m f_i}{m} \quad (2.22)$$

$$a_n = \frac{\sum_{i=1}^m f_i \cos(n\theta)}{m} \quad (2.23)$$

$$b_n = \frac{\sum_{i=1}^m f_i \sin(n\theta)}{m} \quad (2.24)$$

The contribution to entropy and heat capacity are determined according to standard expressions of statistical thermodynamics from the obtained partition functions. Rotator²⁷, accounts directly for contributions to entropy from the optical isomers. Coupling of the low barrier internal rotors with vibrations is not included.

2.2 Kinetic Analysis

The Transition State Theory (TST) describe the hypothetical transition state that occurred between the reactant and product in the reaction path that involved in both forward and reverse reactions. The reaction take place behavior will be generated and explained by this theory.

2.2.1 Canonical Transition State Theory (CTST)

The high-pressure rate constant, $k(T)$, in 300-2000 K is calculated by Canonical transition state theory (CTST) where a transition state maximum energy barrier (saddle point) exists and connected between the reactants and products. The calculation method needs parameters as enthalpies, entropies, and heat capacities for the reactants and transition state (TS) species.

$$k(T) = \frac{k_b T}{h} \exp\left(\frac{\Delta S^\ddagger}{R}\right) \exp\left(\frac{-\Delta H^\ddagger}{RT}\right) \left(\frac{RT}{P^0}\right)^{\Delta n^\ddagger} \quad (2.25)$$

where k_b is Boltzmann's constant, h is Planck's constant, T is temperature, P^0 is standard pressure, R is the ideal gas constant, and ΔS^\ddagger , ΔH^\ddagger , and Δn^\ddagger are the changes in entropy, enthalpy, and the number of molecules between the reactant and transition state, respectively. The rate constant is defined in nonlinear least-squares as the Arrhenius form:

$$k_f = AT^n e^{(-Ea/RT)} \quad (2.26)$$

Where A is the pre-exponential factor, T is the temperature (K), n is the temperature exponent, Ea is the activation energy, and R is the ideal gas constant.

2.2.2 Variational Transition State Theory (VTST)

The minimum-flux or maximum-free-energy-of –activation criteria is used to determine the transition state in VTST²⁸. The transition state is not necessarily located at a saddle point, and it can be variational point which has the maximum-free-energy-of –activation criteria. VTST is used for determination in barrier-less reaction, no transition state structure, which common found in reaction O_2 react (adduct) with radical species.

The variational transition state is determined by a scan (internal rotational analysis) of the interested bond with incrementing the length until a limit in the maximum energy is reached. High-pressure rate constants are determined from the reactant to each of these points for the 300-2000 K temperature range. At each temperature, the distance that has the minimum rate constant is identified (resulting on the information of the

minimum rate constant at each temperature), and the variational rate constant is determined from the fit of these rate constants to the Arrhenius equation (Equation 2.26).

2.2.3 Chemical Activation Reaction

Unimolecular reactions which involve a molecular collision reaction, where a new bond is formed, and the molecule now contains a large excess of energy from the newly formed bond; i.e., results in an ‘energized adduct*’ from the bond formation. This situation may produce a non-equilibrium situation in which molecules acquire energies far in excess of the average thermal energy and this presence of excess energy in the energized adduct allows reactions to occur that would not normally be feasible in a thermal molecule. These chemical activation reactions are important in combustion and in some atmospheric processes. The energized adduct can undergo unimolecular reactions such as photon emission, isomerization, dissociation, reverse reaction back to the original reactants, and deactivation through collisional stabilization. The energy dependence of the rate constant, $k(E)$, must also be considered to correctly account for product distributions, because chemical activation also compete with both pressure-and temperature dependence. Sheng, et al.²⁹ has provided more complete descriptions and utilized modelling details for chemical activation and unimolecular dissociation reactions.

2.2.4 Quantum Rice-Ramsperger-Kassel (QRRK)

Multi frequency quantum Rice Ramsperger-Kassel (QRRK) analysis is used for $k(E)$ ³⁰⁻³² and master equation analysis³³⁻³⁵ is used for falloff. The QRRK analysis is described by Chang et al³⁰. The calculation of $k(E)$ is based on statistical assumptions for the number of ways in which energy can be distributed among the vibrational degrees of freedom in a

molecule. The thermochemical properties along with the forward and reverse rate constants (high-pressure limit) are calculated for each elementary reaction step.

The computer program CHEMASTER, based on the QRRK theory outlined as above. It allows calculation of unimolecular dissociation and chemical activation reaction systems. The formalism in these codes is carried out in all unimolecular and chemical activation reactions involved in this thesis.

The input parameters for CHEMASTER are: (1) High-pressure limit rate constants (Arrhenius A factor and activation energy E_a) for each reaction included for analysis; (2) A reduced set of three vibration frequencies and their associated degeneracy. Reduced sets of three vibration frequencies and their associated degeneracies are computed from fits to heat capacity data, as described by Ritter and Bozzelli et al.³⁶⁻³⁷ These have been shown by Ritter to accurately reproduce molecular heat capacities, $C_p(T)$, and by Bozzelli et al.³⁶ to yield accurate ratios of density of states to partition coefficient, $\rho(E)/Q$; (3) Lennard-Jones transport parameters, (s (Angstroms) and e/k (Kelvin)), and (4) molecular weight of well species.

Although more accurate models exist, such as Rice-Ramsperger-Kassel-Marcus (RRKM), higher demands for specific details about the transition state species are necessary. With uncertainty and questionable accuracy of geometrical structure and modes of vibration in some of these transition state structures, QRRK provides acceptable analysis with fewer input parameters.

CHAPTER 3

DIPOLE MOMENTS, POLARIZABILITY AND LENNARD JONES DIAMETERS OF OXY-HYDROCARBONS: ALCOHOLS, ETHERS, ALDEHYDES, KETONES, AND RADICALS CORRESPONDING TO LOSS OF H ATOMS, FOR ESTIMATION OF TRANSPORT PROPERTIES: A THEORETICAL STUDY

3.1 Overview

Polarizabilities are important properties for use in estimating transport properties of organic molecules. There are some estimation methods for polarizability such as the *ab-initio* structure calculations used by Stout and Dykstra³⁸ to find polarizabilities of over 30 organic molecules, and then used to show that polarizabilities can be divided into transferable atomic contributions. They also demonstrated the important implications of near-additivity of atomic contributions to modeling polarization arising from intermolecular interactions. Maroulis et al.³⁹ compared *ab initio* and density functional theory calculations for polarizability of small silicon clusters of Si₃ to Si₇ and concluded both calculation methods yielded distinctly different polarizability values of the silicon clusters. The *ab initio* methods provided higher predictive capability while density function theory resulted in more reliable values of mean polarizability. Rigorous *ab initio* methods are expensive in use of computation time and density function theory is not always sufficiently accurate for properties of large molecules, Das and Dudis⁴⁰ proposed a simplified and approximate *ab initio* method for calculation of benzene and polyenes of various sizes. A benchmark for dipole moment and polarizability data by calculation has been recently reported by Hickey and Rowley⁴¹. They compare calculation values with experimental data on a set of 46 molecules using the hybrid density functional methods (M06, B3PLYP, B2PYLYP) with the aug-cc-pVTZ basis set.

They report small, systematic errors of ± 0.13 Debye for dipole moments and ± 0.38 (Å)³ for polarizability.

Limited computations on experimental dipole moments are available in the literature. Muller et al.⁴² proposed an estimation method based on structural information of each molecule as well as data found from literature to estimate dipole moments of molecules of high value of and also hydrocarbons of small yet finite dipole moments. Halpern et al.⁴³ used an Monte Carlo integration of electron density distribution of HF/6-31 G* structures with the keywords Standard Volume, to estimate molecular volumes thus obtain the resulting of diameters of both nonpolar and polar molecule species. These were compared with Lennard Jones diameter data in the literature.

The use of Dipole moments, Polarizability and Lennard Jones diameter parameters to the determination of transport properties is described below. Viscosities, diffusion coefficients, and thermal conductivities are required to characterize the molecular transport of species in a multicomponent gaseous mixture. The viscosities of single component are given by the standard kinetic theory⁴⁴ as following equation.

$$\eta_k = \frac{5}{16} \frac{\sqrt{\pi m_k k_B T}}{\pi \sigma_k^2 \Omega^{(2,2)*}} \quad (3.1)$$

Where m_k is the molecular mass, k_B is the Boltzmann constant, and T is the temperature. σ_k is the Lennard-Jones collision diameter, which is related to molecular diameter (d) which can be calculates from molecular volumes. $\Omega^{(2,2)*}$ is the collision integral which depends on the reduced temperature given by formula 3.2, and the reduced dipole moment is calculated by the expression of formula 3.3.

$$T_k^* = \frac{k_B T}{\epsilon_k} \quad (3.2)$$

$$\delta_k^* = \frac{1}{2} \frac{\mu_k^2}{\epsilon_k \sigma_k^3} \quad (3.3.2)$$

Here the term ϵ_k is the Lennard-Jones potential well depth and μ_k is the dipole moment. The binary diffusion coefficients⁴⁴ are given in terms of pressure and temperature.

$$D_{jk} = \frac{3}{16} \frac{\sqrt{2\pi k_B^3 T^3 / m_{jk}}}{P \pi \sigma_{jk}^2 \Omega^{(1,1)*}} \quad (3.4)$$

Where m_{jk} is the reduced molecular mass for the (j,k) species pair is express in equation 3.5, and σ_{jk} is the reduced collision diameter. $\Omega^{(1,1)*}$ is the collision integral which (based on stockmayer potentials) depends on the reduced temperature, T_{jk}^* , which in turn may depend on the species dipole moments μ_k , and polarizabilities α_k . According to whether the collision partners are polar or nonpolar, two cases are considered in computing the reduced quantities. For the case that the partners are either both polar or both nonpolar, equations in 3.5 below are applied.

$$m_{jk} = \frac{m_j m_k}{m_j + m_k} \quad (3.5)$$

$$\frac{\epsilon_{jk}}{k_B} = \sqrt{\frac{\epsilon_j}{k_B} \frac{\epsilon_k}{k_B}} \quad (3.6)$$

$$\sigma_{jk} = \frac{1}{2} (\sigma_j + \sigma_k) \quad (3.7)$$

$$\mu_{jk}^2 = \mu_j \mu_k \quad (3.8)$$

For the case of a polar molecule interacting with a nonpolar molecule, equations 3.9 to 3.11 are used.

$$\frac{\epsilon_{np}}{k_B} = \xi^2 \sqrt{\frac{\epsilon_n}{k_B} \frac{\epsilon_p}{k_B}} \quad (3.9)$$

$$\sigma_{np} = \frac{1}{2}(\sigma_n + \sigma_p)\xi^{-\frac{1}{6}} \quad (3.10)$$

$$\mu_{np}^2 = 0 \quad (3.11)$$

Epsilon can be calculated by equation 3.12, 3.13, and 3.14 give α_n^* value calculation as the reduced polarizability for the nonpolar molecule and μ_p^* as the reduced dipole moment for the polar molecule.

$$\xi = 1 + \frac{1}{4} \alpha_n^* \beta_n^* \sqrt{\frac{\epsilon_p}{\epsilon_n}} \quad (3.12)$$

$$\alpha_n^* = \frac{\alpha_n}{\sigma_n^3} \quad (3.13)$$

$$\mu_p^* = \frac{\mu_p}{\sqrt{\epsilon_p \sigma_p^3}} \quad (3.14)$$

3.2 Dipole Moments

Electric dipole moment represents the arrangement of charges of a molecule with an electric dipole. The moment consists of two electric charges q and $-q$ separated by a distance R . The moment points from the negative charge to the positive charge. The magnitudes of dipole moments are commonly reported in the non-SI unit Debye, D, where $1 \text{ D} = 3.33564 \times 10^{-30} \text{ Coulomb meter}$ and for reference 1 electron e^- is $1.6 \times 10^{-19} \text{ coulombs}$.

A method to estimate polarizability and Lennard-Jones parameters was proposed by Joback and Reid⁴⁵ in 1987 based on the assumption that individual Benson type

groups could be assigned representing partial contributions to the value of a molecule. Then the contributions could be summed to the total value of each parameter to represent that value of a molecule. This method has the limitation that there is a limited set of data points from experiments that can be used to estimate the group contribution values.

Mopac¹ using the semiempirical methods PM3 and PM6 along with two modern Density Functional Methods: BMK¹¹ and the B3LYP²⁻³ were used in this study to calculate the dipole moments, polarizability and molecular diameters of the oxyhydrocarbons in this study. The largest basis set, used with the DFT calculations, in this study is the 6-311+G(d,p) with the tight command. It was used to calculate the dipole electric field induced the Dipole Moments of the alcohol, aldehyde, ether and ketone parent molecules and radicals corresponding to loss of hydrogen atom from the respective carbon atoms. Dipole Moments are reported in units of Debye. The B3LYP DFT method is chosen because it is known to yield accurate geometries. The B3LYP functional is widely used to calibrate and evaluate lower level semi-empirical calculations, where the semi-empirical method is needed for larger molecule systems⁴⁶⁻⁴⁸.

3.2.1 Results Alcohols

Tables 3.1, 3.2 and 3.3 show the dipole moment calculation values of target molecule and corresponding radical species of the C1 to C10 alcohols in this study. Figures 3.1, 3.2, and 3.3 illustrate the consistency with number of carbons and the trends versus number of carbons.

Table 3.1 Calculated Dipole Moment of Alcohols with Comparison to Literature

Name	Molecules	Dipole Moments (Debye)				
		PM6	B3LYP/ 6-31G(d,p)	B3LYP/ 6-311+G(d,p)	BMK/ 6-31G(d,p)	Ref.
methanol	coh	2.05	1.66	1.89	1.74	1.70 ^{a,b}
Ethanol	ccoh	1.84	1.50	1.73	1.57	1.44 ^a 1.69 ^b
1-propanol	cccoh	1.79	1.60	1.71	1.65	1.55 ^a 1.68 ^b
1-pentanol	cccccch	1.96	1.44	1.62	1.49	NA
1-heptanol	cccccccch	1.80	1.43	1.61	1.48	NA
1-decanol	cccccccccccch	1.14	1.29	1.30	1.33	NA

Note: NA = Not Available, Source: ^a[49], ^b[50]

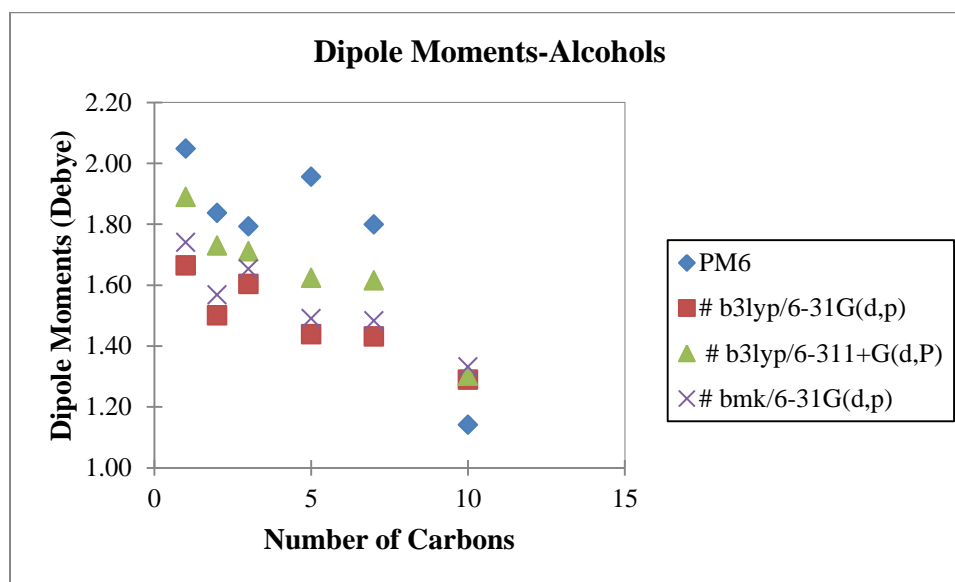
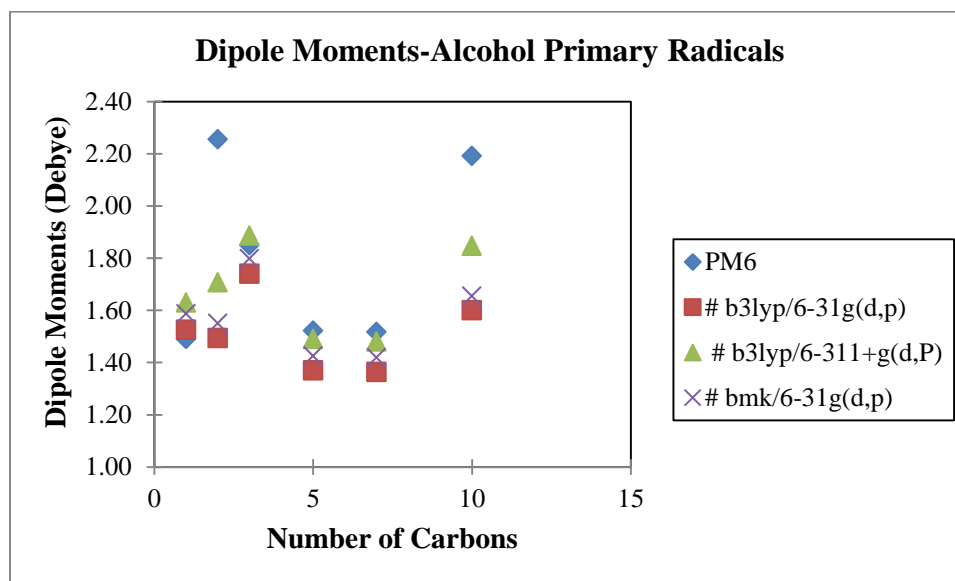
**Figure 3.1** Trends in dipole moment versus carbon number for alcohols and extending equations.

Table 3.2 Calculated Dipole Moment of Alcohol Primary Radicals

Molecules	Dipole moments (Debye)			
	PM6	# b3lyp/ 6-31G(d,p)	# b3lyp/ 6-311+G(d,p)	# bmk/ 6-31G(d,p)
cjoh	1.49	1.53	1.63	1.59
cjcoh	2.26	1.49	1.71	1.55
cjccoh	1.85	1.74	1.89	1.80
cjcccooh	1.52	1.37	1.49	1.43
cjcccccooh	1.52	1.36	1.48	1.42
cjcccccccccooh	2.19	1.60	1.85	1.65

Note: J = radical sites

**Figure 3.2** Dipole moment of alcohol primary radical species and extending equations.**Table 3.3** Calculated Dipole Moment of Alcohol Secondary Radicals

Molecules	Dipole moments (Debye)			
	PM6	# b3lyp/ 6-31G(d,p)	# b3lyp/ 6311+G(d,p)	# bmk/ 6-31G(d,p)
ccjccoh	1.46	1.54	1.64	1.60
ccccjcccooh	2.41	1.57	1.80	1.63
cccccjcccccooh	2.33	1.61	1.88	1.66

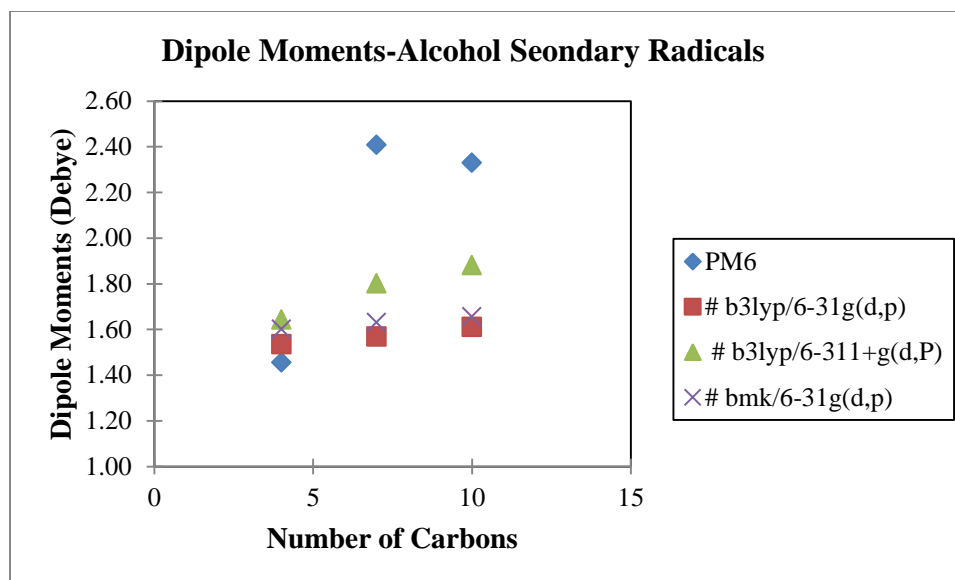


Figure 3.3 Dipole moment of alcohol secondary radicals and trends with carbon number.

A summary of recommended linear equations in for calculating a dipole moment of a normal alcohol using group estimation in Debye unit is present in Table 3.4. The equations were selected from the B3LYP/6-31G(d,p) calculation method values, which showed the best agreement with the available dipole moments data from experiment. Table 3.1 also shows the average ratio of experimental values to calculated values for this method. The scaling factor correction (0.98) is applied to the equation for estimation of the alcohol and alcohol radical dipole moments. Calculated dipole moments with scaling are within ± 0.1 Debye of experimental data.

Table 3.4 Equations to Estimate Dipole Moment of Alcohols and Alcohol Radicals

Species	Equations (N= carbons number)
Alcohol	Dipole = $(-3.63\text{E-}2 \cdot N + 1.66) \cdot 0.98$
Alcohol Primary Radicals	Dipole = $(-5.3\text{E-}3 \cdot N + 1.54) \cdot 0.98$
Alcohol Secondary Radicals	Dipole = $(1.26\text{E-}2 \cdot N + 1.48) \cdot 0.98$

3.2.2 Results Aldehydes

Tables 3.5, 3.6 and 3.7 show the dipole moment calculation values of target molecule and corresponding radical species of the C1 to C10 aldehydes in this study. Figures 3.4, 3.5, and 3.6 illustrate the consistency with number of carbons and the trends versus number of carbons.

Table 3.5 Calculated Dipole Moment of Aldehydes with Comparison to Literature

Name	Molecules	Dipole moments (Debye)				Ref.
		PM6	# b3lyp/ 6-31G(d,p)	# b3lyp/ 6-311+G(d,p)	# bmk/ 6-31G(d,p)	
acetaldehyde	cc*o	3.21	2.65	2.95	2.75	2.69 ^{a,b}
propanal	ccc*o	3.27	2.75	3.07	2.83	2.52 ^{a,b}
pentanal	ccccc*o	3.37	2.88	3.21	3.00	NA
heptanal	cccccc*o	3.39	2.95	3.27	3.07	NA

Note: * = double bond, NA = Not Available, Source: ^a[49], ^b[50]

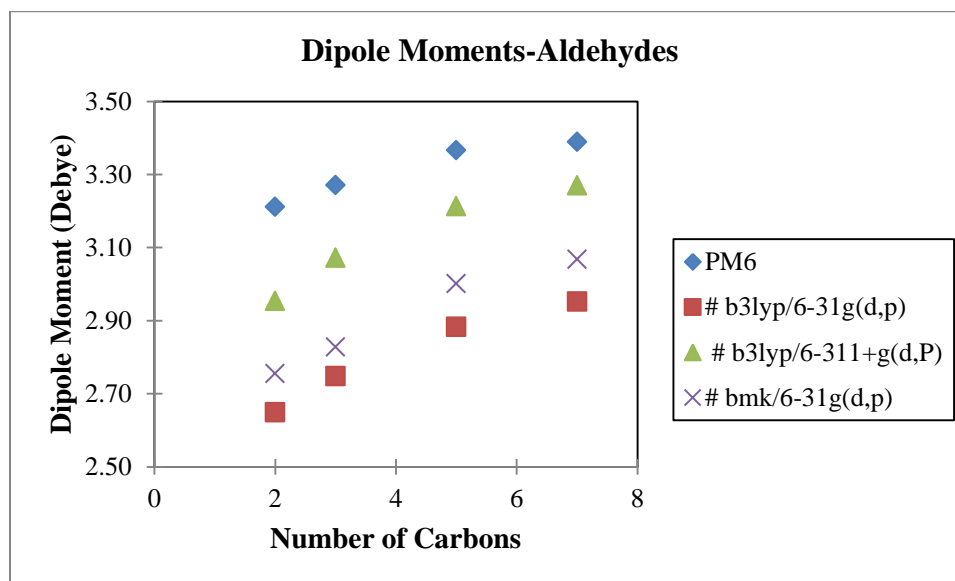
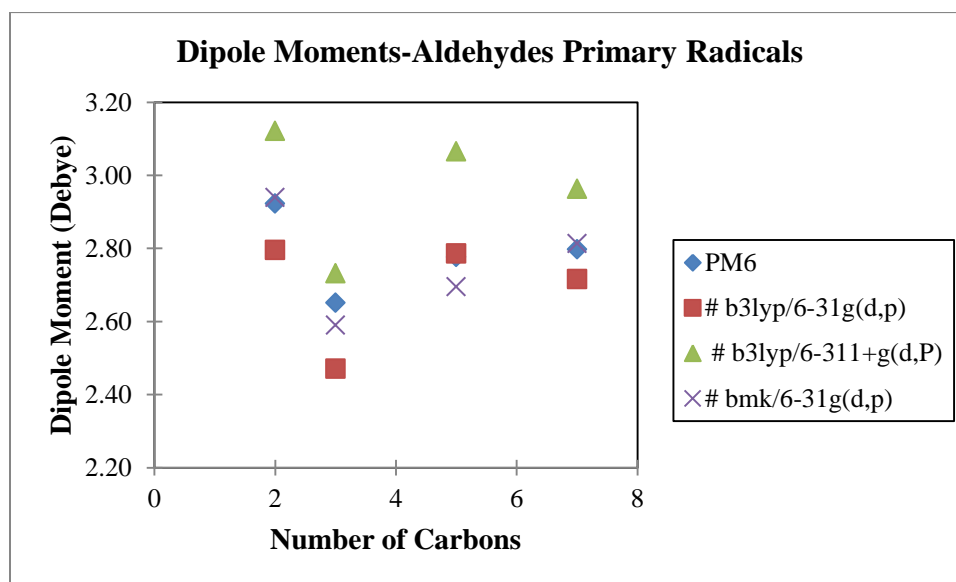


Figure 3.4 Dipole moment of aldehyde vs. carbon number.

Table 3.6 Calculated Dipole Moment of Aldehyde Primary Radical Species

Molecules	Dipole moments (Debye)			
	PM6	# b3lyp/ 6-31g(d,p)	# b3lyp/ 6-311+g(d,p)	# bmk/ 6-31g(d,p)
cjc*o	2.92	2.80	3.12	2.94
cjcc*o	2.65	2.47	2.73	2.59
cjcccc*o	2.78	2.79	3.07	2.70
cjcccccc*o	2.80	2.72	2.96	2.81

Note: * = double bond, j = radical site

**Figure 3.5** Dipole moment of aldehyde primary radical species vs. carbon number.**Table 3.7** Calculated Dipole Moment of Aldehyde Secondary Radical Species

Molecules	Dipole moments (Debye)			
	PM6	# b3lyp/ 6-31g(d,p)	# b3lyp/ 6-311+g(d,p)	# bmk/ 6-31g(d,p)
ccjc*o	4.37	3.46	3.87	3.58
cccjcc*o	2.93	2.88	3.26	2.93
ccccjccc*o	3.72	3.09	3.44	3.23

Note: * = double bond, j = radical site

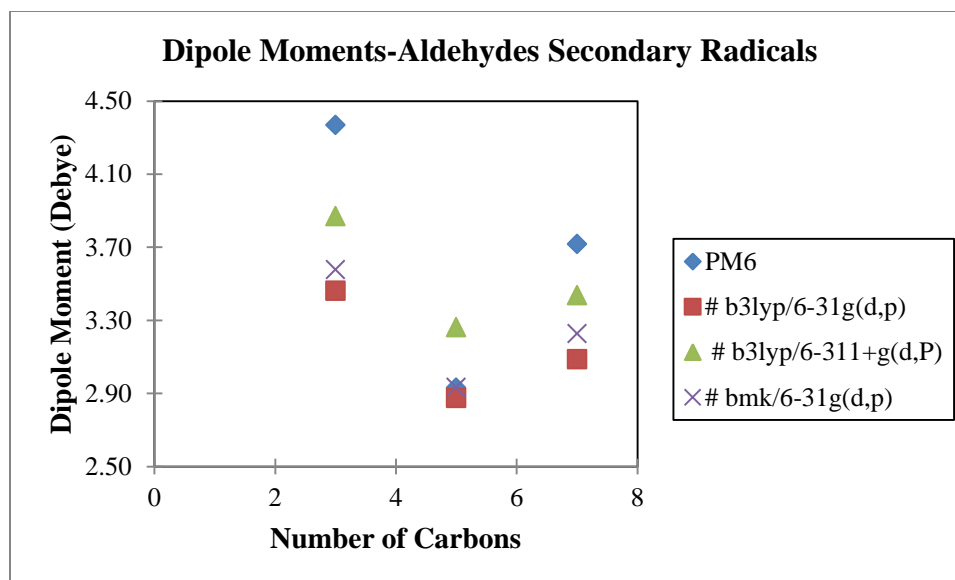


Figure 3.6 Dipole moment of aldehyde secondary radical species vs. carbon number.

A Summary linear equations for dipole moments estimation of aldehydes and corresponding radical species is presented in Table 3.8 via equations obtained from B3LYP with basis set 6-31G(d,p). The average ratio between reference experimental data to the calculation values is 0.97, and this scaling factor is applied to the equation for estimated Aldehyde and Aldehyde radical species dipole moments calculation. Calculated dipole moments with scaling are within ± 0.3 Debye of experimental data for Aldehydes.

Table 3.8 Equations to Estimate Dipole Moment of Aldehydes and Aldehydes Radicals

Species	Equations (N= carbon number)
Aldehyde	Dipole = $(6 \text{ E-}2 \cdot \text{N} + 2.55) \cdot 0.97$
Aldehyde Primary Radicals	Dipole = $(1.22 \text{ E-}2 \cdot \text{N} + 2.64) \cdot 0.97$
Aldehyde Secondary Radicals	Dipole = $(-9.37 \text{ E-}2 \cdot \text{N} + 3.61) \cdot 0.97$

3.2.3 Results Ethers

Tables 3.9, 3.10 and 3.11 show the dipole moment calculation values of target ether molecules and corresponding radicals of C1 to C10 ethers in this study. Figures illustrate the consistency with number of carbons and the trends versus number of carbons.

Table 3.9 Calculated Dipole Moment of Ethers with Comparisons to Literature

Name	Molecules	Dipole moments (Debye)				
		PM6	# b3lyp/ 6-31g(d,p)	# b3lyp/ 6-311+g(d,p)	# bmk/ 6-31g(d,p)	Ref.
dimethyl ether	coc	1.83	1.28	1.45	1.33	1.30 ^{a,b}
ethyl methyl ether	cocc	1.85	1.28	1.47	1.31	1.23 ^{a,b}
methyl propyl ether	coccc	1.74	1.26	1.45	1.29	NA
diethyl ether	ccocc	1.66	1.15	1.35	1.17	1.15 ^{a,b}
buthyl methyl ether	cocccc	1.80	1.20	1.34	1.23	NA

Note: NA = Not Available, Source: ^a[49], ^b[50]

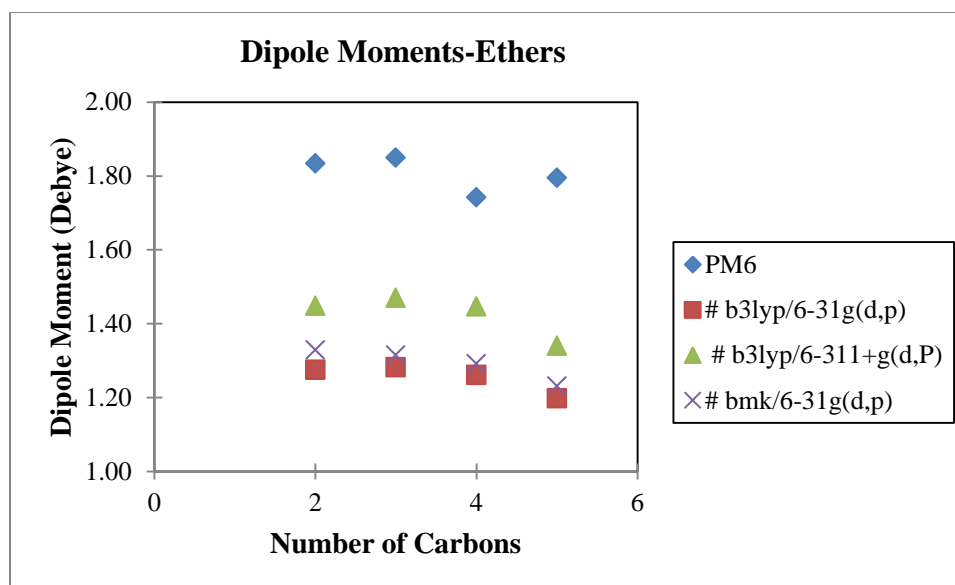
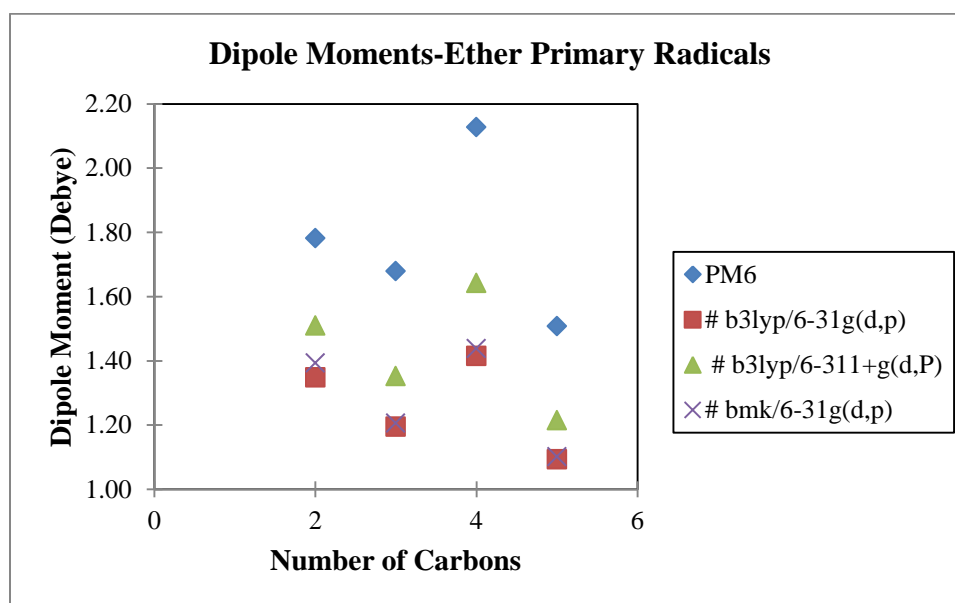


Figure 3.7 Dipole moment of ethers vs. carbon number.

Table 3.10 Calculated Dipole Moment of Ether Primary Radical Species

Molecules	Dipole moments (Debye)			
	PM6	# b3lyp/ 6-31g(d,p)	# b3lyp/ 6-311+g(d,p)	# bmk/ 6-31g(d,p)
cocj	1.78	1.35	1.51	1.39
coccj	1.68	1.19	1.35	1.21
cocccj	2.13	1.42	1.64	1.44
ccoccj	1.50	1.06	1.24	1.07
coccccj	1.51	1.09	1.22	1.10

Note: j = radical site

**Figure 3.8** Dipole moment of ether primary radicals species vs. carbon number.**Table 3.11** Calculated Dipole Moment of Ether Secondary Radical Species

Molecules	Dipole moments (Debye)			
	PM6	# b3lyp/ 6-31g(d,p)	# b3lyp/ 6-311+g(d,p)	# bmk/ 6-31g(d,p)
coccjc	1.53	1.16	1.33	1.16
coccjcc	1.46	1.23	1.36	1.11
cocccjc	2.15	1.37	1.57	1.43

Note: j = radical site

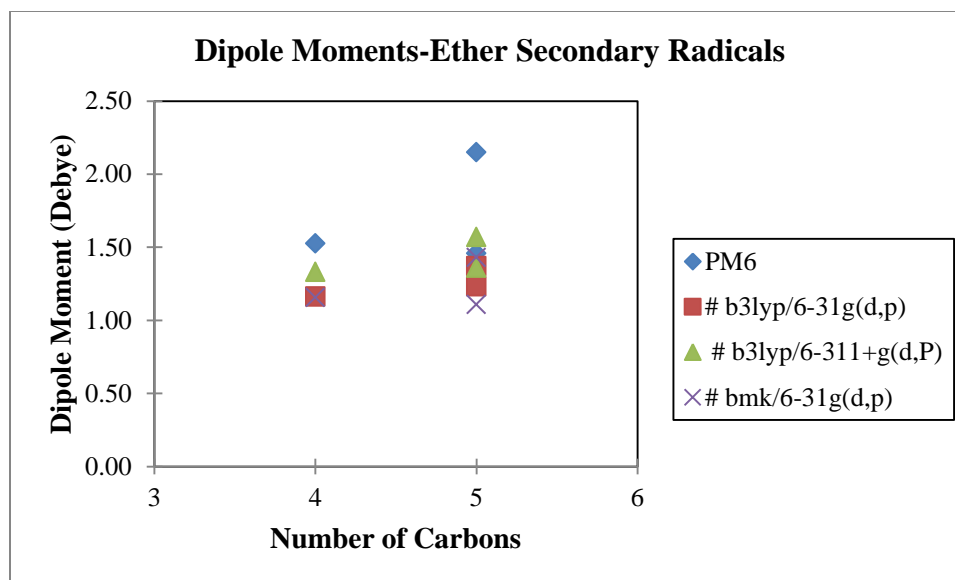


Figure 3.9 Dipole moment of ether secondary radicals species vs. carbon number.

Linear equations for dipole moment estimation of ethers and corresponding radicals in Table 3.12 are obtained from the B3LYP/6-31G(d,p) level of calculation. The comparison between available experimental dipole moments data⁴⁹ and calculation in this work as shown in Table 3.9. The ratio between reference experimental data to the calculation values is 0.99. This scaling factor is applied to the equation for estimated Ether and Ether radical species dipole moments calculation. Calculated dipole moments with scaling are within ± 0.1 Debye of experimental data.

Table 3.12 Equations to Estimate Dipole Moment for Ethers and Ethers Radicals

Species	Equations (N= carbon number)
Ether	Dipole = $(-2.52\text{E-}2 * N + 1.34) * 0.99$
Ether primary radicals	Dipole = $(-5.43\text{E-}2 * N + 1.45) * 0.99$
Ether secondary radicals	Dipole = $(1.39\text{E-}1 * N + 0.61) * 0.99$

3.2.4 Results Ketones

Tables 3.13, 3.14 and 3.15 show the dipole moment calculation values of target ketones and corresponding radical species of the C1 to C10 ketones. Figures illustrate the consistency with number of carbons and the trends versus number of carbons.

Table 3.13 Calculated Dipole Moment of Ketones with Comparison to Literature

Name	Molecules	Dipole moments (Debye)				Ref.
		PM6	# b3lyp/ 6-31g(d,p)	# b3lyp/ 6-311+g(d,p)	# bmk/ 6-31g(d,p)	
Acetone	cc*oc	3.43	2.75	3.08	2.84	2.88 ^{a,b}
butanone	cc*occ	3.48	2.70	2.99	2.77	2.78 ^a
2-heptanone	cc*occcccc	3.36	2.60	3.13	2.67	NA
2-decanone	cc*occcccccc	3.27	2.64	2.92	2.72	NA

Note: * = double bond, NA = Not Available, Source: ^a[49] , ^b[50]

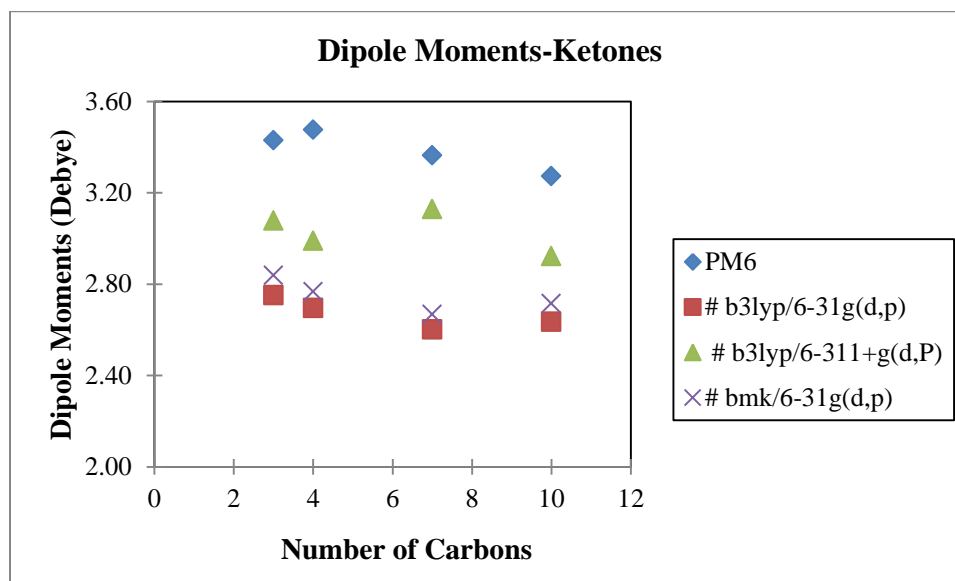
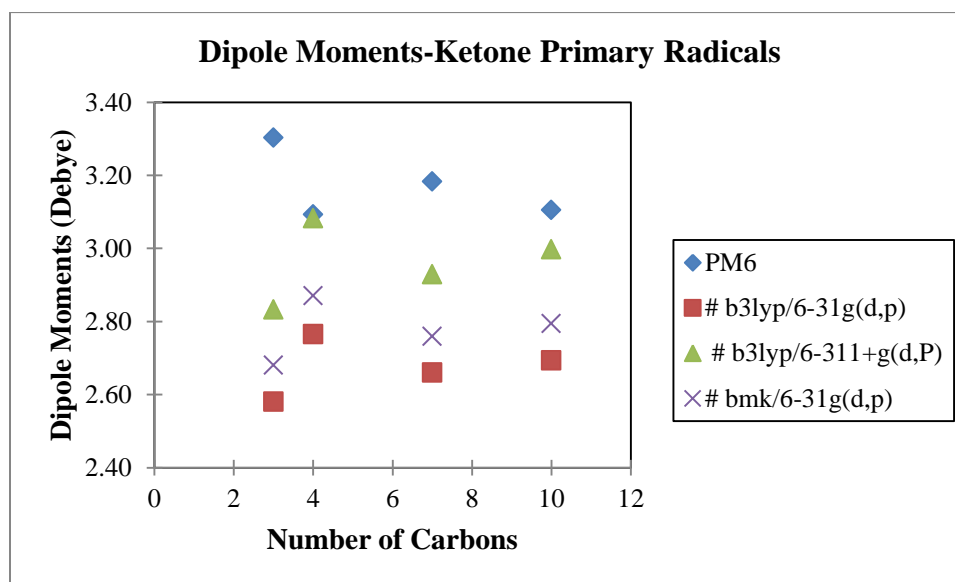


Figure 3.10 Dipole moment of ketone vs. carbon number.

Table 3.14 Calculated Dipole Moment of Ketone Primary Radical Species

Molecules	Dipole moments (Debye)			
	PM6	# b3lyp/ 6-31g(d,p)	# b3lyp/ 6-311+g(d,p)	# bmk/ 6-31g(d,p)
cjc*oc	3.30	2.58	2.83	2.68
cjc*occ	3.09	2.77	3.08	2.87
cjc*occccc	3.18	2.66	2.93	2.76
cjc*occcccccc	3.11	2.69	3.00	2.79

Note: * = double bond, j = radical site

**Figure 3.11** Dipole moment of ketone primary radical species vs. carbon number.**Table 3.15** Calculated Dipole Moment of Ketone Secondary Radical Species

Molecules	Dipole moments (Debye)			
	PM6	# b3lyp/ 6-31g(d,p)	# b3lyp/ 6-311+g(d,p)	# bmk/ 6-31g(d,p)
cc*ocjc	3.41	2.90	3.24	2.99
cc*occccjc	3.63	2.76	3.08	2.82
cc*ocjccccccc	3.55	2.90	3.14	2.96
cc*occcccccjc	2.90	2.48	2.68	2.57

Note: * = double bond, j = radical site

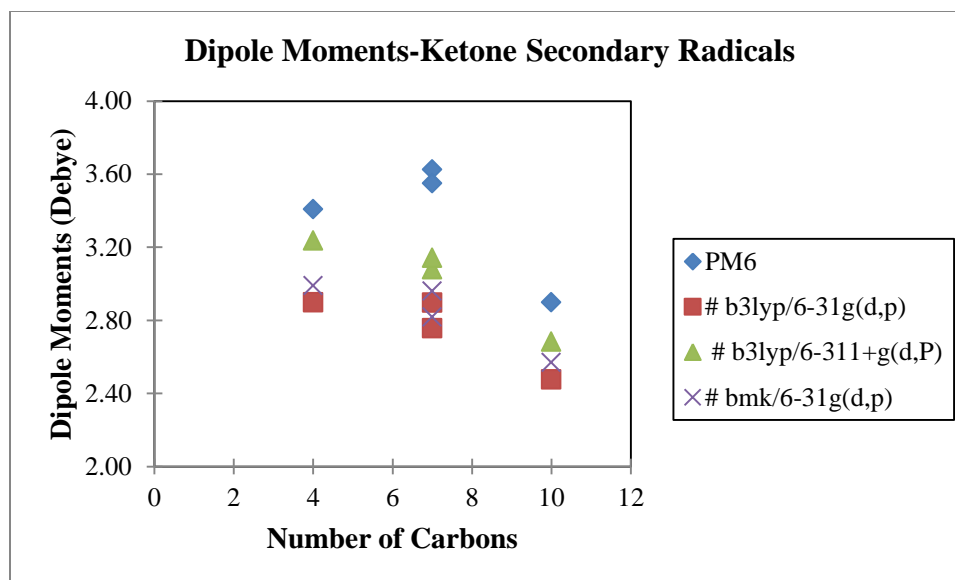


Figure 3.12 Dipole moment of ketone secondary radical species vs. carbon number.

Summary linear equations for estimating the dipole moments of the ketones and corresponding radical species in Table 3.16 are obtained from B3LYP/6-31G(d,p) level of calculation. The comparison between available experimental dipole moments data⁴⁹ and calculation in this work as shown in Table 3.13. The ratio between reference experimental data to the calculation values 1.04. This scaling factor is applied to the equation for estimated ketones and ketone radical species dipole moments calculation. Calculated dipole moments with scaling are within ± 0.1 Debye of ketone experimental data.

Table 3.16 Equations to Estimate Dipole Moment for Ketone and Ketones Radicals

Species	Equations (N = number of carbons)
Ketone	Dipole = $(-1.67\text{E-}2 \cdot N + 2.77) \cdot 1.04$
Ketone Primary Radicals	Dipole = $(5.4\text{E-}3 \cdot N + 2.64) \cdot 1.04$
Ketone Secondary Radicals	Dipole = $(-3.44\text{E-}2 \cdot N + 3.02) \cdot 1.04$

3.3 Polarizability

Polarizability, (α : alpha), is a constant of proportionality of induced dipole moment, μ^* , which is caused by applying electric field resulting in molecular distortion and alignment of its permanent electric dipole moment. The expression of induced dipole moment is as follows,

$$\mu^* = \alpha E \quad (3.15)$$

Where E is field strength. The greater the polarizability, the larger is the induced dipole moment for a given applied field. The unit of polarizability is $\text{C}^2\text{m}^2\text{J}^{-1}$. The expression of polarizability volume, α' , is introduced as follows,

$$\alpha' = \frac{\alpha}{4\pi\epsilon_0} \quad (3.16)$$

The ϵ_0 is the vacuum permittivity. Polarizability volumes are similar in magnitude to actual molecular volumes (of the order of 10^{-30} , 1 \AA^3). Polarizability volumes correlate with the HOMO-LUMO separations in atoms and molecules. Polarizability is large if LUMO lies close to the HOMO in energy so that electron distribution can be distorted readily, and it is low if LUMO lies high above the HOMO so that electron distribution cannot be perturbed significantly by an applied field⁵¹.

The DFT B3LYP/6-31g(d,p) computational chemistry method with the tight command is used to calculate the dipole electric field induced Polarizability of the alcohol, aldehyde, ether and ketone parent molecules, and carbon radicals corresponding to loss of hydrogen atom from the primary and secondary carbon sites and. The isotropic polarizability is reported in units of Bohr³ in the Gaussian 09 code, one Bohr is 0.529 Angstroms (\AA^0)⁴⁶⁻⁴⁸. Units reported in this study are in (\AA^0)³. Values reported as the isotropic polarizability α (\AA^0)³.

3.3.1 Results Alcohols

Tables 3.17, 3.18 and 3.19 show the polarizability calculation values of target molecule and corresponding radicals of the C1 to C10 alcohols in this study. Figures illustrate the consistency with number of carbons and the trends versus number of carbons.

Table 3.17 Calculated Polarizability for Alcohols with Comparison to Literature

Name	Molecules	Polarizability (\AA^3)					
		PM6	# b3lyp/ 6-31g(d,p)	# b3lyp/ 6-311+g(d,p)	# bmk/ 6-31g(d,p)	Joback	Ref.
methanol	coh	3.25	2.37	2.77	2.35	2.60	3.08 ^a 3.26 ^b 3.20 ^c 3.23 ^d
ethanol	ccoh	5.04	3.91	4.54	3.91	4.40	5.11 ^a 5.07 ^b 4.94 ^c
1-propanol	cccoh	8.64	7.11	8.10	7.13	6.20	NA
1-pentanol	cccccch	10.51	8.76	9.91	8.78	9.8	NA
1-heptanol	cccccccch	14.14	12.04	13.54	12.08	13.40	NA
1-decanol	ccccccccch	19.66	17.02	19.04	17.18	18.80	NA

Note: NA = Not Available, Source: ^a[49], ^b[52], ^c[53], ^d[54]

Table 3.18 Calculated Polarizability for Alcohol Primary Radical Species

Molecules	Polarizability (\AA^3)			
	PM6	# b3lyp/ 6-31g(d,p)	# b3lyp/ 6-311+g(d,p)	# bmk/ 6-31g(d,p)
cjoh	3.36	2.07	2.71	2.04
cjcoh	5.92	3.67	4.51	3.63
cjccoh	6.98	5.25	6.30	5.22
cjccccch	10.72	8.43	9.79	8.45
cjcccccccch	14.38	11.71	13.42	11.78
cjccccccccch	19.88	16.70	18.92	16.83

Note: j = radical site

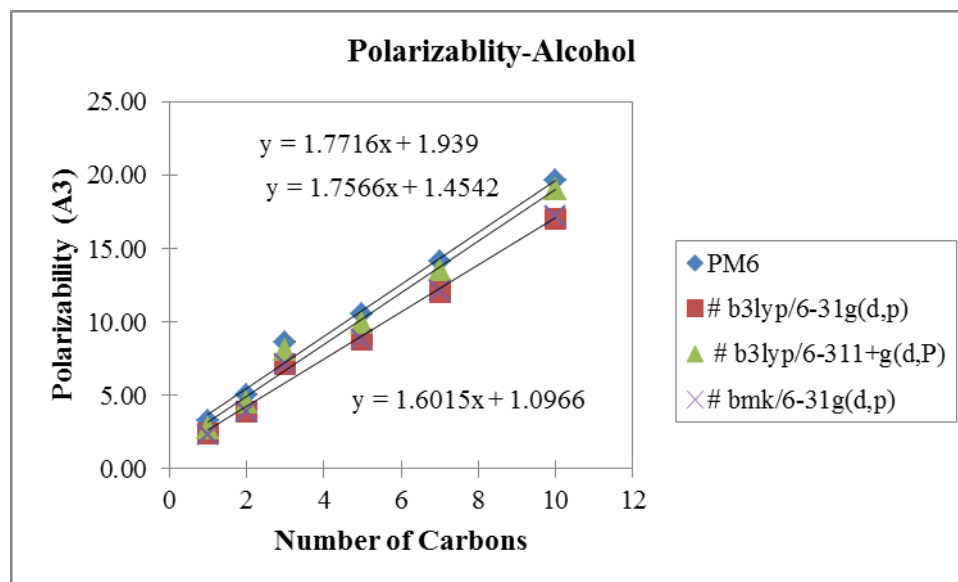


Figure 3.13 Polarizability of alcohols vs. carbon number.

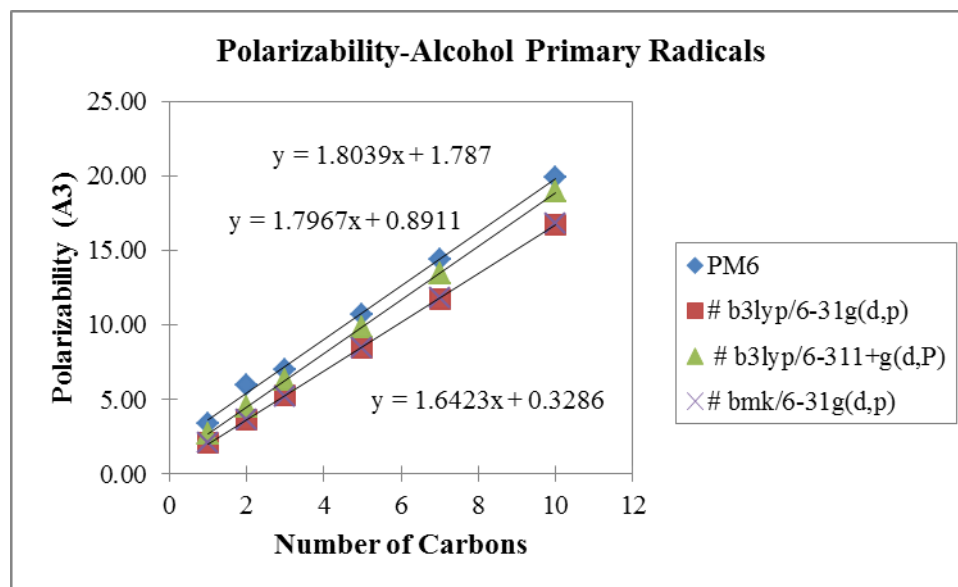
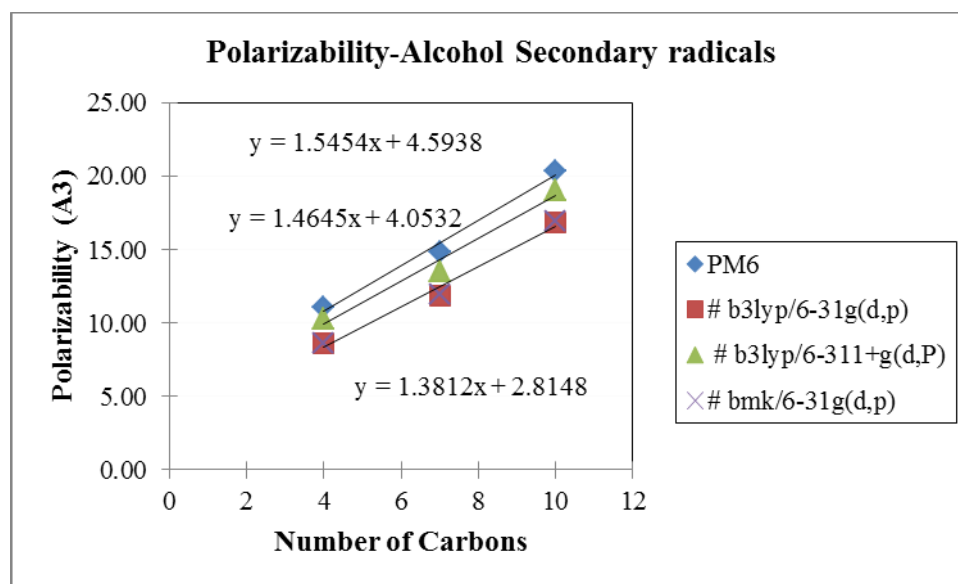


Figure 3.14 Polarizability of alcohol primary radical species vs. carbon number.

Table 3.19 Calculated Polarizability for Alcohol Secondary Radical Species

Molecules	Polarizability (\AA^3)			
	PM6	# b3lyp/ 6-31g(d,p)	# b3lyp/ 6-311+g(d,p)	# bmk/ 6-31g(d,p)
ccjccoh	11.08	8.66	10.29	8.63
ccccjccoh	14.80	11.89	13.56	11.91
cccccjcccooh	20.35	16.88	19.07	16.91

Note: j = radical site

**Figure 3.15** Polarizability of alcohol secondary radical species vs. carbon number.

Linear equations for estimation of Polarizability (α) vs carbon number are listed in Table 3.20. They are obtained from PM6 calculations which show the best agreement with the reference experimental data when compared to the other calculation results from DFT method. PM6 result calculation is almost identical to the reference data from experiment.

Table 3.20 Equations to Estimate Polarizability for Alcohol and Alcohol Radicals

Species	Equations (N= carbon number)
Alcohol	$\alpha = 1.77*N + 1.94$
Alcohol Primary Radicals	$\alpha = 1.80*N + 1.79$
Alcohol Secondary Radicals	$\alpha = 1.55*N + 4.59$

3.3.2 Results Aldehydes

Tables 3.21, 3.22, 3.23 and 3.24 are presented polarizability calculation values for aldehydes and corresponding aldehydes radical, respectively.

Table 3.21 Calculated Polarizability for Aldehydes with Comparison to Literature

Name	Molecules	Polarizability (\AA^3)					
		PM6	# b3lyp ^a	# b3lyp ^b	# bmk ^a	Joback	Ref.
Formaldehyde	c*o	2.69	1.96	2.29	1.95	2.60	2.77 ^c 2.45 ^d
acetaldehyde	cc*o	4.58	3.56	4.20	3.55	4.40	4.28 ^c 4.59 ^d
propanal	ccc*o	6.42	5.13	5.93	5.09	6.20	NA
pentanal	ccccc*o	10.04	8.32	9.46	8.32	9.80	NA
heptanal	cccccc*o	13.69	11.59	13.09	11.60	13.40	NA

Note: * = double bond, NA = Not Available, ^a = 6-31g(d,p), ^b = 6-311+g(d,p), Source: ^c[49], ^d[55]

Table 3.22 Calculated Polarizability for Aldehydes Primary Radicals Species

Molecules	Polarizability (\AA^3)			
	PM6	# b3lyp/ 6-31g(d,p)	# b3lyp/ 6-311+g(d,p)	# bmk/ 6-31g(d,p)
cj*o	2.53	1.78	2.20	1.77
cjc*o	-	3.39	4.13	3.35
cjcc*o	6.55	5.03	6.05	4.94
cjcccc*o	10.24	8.02	9.39	7.99
cjcccccc*o	13.89	11.38	13.12	11.35

Note: * = double bond, j = radical site

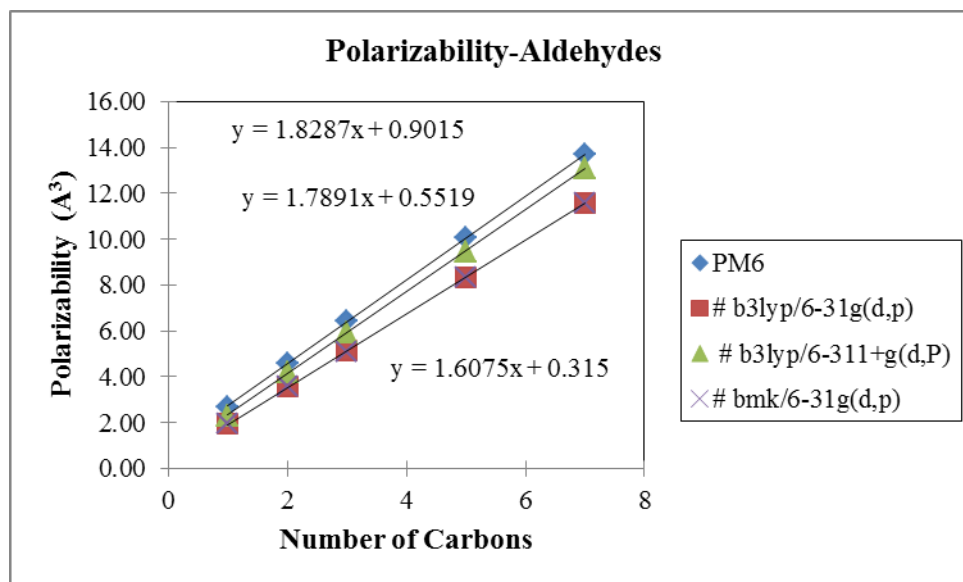


Figure 3.16 Polarizability of aldehydes vs. carbon number.

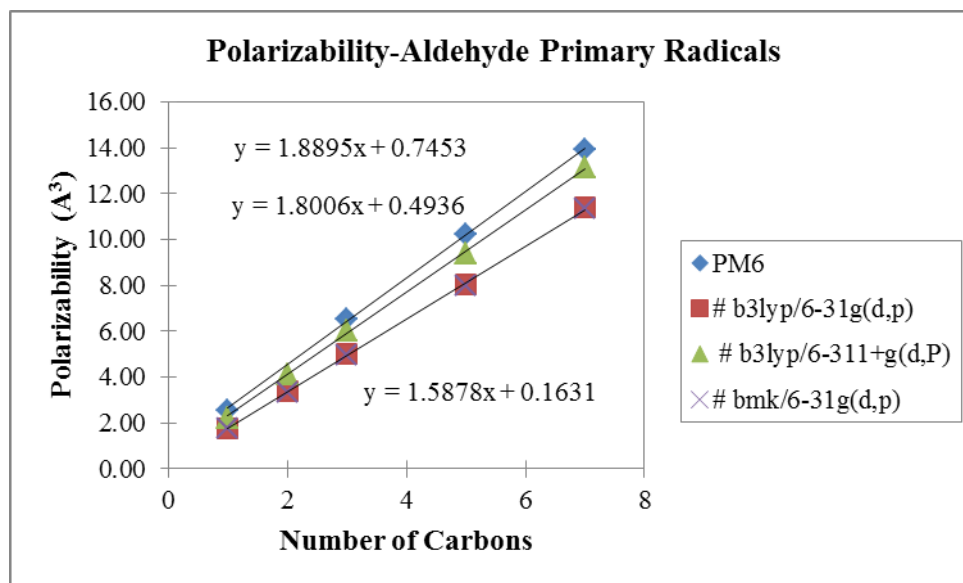
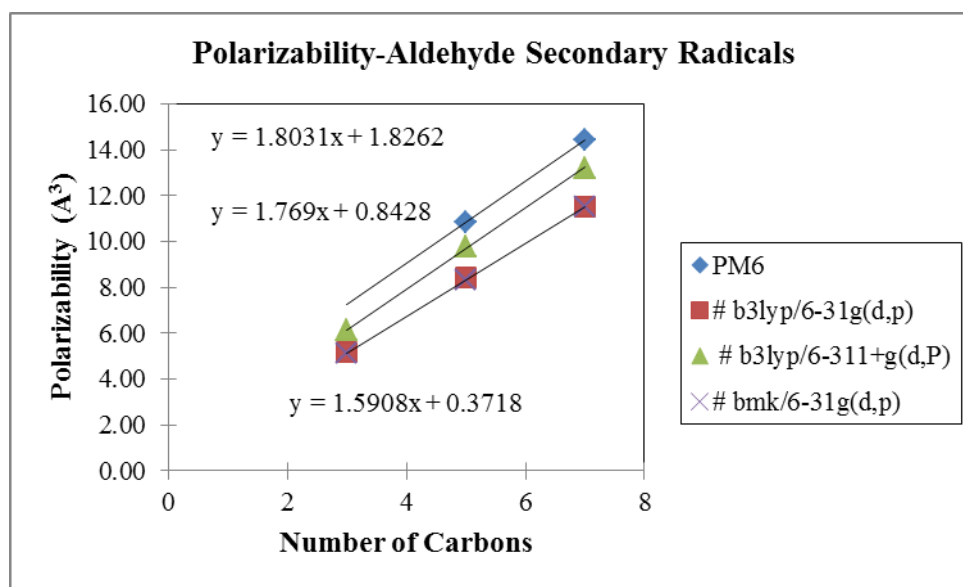


Figure 3.17 Polarizability of aldehydes primary radicals species vs. carbon number.

Table 3.23 Calculated Polarizability of Aldehydes Secondary Radicals Species

Molecules	Polarizability (\AA^3)			
	PM6	# b3lyp/ 6-31g(d,p)	# b3lyp/ 6-311+g(d,p)	# bmk/ 6-31g(d,p)
ccjc*o	-	5.20	6.11	5.15
cccjcc*o	10.84	8.44	9.77	8.31
ccccjccc*o	14.45	11.52	13.19	11.51

Note: * = double bond, j = radical site

**Figure 3.18** Polarizability of aldehydes secondary radicals species vs. carbon number.

The comparison between the calculated polarizability of Aldehyde and corresponding radical species in this work and the experimental data is presented in Table 3.21. Summary linear equations in carbon number for estimation of Aldehyde group Polarizability (α) in \AA^3 is in table 3.24 obtained from PM6 calculation which values are closest to the experimental data.

Table 3.24 Equations to Estimated Polarizability of Aldehydes and Aldehydes Radicals

Species	Equations (N= carbon number)
Aldehyde	$\alpha = 1.83 \cdot N + 0.90$
Aldehyde Primary Radicals	$\alpha = 1.89 \cdot N + 0.75$
Aldehyde Secondary Radicals	$\alpha = 1.80 \cdot N + 1083$

3.3.3 Results Ethers

Tables 3.25, 3.26, 3.27 and 3.28 list the polarizability calculated values for ethers and corresponding ethers radical, respectively.

Table 3.25 Calculated Polarizability for Ethers Group with Comparison to Literature

Name	Molecules	Polarizability (\AA^3)					
		PM6	# b3lyp/ 6-31g(d,p)	# b3lyp/ 6-311+g(d,p)	# bmk/ 6-31g(d,p)	Joback	Ref.
dimethyl ether	coc	5.16	4.00	4.60	3.99	5.20	5.16 ^a
ethyl methyl ether	cocc	6.98	5.56	6.36	5.54	7.00	NA
methyl propyl ether	coccc	8.78	7.10	8.11	7.10	8.80	8.86 ^b 8.64 ^c
diethyl ether	ccocc	8.83	7.22	8.21	7.20	8.80	8.73 ^d
buthyl methyl ether	cocccc	10.58	8.71	9.90	8.71	10.6	NA

Note: NA = Not Available, Source: ^a[49], ^b[52], ^c[53], ^d[54]

Table 3.26 Calculated Polarizability for Ethers Primary Radicals Species

Molecules	Polarizability (\AA^3)			
	PM6	# b3lyp/ 6-31g(d,p)	# b3lyp/ 6-311+g(d,p)	# bmk/ 6-31g(d,p)
cocj	5.42	4.00	4.66	3.72
coccj	-	5.27	6.23	5.23
cocccj	8.92	6.81	8.04	6.77
ccoccj	-	6.94	8.10	6.89
coccccj	10.85	8.41	9.83	8.39

Note: j = radical site

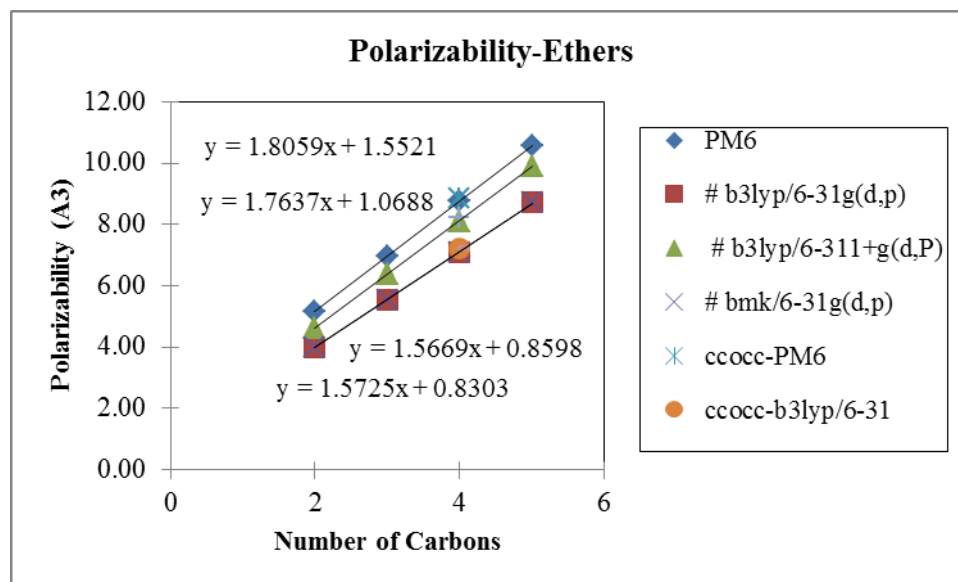


Figure 3.19 Polarizability of ethers vs. carbon number.

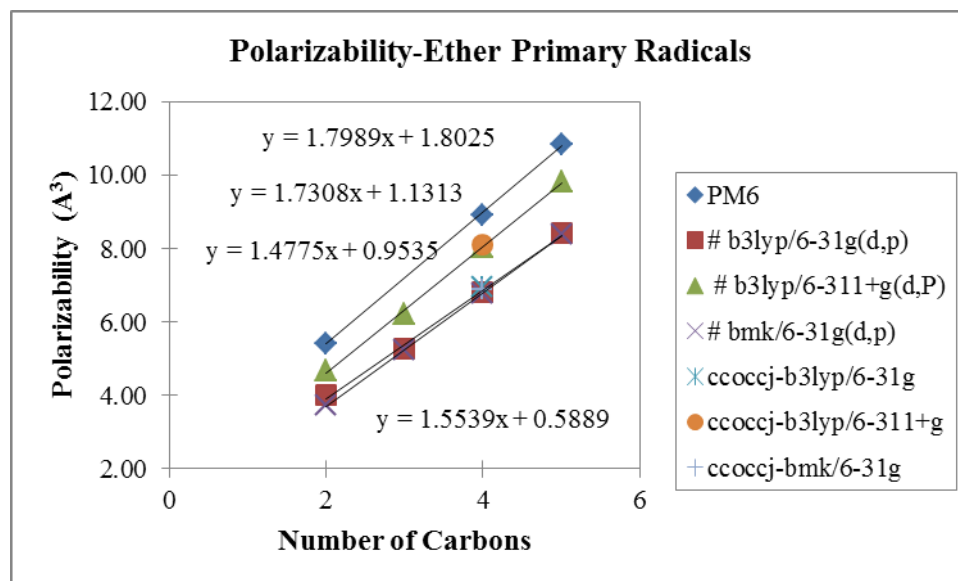


Figure 3.20 Polarizability of ethers primary radicals species vs. carbon number.

Table 3.27 Calculated Polarizability for Ethers Secondary Radicals Species

Molecules	Polarizability (\AA^3)			
	PM6	# b3lyp/ 6-31g(d,p)	# b3lyp/ 6-311+g(d,p)	# bmk/ 6-31g(d,p)
cocccjc	9.54	6.92	8.07	6.89
cocccjcc	12.80	8.52	9.91	8.52
cocccjc	11.01	8.55	9.91	8.51

Note: J = radical site

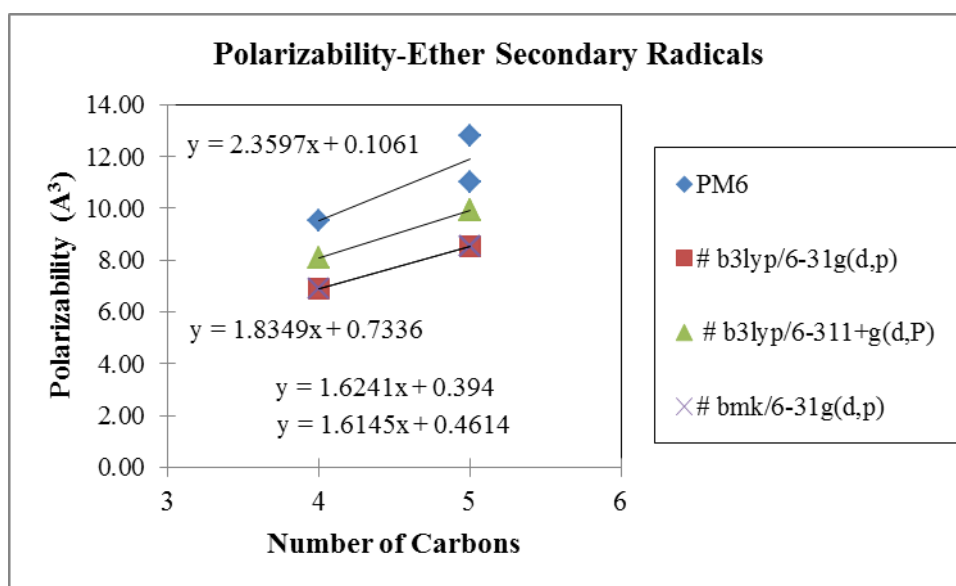
**Figure 3.21** Polarizability of ethers secondary radicals species vs. carbon number.

Table 3.28 is presents a summary linear equations for estimation of polarizability of the ethers and corresponding radicals obtained from PM6 method calculations. The comparison between available experimental data and calculation in this work is in Table 3.25 and shows good agreement between experimental data and the calculation values from PM6.

Table 3.28 Equations to Estimate Polarizability of Ethers and Ethers Radicals

Species	Equations (N= carbon number)
Ether	$\alpha = 1.81 * N + 1.55$
Ether primary radicals	$\alpha = 1.80 * N + 1.80$
Ether secondary radicals	$\alpha = 2.36 * N + 0.11$

3.3.4 Results Ketones

Tables 3.29, 3.30, 3.31 and 3.32 present the polarizability calculation values for Ketone and corresponding ketone radicals.

Table 3.29 Calculated Polarizability for Ketones with Comparison to Literature

Name	Molecules	Polarizability (\AA^3)					
		PM6	# b3lyp ^a	# b3lyp ^b	# bmk ^a	Joback	Ref.
Acetone	cc*oc	6.39	5.06	5.95	5.08	6.20	6.1 ^c 6.40 ^d 6.33 ^e 6.39 ^f
Butanone	cc*occ	8.22	6.63	7.64	6.66	8.00	8.19 ^c 8.13 ^e
2-heptanone	cc*occcccc	13.69	11.52	13.13	11.59	13.40	NA
2-decanone	cc*occcccccc	19.17	16.49	18.55	16.61	18.80	NA

Note: NA = Not Available, ^a = 6-31g(d,p), ^b = 6-311+g(d,p), Source: ^c[49], ^d[52], ^e[54], ^f[55]

Table 3.30 Calculated Polarizability for Ketone Primary Radicals Species

Molecules	Polarizability (\AA^3)		
	# b3lyp/6-31g(d,p)	# b3lyp/6-311+g(d,P)	# bmk/6-31g(d,p)
cjc*oc	4.80	5.81	4.75
cjc*occ	6.48	7.58	6.47
cjc*occcccc	11.39	13.02	11.43
cjc*occcccccc	16.37	18.52	16.48

Note: * = double bond, j = radical site

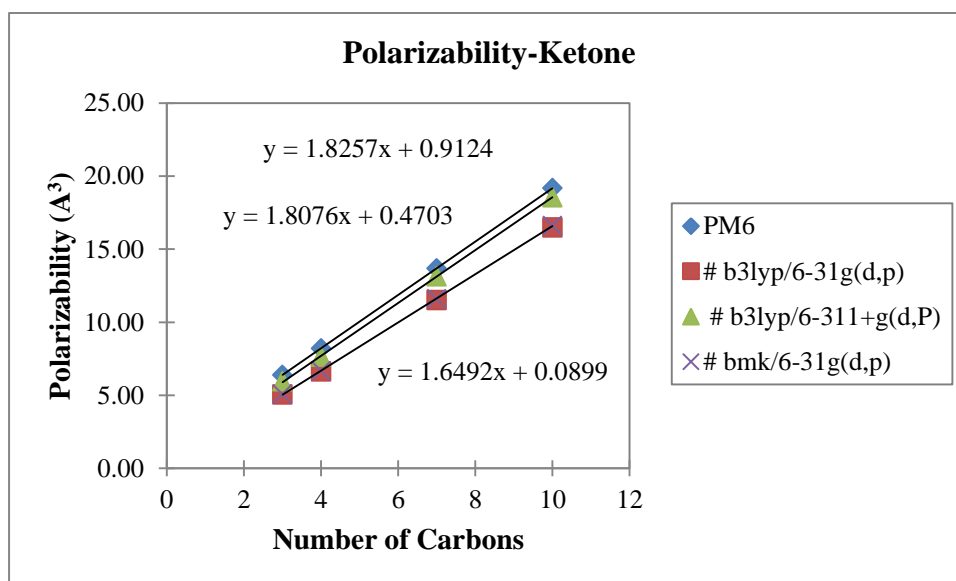


Figure 3.22 Polarizability of ketones vs. carbon number.

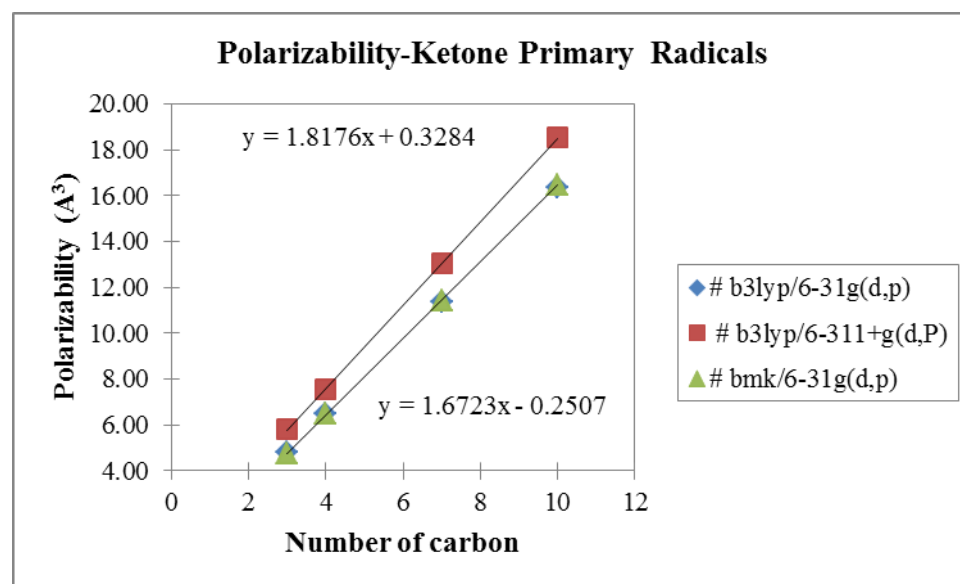


Figure 3.23 Polarizability of ketone primary radicals species vs. carbon number.

Table 3.31 Calculated Polarizability for Ketone Secondary Radicals Species

Molecules	Polarizability (\AA^3)		
	# b3lyp/6-31g(d,p)	# b3lyp/6-311+g(d,p)	# bmk/6-31g(d,p)
cc*ocjc	6.65	7.76	6.65
cc*ocjccc	11.73	13.43	11.61
cc*occcccjc	11.35	13.04	11.38
cc*ocjccccccc	16.77	19.03	16.76
cc*occcccccjc	16.32	18.55	16.41

Note: * = double bond, j = radical site

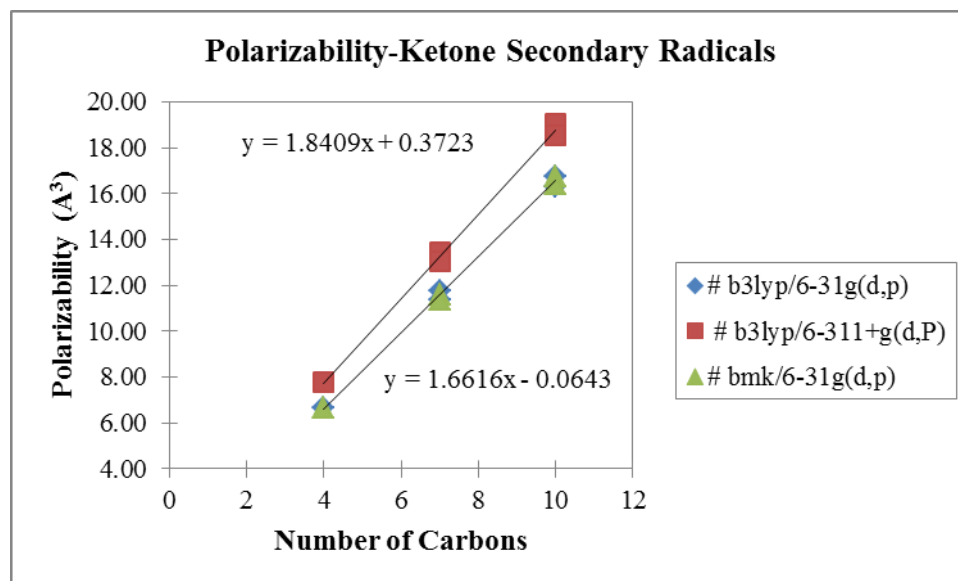
**Figure 3.24** Polarizability of ketone secondary radicals species vs. carbon number.

Table 3.2 is show the comparison between experimental data and the calculation values in this study. The results from the PM6 calculation method show the best agreement with experimental data. Unfortunately, PM6 unable performed the polarizability calculation for the Ketone primary and secondary radical species. Therefore, the linear equation in Table 3.32 for Ketone stable molecules are obtained from PM6 calculation, and the Ketone primary and secondary radical species are obtain

the linear equation from B3LYP/6-311+G(d,p) level of calculation that has result close to the PM6 calculation. The scaling factor 1.05 from ratio between the reference data and B3LYP/6-311+G(d,p) values is applied to the linear equation in Table 3.32.

Table 3.32 Equations to Estimate Polarizability for Ketones and Ketones Radicals

Species	Equations (N= carbon number)
Ketone	$\alpha = 1.83*N + 0.91$
Ketone Primary Radicals	$\alpha = (1.82*N + 0.33) * 1.05$
Ketone Secondary Radicals	$\alpha = (1.84*N + 0.37) * 1.05$

3.4 Lennard Jones Diameters (σ)

The data presented in this section are molecular diameters that are calculated from molecular volumes. In continuing work we will validate the relationship between molecular diameter and Lennard Jones Diameter as a function of class of molecule. In this study we utilized the “Volume” command in Mopac 2009 to calculate molar volumes. In comparisons of methods for calculations of volumes with literature data we observed that the Mopac2009 calculation data was closer to literature than the Density functional (B3LYP) calculations. From the volume, we calculated a dvol (molecular diameter computed from the volume) which has been shown to be closely related to the Lennard-Jones collision parameter σ_0 . the Mopac PM6 method is used for volumes and found to be more consistent than the calculated volumes from Gaussian Code calculations of volume at the B3LYP/6-311+ level, where standard deviations were on the order of 30%.

3.4.1 Results Alcohols

Tables 3.33, 3.34, 3.35 and 3.36 present the Lennard Jones diameters calculation values for Alcohols and corresponding alcohol radicals with comparison to literature.

Table 3.33 Calculated L. J. Diameters for Alcohols with Comparison to Literature

Name	Molecules	L J diameter (A/mol)		
		PM6	Joback	Ref.
methanol	coh	4.51	3.88	3.63 ^a 3.80 ^b 3.66 ^c 3.48 ^d
ethanol	ccoh	5.10	4.45	4.53 ^a 4.37 ^b 4.32 ^c
1-propanol	cccoh	5.99	4.90	4.82 ^b
1-pentanol	cccccch	6.36	5.61	NA
1-heptanol	cccccccch	6.99	6.18	NA
1-decanol	ccccccccch	7.76	6.88	NA

Note: NA = Not Available, Source: ^a[56], ^b[57], ^c[58], ^d[59]

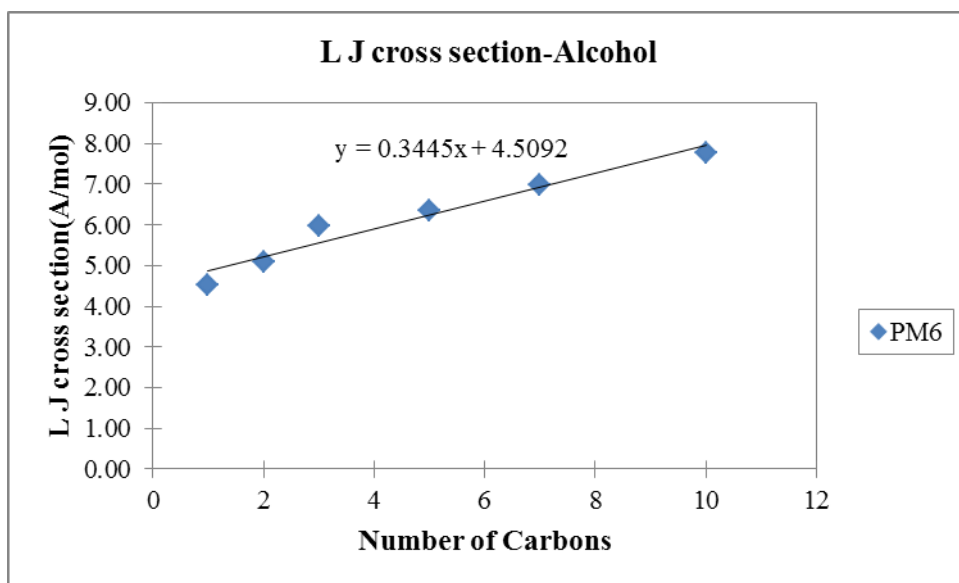
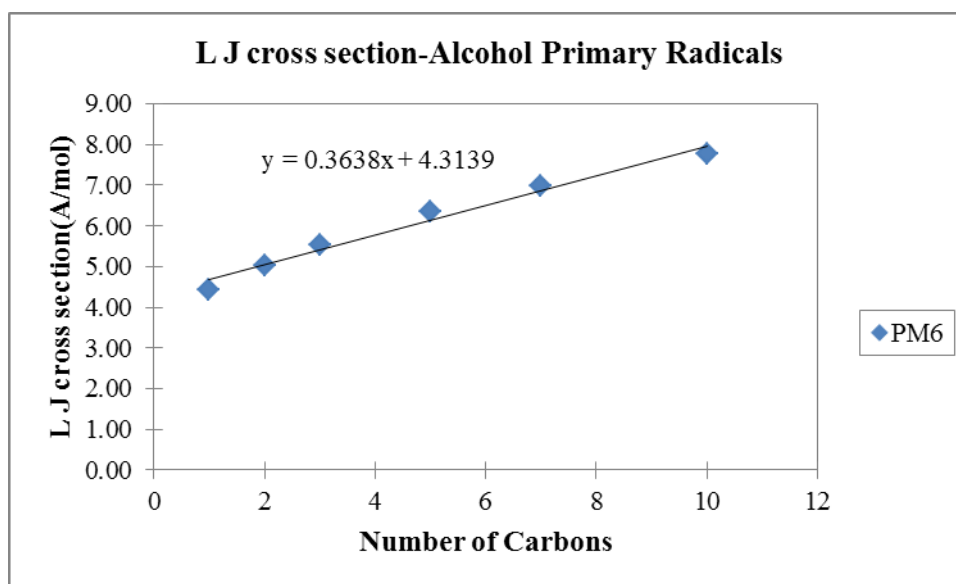


Figure 3.25 L J diameters for alcohols vs. carbon number.

Table 3.34 Calculated L J Diameters for Alcohol Primary Radicals Species

Molecules	L J diameter (A/mol)
cjoh	4.43
cjcoh	5.03
cjccoh	5.54
cjcccooh	6.34
cjcccccooh	6.97
cjcccccccooh	7.76

Note: j = radical site

**Figure 3.26** L J diameters for alcohol primary radicals vs. carbon number.**Table 3.35** Calculated L J Diameters for Alcohol Secondary Radicals Species

Molecules	L J diameter (A/mol)
ccjccoh	6.32
ccccjcccooh	6.94
cccccjcccccooh	7.73
ccccccccccjoh	7.72

Note: j = radical site

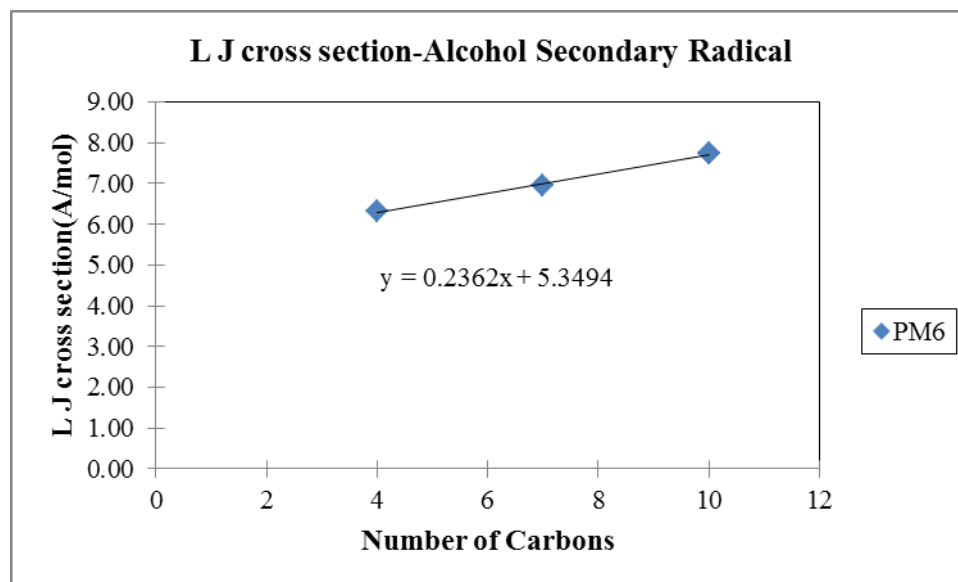


Figure 3.27 L J diameters for alcohol secondary radicals vs. carbon number.

Linear equations in carbon number for estimation of L. J. diameters (σ) in A/mol for Alcohol and corresponding radical species are obtained from MOPAC2009 (PM6). The average ratio of the experiential data (Svehla, 1962⁵⁶) to the the calculation values in this work is 0.85. This scaling factor is applied to correct the estimated linear equation in Table 3.36.

Table 3.36 Equations to Estimate L. J Diameters for Alcohols and Alcohols Radicals

Species	Equations (N= carbon number)
Alcohol	L J diameter = $(3.45\text{E-}1 \cdot N + 4.51) \cdot 0.85$
Alcohol Primary Radicals	L J diameter = $(3.64\text{E-}1 \cdot N + 4.31) \cdot 0.85$
Alcohol Secondary Radicals	L J diameter = $(3.29\text{E-}1 \cdot n + 4.53) \cdot 0.85$

3.4.2 Results Aldehydes

Lennard Jones diameters calculation values for Aldehyde and corresponding Aldehyde radicalspecies are shown in Tables 3.37, 3.38, 3.39 and 3.40, respectively with comparison with literature values.

Table 3.37 Calculated L. J. Diameters for Aldehydes with Comparison to Literature

Name	Molecules	L J diameter (A/mol)		
		PM6	Joback	Ref.
Formaldehyde	c*o	4.33	3.75	3.35 ^a
acetaldehyde	cc*o	4.94	4.43	4.86 ^b
propanal	ccc*o	5.46	4.89	NA
pentanal	ccccc*o	6.26	5.60	NA
heptanal	cccccc*o	6.91	6.17	NA

Note: * = double bond , Source: ^a[59] , ^b[43]

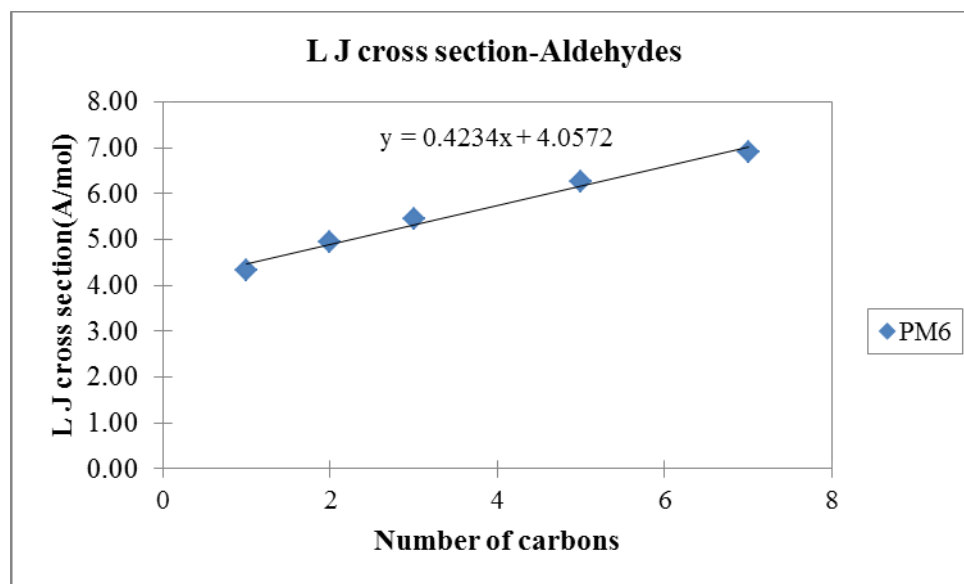
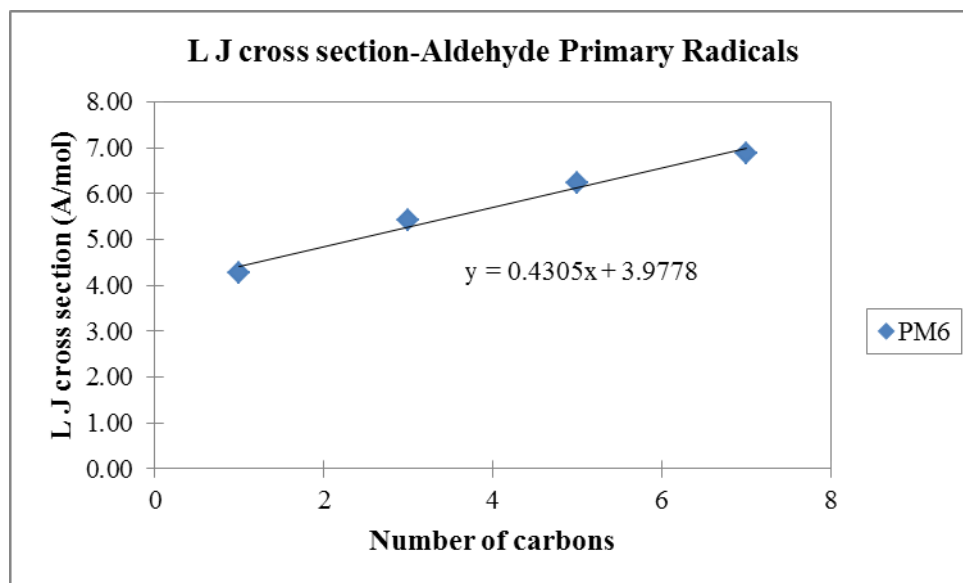


Figure 3.28 L J diameters for aldehydes vs. carbon number.

Table 3.38 Calculated L. J. Diameters for Aldehyde Primary Radicals Species

Molecules	L J diameter (A/mol)
cj*o	4.28
cjcc*o	5.41
cjcccc*o	6.23
cjcccccc*o	6.88

Note: * = double bond, j = radical site

**Figure 3.29** L. J. diameters for aldehyde primary radicals vs. carbon number.**Table 3.39** Calculated L J Diameters for Aldehyde Secondary Radicals Species

Molecules	L J diameter (A/mol)
ccjc*o	5.4
cccjcc*o	6.19
ccccjccc*o	6.87

Note: * = double bond, j = radical site

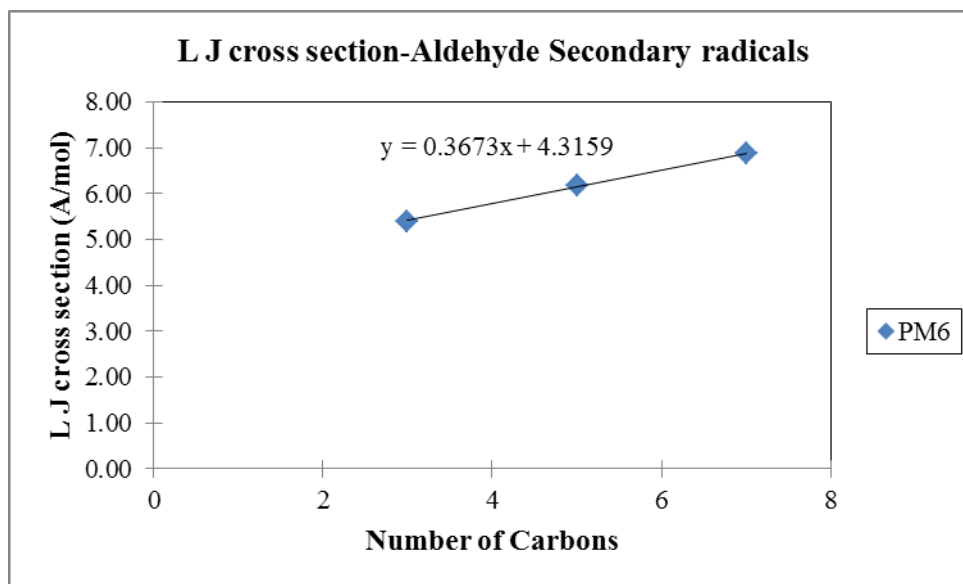


Figure 3.30 L. J. diameters for aldehyde secondary radical vs. carbon number.

Lennard Jones parameter reference data are presented in Table 3.37. They show lower values compared to values from volume calculations in this study. The average ratio of reference data to this study is 0.88. This scaling factor is used in the linear equation for estimation Lennard Jones parameters of Aldehydes and corresponding radicals.

Table 3.40 Equations to Estimate L. J. Diameters for Aldehydes and Aldehydes Radicals

Species	Equations (N= carbon number)
Aldehyde	L J diameter= $(4.23\text{E-}1 \cdot \text{N} + 4.06) \cdot 0.88$
Aldehyde Primary Radicals	L J diameter= $(4.31\text{E-}1 \cdot \text{N} + 3.98) \cdot 0.88$
Aldehyde Secondary Radicals	L J diameter= $(3.67\text{E-}1 \cdot \text{N} + 4.32) \cdot 0.88$

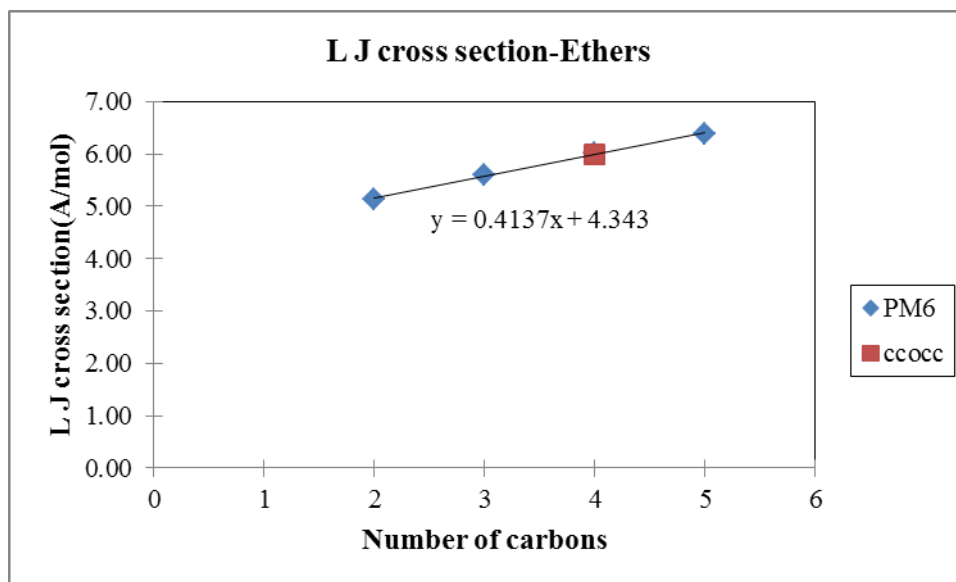
3.4.3 Results Ethers

Lennard Jones Diameters calculation values for Ether and corresponding Ether radicals along with literature values are presented in Tables 3.41, 3.42, 3.43 and 3.44, respectively.

Table 3.41 Calculated L J Diameters for Ether group with Comparison to Literature

Name	Molecules	L J diameter (A/mol)		
		PM6	Joback	Ref.
dimethyl ether	coc	5.15	4.44	4.31 ^a 4.23 ^b 4.75 ^c
ethyl methyl ether	cocc	5.61	4.89	NA
diethyl ether	coccc	6.02	5.27	NA
methyl propyl ether	cocccc	6.39	5.61	NA
buthyl methyl ether	ccocc	6.00	5.27	5.68 ^a 5.55 ^b

Note: NA = Not Available, Source: ^a[56], ^b[58], ^c[43]

**Figure 3.31** L J diameters for ethers vs. carbon number.

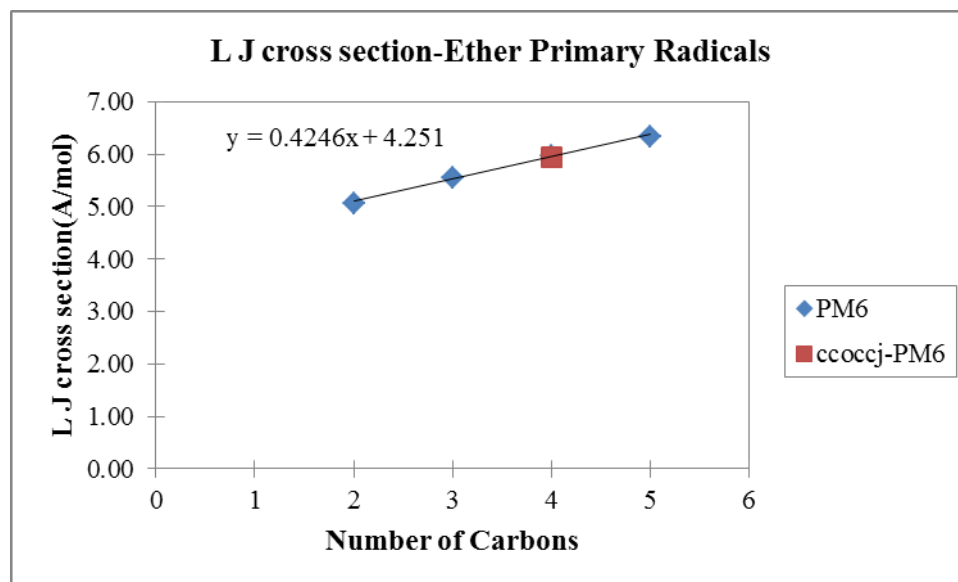


Figure 3.32 L J diameters for ether primary radicals vs. carbon number.

Table 3.42 Calculated L. J. Diameters for Ether Primary Radicals Species

Molecules	L J diameter (A/mol)
cocj	5.07
coccj	5.56
cocccj	5.95
ccoccj	5.98
coccccj	6.34

Note: j = radical site

Table 3.43 Calculated L. J. Diameters for Ether Secondary Radicals Species

Molecules	L J diameter (A/mol)
cocjcc	5.93
coccjc	5.94
cocccjc	6.32

Note: j = radical site

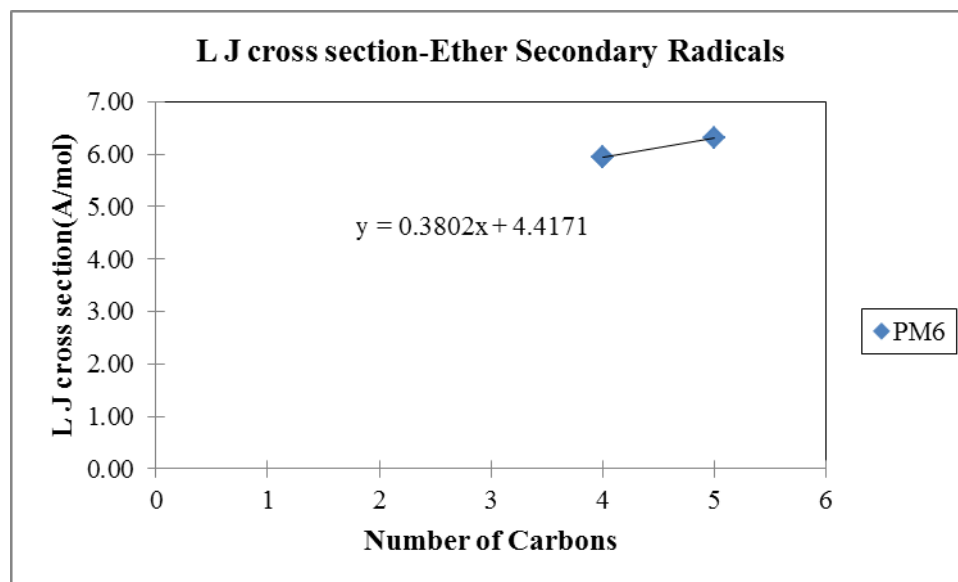


Figure 3.33 L J diameters for ether secondary radicals vs. carbon number.

Table 3.41 shows a comparison of values from PM6 calculation to literature data⁵⁶. The PM6 calculation values over estimate the diameters, they show a factor 0.89 for the ratio of the experimental to PM6 calculation. The recommended values for Lennard Jones diameters of Ethers and corresponding radicals in the reported equations are corrected by this factor.

Table 3.44 Equations to Estimate L. J. Diameters for Ethers and Ethers Radicals

Species	Equations (N= carbon number)
Ether	L J diameter = $(0.41 \cdot N + 4.34) \cdot 0.89$
Ether primary radicals	L J diameter = $(0.42 \cdot N + 4.25) \cdot 0.89$
Ether secondary radicals	L J diameter = $(0.38 \cdot N + 4.42) \cdot 0.89$

3.4.4 Results Ketones

Tables 3.45, 3.46, 3.47 and 3.48 present Lennard Jones Diameters calculation values for Ketone and corresponding Ketone radicals, respectively.

Table 3.45 Calculated L. J. Diameters for Ketones with Comparison to Literature

Name	Molecules	L J crosssection (A/mol)		
		PM6	Joback	Ref.
acetone	cc*oc	5.44	4.80	4.60 ^{a,b} 4.76 ^c
butanone	cc*occ	5.89	5.20	NA
2-heptanone	cc*occcccc	6.90	6.12	NA
2-decanone	cc*occcccccc	7.69	6.83	NA

Note: * = double bond, Source: ^a[56], ^b[58], ^c[56]

Table 3.46 Calculated L J Diameters for Ketone Primary Radicals Species

Molecules	L J diameter (A/mol)
cjc*oc	5.39
cjc*occ	5.82
cjc*occcccc	6.86
cjc*occcccccc	7.66

Note: * = double bond, j = radical site

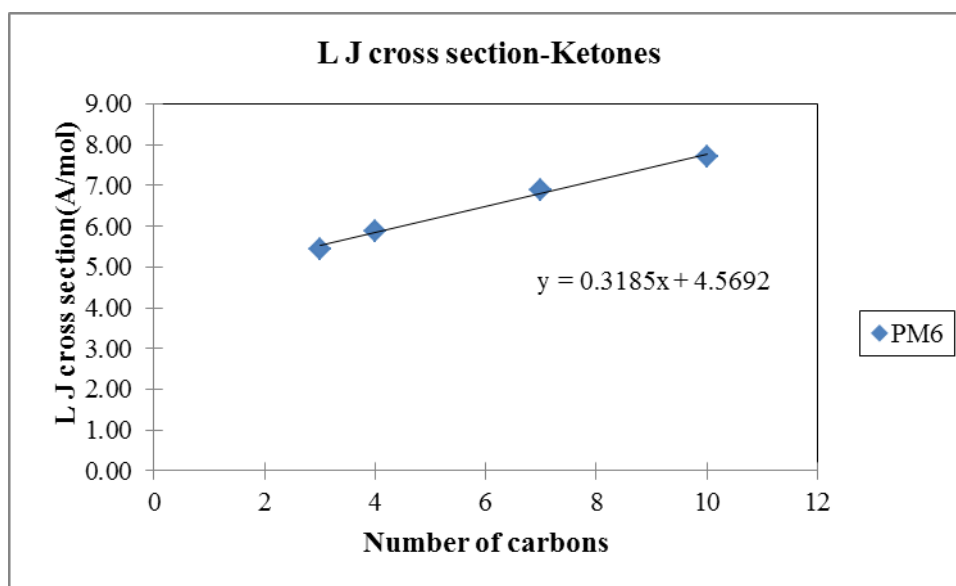


Figure 3.34 L J diameters for Ketones vs. carbon number.

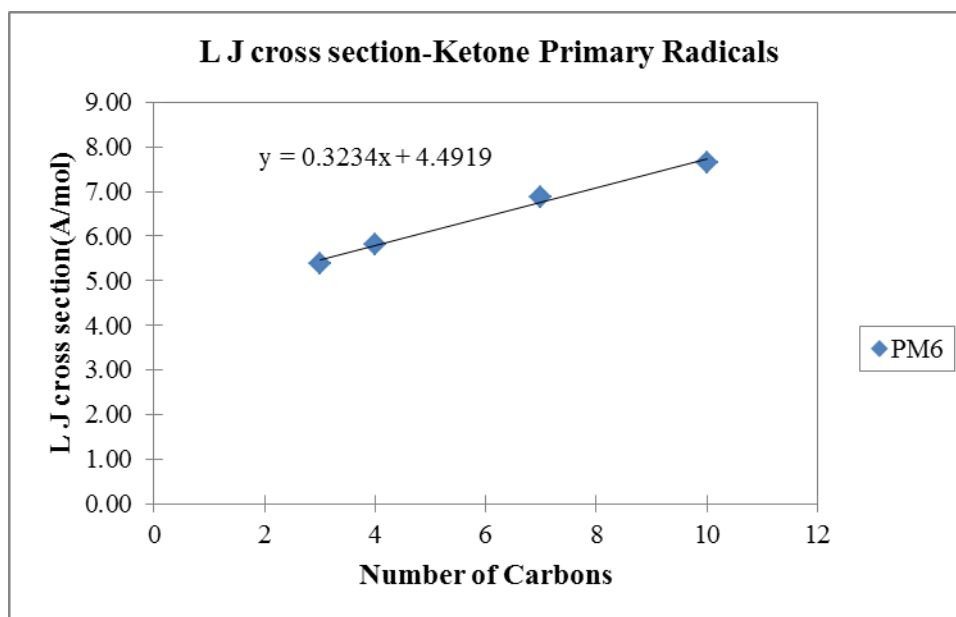


Figure 3.35 L J diameters for ketone primary radicals vs. carbon number.

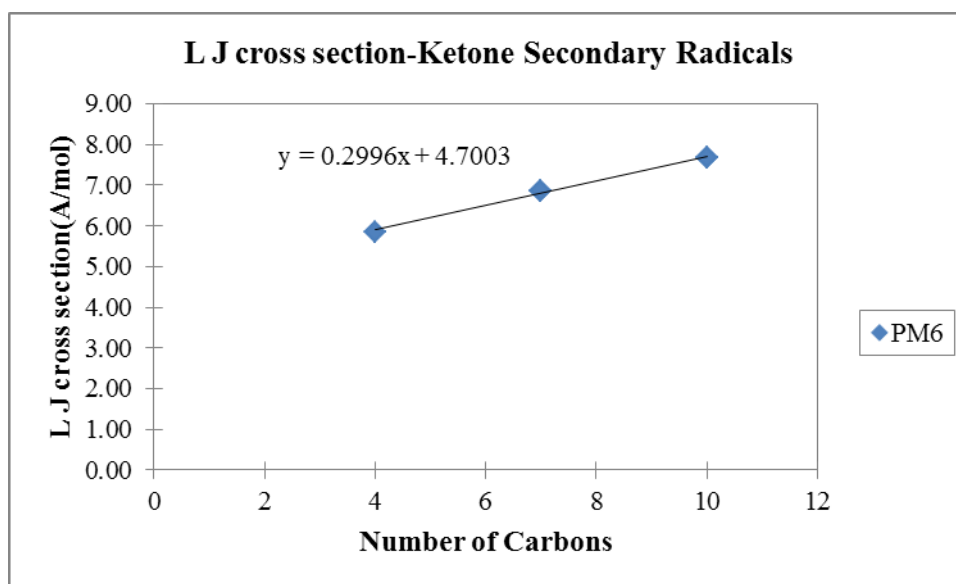


Figure 3.36 L J diameters for ketone secondary radicals vs. carbon number.

Table 3.47 Calculated L. J. Diameters for Ketone Secondary Radicals

Molecules	L J diameter (A/mol)
cc*ocjc	5.83
cc*ocjccc	6.86
cc*occccccjc	6.87
cc*ocjccccccc	7.66
cc*occccccccjc	7.66

Note: * = double bond, j = radical site

Table 3.48 Equations to Estimate L. J. Diameters for Ketones and Ketones Radicals

Species	Equations (N= carbon number)
Ketone	L J diameter = $(0.32*N + 4.57) * 0.84$
Ketone Primary Radicals	L J diameter = $(0.32*N + 4.49) * 0.84$
Ketone Secondary Radicals	L J diameter = $(0.3*N + 4.7) * 0.84$

3.5 Summary

Parameters for estimation of dipole moment, polarizability and Lennard-Jones diameters needed to calculate transport properties of alcohols, aldehydes, ethers, and ketones and corresponding radicals are calculated. Linear relationships vs. carbon number are shown and linear equations with a scaling factor for individual parameters and molecule species are presented.

Dipole moment calculation values from B3LYP/6-31G(d,p) show better agreement with the experimental data when compared to the other calculation methods in this study. BMK/6-31G(d,p) also has a good potential in an efficiency dipole moment calculation and can compete with B3LYP/6-31G9(d,p) in some cases of this study. The dipole moments do not show consistent increasing values with the number of carbon atoms in the compound.

PM6 method has the significant capability for calculation the molecular polarizability of alcohols, aldehydes, ethers, and ketones group of species. Polarizability (Alpha) and Lennard Jones diameter (Sigma) increase near linearly with the number of carbon atoms in compounds (more carbon atoms, higher polarizability and larger L. J. diameters) for all stable molecules, Primary radicals, and secondary radicals species of Alcohol, Aldehyde, Ethers, and Ketones group.

Diameters from PM6 Volumes multiplied by factors of ~ 0.86 provide good results compared to literature data and are recommended.

CHAPTER 4

CYCLOPENTADIENONE OXIDATION REACTION KINETICS AND THERMOCHEMISTRY FOR THE ALCOHOLS, HYDROPEROXIDES, VINYLIC, ALKOXY AND ALKYLPEROXY RADICALS

4.1 Overview

Cyclopentadienone has a $4n + 2$ pi electron configuration similar to that of benzene and furans and reactions of the ring radical sites appear to undergo chain branching to a more significant extent than vinyl radicals or phenyl radicals⁶⁰⁻⁶¹. Evaluation of its thermochemistry shows the effect of the carbonyl group on the electronegative carbonyl oxygen moiety; its thermochemistry and the effects of alcohol and hydroperoxy groups on C-H bond dissociation energies are to understand its reactions under thermal and combustion conditions. To our knowledge no one has studied the extensive thermochemistry or kinetics of these oxygenated derivatives and corresponding radicals. Thermal decomposition studies on methoxy and dimethoxy benzenes, methoxy phenols, and di-phenols have been shown to form cyclopentadienone as an important intermediate.⁶²⁻⁶⁵ Cyclopentadienone (C_5H_4O) has also been considered an oxidation product of cyclopentadiene (C_5H_6), and a decomposition product of mono aromatics and benzoquinones. Experimental oxidation studies are however inconclusive as to formation of cyclopentadienone as a stable intermediate from reactions of cyclopentadiene.^{61, 66}

Da Costa et al.⁶⁰ reported that cyclopentadienone is one of the main products from the thermal decomposition benzoquinone ($C_6H_4O_2$) as a result of CO elimination, where it further reacts to unsaturated non-cyclic products of acetylene and vinylacetylene⁶⁴. Alzueta et al.⁶⁷ have constructed a detail kinetic reaction model of benzene oxidation forming cyclopentadienone (C_5H_4O) as a major product but they needed rapid

dimerization and radical addition reactions to convert their calculated cyclopentadienone intermediate to new products, in order to describe its lack of buildup and observation in their experimental results. Schraa et al.⁶⁸ reported results from thermal decomposition of two cyclopentadienone precursors, orthobenzoquinone, and dihydro-benzodioxin. They proposed that cyclopentadienone was formed, but not observed due to rapid consumption at temperatures between 850-1100 K and low radical concentrations. They suggested that it was lost to a fast dimerization product with a reaction rate of $4.0 \times 10^{11} \text{ cm}^3 \text{ mol}^{-1} \text{ s}^{-1}$ at 850 K via observation the cyclopentadienone dimer. Dejong et al.⁶⁹ studied thermal reactions of phenylene sulfite which was indicated to decompose to form cyclopentadienone. They also reported the need for rapid conversion or dimerization of the initially formed cyclopentadienone to explain the formation of the observed product dimer.

Butler and Glassman⁶⁶ conducted experiments to investigate the formation of cyclopentadienone from oxidation studies of cyclopentadiene from 1100 to 1200 K. They considered that the ketone would be a significant intermediate in C₅ ring oxidation processes under combustion conditions; but cyclopentadienone was not detected under their high temperature oxidation conditions. Because of the lack of observation of cyclopentadienone in the experiments, Wang and Brezinsky⁶¹ studied its unimolecular decomposition to determine stability relative to the formation of cyclobutadiene (C₄H₄) via elimination of CO. They reported a several step mechanism with overall barrier of 59 kcal mol⁻¹. Cyclopentadienones are considered important products in the thermal oxidation of aromatic species (Sebbar et al.⁷⁰) where a phenyl radical reacts with O₂ to form a peroxy radical and the peroxy radical reacts to insert an oxygen atom into the ring,

forming a seven membered cyclic radical. This seven member cyclic radical undergoes ring opening and then a ring closing to form a new 5 member - 2-formyl-cyclopentadienone -3-yl radical, which loses the HC•O group to form cyclopentadienone. The intermediate was identified by work of Kirk et al.⁷¹ in their experiment. As noted above dissociation reaction of cyclopentadienone involves loss CO to form cyclobutadiene with a barrier of 59 kcal mol⁻¹ or formation of two acetylenes plus CO⁷², where the reaction is 78 kcal mol⁻¹ endothermic.

In 2014, Ormand et al.⁷³ used flash pyrolysis of o-phenylene sulfite (C₆H₄O₂SO) to provide a molecular beam of cyclopentadienone (for collection by matrix isolation. They confirmed products via photo-ionization mass spectroscopy (PIMS) and infrared. They reported symmetry and frequencies, which were further validated with calculations. Scheer et al.⁶⁴ reported that cyclopentadienone is detected and confirmed by IR spectroscopy as an intermediate in a unimolecular decomposition of methoxyphenols. Sirjean et al.⁷⁴ used theoretical chemistry to evaluate pathways leading to cyclopentadienone with both Density Function Theory (DFT) methods and Coupled Cluster Theory. They reported the thermal deposition pathways leading to cyclopentadienone from phenylperoxy radical, similar to that of Sebbar et al.⁷⁰. Battin-Leclerc reported that the kinetics and thermochemistry of cyclopentadienone (C₅H₄O), along with its peroxy radicals and alkoxy aromatic group needed to be investigated in order to have a full understanding of the chemistry for C₅ oxygenated compounds⁷⁵.

In an early study Zhong and Bozzelli⁷⁶ carried out the study thermochemistry and kinetic analysis with thermochemical known reactants, intermediates, and product species with evaluations based on literature data and group additivity contributions with

available hydrogen bond increments; they estimated $\Delta_f H^\circ_{298}$ of cyclopentadienone at 7.4 kcal mol⁻¹. The $\Delta_f H^\circ_{298}$ of cyclopentadienone was subsequently calculated by Wang and Brezinsky¹ at 13.2 kcal mol⁻¹ using ab initio molecular orbital calculations at the G2(MP2,SVP) and G2(B3LYP/MP2,SVP) levels of theory and with the use of isodesmic reactions. In a separate study the heat of formation data of cyclopentadienone (12.75 kcal mol⁻¹) was calculated by Robinson and Lindstedt in 2011⁷⁷, where the kinetic and thermochemical parameters were calculated using G4/G4MP2 and G3B3 composite methods. Lindstedt also obtained the equilibrium structure from B3LYP with the 6-31G (2df,p) basis set and determined the thermochemical data relative to the oxidation reactions of the cyclopentadiene and oxygenated cyclopentadienyl intermediates.

Under combustion conditions, cyclopentadienone can react to form radicals from loss (abstraction) of the ring hydrogen atoms, and the formed alken-yl radicals will react with O₂ to form peroxy and alkoxy radicals at the different sites on the ring. The radicals can also undergo unimolecular beta scission reactions leading to ring opening and formation of reactive, unsaturated non-cyclic species. Thermochemical properties: formation enthalpies ($\Delta_f H^\circ_{298}$), entropies (S°), heat capacities ($C_p^\circ(T)$), and bond dissociation enthalpies (BDEs) for the vinylic carbon radicals, hydroperoxides, peroxy radicals, alcohols and alkoxy radicals of cyclopentadienone are needed to understand reaction paths and to assist in developing the chemical kinetic mechanisms. Ab initio composite and Density Functional Theory methods were used with work reactions to calculate the thermochemical properties for of these target molecules and radical intermediates and kinetic parameters for ring opening reactions of the vinylic radicals and the R + O₂ initial reaction steps.

Results show the $R^\bullet + O_2$ association reactions to have an unusually deep well ($\sim 50 \text{ kcal mol}^{-1}$) relative to ~ 46 in vinyl and phenyl + O_2 systems and the chemical activation reactions of $R^\bullet + O_2$ to $RO^\bullet + O$ atom (chain branching) for the cyclopentadienone -2-yl and 3-yl carbon radicals have reaction enthalpies which are well below the entrance channel. The kinetic analysis in this study suggests that the $R + O_2$ chain branching reaction to $RO + O$ is an important path in the cyclopentadienone vinyl radical reactions with molecular oxygen under combustion conditions and to some extent under atmospheric conditions.

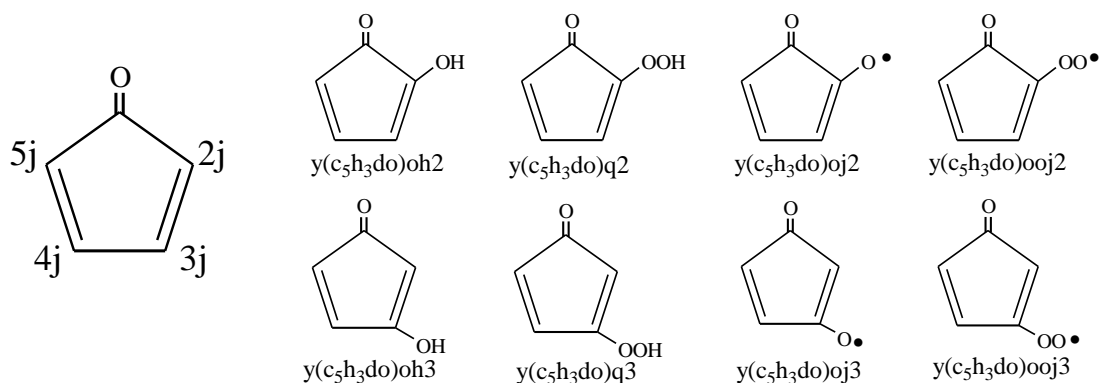


Figure 4.1 Nomenclature for radical and functional group sites.

4.2 Thermochemical Properties

The structures of cyclopentadienone and alcohols and hydroperoxides, the radicals corresponding to the loss of H atoms, plus standard enthalpies of formation for the parents and radicals have been calculated using B3LYP hybrid density functional theory in conjunction with the 6-31G(d,p)²⁻³ basis set and the composite CBS-QB3 level of theory⁴. The B3LYP method combines the three-parameter Becke exchange functional,

B3, with Lee-Yang-Parr correlation functional as LYP. CBS-QB3 is a multilevel model chemistry that combines the results of several ab initio and density functional theory (DFT) individual methods and empirical correction terms to predict molecular energies with high accuracy and reasonably low computational cost. All quantum chemical calculation has been performed within the Gaussian 03 suite of programs¹⁴.

4.2.1 Uncertainty and Confidence Limits

The uncertainty is determined from comparison of calculated ΔH_{rxn} with the literature ΔH_{rxn} , on a set of twelve work reactions involving species with known, standard enthalpies of formation. Table 4.1 lists the 12 reference reactions using known thermochemical values and our calculated ΔH reaction energies. Overall of Root Mean Square (RMS) deviation values for the twelve reaction set are $0.48 \text{ kcal mol}^{-1}$ for CBS-QB3 and $0.98 \text{ kcal mol}^{-1}$ for B3LYP/6-31G(d,p). Table 4.2 lists the confidence limit obtained from this data for different numbers of work reactions, as to use of different numbers of work reactions for have been use in several target species. The uncertainty in enthalpy values of each reference species in each of the work reactions for our target molecules and radicals is also incorporated into the error analysis. Further calculation details for uncertainties include error limits for the reference species and are included in the appendix material. The set of isodesmic reactions for each target molecule can be observed in Table 4.1, which also includes the 95% confidence limits.

Table 4.1 Comparison of Experiment $\Delta_f H^\circ_{298}$ with Values from CBS-QB3 and B3LYP/6-31G(d,p) Calculation (kcal mol⁻¹)

Reaction	Experiment	CBS-QB3	B3LYP/6-31G(d,p)
coh + ccc → ccoh + cc	-3.07	-2.95	-3.86
ccoh + ccc → cccoh + cc	0.22	-0.01	-0.15
ccco + cc → ccoh + ccc	-0.22	0.01	0.15
cdcc + cc → cdc + ccc	2.78	2.72	3.89
cj + cdcc → i-c ₄ h ₉	-22.88	-22.21	-21.34
cdcj + cj → cdcc	-101.32	-101.32	-102.05
y(c ₄ h ₄ o) + cdccdc → y(c ₅ h ₆) + y(c ₃ h ₄ do)	18.20	18.77	18.55
Phenol + cc → y(c ₆ h ₆) + ccoh	6.66	6.18	8.20
y(c ₆ h ₅)oh + ccj → y(c ₆ h ₅)j + ccoh	19.42	19.92	19.09
cdcc + cdcd → cdc + y(c ₃ h ₄ do)	22.91	23.67	23.86
y(c ₄ h ₆) + cccoh → Phenol + ccc	-6.88	-6.17	-8.05
cdcoh + Benzene → Phenol + cdc	-0.49	0.05	0.70
RMS		0.48	0.98

Note: y = cyclic, d = double bond, j = radical

Table 4.2 Confidence Limits (95%) for Each of the Work Reaction Sets

Number of Work Reactions	CBS-QB3	B3LYP/6-31G(d,p)
7	0.44	0.90
5	0.59	1.21
4	0.76	1.54
3	1.18	2.42

4.2.2 Standard Enthalpies of Formation ($\Delta_f H^\circ_{298}$)

Standard enthalpies of formation ($\Delta_f H^\circ_{298}$) were determined using calculated energies, zero point vibration energy (ZPVE), plus thermal contributions (to 298K) at the B3LYP/6-31 g(d,p) and CBS-QB3 levels of theory plus use of work reactions¹⁶⁻¹⁷. The calculated total energy at B3LYP/6-31 g(d,p) is corrected by the ZPVE, which is scaled by 0.9806 , as recommended by Scott and Radom¹⁸. The CBS-QB3 uses geometry from B3LYP/CBSB7 calculations. To more accurately evaluate the standard enthalpy of formation ($\Delta_f H^\circ_{298}$), a number of homodesmic and isodesmic work reactions have been

used to calculate the standard enthalpy of formation for both parent molecules and radicals at each level of theory. An isodesmic reaction is a hypothetical reaction where the number and type of bonds is conserved on each side of the work reaction, and a homodesmic reaction conserves number and type of bonds, but also conserves hybridization¹⁹. The thermal enthalpy of each species in the work reaction is determined, which allows calculation of $\Delta_f H^{\circ}_{298}$ reaction. The known $\Delta_f H^{\circ}_{298}$ values of the three reference molecules are used with the calculated $\Delta_f H^{\circ}_{298}$ reaction to determine the standard enthalpies of formation. The use of similar structural components on both sides of the work reaction provide a cancellation of systematic errors that may exist in the calculation of $\Delta_f H^{\circ}_{298}$ for each species and allows for an increase in accuracy for the standard enthalpy analysis.

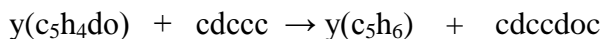
The work reactions in this work have used to calculate the $\Delta_f H^{\circ}_{298}$ of the target molecule as following:

$$\Delta_{\text{rxn}} H^{\circ}_{298} = \sum \Delta H_f (\text{Product}) - \sum \Delta H_f (\text{Reactant}) \quad (4.1)$$

Where the two products and one reactant are the reference molecules that are known, and the three evaluated $\Delta_f H^{\circ}_{298}$ reference species from the literature thermodynamic properties have been use.

The standard enthalpies of formation at 298.15 K of the reference species used in the reactions are summarized in Table 4.3.

As an example the following equation is used to estimate $\Delta_f H^{\circ}_{298}$ for y(c₅h₄do)



$$\Delta_f H_{298}^{\circ} \text{ (kcal mol}^{-1}\text{): Target} \quad \quad \quad \mathbf{-0.15} \quad \mathbf{32.1} \quad \mathbf{-27.40}$$

The standard enthalpy of formation for each species in the reaction is calculated, and the heat of reaction, $\Delta_{\text{rxn}} H_{298}^{\circ}$, is calculated. Literature values for enthalpies of formation of the three reference compounds (values above in bold) are used with the $\Delta_{\text{rxn}} H_{298}^{\circ}$ to obtain the enthalpy of formation on the target molecule, $y(C_5H_4dO)$. The values in brackets correspond to B3LYP/6-31 g(d,p) calculated values.

$$\begin{aligned} \Delta_{\text{rxn}} H_{298}^{\circ} &= [(-194.012906) + (-231.147354)] - [(-268.030211) + (-157.117923)] \times 627.51 \\ &= -7.61 \text{ kcal mol}^{-1} \end{aligned}$$

Using the calculated $\Delta_{\text{rxn}} H_{298}^{\circ}$ and reference species to find $\Delta_f H_{298}^{\circ}$ of the target molecule in kcal mol^{-1} as follow:

$$-7.61 \text{ kcal mol}^{-1} = (-27.40) + (32.1) - (-0.15) - \Delta_f H_{298}^{\circ} y(C_5H_4dO)$$

$$\Delta_f H_{298}^{\circ} y(C_5H_4dO) = 12.46 \text{ kcal mol}^{-1}$$

The target molecule and radical structure corresponding abbreviated nomenclature are presented in Figures 4.2 and 4.3, respectively. Calculation of the standard enthalpies of formation and for the stable parent molecules of cyclopentadienone, hydroxyl cyclopentadienones and cyclopentadienone-hydroperoxides are listed in Table 4.5.

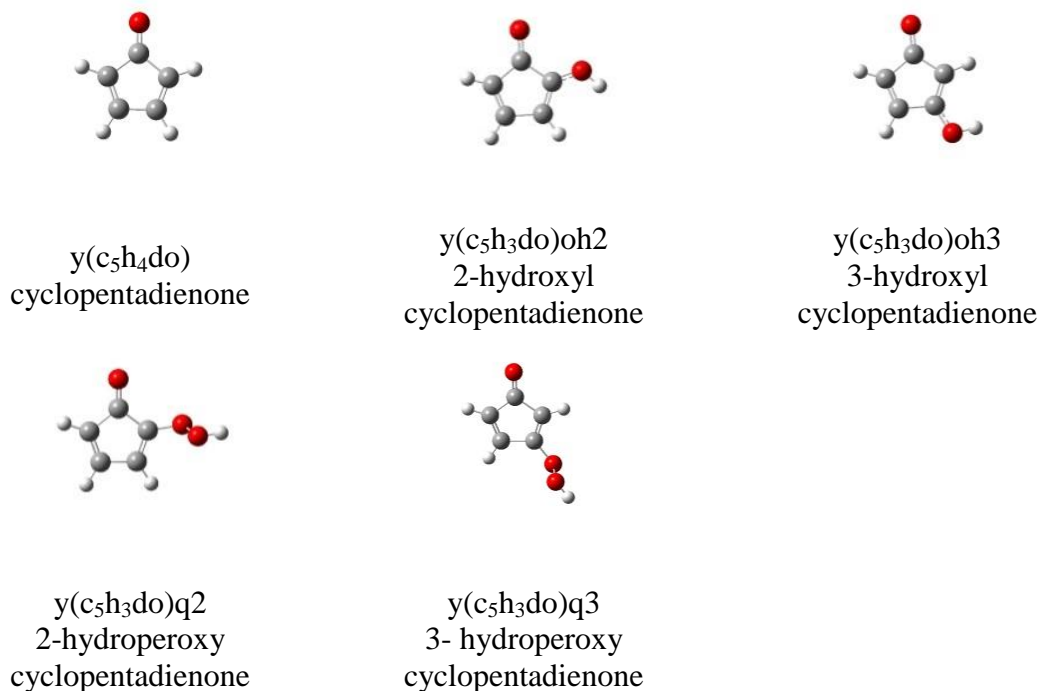


Figure 4.2 Structure and abbreviated nomenclature of the target molecules.

The calculated standard enthalpies of formation and work reactions for each of these target parent molecules, with the corresponding uncertainty value including standard deviation are listed in Table 4.5. The calculated values from CBS-QB3, which shows the lowest standard deviation and is the highest level calculation method in this work are recommended. Evaluation of accuracy for enthalpy of formation, we calculate $\Delta_f H_{298}^0$ of the target cyclopentadienone y(c₅h₄do) using seven work reactions as shown in Table 4.4, resulted in $13.0 \pm 1.88 \text{ kcal mol}^{-1}$ for $\Delta_f H_{298}^0$. This value is in agreement with the literature data ($13.2 \text{ kcal mol}^{-1}$) by Wang and Brezinsky⁶¹ and by Burcat and Ruscic²⁰, the data is $0.25 \text{ kcal mol}^{-1}$ higher than work of Robinson and Lindstedt⁷⁷ ($12.75 \text{ kcal mol}^{-1}$). Five isodesmic reactions schemes are used for evaluation the $\Delta_f H_{298}^0$ values on the cyclopentadienone-alcohols, y(c₅h₃do)oh2 and y(c₅h₃do)oh3, where values show a 2.2

kcal mol⁻¹ higher enthalpy for the 2 position alcohol relative to the 3 position, -31.3 ± 2.67 and -33.5 ± 2.67 kcal mol⁻¹, respectively.

Enthalpies of formation of two parent cyclopentadienone hydroperoxides, y(c₅h₃do)q₂ and y(c₅h₃do)q₃, were calculated with five isodesmic reactions. The enthalpies determined show that y(c₅h₃do)q₂ is five kcal mol⁻¹ higher in enthalpy at -8.2 ± 2.41 kcal mol⁻¹, versus the lower enthalpy of y(c₅h₃do)q₃ at -13.2 ± 2.41 kcal mol⁻¹.

Table 4.3 Standard Enthalpies of Formation at 298.15 K of Reference Species Used in Work Reactions

Species	$\Delta_f H^\circ_{298}$ kcal mol ⁻¹	reference	Species	$\Delta_f H^\circ_{298}$ kcal mol ⁻¹	reference
cdcc	4.78 ± 0.19	78	cdcj	71 ± 1.0	79
y(c ₅ h ₆)	32.1 ± 0.36	78	y(c ₆ h ₅)j	81 ± 2.0	79
cdccdo	-16.7 ± 1.0	80	Cdcjc	58.89 ± 0.12	81
cdccc	-0.15 ± 0.19	82	y(c ₄ h ₄ o)	-8.3 ± 0.2	83
cdccdoc	-27.4 ± 2.6	84	y(c ₄ h ₃ o)j ₂	61.67 ± 0.3	85
y(c ₆ h ₈)	25.00 ± 0.15	86	cdccdc	26.00 ± 0.19	82
y(c ₆ h ₆ do)	-4.4 ± 2.4	87	cdcjcdc	75 ± 1^a	88
y(c ₆ h ₁₂)	-29.43 ± 0.19	89	cdccjdo	21.9 ± 1^a	88
y(c ₆ h ₁₀ do)	-55.23 ± 0.21	90	cdccdcj	85.4 ± 1^a	91
y(c ₄ h ₆)	38.53 ± 0.4	92	y(c ₄ h ₃ o)j ₃	61.80 ± 0.3	85
y(c ₄ h ₄ do)	10.32 ± 1.0	93	coh	-48.16 ± 0.07	78
y(c ₆ h ₁₀)	-1.03 ± 0.2	94	ccoh	-56.21 ± 0.1	78
y(c ₅ h ₈)	8.10 ± 0.33	78	cccoh	-60.97 ± 0.12	78
cdc	12.54 ± 0.1	78	coj	5.02 ± 0.5	95
cdcoh	-29.8 ± 2.0	96	cco	-3.1 ± 0.31	97
Benzene	19.8 ± 0.2	98	cccoj	-7.91 ± 0.33	97
Phenol	-23.03 ± 0.14	99	cq	-30.93 ± 0.21	97
ccohdc	-42.1 ± 1^a	100	ccq	-39.9 ± 1.5	101
y(c ₆ h ₆ do) ₂	-6.0 ± 2.4	87	cccq	-44.37 ± 0.2	102
cdcq	-10.87 ± 1^a	103	cooj	2.91 ± 0.21	97
y(c ₆ h ₅)q	-2.68 ± 0.49	81	ccooj	-6.8 ± 2.3	104
cc	-20.04 ± 0.07	105	cccooj	-10.53 ± 0.26	97
ccc	-25.02 ± 0.12	105	cj	35.1 ± 0.2	79
i-c ₄ h ₉	17 ± 0.5	79	y(c ₄ h ₄ o)	-8.3 ± 0.2	106
y(c ₃ h ₄ do)	3.8 ± 1.0	107	cdccdo	-11.35 ± 0.38	78

Note: ^a Error not provided (error ± 1 assigned), y= cyclic, d= double bond, j= radical, q= OOH group

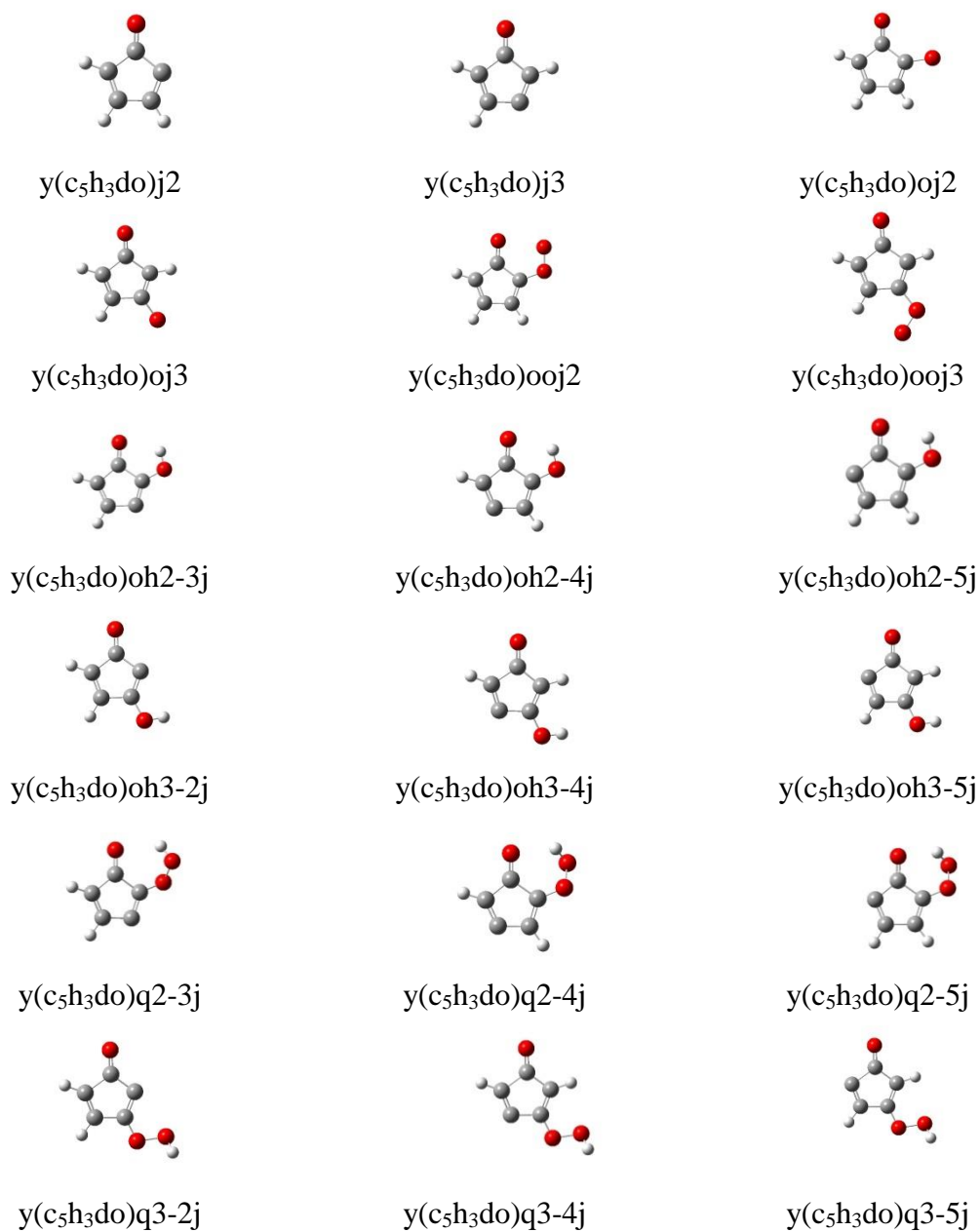


Figure 4.3 Structure and abbreviated nomenclature of the cyclopentadienone radical corresponding to the loss of a hydrogen atom from the parent molecules.

Table 4.4 Name and Nomenclature of Radical Species

Cyclopentadienone, hydroxyl-, and hydroperoxyl- cyclopentadienone vinyl radicals
Cyclo-pentadienone-2yl: $(y(c_5h_3do))j_2$
Cyclo-pentadienone-3yl: $y(c_5h_3do)j_3$
Cyclo-pentadienone-2-hydroxyl-3-yl: $y(c_5h_3do)oh_2-3j$
Cyclo-pentadienone-2-hydroxyl-4-yl: $y(c_5h_3do)oh_2-4j$
Cyclo-pentadienone-2-hydroxyl-5-yl: $y(c_5h_3do)oh_2-5j$
Cyclo-pentadienone-3-hydroxyl-2-yl: $y(c_5h_3do)oh_3-2j$
Cyclo-pentadienone-3-hydroxyl-4-yl: $y(c_5h_3do)oh_3-4j$
Cyclo-pentadienone-3-hydroxyl-5-yl: $y(c_5h_3do)oh_3-5j$
Cyclo-pentadienone-2-hydroperoxyl-3-yl: $y(c_5h_3do)q_2-3j$
Cyclo-pentadienone-2-hydroperoxyl-4-yl: $y(c_5h_3do)q_2-4j$
Cyclo-pentadienone-2-hydroperoxyl-5-yl: $y(c_5h_3do)q_2-5j$
Cyclo-pentadienone-3-hydroperoxyl-2-yl: $y(c_5h_3do)q_3-2j$
Cyclo-pentadienone-3-hydroperoxyl-4-yl: $y(c_5h_3do)q_3-4j$
Cyclo-pentadienone-3-hydroperoxyl-5-yl: $y(c_5h_3do)q_3-5j$
O—H bond dissociation energies for cyclopentadienone to form an alkoxy radical
Cyclo-pentadienone-alkoxyl-2-yl: $(y(c_5h_4do))oj_2$
Cyclo-pentadienone-alkoxyl-3-yl: $y(c_5h_4do)oj_3$
OO-H bond dissociation energies for cyclopentadienone to form a peroxy radical
Cyclo-pentadienone-peroxyl-2-yl $(y(c_5h_3do))ooj_2$
Cyclo-pentadienone-peroxyl-3-yl: $y(c_5h_3do)ooj_3$
Note : Nomenclature – carbon site adjacent to the C=O group is 1, secondary vinyl carbon is 2, q is OOH group, structures of radical species are illustrated in the figure 4.3

Table 4.5 Evaluated Enthalpies of Formation at 298 K of Target Molecules

Work Reactions	$\Delta_f H^\circ_{298}$ kcal mol ⁻¹		
	CBS-QB3	B3LYP/ 6-31G(d,p)	Literature
y(c₅h₄do)			
y(c ₅ h ₄ do) + cdcc → y(c ₅ h ₆) + cdccdo	12.34 ± 1.17	12.01 ± 1.41	13.2 ⁶¹
y(c ₅ h ₄ do) + cdccc → y(c ₅ h ₆) + cdccdoc	12.79 ± 2.67	12.46 ± 2.78	12.75 ⁷⁷
y(c ₅ h ₄ do) + y(c ₆ h ₈) → y(c ₅ h ₆) + y(c ₆ h ₆ do)	13.65 ± 2.47	15.58 ± 2.59	13.20 ²⁰
y(c ₅ h ₄ do) + y(c ₆ h ₁₂) → y(c ₅ h ₆) + y(c ₆ h ₁₀ do)	13.02 ± 0.64	12.24 ± 1.01	
y(c ₅ h ₄ do) + y(c ₄ h ₆) → y(c ₅ h ₆) + y(c ₄ h ₄ do)	13.84 ± 1.22	13.81 ± 1.45	
y(c ₅ h ₄ do) + y(c ₆ h ₁₀) → y(c ₅ h ₈) + y(c ₆ h ₆ do)	12.53 ± 2.47	15.12 ± 2.59	
y(c ₅ h ₄ do) + y(c ₅ h ₈) → y(c ₄ h ₆) + y(c ₆ h ₆ do)	12.99 ± 2.49	16.33 ± 2.62	
Average $\Delta_f H^\circ_{298}$	13.02 ± 1.88	13.94 ± 2.06	
Standard Deviation	0.55	1.76	
y(c₅h₃do)oh2			
y(c ₅ h ₃ do)oh2 + cdc → y(c ₅ h ₄ do) + cdcoh	-30.91 ± 2.80	-31.87 ± 3.00	
y(c ₅ h ₃ do)oh2 + benzene → y(c ₅ h ₄ do) + phenol	-31.45 ± 1.98	-33.06 ± 2.24	
y(c ₅ h ₃ do)oh2 + cdcc → y(c ₅ h ₄ do) + ccohdcc	-32.29 ± 2.21	-34.41 ± 2.45	
y(c ₅ h ₃ do)oh2 + cdcc → y(c ₆ h ₆ do) + cdcoh	-30.94 ± 3.18	-30.88 ± 3.36	
y(c ₅ h ₃ do)oh2 + cdcc → y(c ₆ h ₆ do)2 + cdcoh	-30.98 ± 3.18	-31.61 ± 3.36	
Average $\Delta_f H^\circ_{298}$	-31.32 ± 2.67	-32.37 ± 2.88	
Standard Deviation	0.59	1.39	
y(c₅h₃do)oh3			
y(c ₅ h ₃ do)oh3 + cdc → y(c ₅ h ₄ do) + cdcoh	-33.12 ± 2.80	-33.32 ± 3.00	
y(c ₅ h ₃ do)oh3 + benzene → y(c ₅ h ₄ do) + phenol	-33.66 ± 1.98	-34.51 ± 2.24	
y(c ₅ h ₃ do)oh3 + cdcc → y(c ₅ h ₄ do) + ccohdcc	-34.50 ± 2.21	-35.86 ± 2.45	
y(c ₅ h ₃ do)oh3 + cdcc → y(c ₆ h ₆ do) + cdcoh	-33.15 ± 3.18	-32.33 ± 3.36	
y(c ₅ h ₃ do)oh3 + cdcc → y(c ₆ h ₆ do)2 + cdcoh	-33.18 ± 3.18	-33.05 ± 3.36	
Average $\Delta_f H^\circ_{298}$	-33.52 ± 2.67	-33.81 ± 2.88	
Standard Deviation	0.59	1.39	
y(c₅h₃do)q2			
y(c ₅ h ₃ do)q2 + cdc → y(c ₅ h ₄ do) + cdccq	-8.25 ± 2.20	-8.90 ± 2.44	
y(c ₅ h ₃ do)q2 + benzene → y(c ₅ h ₄ do) + y(c ₆ h ₅)q	-8.37 ± 2.03	-9.55 ± 2.29	
y(c ₅ h ₃ do)q2 + cc → y(c ₅ h ₄ do) + ccq	-7.93 ± 2.47	-10.74 ± 2.69	
y(c ₅ h ₃ do)q2 + cdcc → y(c ₆ h ₆ do) + cdccq	-8.27 ± 2.67	-7.91 ± 2.87	
y(c ₅ h ₃ do)q2 + cdcc → y(c ₆ h ₆ do)2 + cdccq	-8.30 ± 2.67	-8.64 ± 2.87	
Average $\Delta_f H^\circ_{298}$	-8.22 ± 2.41	-9.15 ± 2.63	
Standard Deviation	0.17	1.07	

Table 4.5 Evaluated Enthalpies of Formation at 298 K of Target Molecules
(Continued)

Work Reactions	$\Delta_f H^\circ_{298}$ kcal mol ⁻¹		
	CBS-QB3	B3LYP/ 6-31G(d,p)	Literature
y(c₅h₃do)q3			
y(c ₅ h ₃ do)q3 + cdc → y(c ₅ h ₄ do) + cdcq	-13.26 ± 2.20	-13.14 ± 2.44	
y(c ₅ h ₃ do)q3 + benzene → y(c ₅ h ₄ do) + y(c ₆ h ₅)q	-13.38 ± 2.03	-13.78 ± 2.29	
y(c ₅ h ₃ do)q3 + cc → y(c ₅ h ₄ do) + ccq	-12.94 ± 2.47	-14.97 ± 2.69	
y(c ₅ h ₃ do)q3 + cdcc → y(c ₆ h ₆ do) + cdcq	-13.28 ± 2.67	-12.14 ± 2.87	
y(c ₅ h ₃ do)q3 + cdcc → y(c ₆ h ₆ do)2 + cdcq	-13.32 ± 2.67	-12.87 ± 2.87	
Average $\Delta_f H^\circ_{298}$	-13.24 ± 2.41	-13.38 ± 2.63	
Standard Deviation	0.17	1.07	

Note: y = cyclic, d = double bond, j = radical, q = OOH group, 2 is carbon beta to carbonyl. CBS-QB3 values recommended, standard deviation is for the method work reaction sets.

Table 4.6 Enthalpies of Formation at 298 K and Bond Dissociation Enthalpy (BDE) for Radicals

Work Reactions	$\Delta_f H^\circ_{298}$ kcal mol ⁻¹	
	CBS-QB3	B3LYP/ 6-31g(d,p)
y(c₅h₃do)j2		
y(c ₅ h ₃ do)j2 + cdc → y(c ₅ h ₄ do) + cdcj	78.62 ± 2.17	75.55 ± 2.31
y(c ₅ h ₃ do)j2 + benzene → y(c ₅ h ₄ do) + y(c ₆ h ₅)j	76.51 ± 2.78	80.12 ± 2.89
y(c ₅ h ₃ do)j2 + cdcc → y(c ₅ h ₄ do) + cdcjc	77.31 ± 1.93	78.70 ± 2.09
y(c ₅ h ₃ do)j2 + y(c ₄ h ₄ o) → y(c ₅ h ₄ do) + y(c ₄ h ₃ o)j	78.92 ± 1.95	79.80 ± 2.11
y(c ₅ h ₃ do)j2 + cdccdc → y(c ₅ h ₄ do) + cdcjcdc	79.34 ± 2.17	82.11 ± 2.31
y(c ₅ h ₃ do)j2 + cdccdo → y(c ₅ h ₄ do) + cdccjdo	78.76 ± 2.39	81.12 ± 2.51
y(c ₅ h ₃ do)j2 + cdccdc → y(c ₅ h ₄ do) + cdccdcj	78.63 ± 2.17	78.62 ± 2.31
Average $\Delta_f H^\circ_{298}$	78.30 ± 2.22	79.43 ± 2.36
Standard Deviation	1.01	2.12
BDE	117.38	118.51
y(c₅h₃do)j3		
y(c ₅ h ₃ do)j3 + cdc → y(c ₅ h ₄ do) + cdcj	75.06 ± 2.17	71.81 ± 2.31
y(c ₅ h ₃ do)j3 + benzene → y(c ₅ h ₄ do) + y(c ₆ h ₅)j	72.95 ± 2.78	76.37 ± 2.89
y(c ₅ h ₃ do)j3 + cdcc → y(c ₅ h ₄ do) + cdcjc	73.75 ± 1.93	74.95 ± 2.09
y(c ₅ h ₃ do)j3 + y(c ₄ h ₄ o) → y(c ₅ h ₄ do) + y(c ₄ h ₃ o)j2	75.26 ± 1.95	76.18 ± 2.11
y(c ₅ h ₃ do)j3 + cdccdc → y(c ₅ h ₄ do) + cdcjcdc	75.78 ± 2.17	78.37 ± 2.31
y(c ₅ h ₃ do)j3 + cdccdo → y(c ₅ h ₄ do) + cdccjdo	75.20 ± 2.39	77.38 ± 2.51
y(c ₅ h ₃ do)j3 + cdccdc → y(c ₅ h ₄ do) + cdccdcj	75.07 ± 2.17	74.88 ± 2.31
Average $\Delta_f H^\circ_{298}$	74.72 ± 2.22	75.71 ± 2.36
Standard Deviation	1.01	2.12
BDE	113.80	114.79

Table 4.6 Enthalpies of Formation at 298 K and Bond Dissociation Enthalpy (BDE) for Radicals (Continued)

Work Reactions	$\Delta_f H^\circ_{298}$ kcal mol ⁻¹	
	CBS-QB3	B3LYP/ 6-31g(d,p)
y(c₅h₄do)oj2		
y(c ₅ h ₃ do)oj2 + coh → y(c ₅ h ₃ do)oh + coj	-9.38 ± 3.07	-6.22 ± 3.73
y(c ₅ h ₃ do)oj2 + ccoh → y(c ₅ h ₃ do)oh + ccoj	-9.36 ± 3.05	-6.10 ± 3.71
y(c ₅ h ₃ do)oj2 + cccoh → y(c ₅ h ₃ do)oh + cccoj	-9.34 ± 3.05	-6.08 ± 3.71
Average $\Delta_f H^\circ_{298}$	-9.36 ± 3.06	-6.13 ± 3.72
Standard Deviation	0.02	0.08
BDE	74.06	77.29
y(c₅h₃do)oj3		
y(c ₅ h ₃ do)oj3 + coh → y(c ₅ h ₃ do)oh2 + coj	-6.67 ± 3.07	-3.81 ± 3.73
y(c ₅ h ₃ do)oj3 + ccoh → y(c ₅ h ₃ do)oh2 + ccoj	-6.65 ± 3.05	-3.69 ± 3.71
y(c ₅ h ₃ do)oj3 + cccoh → y(c ₅ h ₃ do)oh2 + cccoj	-6.64 ± 3.05	-3.67 ± 3.71
Average $\Delta_f H^\circ_{298}$	-6.65 ± 3.06	-3.72 ± 3.72
Standard Deviation	0.02	0.08
BDE	78.97	81.90
y(c₅h₃do)ooj2		
y(c ₅ h ₃ do)ooj2 + cooh → y(c ₅ h ₃ do)q + cooj	27.67 ± 2.70	28.75 ± 3.43
y(c ₅ h ₃ do)ooj2 + ccooh → y(c ₅ h ₃ do)q + ccooj	27.56 ± 3.84	28.56 ± 4.38
y(c ₅ h ₃ do)ooj2 + cccooH → y(c ₅ h ₃ do)q + cccooj	28.15 ± 2.70	29.27 ± 3.43
Average $\Delta_f H^\circ_{298}$	27.79 ± 3.08	28.86 ± 3.75
Standard Deviation	0.31	0.37
BDE	88.11	89.18
y(c₅h₃do)ooj3		
y(c ₅ h ₃ do)ooj3 + cooh → y(c ₅ h ₃ do)q2 + cooj	23.86 ± 2.70	24.60 ± 3.43
y(c ₅ h ₃ do)ooj3 + ccooh → y(c ₅ h ₃ do)q2 + ccooj	23.75 ± 3.84	24.41 ± 4.38
y(c ₅ h ₃ do)ooj3 + cccooH → y(c ₅ h ₃ do)q2 + cccooj	24.34 ± 2.70	25.12 ± 3.43
Average $\Delta_f H^\circ_{298}$	23.98 ± 3.08	24.71 ± 3.75
Standard Deviation	0.31	0.37
BDE	89.32	90.05
y(c₅h₃do)oh2-3j		
y(c ₅ h ₃ do)oh2-3j + cdc → y(c ₅ h ₃ do)oh + cdcj	33.66 ± 3.06	30.86 ± 3.35
y(c ₅ h ₃ do)oh2-3j + cdcedo → y(c ₅ h ₃ do)oh + cdccjdo	33.81 ± 3.22	36.42 ± 3.49
y(c ₅ h ₃ do)oh2-3j + cdccdc → y(c ₅ h ₃ do)oh + cdccjcdc	34.39 ± 3.07	37.41 ± 3.35
y(c ₅ h ₃ do)oh2-3j + cdccdc → y(c ₅ h ₃ do)oh + cdccdcj	33.68 ± 3.07	33.93 ± 3.35
Average $\Delta_f H^\circ_{298}$	33.88 ± 3.12	34.66 ± 3.40
Standard Deviation	0.34	2.93
BDE	117.30	118.08

Table 4.6 Enthalpies of Formation at 298 K and Bond Dissociation Enthalpy (BDE) for Radicals (Continued)

Work Reactions	$\Delta_f H^\circ_{298}$ kcal mol ⁻¹	
	CBS-QB3	B3LYP/ 6-31g(d,p)
y(c₅h₃do)oh2-4j		
y(c ₅ h ₃ do)oh2-4j + cdc → y(c ₅ h ₃ do)oh + cdcj	30.24 ± 3.06	27.00 ± 3.35
y(c ₅ h ₃ do)oh2-4j + cdccdo → y(c ₅ h ₃ do)oh + cdccjdo	30.38 ± 3.22	32.56 ± 3.49
y(c ₅ h ₃ do)oh2-4j + cdccdc → y(c ₅ h ₃ do)oh + cdccjcdc	30.96 ± 3.07	33.55 ± 3.35
y(c ₅ h ₃ do)oh2-4j + cdccdc → y(c ₅ h ₃ do)oh + cdccdcj	30.26 ± 3.07	30.07 ± 3.35
Average $\Delta_f H^\circ_{298}$	30.46 ± 3.12	30.79 ± 3.40
Standard Deviation	0.34	2.93
BDE	113.88	114.22
y(c₅h₃do)oh2-5j		
y(c ₅ h ₃ do)oh2-5j + cdc → y(c ₅ h ₃ do)oh + cdcj	34.63 ± 3.06	31.95 ± 3.35
y(c ₅ h ₃ do)oh2-5j + cdccdo → y(c ₅ h ₃ do)oh + cdccjdo	34.78 ± 3.22	37.52 ± 3.49
y(c ₅ h ₃ do)oh2-5j + cdccdc → y(c ₅ h ₃ do)oh + cdccjcdc	35.36 ± 3.07	38.51 ± 3.35
y(c ₅ h ₃ do)oh2-5j + cdccdc → y(c ₅ h ₃ do)oh + cdccdcj	34.65 ± 3.07	35.02 ± 3.35
Average $\Delta_f H^\circ_{298}$	34.86 ± 3.12	35.75 ± 3.40
Standard Deviation	0.34	2.93
BDE	118.27	119.17
y(c₅h₃do)oh3-2j		
y(c ₅ h ₃ do)oh3-2j + cdc → y(c ₅ h ₃ do)oh2 + cdcj	33.93 ± 3.06	30.94 ± 3.35
y(c ₅ h ₃ do)oh3-2j + cdccdo → y(c ₅ h ₃ do)oh2 + cdccjdo	34.07 ± 3.22	36.51 ± 3.49
y(c ₅ h ₃ do)oh3-2j + cdccdc → y(c ₅ h ₃ do)oh2 + cdccjcdc	34.65 ± 3.07	37.50 ± 3.35
y(c ₅ h ₃ do)oh3-2j + cdccdc → y(c ₅ h ₃ do)oh2 + cdccdcj	33.94 ± 3.07	34.01 ± 3.35
Average $\Delta_f H^\circ_{298}$	34.15 ± 3.12	34.74 ± 3.40
Standard Deviation	0.34	2.93
BDE	119.77	120.36
y(c₅h₃do)oh3-4j		
y(c ₅ h ₃ do)oh3-4j + cdc → y(c ₅ h ₃ do)oh2 + cdcj	30.16 ± 3.06	26.42 ± 3.35
y(c ₅ h ₃ do)oh3-4j + cdccdo → y(c ₅ h ₃ do)oh2 + cdccjdo	30.30 ± 3.22	31.99 ± 3.49
y(c ₅ h ₃ do)oh3-4j + cdccdc → y(c ₅ h ₃ do)oh2 + cdccjcdc	30.88 ± 3.07	32.97 ± 3.35
y(c ₅ h ₃ do)oh3-4j + cdccdc → y(c ₅ h ₃ do)oh2 + cdccdcj	30.18 ± 3.07	29.49 ± 3.35
Average $\Delta_f H^\circ_{298}$	30.38 ± 3.12	30.22 ± 3.40
Standard Deviation	0.34	2.93
BDE	116.00	115.84

Table 4.6 Enthalpies of Formation at 298 K and Bond Dissociation Enthalpy (BDE) for Radicals (Continued)

Work Reactions	$\Delta_f H^\circ_{298}$ kcal mol ⁻¹	
	CBS-QB3	B3LYP/ 6-31g(d,p)
y(c₅h₃do)oh3-5j		
y(c ₅ h ₃ do)oh3-5j + cdc → y(c ₅ h ₃ do)oh2 + cdcj	31.74 ± 3.06	28.28 ± 3.35
y(c ₅ h ₃ do)oh3-5j + cdccdo → y(c ₅ h ₃ do)oh2 + cdccjdo	31.88 ± 3.22	33.85 ± 3.49
y(c ₅ h ₃ do)oh3-5j + cdccdc → y(c ₅ h ₃ do)oh2 + cdccjcdc	32.46 ± 3.07	34.84 ± 3.35
y(c ₅ h ₃ do)oh3-5j + cdccdc → y(c ₅ h ₃ do)oh2 + cdccdcj	31.75 ± 3.07	31.35 ± 3.35
Average $\Delta_f H^\circ_{298}$	31.96 ± 3.12	32.08 ± 3.40
Standard Deviation	0.34	2.93
BDE	117.58	117.70
y(c₅h₃do)q2-3j		
y(c ₅ h ₃ do)q2-3j + cdc → y(c ₅ h ₃ do)q + cdcj	56.83 ± 2.72	53.55 ± 3.04
y(c ₅ h ₃ do)q2-3j + cdccdo → y(c ₅ h ₃ do)q + cdccjdo	56.98 ± 2.90	59.11 ± 3.20
y(c ₅ h ₃ do)q2-3j + cdccdc → y(c ₅ h ₃ do)q + cdccjcdc	57.56 ± 2.75	60.10 ± 3.06
y(c ₅ h ₃ do)q2-3j + cdccdc → y(c ₅ h ₃ do)q + cdccdcj	56.85 ± 2.72	56.61 ± 3.07
Average $\Delta_f H^\circ_{298}$	57.06 ± 2.79	57.34 ± 3.10
Standard Deviation	0.34	2.93
BDE	117.38	117.66
y(c₅h₃do)q2-4j		
y(c ₅ h ₃ do)q2-4j + cdc → y(c ₅ h ₃ do)q + cdcj	53.76 ± 2.72	50.32 ± 3.04
y(c ₅ h ₃ do)q2-4j + cdccdo → y(c ₅ h ₃ do)q + cdccjdo	53.91 ± 2.90	55.89 ± 3.20
y(c ₅ h ₃ do)q2-4j + cdccdc → y(c ₅ h ₃ do)q + cdccjcdc	54.49 ± 2.75	56.88 ± 3.06
y(c ₅ h ₃ do)q2-4j + cdccdc → y(c ₅ h ₃ do)q + cdccdcj	53.78 ± 2.72	53.39 ± 3.07
Average $\Delta_f H^\circ_{298}$	53.98 ± 2.79	54.12 ± 3.10
Standard Deviation	0.34	2.93
BDE	114.30	144.40
y(c₅h₃do)q2-5j		
y(c ₅ h ₃ do)q2-5j + cdc → y(c ₅ h ₃ do)q + cdcj	57.45 ± 2.72	53.94 ± 3.04
y(c ₅ h ₃ do)q2-5j + cdccdo → y(c ₅ h ₃ do)q + cdccjdo	57.60 ± 2.90	59.51 ± 3.20
y(c ₅ h ₃ do)q2-5j + cdccdc → y(c ₅ h ₃ do)q + cdccjcdc	58.18 ± 2.75	60.50 ± 3.06
y(c ₅ h ₃ do)q2-5j + cdccdc → y(c ₅ h ₃ do)q + cdccdcj	57.47 ± 2.72	57.01 ± 3.07
Average $\Delta_f H^\circ_{298}$	57.67 ± 2.79	57.74 ± 3.10
Standard Deviation	0.34	2.93
BDE	117.99	118.06

Table 4.6 Enthalpies of Formation at 298 K and Bond Dissociation Enthalpy (BDE) for Radicals (Continued)

Work Reactions	$\Delta_f H^\circ_{298}$ kcal mol ⁻¹	
	CBS-QB3	B3LYP/ 6-31g(d,p)
y(c₅h₃do)q3-2j		
y(c ₅ h ₃ do)q3-2j + cdc → y(c ₅ h ₃ do)q2 + cdcj	55.17 ± 2.72	52.14 ± 3.04
y(c ₅ h ₃ do)q3-2j + cdccdo → y(c ₅ h ₃ do)q2+ cdccjdo	55.32 ± 2.90	57.70 ± 3.20
y(c ₅ h ₃ do)q3-2j + cdccdc → y(c ₅ h ₃ do)q2 + cdcjcdc	55.90 ± 2.75	58.69 ± 3.06
y(c ₅ h ₃ do)q3-2j + cdccdc → y(c ₅ h ₃ do)q2 + cdccdcj	55.19 ± 2.72	55.20± 3.07
Average $\Delta_f H^\circ_{298}$	55.40 ± 2.79	55.93 ± 3.10
Standard Deviation	0.34	2.93
BDE	120.74	121.27
y(c₅h₃do)q3-4j		
y(c ₅ h ₃ do)q3-4j + cdc → y(c ₅ h ₃ do)q2 + cdcj	50.28 ± 2.72	46.69 ± 3.04
y(c ₅ h ₃ do)q3-4j + cdccdo → y(c ₅ h ₃ do)q2+ cdccjdo	50.43 ± 2.90	52.26 ± 3.20
y(c ₅ h ₃ do)q3-4j + cdccdc → y(c ₅ h ₃ do)q2 + cdcjcdc	51.01 ± 2.75	53.25 ± 3.06
y(c ₅ h ₃ do)q3-4j + cdccdc → y(c ₅ h ₃ do)q2 + cdccdcj	50.30 ± 2.72	49.76± 3.07
Average $\Delta_f H^\circ_{298}$	50.50 ± 2.79	50.49 ± 3.10
Standard Deviation	0.34	2.93
BDE	115.84	115.83
y(c₅h₃do)q3-5j		
y(c ₅ h ₃ do)q3-5j + cdc → y(c ₅ h ₃ do)q2 + cdcj	51.82 ± 2.72	48.53 ± 3.04
y(c ₅ h ₃ do)q3-5j + cdccdo → y(c ₅ h ₃ do)q2+ cdccjdo	51.97 ± 2.90	54.10 ± 3.20
y(c ₅ h ₃ do)q3-5j + cdccdc → y(c ₅ h ₃ do)q2 + cdcjcdc	52.55 ± 2.75	55.09 ± 3.06
y(c ₅ h ₃ do)q3-5j + cdccdc → y(c ₅ h ₃ do)q2 + cdccdcj	51.84 ± 2.72	51.60± 3.07
Average $\Delta_f H^\circ_{298}$	52.04 ± 2.79	52.33 ± 3.10
Standard Deviation	0.34	2.93
BDE	117.38	117.67

Note: y = cyclic, d = double bond, j = radical, q = OOH group, BDE = Bond Dissociation Enthalpy, CBS-QB3 values are recommended, standard deviation is for the method work reaction sets.

4.2.3 Internal Rotation Potentials

The C—C,C—H, C—OH, and O—OH bonds in the target molecules are needed to determine the lowest energy conformer and internal rotor energy contributions to entropy and heat capacity versus temperature. The resulting potential energy barriers for internal rotations in the hydroperoxides, alcohols and peroxy radicals are shown in Appendix C along with data for the potentials.

4.2.4 Entropy and Heat Capacity

Entropy and heat capacity values as a function of temperature are determined from the calculated structures, moments of inertia, vibration frequencies, internal rotor potentials, symmetry, electron degeneracy, number of optical isomers and the known mass of each molecule. The calculations use standard formulas from statistical mechanics for the contributions of translation, vibrations and external rotation (TVR) using the SMCPS (Statistical Mechanics – Heat Capacity, Cp, and Entropy, S) program²³. This program utilizes the rigid-rotor-harmonic oscillator approximation from the frequencies along with moments of inertia from the optimized B3LYP/6-31G(d,p) level.

Entropy and heat capacity contributions from lower frequency vibrational modes that represent torsions around single bonds were calculated as hindered internal rotors, with this data substituted for the torsion frequencies. Energy profiles for internal rotations were calculated to determine energies of the rotational conformers and inter-conversion barriers along with contributions to entropy and heat capacity for the low barrier rotors. All internal: (R--OH) and hydroperoxide rotors (R--OOH) and (R-O--OH), were treated as hindered rotors. Coupling of the low barrier internal rotors with vibrations is not included. For hindered rotors, a relaxed rotational scan was done with dihedral angle increments of 10° using B3LYP/6-31G(d,p) and the potential obtained was fitted to a truncated Fourier series expansion of the form:

$$V(\theta) = a_0 + \sum_{n=1}^{10} a_n \cos(n\theta) + \sum_{n=1}^{10} b_n \sin(n\theta) \quad (4.2)$$

$$a_0 = \frac{\sum_{i=1}^m f_i}{m} ; \quad a_n = \frac{\sum_{i=1}^m f_i \cos(n\theta)}{m} ; \quad b_n = \frac{\sum_{i=1}^m f_i \sin(n\theta)}{m} \quad (4.3)$$

Table 4.7 Ideal Gas-Phase Thermochemical Properties^a vs. Temperature ($^{\circ}\text{K}$)

Species	S ^o (298K)	C _p ^o (T)						
		300K	400K	500K	600K	800K	1000K	1500K
y(c ₅ h ₄ do)	69.27	19.58	25.35	30.08	33.82	39.23	42.93	48.34
y(c ₅ h ₃ do)oh2	75.91	24.06	30.40	35.64	39.83	45.78	49.57	54.54
y(c ₅ h ₃ do)oh3	76.05	24.70	31.21	36.28	40.15	45.51	49.00	53.92
y(c ₅ h ₃ do)q2	86.12	29.01	35.72	41.18	45.41	51.13	54.65	59.35
y(c ₅ h ₃ do)q3	86.06	29.09	35.69	40.76	44.64	50.08	53.68	58.80
y(c ₅ h ₃ do)j2	72.07	19.26	24.35	28.45	31.67	36.28	39.38	43.84
y(c ₅ h ₃ do)j3	71.82	19.33	24.46	28.56	31.77	36.34	39.42	43.85
y(c ₅ h ₃ do)oj2	72.08	19.26	24.35	28.45	31.67	36.28	39.38	43.84
y(c ₅ h ₃ do)oj3	71.82	19.33	24.46	28.56	31.77	36.35	39.42	43.85
y(c ₅ h ₃ do)ooj2	83.63	26.85	33.70	38.94	42.77	47.76	51.07	55.81
y(c ₅ h ₃ do)ooj3	83.42	26.94	33.09	38.02	41.85	47.17	50.57	55.13
y(c ₅ h ₃ do)oh2-3j	77.74	24.06	29.87	34.49	38.00	42.69	45.57	49.46
y(c ₅ h ₃ do)oh2-4j	77.33	23.94	29.71	34.38	38.04	43.03	46.08	49.92
y(c ₅ h ₃ do)oh2-5j	78.75	23.89	29.56	34.25	37.96	43.03	46.07	49.86
y(c ₅ h ₃ do)oh3-2j	78.65	23.85	29.81	34.50	38.02	42.69	45.56	49.44
y(c ₅ h ₃ do)oh3-4j	78.64	23.70	29.28	33.68	37.10	41.88	44.98	49.24
y(c ₅ h ₃ do)oh3-5j	77.99	24.69	30.31	34.58	37.82	42.29	45.18	49.23
y(c ₅ h ₃ do)q2-3j	87.10	29.95	36.07	40.62	43.92	48.20	50.85	54.55
y(c ₅ h ₃ do)q2-4j	88.04	28.76	34.92	39.74	43.35	48.07	50.91	54.67
y(c ₅ h ₃ do)q2-5j	87.19	29.32	35.57	40.29	43.76	48.28	51.01	54.68
y(c ₅ h ₃ do)q3-2j	88.29	28.51	34.32	38.73	42.10	46.79	49.85	54.12
y(c ₅ h ₃ do)q3-4j	87.45	28.66	34.50	38.96	42.37	47.12	50.19	54.39
y(c ₅ h ₃ do)q3-5j	87.63	28.85	34.78	39.21	42.56	47.19	50.18	54.32

Note: ^a Units: kcal mol⁻¹, S = entropy, Cp = heat capacity

4.3 Bond Dissociation Enthalpies (BDE)

The C—H bond dissociation Enthalpies are reported from the calculated $\Delta_f H^\circ_{298}$ of the parent molecule and the radical corresponding to loss of hydrogen atom at each carbon or oxygen site. The enthalpies of the parent molecule and product species are both calculated in this study and used with the value of 52.10 kcal mol⁻¹ for the H atom²⁰ to determine the corresponding BDE. The individual BDE values computed from isodesmic work reaction enthalpies of formation with the corresponding error limits (sum of calculated standard deviation and reported error of all species) are listed in Tables 4.6. The standard enthalpy for cyclopentadienone -1yl radical (117.4) 3.6 kcal mole⁻¹ stronger than the C—H bond on cyclopentadienone-2yl radical (113.8). The 2-yl C—h bond is similar to that on benzene⁵⁰ (113.5 kcal mol⁻¹); but the -1yl bond is significantly stronger. The presence of alcohol, hydroperoxide or peroxy group on a carbon adjacent to the C-H bond increase bond dissociation enthalpy somewhat; the data show an average of 0.5 kcal mol⁻¹ here. Table 4.8 provides a comparison of the C—H, O—H, OO--H bond dissociation enthalpies for cyclopentadienone related species and literature value for cyclic and linear compounds.

The C—H bond dissociation enthalpies are important properties that relate the respective reactivity / stability at specific carbon sites. Table 6 shows and compares BDE values of this study with that of the literature, where data are available.

- C—H bond dissociation enthalpies for the carbonyl-vinyl site [y(c₅h₃do)j2] is 117.4 kcal mol⁻¹. This is lower than the corresponding bond on furan 1-3 kcal mol⁻¹ and higher than on benzene by ~ 4 kcal mol⁻¹.

- C—H bond dissociation enthalpies for secondary vinyl-3-yl site [y(c₅h₃do)j3] is 113.8 kcal mol⁻¹, similar to that on benzene.
- C—H bond dissociation enthalpies for 2-hydroxyl-3-yl and 2-hydroperoxyl-3-yl sites [y(c₅h₃do)oh2-3j and y(c₅h₃do)q-2j] are 117.2 and 117.4 kcal mol⁻¹.
- C—H bond dissociation enthalpies for 2-hydroxyl-4-yl and 2-hydroperoxyl-4-yl sites [y(c₅h₃do)oh2-4j and y(c₅h₃do)q-3j] are 113.9 and 114.3 kcal mol⁻¹, respectively.
- C—H bond dissociation enthalpies for 2-hydroxyl-5-yl and 2-hydroperoxyl-5-yl sites [(y(c₅h₃do)oh2-5j and y(c₅h₃do)q-3j] are 118.3 and 118.0 kcal mol⁻¹, respectively.
- C—H bond dissociation enthalpies for 3-hydroxyl-2-yl sites [(y(c₅h₃do)oh3-2j] is 119.8 kcal mol⁻¹, similar to that on furans.
- C—H bond dissociation enthalpies for 3-hydroxyl-4-yl and 3-hydroperoxyl-4-yl sites [(y(c₅h₃do)oh3-4j and y(c₅h₃do)q3-4j] are 116.0 and 115.8 kcal mol⁻¹, respectively.
- C—H bond dissociation enthalpies for 3-hydroxyl-5-yl and 3-hydroperoxyl-5-yl sites [(y(c₅h₃do)oh3-5j and y(c₅h₃do)q3-5j] are 117.6 and 117.4 kcal mol⁻¹ about 2 kcal mol⁻¹ weaker than the C—H bond on furans.

C—H bond dissociation enthalpies for cyclopentadienone with a peroxy or a hydroperoxy group at the respective one similar radical site vary by less than 1 kcal mol⁻¹ (between 0.2-0.9 kcal mol⁻¹).

Table 4.8 Comparison of C—H, O—H, and OO—H Bond Dissociation Enthalpies

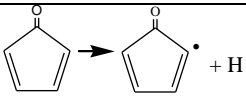

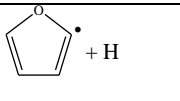
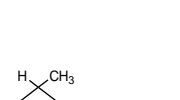
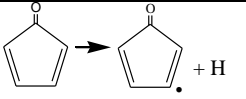
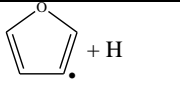
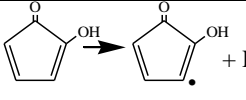
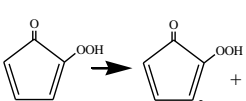
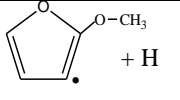
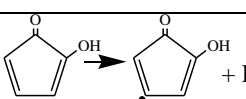
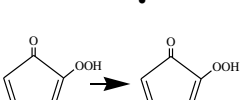
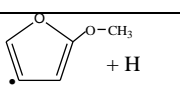
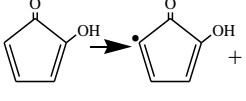
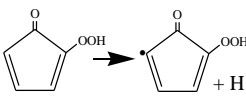
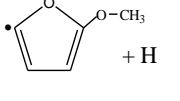
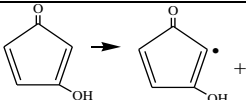
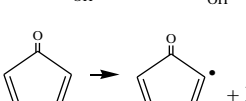
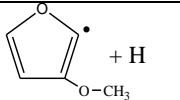
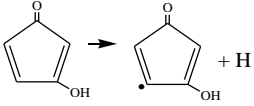
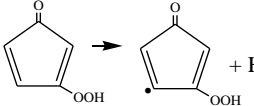
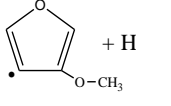
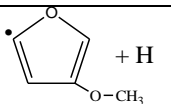
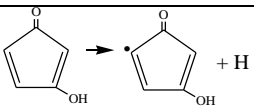
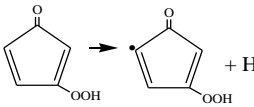
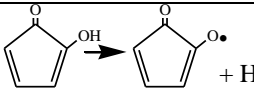
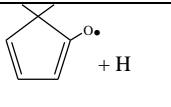
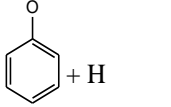
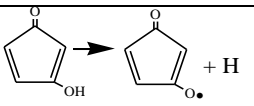
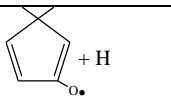
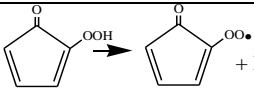
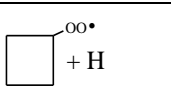
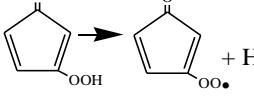
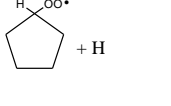
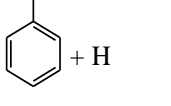
C—H Bond Dissociation Enthalpies (kcal mol ⁻¹)		Values for comparison
 	 	(cdcjqc + H) 110.17 ¹⁰⁸ (cdcjc + H) 106.28 ⁸¹ (ccjdcc + H) 108.6 ¹¹⁰ (cdcjcdo + H) 112.82 ¹¹¹
		
 		
 		
 		
 		

Table 4.8 Comparison of C—H, O—H, and OO—H Bond Dissociation Enthalpies (Continued)

C—H Bond Dissociation Enthalpies (kcal mol ⁻¹)		Values for comparison
 	 	
 		
O—H Bond Dissociation Enthalpies (kcal mol ⁻¹)		
	 	(cdccoj + H) 105.9 ¹¹⁰ alkoxy radical
		(cdcoj + H) 86.4 ¹¹⁰ vinoxyl radical
OO—H Bond Dissociation Enthalpies (kcal mol ⁻¹)		
		(cdcc(ooj) + H) 86.61 ¹⁰⁸
	 	(c(ooj)cdo + H) 87.28 ¹¹⁴ (cdc(ooj)c + H) 84.81 ⁸¹ (ccdc(ooj)c + H) 85.52 ⁸¹ Peroxy radical

Note: • and j = radical site, d = double bond, q = OOH group

Alkoxy and Peroxide bonds

The O—H bond dissociation enthalpies for different alcohols forming an alkoxy radical site on the ring.

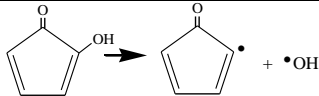
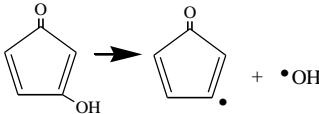
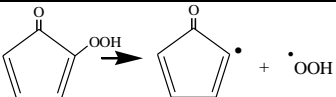
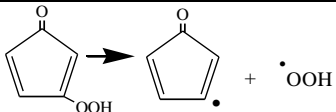
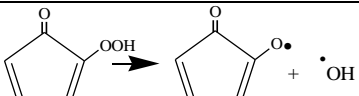
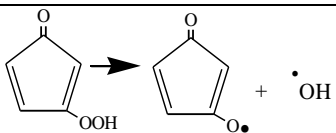
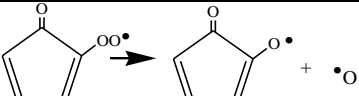
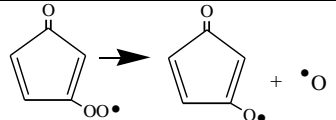
- O—H bond dissociation enthalpies at alkoxy-2-yl site [y(c₅h₃do)oj2] is 74.1 kcal mol⁻¹ that close to the 1,3-c₅h₅o reference species from Wang and Brezinsky⁶¹ (73.5 kcal mol⁻¹), and lower than a phenol - phenoxy radical by more than 10 kcal mol⁻¹.
- O—H bond dissociation enthalpies at alkoxy-3-yl site [y(c₅h₃do)oj3] is 79.0 kcal mol⁻¹.

The O—OH bond dissociation enthalpies are from the calculated $\Delta_f H^\circ_{298}$ of parent hydroperoxide molecule and their alkoxy radical corresponding to loss of [•]OH, where the enthalpies of parent molecule and radicals are calculated in this study in conjunction with the value of 8.95²¹ kcal mol⁻¹ for [•]OH at 298.15 K. The hydroperoxide carbon bond, the RC—OOH bond dissociation enthalpies are report from the calculated $\Delta_f H^\circ_{298}$ of parent hydroperoxide molecule corresponding to loss of [•]OOH ($\Delta_f H^\circ_{298}$ of 2.94²² kcal mol⁻¹) used in the calculation. The RO—O bond dissociated enthalpies were calculate with the value of 59.55²⁰ kcal mol⁻¹ for [•]O at 298.15 K. Table 5 provides the C—OOH, RO—OH, and RO—O bond dissociations enthalpies from this study.

Bond dissociation enthalpies for peroxy radical sites ROO—H on the ring.

- OO—H bond dissociation enthalpies at peroxy-2-yl site [y(c₅h₃do)ooj2] is 88.1 kcal mol⁻¹, which is stronger linear alkyl peroxides by 2-3 kcal mol⁻¹.
- OO—H bond dissociation enthalpies at peroxy-3-yl site [y(c₅h₃do)ooj3] is 89.3 kcal mol⁻¹.

Table 4.9 Comparison of R—OH, R—OOH, RO—OH, RO—O Bond Dissociation Enthalpies (kcal mol⁻¹)

Bond Dissociated	C—OH Bond dissociation enthalpies
	118.52
	117.14
Bond Dissociated	C—OOH Bond dissociation enthalpies
	89.46
	90.90
Bond Dissociated	RO—OH Bond dissociation enthalpies
	7.76 <i>Hydroperoxide not stable</i>
	15.49
Bond Dissociated	RO—O Bond dissociation enthalpies
	22.40
	28.92

Note: • = radical site

4.4 Kinetic Properties

4.4.1 Ring Opening Reactions of Cyclopentadienone Vinyl Radicals

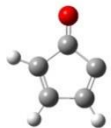
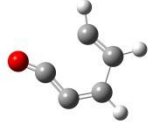
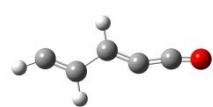
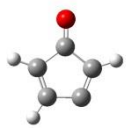
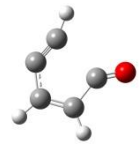
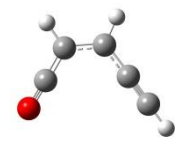

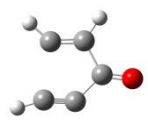
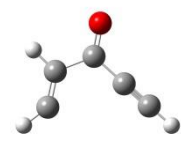
Canonical transition state theory was used to calculate the ring opening kinetic parameters for Cyclo-pentadienone-2yl [y(c₅h₃do)j2] and Cyclo-pentadienone-3yl [y(c₅h₃do)j3] radicals. The M062X⁵ and wB97X⁶ hybrid density functional theory methods were used with the 6-311+G(d,p) basis set, along with the composite CBS-QB3⁴ level of theory. There are two paths, both beta scissions for ring opening reaction of Cyclo-pentadienone-2yl radical; one is to transition state (TS3) at 35.6 kcal mol⁻¹ as shown in Table 8 forming C≡C-C(=O)C=C•. A second is TS1 to form C•=C--C=C=C=O with a barrier of 30.7, both barriers at the CBS-QB3 level.

A lower barrier exists for the y(c₅h₃do)j3 radical at 23.7 kcal mol⁻¹ for the ring opening, beta scission reaction to form C≡CC=C-C•=O from the Cyclo-pentadienone-3yl radical. High pressure limit Rate parameter expressions in table 4.10 is calculated based on B3LYP/CBSB7 structure.

Table 4.10 High Pressure-Limit Rate Parameters for Ring Opening Reactions

Reactions	$k = A(T)^n \exp(-Ea/RT) \text{ cm}^3/\text{mol}\cdot\text{s}$		
	<i>A</i>	<i>n</i>	<i>Ea</i> (kcal mol ⁻¹)
y(c ₅ h ₃ do) j2 → TS1	1.03 x 10 ¹¹	0.93	30.7
y(c ₅ h ₃ do) j3 → TS2	3.61 x 10 ¹⁰	1.15	23.7
y(c ₅ h ₃ do) j3 → TS3	1.07 x 10 ¹⁰	1.30	35.6

Table 4.11 Ring Opening Reactions of Cyclo-Pentadienone-2yl and Cyclo-Pentadienone-3yl Radicals. Enthalpies of Reactants, Transition State Structures and Products

Methods	Reactant	TS	Product	
				<i>Ea</i>
	y(c5h3do)j2	TS1	cj=c--c=c=c=o	
M062X/ 6-311+G(d,p)	78.30	110.43	98.21	32.13
ωB97X/ 6-311+G(d,p)	78.30	112.02	101.03	33.72
CBS-QB3	78.30	108.97	102.14	30.67
				
	y(c5h3do)j3	TS2	c≡c-c=c-cj=o	
M062X/ 6-311+G(d,p)	74.72	97.98	69.14	23.26
ωB97X/ 6-311+G(d,p)	74.72	100.94	70.52	26.22
CBS-QB3	74.72	98.44	72.42	23.72
				
	y(c5h3do)j2	TS3	c≡c-c(=o)c=cj	
M062X/ 6-311+G(d,p)	78.30	116.27	100.30	37.97
ωB97X/ 6-311+G(d,p)	78.30	117.63	102.99	39.33
CBS-QB3	78.30	113.89	102.27	35.59

Note: unit is kcal mol⁻¹, y= cyclic ring, TS = transition state

4.4.2 $R\cdot + O_2$ Potential Energy Surface and Chemical Activation Reactions

Figures 4.4 and 4.5 show potential energy diagrams for the chemical activation reactions of O_2 addition with the 2 and 3 carbon radical sites on cyclopentadienone and the further reactions involving: stabilization to $ROO\cdot$, $RO\cdot + O$ (chain branching), intramolecular H atom transfers from the carbon atom sites to the peroxy radical, and intramolecular peroxy radical additions to the sp^2 carbons.

The C_2 and C_3 carbon radical sites on the ring have deep $R\cdot + O_2 \rightarrow ROO\cdot$ reaction well depths of 50.5 and 50.8 kcal mol⁻¹, respectively. The Enthalpy of Reaction (ΔH_{RXN}^0) for the chain branching reaction to cleave the $RO-O$ bond is only 22.4 and 29 kcal mol⁻¹ for the C_2 and C_3 peroxy sites as shown in figures 3 and 4 and Table 5. The reverse reactions of the peroxy radicals back to parent radical + O_2 , which often dominate over the branching reactions in conventional alkyl peroxy radicals, each have an endothermicity (barrier) of slightly over 50 kcal mol⁻¹ and will not be competitive.

Reactions involving intramolecular hydrogen transfer from the carbon sites on the ring to the peroxy radical sites are also illustrated. The activation enthalpy (E_a) for these reactions is 10 kcal mol⁻¹ or more above that of the $RO + O$ branching channel for the H transfer reaction of $y(c_5h_3do)ooj2$ to $y(c_5h_3do)q2-3j$. The intramolecular transfer reaction of the $y(c_5h_3do)ooj3$ peroxy radical can abstract a hydrogen atom from two sites, forming products $y(c_5h_3do)q3-2j$ and $y(c_5h_3do)q3-4j$, where the barriers to these H atom transfers are more than 13 kcal mol⁻¹ above the branching path. There is one low energy reaction path that competes with the chain branching reactions in the cyclopentadienone 2 and 3 peroxy radical systems: this is the ipso addition of the peroxy radical to the ring forming a dio-oxirane ring, which occurs for both the C_2 and C_3 peroxy radicals. The peroxy

radical adds to the carbon site of the peroxide group (ipso addition) forming cyclopentadienone-2-dioxirane [ycpdo-2-y(oo)] and Cyclopentadienone-3-dioxirane [ycpdo-3-y(oo)]. The respective barriers are 22.8 and 24.4 kcal mol⁻¹, respectively. The low barriers make these product channels competitive with the chain branching reaction (RO + O) in the Potential Energy (PE) diagrams, figure 3 and 4, but also have somewhat tighter transition state structures.

The intramolecular peroxy radical addition reactions that result in a four member ring shown in Figures 4.4 and 4.5 have barriers that are near 10 kcal mol⁻¹ higher than the chain branching and dioxirane paths.

The R• + O₂ reactions to RO• + O chain branching reactions will be important paths when the cyclopentadienone carbon radicals are formed in combustion systems.

The thermochemical properties along with the forward and reverse rate constants (high-pressure limit) are calculated for each elementary reaction step. Multi frequency quantum Rice Ramsperger-Kassel (QRRK) analysis is used for $k(E)^{30-32}$ with master equation analysis³³⁻³⁵ used for falloff. The QRRK analysis is described by Chang et al.³⁰. Tables 4.12 and 4.13 list the high pressure-limit, elementary rate parameters used as input data to the QRRK calculations.

The chemical activation reaction kinetic results versus temperature and pressure are presented in Figures 4.6 to 4.13 for the Cyclo-pentadienone-2-yl radical and Cyclopentadienone-3-yl radical systems, respectively.

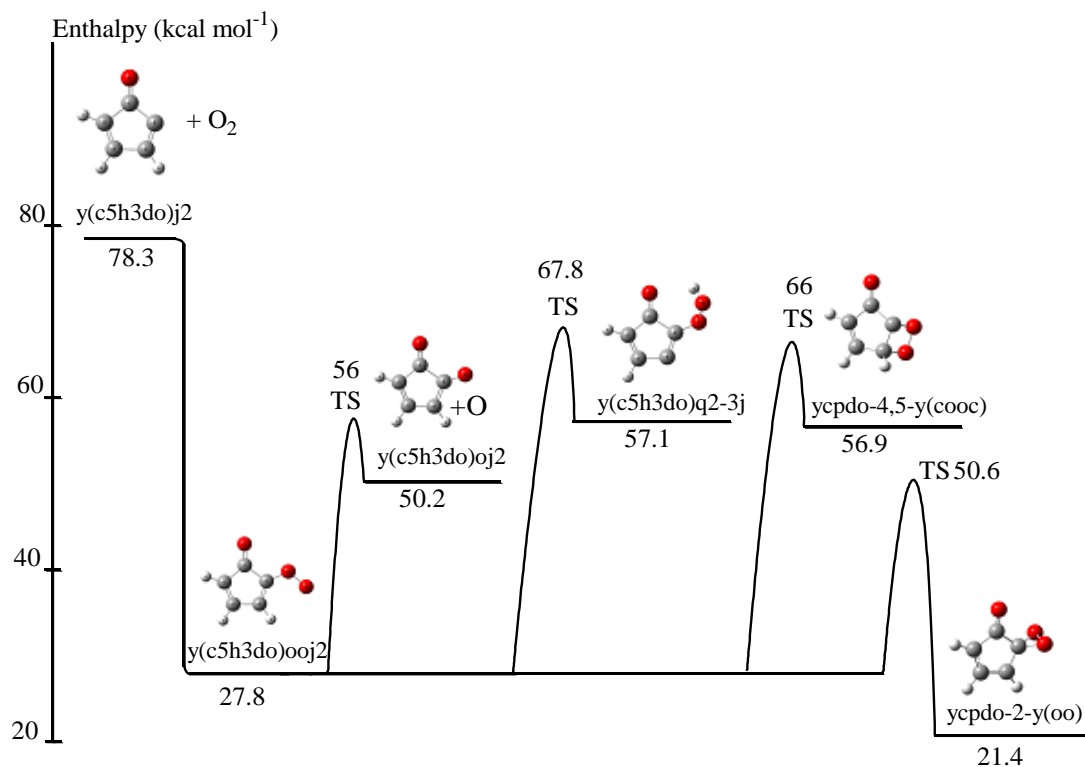


Figure 4.4 Reactions of cyclo-pentadienone-2-yl (TS=Transition State).

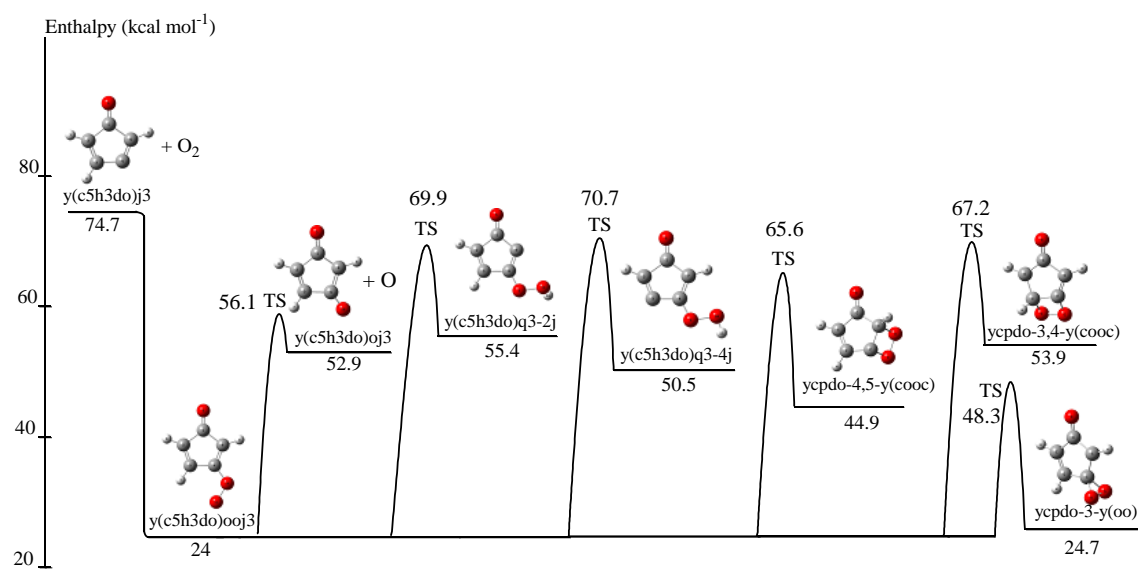
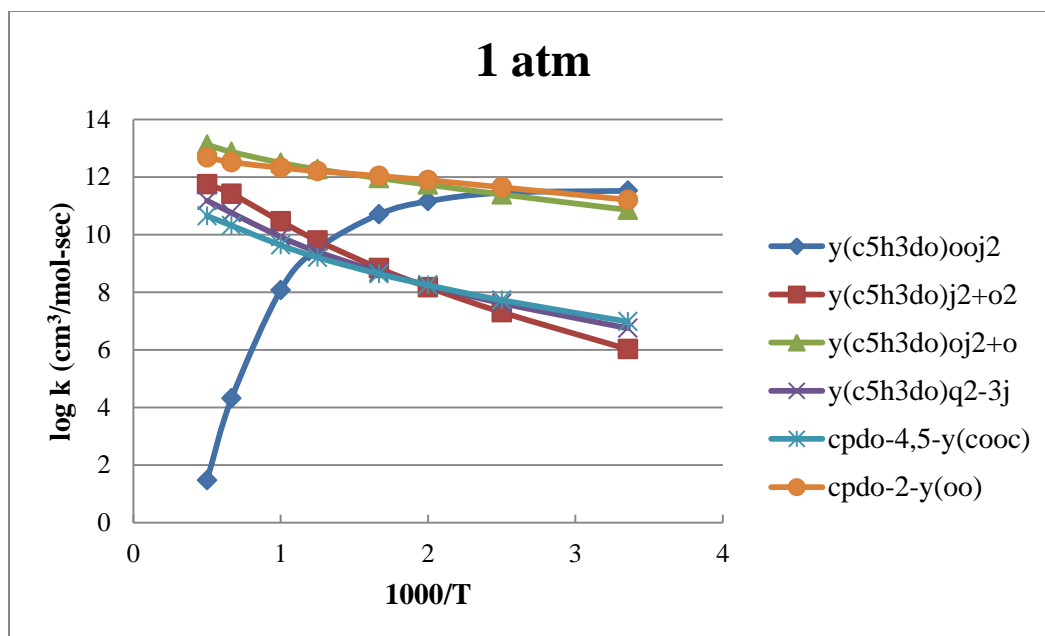


Figure 4.5 Reactions of cyclo-pentadienone-3-yl (TS=Transition State).

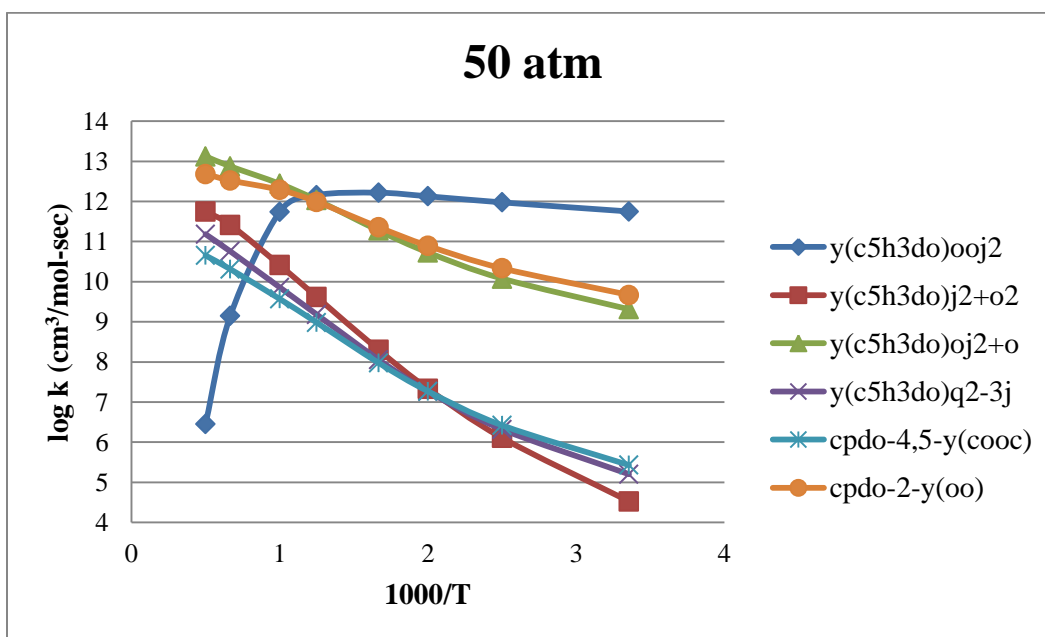
Table 4.12 High Pressure-Limit Rate Parameters for Cyclo-Pentadienone-2-yl Radical Reactions

Reactions	$k = A(T)^n \exp(-Ea/RT)$		
	<i>A</i>	<i>n</i>	<i>Ea</i> (kcal mol ⁻¹)
y(c5h3do)j2 + o ₂ → y(c5h3do)ooj2	1.6 x 10 ⁷	1.84	0.00
y(c5h3do)ooj2 → y(c5h3do)j2 + o ₂	3.22 x 10 ¹⁸	-1.17	50.50
y(c5h3do)ooj2 → y(c5h3do)oj2 + o	5.66 x 10 ¹²	0.26	28.22
y(c5h3do)ooj2 → y(c5h3do)q2-3j	1.97 x 10 ¹¹	0.49	40.20
y(c5h3do)ooj2 → ycpdo-4,5-y(cooc)	2.59 x 10 ¹²	-0.06	38.66
y(c5h3do)ooj2 → ycpdo-2-y(oo)	3.07 x 10 ¹²	0.06	23.25

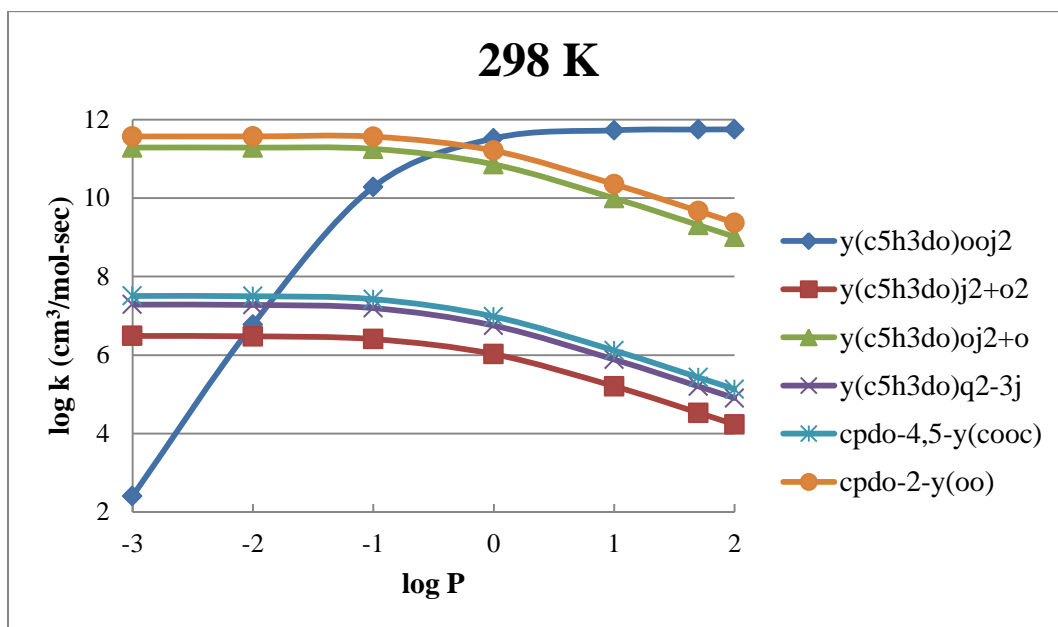
Results from the QRRK / Master Equation analysis show the important channels are the competitive of chain branching (RO• + O), product from intramolecular peroxy addition (cyclopentadienone-2-dioxirane) and products from intramolecular transfer to the peroxy radical. Figure 4.6 shows stabilization (Cyclo-pentadienone-peroxyl-2-yl), is the most important channel up to 400 K. at 1 atm pressure, with the di-oxirane ring (cyclopentadienone-2-dioxirane) and the chain branching RO + O (y(c5k3do)oj+o) slightly lower. Above 400 K the stabilization shows falloff and the dioxirane and the RO• + O channels dominate, with the dioxirane slightly between 400 and 1000K and chain branching dominates above 1000K. At 50 atm. pressure, Figure 4.7 shows that stabilization (Cyclo-pentadienone-peroxyl-2-yl) is the most important product up to 1000 K. Near 1000 K stabilization, chain branching and dioxirane formation are similar. Above 1000K chain branching dominates slightly over dioxirane formation through the higher temperatures, while stabilization shows rapid falloff. The intramolecular hydrogen atom transfer reactions to form a hydroperoxide and alkenyl radical are several orders of magnitude lower.



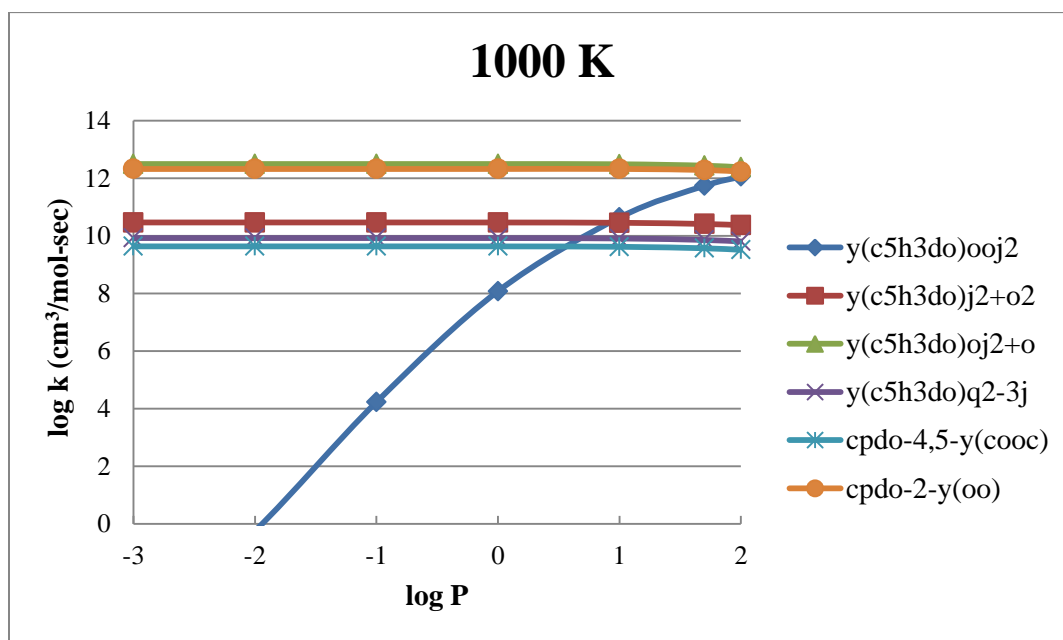
Figures 4.6 Rate constants (log k) vs temperature (1000/T) at 1 atm for of cyclopentadienone-2-yl system.



Figures 4.7 Rate constants (log k) vs temperature (1000/T) at 50 atm of cyclopentadienone-2-yl system.



Figures 4.8 Rate constants ($\log k$) vs tressure ($\log P$) at 298 K of cyclo-pentadienone-2-yl system.



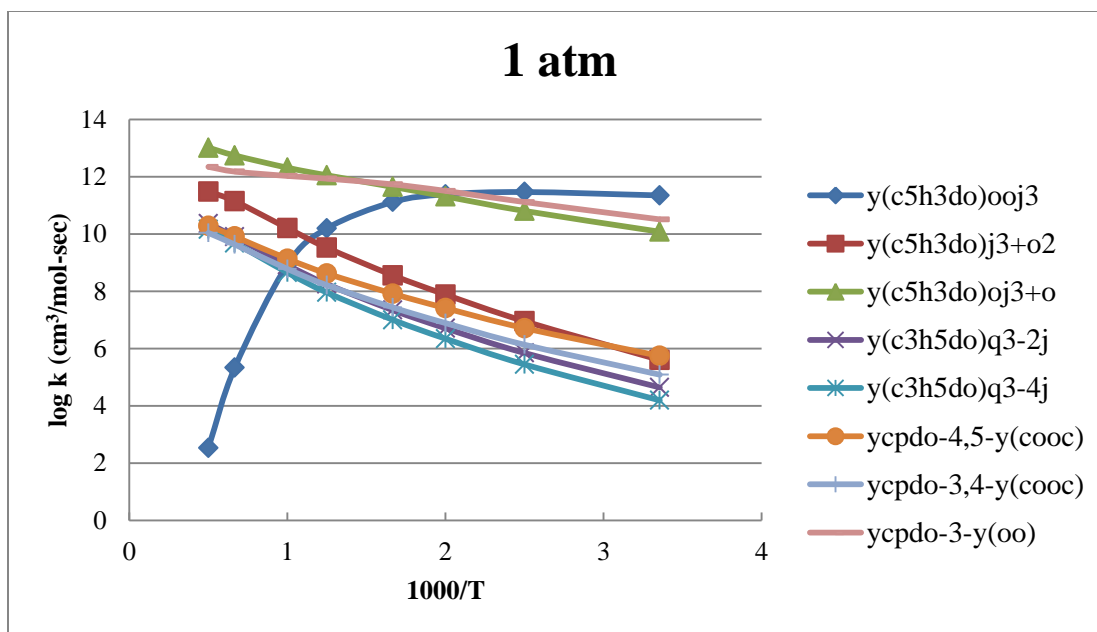
Figures 4.9 Rate constants ($\log k$) vs pressure ($\log P$) at 1000 K of cyclo-pentadienone-2-yl system.

Figure 4.8 illustrates the rate constants as a function of pressure at 298K. At pressures of 1 Atm and above the stabilized Cyclo-pentadienone-peroxyl-2-yl is the dominant channel and cyclopentadienone-2-dioxirane and $y(c5k3do)oj+o$ products are lower. Below 1 Atm., stabilization starts to falloff rapidly with decreasing pressure. The cyclopentadienone-2-dioxirane and the chain branching reaction $[y(c5k3do)oj+o]$ are the dominate reactions below 1Atm pressure. Figure 4.9 shows rate constants versus pressure at 1000 K. Cyclopentadienone-2-dioxirane, and the chain branching channel are near equal and dominate over the entire pressure range with stabilization only approaching these two main channels at 100 Atm. Intramolecular hydrogen atom transfer reactions are considered not important

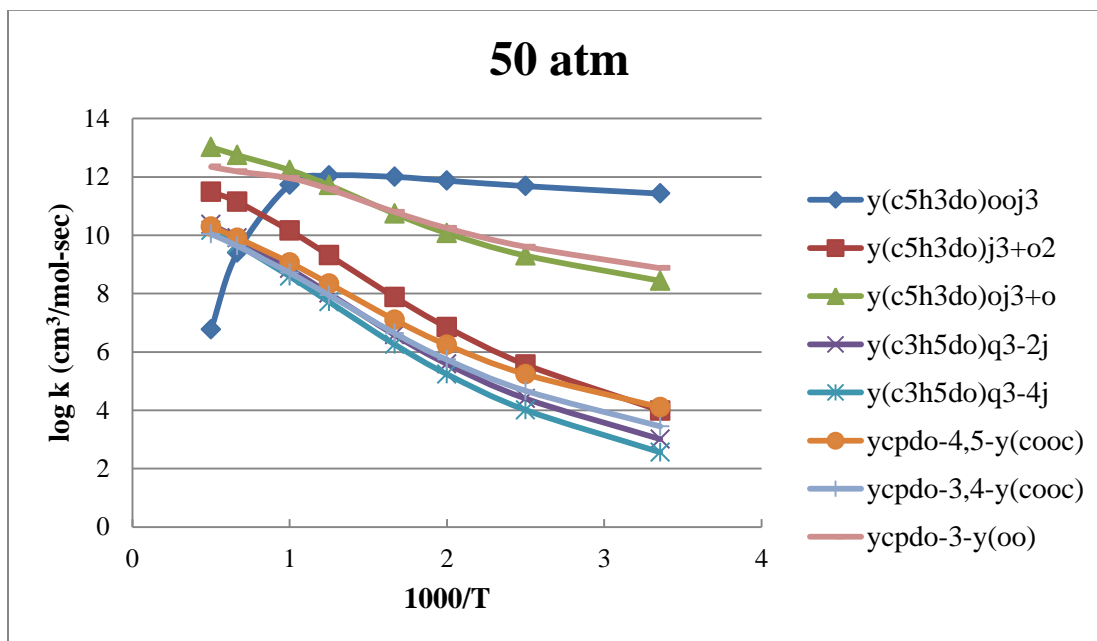
Figures 4.10 and 4.11 illustrate the rate constants for the cyclo-pentadienone-3-yl radical reactions with 3O_2 versus temperature at 1 and 50 atmospheres.

Table 4.13 High Pressure-Limit Rate Parameters for Cyclo-Pentadienone-3-yl Radical Reactions

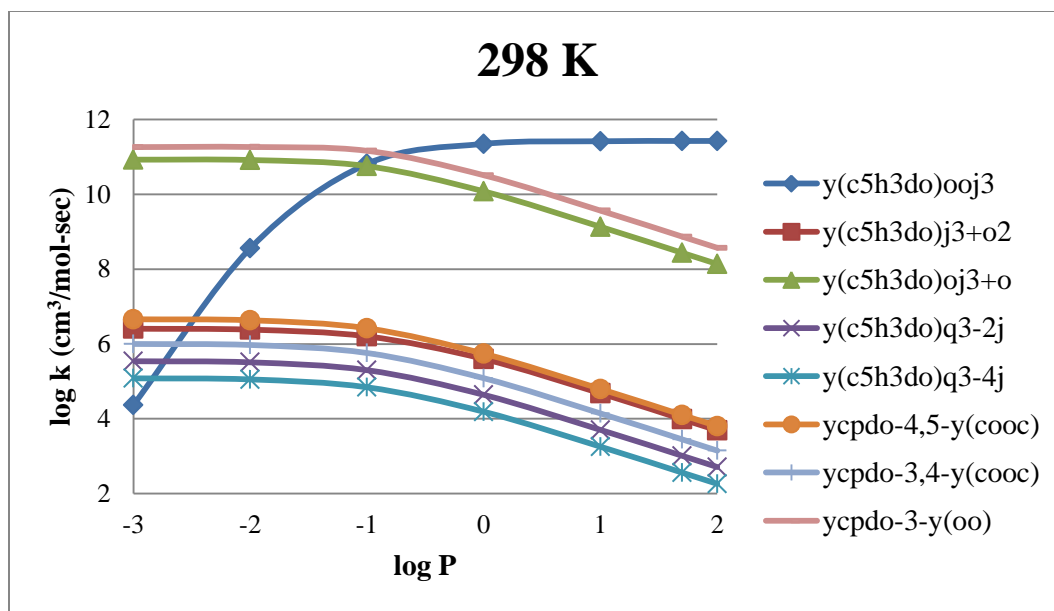
Reactions	$k = A(T)^n \exp(-Ea/RT)$		
	<i>A</i>	<i>n</i>	<i>Ea</i> (kcal mol ⁻¹)
$y(c5h3do)j3 + o_2 \rightarrow y(c5h3do)ooj3$	2.40×10^6	2.04	0.00
$y(c5h3do)ooj3 \rightarrow y(c5h3do)j3 + o_2$	4.94×10^{17}	-0.91	50.70
$y(c5h3do)ooj3 \rightarrow y(c5h3do)oj3 + o$	5.10×10^{12}	0.45	32.09
$y(c5h3do)ooj3 \rightarrow y(c5h3do)q3-2j$	2.47×10^{11}	0.50	46.11
$y(c5h3do)ooj3 \rightarrow y(c5h3do)q3-4j$	1.39×10^{11}	0.54	46.91
$y(c5h3do)ooj3 \rightarrow ycpdo-4,5-y(cooc)$	3.75×10^{11}	0.28	41.90
$y(c5h3do)ooj3 \rightarrow ycpdo-3,4-y(cooc)$	2.00×10^{11}	0.34	43.49
$y(c5h3do)ooj3 \rightarrow ycpdo-3-y(o)$	4.55×10^{12}	0.34	24.63



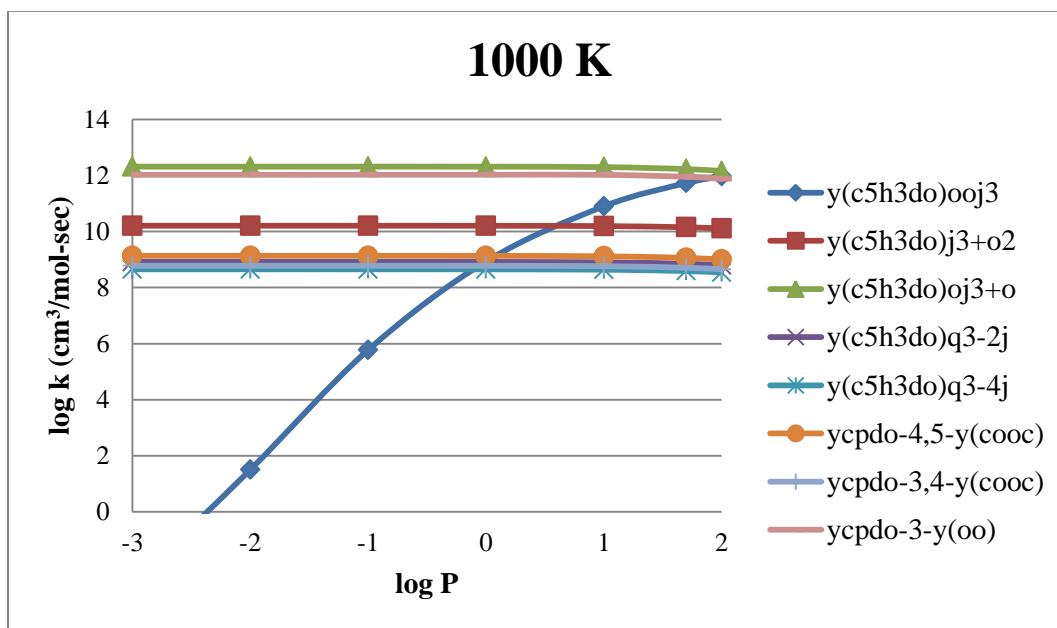
Figures 4.10 Rate constants (log k) vs temperature (1000/T) at 1 atm of cyclopentadienone-3-yl system.



Figures 4.11 Rate constants (log k) vs temperature (1000/T) at 50 atm of cyclopentadienone-3-yl system.



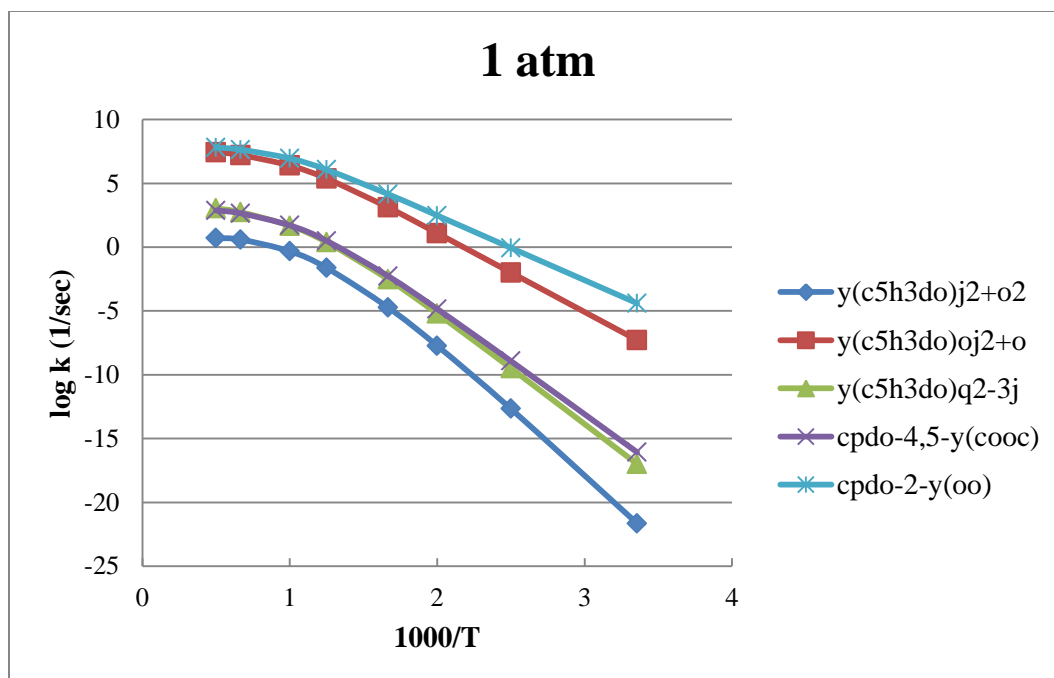
Figures 4.12 Rate constants (log k) vs pressure (log P) at 298 K of cyclo-pentadienone-3-yl system.



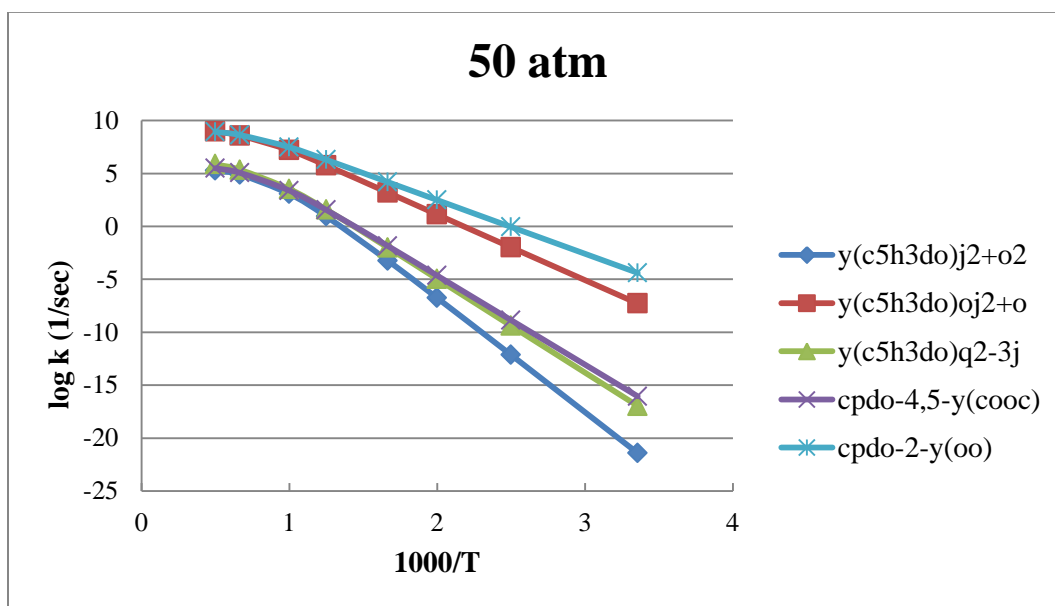
Figures 4.13 Rate constants (log k) vs pressure (log P) at 1000 K of cyclo-pentadienone-3-yl system.

The cyclo-pentadienone-3-yl radical reaction with $^3\text{O}_2$ shows similar results to the cyclo-pentadienone-2-yl radical reactions with $^3\text{O}_2$. Figures 4.10 and 4.11 show rates constants vs temperature, where stabilization dominates at temperatures below 500 K at 1Atm, and below 1000 K at 50 Atm. The chain branching ($\text{RO}\cdot + \text{O}$) and the intramolecular peroxy ipso addition (cyclopentadienone-3-dioxirane) are dominant at higher temperatures with the chain branching channel $[\text{y}(\text{c5h3do})\text{oj3+o}]$ being higher. Figures 4.12 and 4.13 show the rate constants for cyclo-pentadienone-3-yl radical reactions with $^3\text{O}_2$ at temperatures of 298 and 1000K versus log pressure. The results are similar to the cyclo-pentadienone-2-yl radical system, where at 1000 K chain branching dominates over the entire pressure range and stabilization only approaches the high pressure limit at 100 Atm. The dioxirane ring formation is slightly lower than the $\text{RO}\cdot + \text{O}$ branching channel. At 298 K the stabilization is the major product channel above 0.1 Atm, and the branching and dioxirane ring channels dominate at pressures below 0.1 Atm.

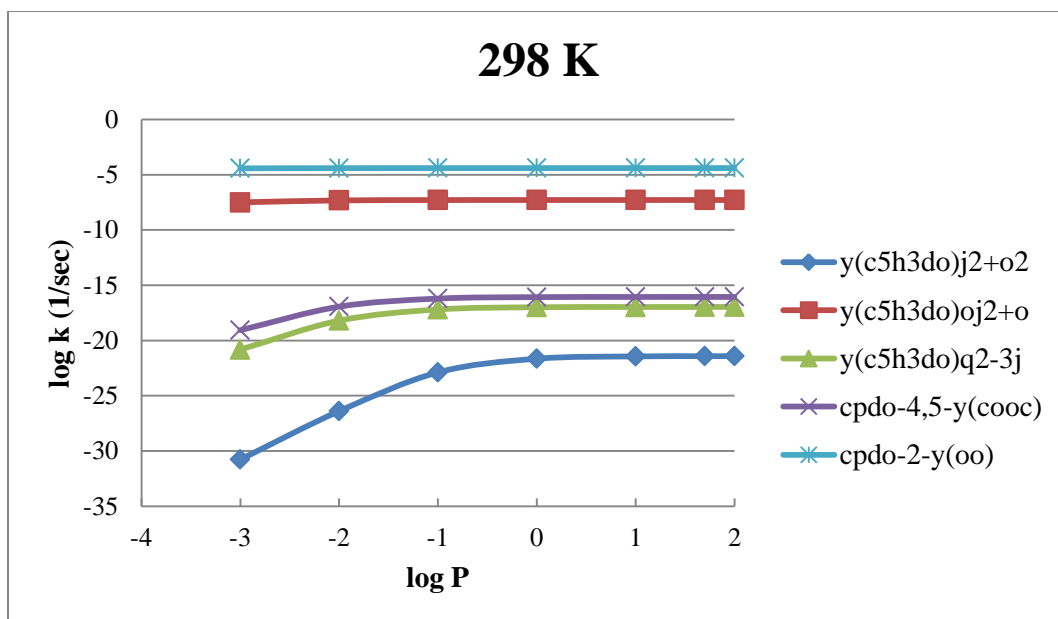
Overall, the cyclopentadienone radical, chemical activation oxidation reactions show a major fraction of the reaction to chain branching ($\text{RO}\cdot + \text{O}$) and to a dioxirane ring radical products in temperature and pressure regions important to internal combustion engines. The products of the dioxirane reaction paths and products need to be further evaluated.



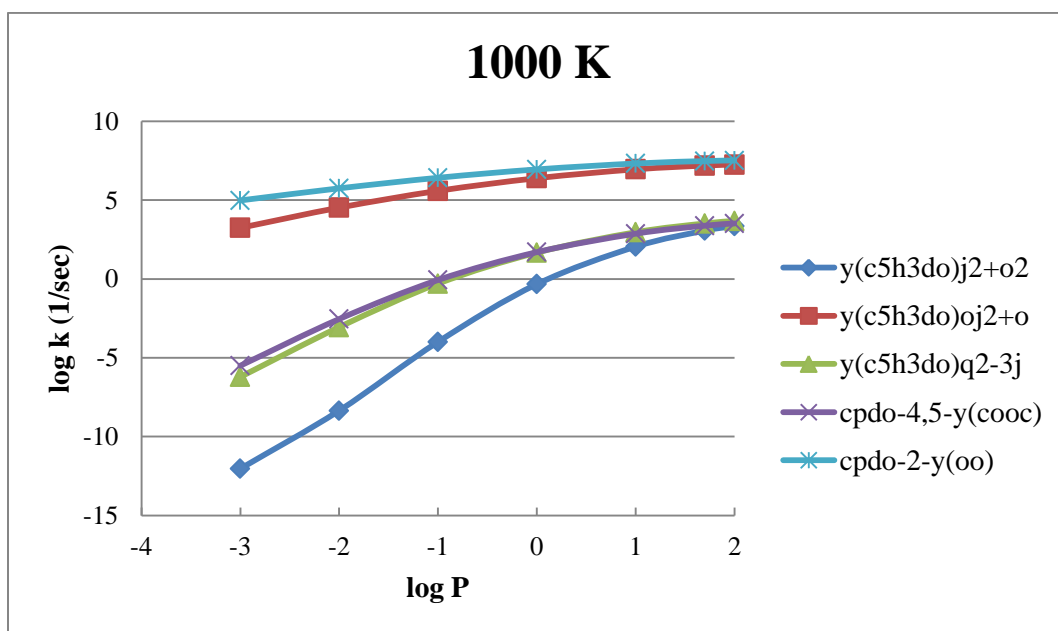
Figures 4.14 Rate constants (log k) vs. temperature (1000/T) at 1 atm. for cyclopentadienone-2-yl dissociation.



Figures 4.15 Rate constants (log k) vs. temperature (1000/T) at 50 atm. for cyclopentadienone-2-yl dissociation.



Figures 4.16 Rate constants ($\log k$) vs. pressure ($\log P$) at 298 K for cyclopentadienone-2-yl dissociation.

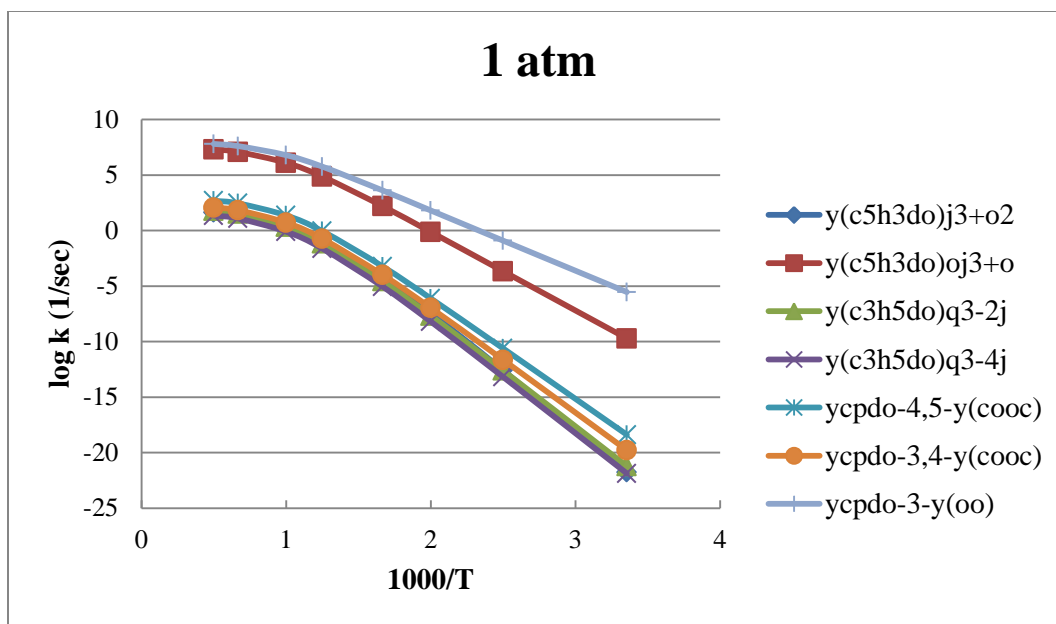


Figures 4.17 Rate constants ($\log k$) vs. pressure ($\log P$) at 1000 K for cyclopentadienone-2-yl dissociation.

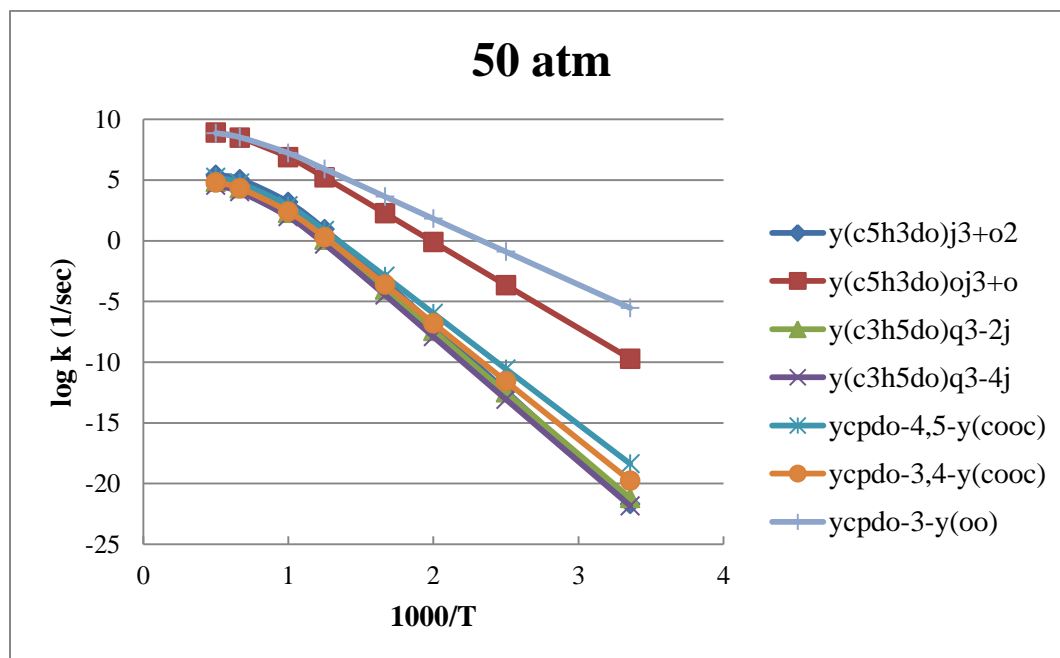
4.4.3 Unimolecular Dissociation Reactions

Unimolecular Dissociation of Cyclo-pentadienone-2-yl and Cyclo-pentadienone-3-yl peroxy radicals Plots of rate constant versus $1000/T$ for dissociation of the stabilized peroxy adduct y(c5h3do)ooj2 at 1 and 50 atm pressure are illustrated in Figures 4.14 and 4.15. The intramolecular peroxy ipso addition (cyclopentadienone-2-dioxirane) and the chain branching ($RO\bullet + O$) reactions are the dominant unimolecular dissociation reaction channels under all conditions. At temperatures below 1000K the cyclic dioxirane adduct dominates the chain branching, and at temperatures above 1000K, the chain branching and dioxirane ring are similar at both pressures. Plots of rate constant versus log pressure at 298 and 1000 K are illustrated in Figure 4.16 and 4.17 at 1 and 50 atm, respectively. At 298 K this cyclo-pentadienone-2-yl peroxy radical dissociates to the dioxirane ring adduct at several molecules per day over the entire pressure range. At 1000 K the dioxirane ring dominates the chain branching at pressures above 5 atm the two channels are competitive.

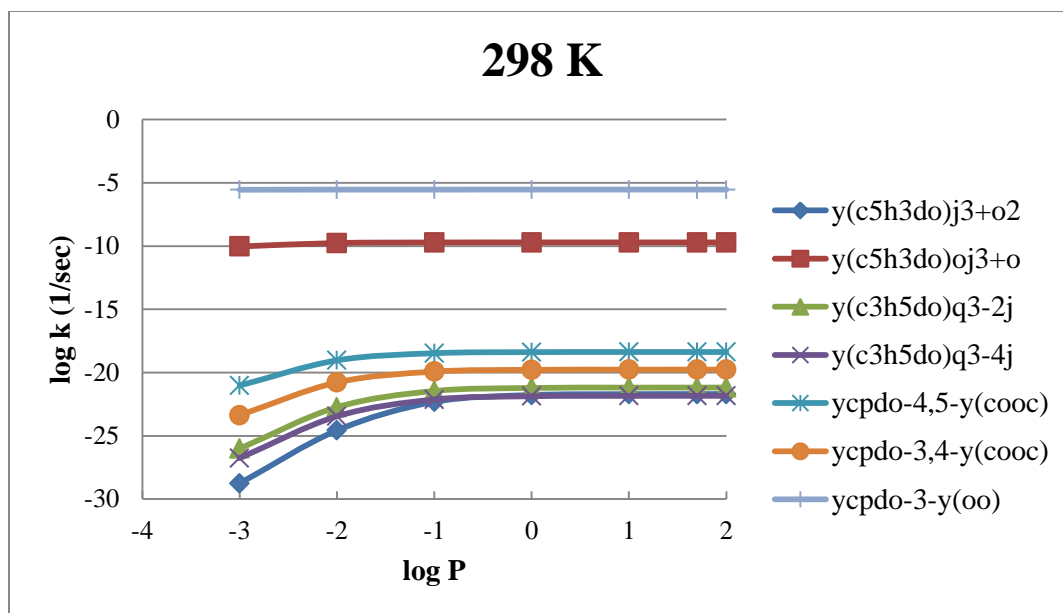
The rate constant for the cyclo-pentadienone-3-yl peroxy radical dissociation reaction at 1 and 50 atm are shown in Figure 4.18 and 4.19. The dominant unimolecular reaction paths are similar to that of the cyclo-pentadienone-2-yl peroxy, dioxirane ring and chain branching paths, with the reaction paths being about one order of magnitude lower than those of the cyclo-pentadienone-2-yl peroxy radical adduct. At pressures above 10 atm at 1000 K the cyclopentadienone-3-dioxirane formation reaction is the dominant path with a smaller fraction to the chain branching.



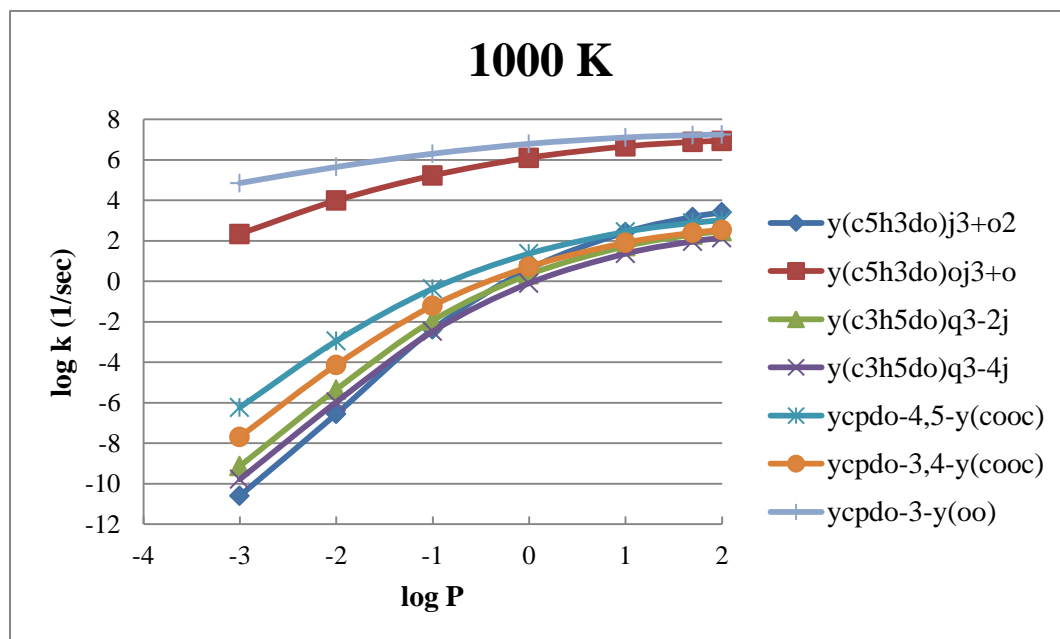
Figures 4.18 Rate constants (log k) vs. temperature (1000/T) at 1 atm. for cyclopentadienone-3-yl dissociation.



Figures 4.19 Rate constants (log k) vs. temperature (1000/T) at 50 atm. for cyclopentadienone-3-yl dissociation.



Figures 4.20 Rate constants (log k) vs. pressure (log P) at 298 K for cyclopentadienone-3-yl dissociation.



Figures 4.21 Rate constants (log k) vs. pressure (log P) at 1000 K for cyclopentadienone-3-yl dissociation.

Table 4.14 High Pressure-Limit Elementary Rate Parameter for Important Paths In Cyclo-Pentadienone-2-yl and Cyclo-Pentadienone-3-yl Peroxy Radical System versus Pressure

Reactions	Pressure (atm)	$k = A(T)^n \exp(-Ea/RT)$		
		A	n	Ea (kcal mol ⁻¹)
y(c5h3do)ooj2 → y(c5h3do)oj2+o	0.1	8.68 x 10 ⁴⁹	-12.05	37.5
	1	6.98 x 10 ⁴¹	-9.22	36.05
	10	8.75 x 10 ³⁴	-6.88	34.6
	50	1.87 x 10 ²⁹	-5.02	33.1
y(c5h3do)ooj2 → cpdo-2-y(oo)	0.1	7.27 x 10 ⁴²	-9.89	31.2
	1	2.24 x 10 ³⁵	-7.35	29.5
	10	4.90 x 10 ²⁹	-5.46	28.2
	50	1.63 x 10 ²⁵	-4	27.0
y(c5h3do)ooj3 → y(c5h3do)oj3+o	0.1	2.26 x 10 ⁵⁵	-13.59	43.0
	1	2.97 x 10 ⁴⁵	-10.18	41.1
	10	3.81 x 10 ³⁷	-7.52	39.3
	50	3.59 x 10 ³¹	-5.56	37.7
y(c5h3do)ooj3 → cpdo-3-y(oo)	0.1	1.69 x 10 ⁴³	-9.92	33.2
	1	6.32 x 10 ³⁴	-7.12	31.15
	10	6.56 x 10 ²⁸	-5.15	29.7
	50	2.87 x 10 ²⁴	-3.74	28.4

Note: j = radical site, y = cyclic ring

The high pressure-limit rate parameters versus pressure of chain branching and dioxirane formation reactions for Cyclo-pentadienone-2-yl and Cyclo-pentadienone-3-yl peroxy radical system are tabulated in Table 4.14 Chemical activation and unimolecular dissociation reaction rate parameters at pressures from 0.001 to 100 atm. and temperatures to 2000 K are in the appendix section.

4.5 Summary

Thermochemical properties of cyclopentadienone and cyclo-pentadienone- alcohols, hydroperoxides, vinylic radicals, alkoxy radicals and peroxy radicals are determined using Density Functional Theory B3LYP/6-31G(d,p) and the CBS-QB3 higher level composite calculation method with use of isodesmic work reactions. Thermochemical properties, standard enthalpy of formation ($\Delta_f H^\circ_{298}$), entropy (S°_{298}) and heat capacity ($C_P^\circ(T)$) for cyclopentadienone and corresponding 2-hydroxyl cyclopentadienone, 3-hydroxyl cyclopentadienone, 2-hydroperoxy cyclopentadienone, and 3- hydroperoxy cyclopentadienone and related radical species are reported. Entropy and heat capacity values versus temperature were also determined.

The computed standard enthalpy of formation for the lowest energy conformer of cyclopentadienone from this study is $13.0 \pm 1.88 \text{ kcal mol}^{-1}$ in agreement with data in the literature. The standard enthalpy of formation for the 2-hydroxyl cyclopentadienone, 3-hydroxyl cyclopentadienone, 2-hydroperoxy cyclopentadienone, and 3- hydroperoxy cyclopentadienone are $-31.3 \pm 2.67 \text{ kcal mol}^{-1}$, $-33.5 \pm 2.67 \text{ kcal mol}^{-1}$, $-8.2 \pm 2.41 \text{ kcal mol}^{-1}$, and $-13.2 \pm 2.41 \text{ kcal mol}^{-1}$, respectively. Bond dissociation enthalpies for C—H, O—H, OO—H, C—OOH, R—OH, R—OOH, RO—OH, and RO—O bonds on cyclopentadienone and the cyclopentadienone alcohols and hydroperoxides were also determined. The vinylic C—H bond dissociation energy for parent cyclopentadienone are 113.8 and 117.4 kcal mol^{-1} for the cyclo-pentadienone-2, and -3-yl peroxy radicals, respectively. The RO—OH bond dissociation energies on the cyclopentadienone via $y(c_5h_3do)oj2-OH$ and $y(c_5h_3do)oj3-OH$ bond are the weak bond at 7.8 and 15.5 kcal mol^{-1} , respectively and the RO—O bonds of $y(c_5h_3do)oj2-O$ and $y(c_5h_3do)oj-O$ are

also low at 22.4 and 29.0 kcal mol⁻¹, respectively. The R—OO bond dissociation energies of $\gamma(\text{C}_5\text{H}_3\text{DO})\beta_2\text{—OO}$ and $\gamma(\text{C}_5\text{H}_3\text{DO})\beta_3\text{—OO}$ system are at 50 kcal mol⁻¹ that stronger than corresponding bonds on phenyl systems⁷⁰ at 44.9 kcal mol⁻¹.

The chemical activation oxidation reactions, of the two vinylic radicals in cyclopentadienone, with oxygen show significant chain branching forming cyclopentadienone-2 and -3-yl alkoxy radicals (RO•) + oxygen atom (O) products, on the order of 50 % in several important temperature and pressure ranges. The other major product from the oxidation reaction product is formation of a dioxirane ring on the carbon of a cyclopentennone radical.

CHAPTER 5

KINETICS OF HYDROGEN ADDITION REACTION AT PRIMARY, SECONDARY AND TERTIARY SITES IN SMALL OLEFINS: COMPARISONS WITH EXPERIMENTAL DATA

5.1 Overview

Addition of Hydrogen atom to alkenes (olefins) and the reverse reaction – the β scission elimination of H atoms from alkane carbon radicals, have been investigated experimentally, primarily for smaller olefin systems. The studies usually involve monitoring the H atom loss and it is often difficult for the experimentalist to identify the products, that is - the addition site, when the olefin is not symmetrical. Both the forward and the reverse reactions are important in combustion systems: (i.) the reverse where a radical is formed on a alkyl carbon by an abstraction reaction and then there is competition between reaction of the radical with O_2 or the beta-scission elimination reaction of which one step is H atom loss and (ii.) where H atoms are present and they can add to the unsaturated bond with low energies of activation.

Olefins are also important reaction species in the formation of aromatics in combustion systems¹¹⁵ where aromatics are strongly linked with soot formation. Under low temperature – atmospheric conditions, olefins are consumed by radical-addition, and loss of hydrogen via abstraction reactions. Under combustion conditions olefins are consumed by simple dissociation, abstraction and less frequently by addition reactions. The addition reactions occur, but at the higher temperatures of combustion systems, the reverse (beta scission is also fast). As an example, in combustion processes the ethyl (C_2H_5) radical play an important role, as it is formed from hydrogen atom addition to stable olefins. Here the reaction energies are relatively small, and these radicals are

formed and also tend to dissociate rapidly in the primary reaction zones of premixed flames¹¹⁶.

H atoms are very important in combustion systems as they are the key specie in the chain branching reaction of H atoms with O₂, where reaction of one radical results in formation of two radicals: $\text{H} + \text{O}_2 = \text{OH} + \text{O}$.

In 2002, Turányi et al.¹¹⁷ investigated the kinetic and thermodynamic uncertainties of the methane flame, and indicated that hydrogen radical is the most active chain carrier (involved in chain-propagating reactions) in hydrocarbon combustion system.

One goal of this work is to use the data from experiments on hydrogen atom addition to small olefins at the primary (p), secondary (s), and tertiary (t) sites to identify a reasonably high level calculation method that reproduces the experimental result. The calculation method can then be recommended for use in calculating activation enthalpy (barrier), structure, and kinetic data for the H atom addition to different types of olefins and the reverse beta scission barriers and rate constants, where experimental data is not available. A second objective in this work is to identify a lower cost (faster) density functional method (DFT) that can be recommended for kinetic and thermochemical parameters on much larger molecules.

The hydrogen atom addition reactions with ethylene (C₂H₄), propene (C₃H₆), 1-butene (C₄H₈), E-2-butene (trans- C₄H₈), Z-2-butene (cis- C₄H₈), isobutene (iso- C₄H₈) and 2,3-dimethy-2-butene (C₆H₁₂: c2c=cc2) as following Table 5.1 are evaluated in this study. The hydrogen reactions with smaller olefins have been investigated in a number of experimental and in some theoretical studies¹¹⁸⁻¹⁴¹. Activation Energy (*E_a*) and rate

constant for the addition reaction (forward reaction) and alkyl radical β -scission reaction (reverse reaction) as a function of structure in the olefin carbons are studied with several higher level calculation methods and with several lower level but much less time consuming DFT methods. Several methods are recommended.

5.2 Thermochemical Properties

5.2.1 Standard Enthalpy of Formation and Transition State

Standard enthalpies of formation at 298 K for reference species used in this study are summarized in Table 5.2. Structural parameters including vibration frequencies, zero-point vibrational, thermal energies, and transition state structure and energies for this set of compounds were initially obtained using the density functional theory (DFT) M062X level of theory as proposed by Truhlar group¹⁴² along with the standard basis sets 6-31G(d,p) and 6-311+G(d,p), and also using composite methods CBS-QB3⁴ and CBS-APNO⁷. CBS-QB3 and CBS-APNO are multilevel model chemistry methods that combines the results of several ab initio and density functional theory (DFT) individual methods and empirical correction terms to predict molecular energies with high accuracy and reasonably low computational cost. A second CBS-QB3 method was modified to incorporate the M062X calculated energies and structures in the subsequent CBS energy calculation (CBS-QB3//M062X), where the geometries and zero-point vibration energies from M062X/6-311+G(d,p) calculation. All quantum chemical calculation has been performed within the Gaussian 09 suite of programs.

Table 5.1 The Mechanism of Hydrogen Additional Reaction in This Study

Reactions	Additional sites
$\text{c}=\text{c} + \text{h} \leftrightarrow \text{ccj}$	Primary
$\text{c}=\text{cc} + \text{h} \leftrightarrow \text{cjcc}$	Secondary
$\text{c}=\text{cc} + \text{h} \leftrightarrow \text{ccjc}$	Primary
$\text{c}=\text{ccc} + \text{h} \leftrightarrow \text{cjccc}$	Secondary
$\text{cis-cc}=\text{cc} + \text{h} \leftrightarrow \text{ccjcc}$	Secondary
$\text{tran-cc}=\text{cc} + \text{h} \leftrightarrow \text{ccjcc}$	Secondary
$\text{c}=\text{cc}_2 + \text{h} \leftrightarrow \text{c}_3\text{cj}$ (tert- C_4H_9)	Primary
$\text{c}=\text{cc}_2 + \text{h} \leftrightarrow \text{c}_2\text{ccj}$ (iso- C_4H_9)	Tertiary
$\text{c}_2\text{c}=\text{cc}_2 + \text{h} \leftrightarrow \text{c}_2\text{cjcc}_2$	Tertiary

Note: j = radical site, equa sign (=) is double bond

Table 5.2 Standard Enthalpies of Formation at 298.15 K of Reference Species

Species	$\Delta_f H^\circ_{298} \text{ kcal mol}^{-1}$	Species	$\Delta_f H^\circ_{298} \text{ kcal mol}^{-1}$
h	52.10 ± 0.003^a	ccj	28.4 ± 0.5^c
c=c	12.54 ± 0.1^b	cjcc	23.9 ± 0.5^c
c=cc	4.78 ± 0.19^b	ccjc	22 ± 0.5^c
c=ccc	0.02 ± 0.22^b	cjccc	19.34 ± 0.53^d
c=cc ₂	-4.04 ± 0.2^b	ccjcc	16 ± 0.5^c
c ₂ c=cc ₂	-16.30 ± 0.26^b	iso- C_4H_9	17 ± 0.5^c
cis-cc=cc	-1.7 ± 0.24^b	tert- C_4H_9	11 ± 0.7^c
tran-cc=cc	-2.72 ± 0.24^b	c ₂ cjcc ₂	0.99^e

Note: j = radical site, Source: ^a[143], ^b[78], ^c[79], ^d[144], ^e This work.

Table 5.3 Thermodynamic Properties vs Temperature

Species	S ^o (298K) Cal mol ⁻¹ K ⁻¹	C _p ^o (T) (Cal mol ⁻¹ K ⁻¹)						
		300K	400K	500K	600K	800K	1000K	1500K
h	27.39	4.97	4.97	4.97	4.97	4.97	4.97	4.97
c=c	55.04	10.04	12.32	14.52	16.44	19.56	21.96	25.88
c=cc	63.70	15.17	18.79	22.21	25.22	30.74	30.10	39.87
c=ccc	77.31	20.89	25.51	30.03	34.05	40.63	45.67	53.78
c=cc2	70.11	20.58	25.52	30.10	34.14	40.69	45.72	53.81
c2c=cc2	87.21	28.39	36.22	43.70	50.30	60.95	69.00	81.62
cis-cc=cc	71.74	19.02	23.99	28.81	33.08	39.99	45.25	53.60
tran-cc=cc	70.83	20.54	25.22	29.76	33.83	40.48	45.58	53.77
ccj	59.29	12.24	14.65	16.99	19.08	22.56	25.31	29.88
cjcc	69.66	17.30	21.32	25.03	28.25	33.47	37.49	44.03
ccjc	69.34	17.24	21.15	24.81	28.04	33.31	37.41	44.03
cjccc	79.37	22.55	28.05	33.11	37.44	44.36	49.63	58.11
ccjcc	81.03	21.76	26.84	31.80	36.21	43.41	48.94	57.79
iso-c4h9	76.52	22.87	28.48	33.50	37.78	44.58	49.77	58.17
tert-c4h9	76.21	21.44	26.21	31.10	35.57	42.93	48.61	57.65
c2cjcc2	67.01	23.42	31.94	40.04	47.15	58.58	67.18	80.61

5.2.2 Entropy and Heat Capacities Data

Entropy and heat capacity calculation were performed using CBS-QB3//M062X determined geometries and harmonic frequencies are summarized in Table 5.3.

5.3 Kinetics

The potential energy surface and thermochemical properties are calculated with forward and reverse rate constants (high-pressure limit) for each elementary reaction step determined. Multifrequency quantum Rice Ramsperger-Kassel (QRRK) analysis is used for $k(E)$ ^{30, 145-146} with master equation analysis³³⁻³⁵ used for falloff. The QRRK analysis is described by Chang et al.³⁰. It is shown to yield reasonable results and provides a

framework by which the effects of temperature and pressure can be evaluated in complex reaction systems. The QRRK code utilizes a reduced set of three vibration frequencies for densities of states which accurately reproduce the molecules' (adduct) heat capacity³⁶⁻³⁷ and include one external rotation in calculation in the density states. Comparisons of ratios of these $\rho(E)/Q$ (partition function Q) with direct count $\rho(E)/Q$ are shown to be in good agreement¹⁴⁷. Nonlinear Arrhenius effects resulting from changes in the thermochemical properties of the respective transition state relative to the adduct with temperature are incorporated using a two-parameter Arrhenius pre-exponential factor (A , n) in AT^n (where T is the temperature).

5.3.1 Activation Energy (E_a)

Canonical transition state theory is used to determine the transition state (TS) and calculated the Activation Energy (E_a) as kinetic parameters. The computational method used in this study included the density functional theory (DFT); M06-2X/6-31G(d,p) and M06-2X/6-311+G(d,p), and the composite method; CBS-QB3 and CBS-APNO level of theory. A second CBS-QB3 method was modified to incorporate the M06-2X/6-311+G(d,p) calculated energies and structures for the barriers in the subsequent CBS energy calculation (CBS-QB3//M062x). Results from calculations at different levels are compared with the experimental data and reviewed data for hydrogen atom addition to Ethylene ($c=c$), Propene ($c=cc$), 1-Butene ($c=ccc$), E-2-Butene ($trans\text{-}cc=cc$), Z-2-Butene ($cis\text{-}cc=cc$), and Isobutene ($iso\text{-}c_4h_8$: $c=cc_2$). Table 5.3 presents the comparison of calculated activation energy from several computational methods for hydrogen additional reactions to the small olefins (forward reactions) with the experimental and review data.

Calculated Activation Energy (E_a) of forward reactions for hydrogen additional reactions are presented in Table 5.4. The E_a for hydrogen addition reactions from literature data are used to compare with the value from 5 calculation methods in this study (M06-2x/6-31G(d,p), M06-2X/6-311+G(d,p), M06-2X/6-311+g(d,p)//CBS-QB3, CBS-QB3, and CBS-APNO). All E_a values from experimental and calculation data show the low values for the forward reaction energy barrier, between 1 to 3 kcal mol⁻¹. An E_a for hydrogen addition to 2, 3-Dimethyl-2-butene (c2c=cc2) at the tertiary carbon site could not be found. The comparisons show a good agreement for E_a 's from the complete basis set methods which include the modified method, viz., M06-2X//CBS-QB3 method, CBS-QB3 could not find a transition state (TS) structure in the reactions of Propene (c=cc) and Isobutene (iso-c4h8: c=cc2), where zero values are shown in Table 5.4. The M06-2x modified CBS-QB3 method and the CBS-APNO show the closet agreement to the experimental data with CBS-QB3 next most accurate. The DFT methods all show a somewhat higher, i.e., over-estimation, of barriers in all the systems studied.

Table 5.5 shows a comparison of the barrier (E_a) for hydrogen elimination reaction (reverse reaction of hydrogen addition) values for calculations in this study vs. experimental data and reviewed literature. The energy barriers for hydrogen elimination from primary, secondary and tertiary carbon sites range from literature range from 30 to 39 kcal mol⁻¹, with no reference data for hydrogen elimination from 2,3-Dimethyl-2-butene (c2c=cc2) at tertiary carbon site. These barriers all include the endothermicity of the reaction, that is, the energy needed to cleave the carbon – hydrogen bond, minus the energy gained from forming a carbon – carbon Π bond. The calculated E_a values from M06-2x modified CBS-QB3 method and the CBS-APNO show good agreement with the

experimental and reviewed literature data. The values from CBS-QB3 are next in accuracy.

Table 5.4 Activation Energy (E_a) of Hydrogen Additional Reactions

Reactions	Add'n Site	M06-2X		M06-2X CBS-QB3	CBS		Literature
		<i>BS1</i>	<i>BS2</i>		QB3	APNO	
$\text{c}=\text{c} + \text{h} \leftrightarrow \text{ccj}$	P	4.11	3.41	1.17	-0.15	1.45	1.29 ^a 2.05 ^b
$\text{c}=\text{cc} + \text{h} \leftrightarrow \text{ccjc}$	P	4.83	4.05	1.44	0.00	2.14	1.30 ^c 1.11 ^d
$\text{c}=\text{cc}2 + \text{h} \leftrightarrow \text{tert-c}_4\text{h}_9$	P	2.13	1.22	-1.38	0.00	-0.69	1.37 ^e 1.41 ^f
$\text{c}=\text{cc} + \text{h} \leftrightarrow \text{cjcc}$	S	4.89	4.31	1.90	1.45	2.55	2.93 ^g 2.53 ^h
$\text{cis-cc}=\text{cc} + \text{h} \leftrightarrow \text{ccjcc}$	S	4.20	2.82	1.40	0.89	1.86	1.92 ⁱ
$\text{tran-cc}=\text{cc} + \text{h} \leftrightarrow \text{ccjcc}$	S	4.07	3.36	1.73	0.59	1.65	2.09 ^k
$\text{c}=\text{ccc} + \text{h} \leftrightarrow \text{cjccc}$	S	5.23	4.47	2.22	1.78	2.80	2.62 ^l
$\text{c}=\text{cc}2 + \text{h} \leftrightarrow \text{iso-c}_4\text{h}_9$	T	5.23	4.78	2.60	2.28	3.12	2.62 ^l
$\text{c}2\text{c}=\text{cc}2 + \text{h} \leftrightarrow \text{c}2\text{cjcc}2$	T	3.63	2.73	0.73	0.20	1.25	NA

Note: j=radical site, *BS1*=6-31G(d,p), *BS2*=6-311+G(d,p), *a,c,e,g,i*, and *k* are values from average or reviewed literature, *b, d, f, h* and *l* are values from average or experimental data; Source: ^a [119, 121, 123, 134, 141, 148], ^b [129, 135-136, 149-150], ^c [121, 124, 139-141], ^d [127, 151-152], ^e [121, 124], ^f [120, 128, 153-156], ^g [121, 124, 139-141], ^h [152, 157], ⁱ [128], ^k [123, 128], ^l [121].

Table 5.5 Activation Energy (E_a) of Hydrogen Elimination Reactions

Reactions	E site	M06-2X		M06-2X CBS-QB3	CBS		Literature
		<i>BS1</i>	<i>BS2</i>		QB3	APNO	
$\text{ccj} \leftrightarrow \text{c}=\text{c} + \text{h}$	P	40.36	39.65	37.41	36.09	37.69	36.42^a 38.01^b
$\text{ccjc} \leftrightarrow \text{c}=\text{cc} + \text{h}$	P	39.71	38.93	36.32	0.00	37.02	37.10^c 37.26^d
$\text{tert-c}_4\text{h}_9 \leftrightarrow \text{c}=\text{cc2} + \text{h}$	P	39.19	38.28	35.68	0.00	36.37	37.36^e 39.10^f
$\text{cjcc} \leftrightarrow \text{c}=\text{cc} + \text{h}$	S	37.87	37.29	34.88	34.43	35.53	36.49^g 33.45^h
$\text{cejcc} \leftrightarrow \text{cis-cc}=\text{cc} + \text{h}$	S	38.60	37.22	35.80	35.29	36.26	34.78^i
$\text{cejcc} \leftrightarrow \text{tran-cc}=\text{cc} + \text{h}$	S	37.45	36.74	35.11	33.97	35.03	33.98^i
$\text{cjccc} \leftrightarrow \text{c}=\text{ccc} + \text{h}$	S	38.01	37.25	35.00	34.56	35.58	35.71^k 39.15^l
$\text{iso-c}_4\text{h}_9 \leftrightarrow \text{c}=\text{cc2} + \text{h}$	T	36.29	35.84	33.66	33.34	34.18	33.68^k 30.60^m
$\text{c2cjcc2} \leftrightarrow \text{c2c}=\text{cc2} + \text{h}$	T	38.44	37.54	35.54	35.01	36.06	NA

Note: j=radical site, E =Elimination, $BS1=6-31\text{G(d,p)}$, $BS2=6-311+\text{G(d,p)}$; $a, c, e, g, i, \text{ and } k$ are values from average or reviewed literature; $b, d, f, h \text{ and } k$ are values from average or experimental data; Sources: a [119, 121, 141, 148, 158], b [130, 158-161], c [121, 141, 162], d [125, 137, 151, 163-167], e [121, 138], f [120, 137, 156, 168], g [121, 141], h [125, 164, 169], i [137], k [121], l [130, 164], m [133].

5.3.2 Rate Constant (k)

Tables 5.6 and 5.7 provide high pressure-limit rate constants in for hydrogen addition reaction (forward reaction) and hydrogen elimination reaction (reverse reaction), respectively with two-parameter of Arrhenius pre-exponential factors (A , n) in AT^n format, where T is the temperature in K, from our calculations and literature data for comparison

The high pressure limit rate parameter expressions in table 5.6 and 5.7 are calculated based on structure from M06-2X//CBS-QB3 method. For comparison rate constants (k) in this study, the calculated rate constant at 298 K are provided and compared with experimental data and reviewed literature data at the same temperature.

The high pressure-limit rate constants (k) at 298K for hydrogen addition reactions to olefins have low E_a barriers, on the order of 0.5 to 3 kcal mol⁻¹, as shown in Table 5.6, and are therefore relatively high rate constants. The low value of activation energy (E_a) for these addition reactions make them highly favorable under atmospheric and low temperature combustion conditions. The forward reactions are also exothermic forming lower energy products.

The majority of the calculated rate constants at 298K in the present study show good agreement with both experimental and reviewed literature. The calculated H atom addition to iso – butene (iso-c₄h₈: c=cc2) shows good agreement at the xx site with the literature and the elimination reaction is calculated to be lower than the values reported in the literature, but there is a wide near 2 order of magnitude difference in the reference data.

Rate constants at 298K in Table 5.7 for hydrogen elimination (beta scission) reactions show the rate constant values in the range of 10⁻¹⁰-10⁻¹⁵ sec⁻¹, which results from their endothermicity, i.e., the high activation barrier range (~30-40 kcal mol⁻¹) as listed in table 5.5. The calculated rate constants are in accord with rate constants from experimental and reviewed literature except the reaction that involve to the hydrogen beta scission elimination from isobutene (iso-c₄h₉ ↔ c=cc2 + h) which has a slightly lower calculated rate constant compared to the reference data.

Table 5.6 High Pressure-Limit Rate Parameter for Hydrogen Additional Reaction

Reactions	Add'n Site	A	n	Ea	k at 298°K	Literature
$c=c + h \leftrightarrow ccj$	P	6.07E+08	1.46	1.43	4.55E+11	7.03E+11 ^a 7.19E+11 ^b
$c=cc + h \leftrightarrow ccjc$	P	1.85E+07	1.96	1.19	1.81E+11	9.63E+11 ^c 7.60E+11 ^d
$c=cc2 + h \leftrightarrow tert-c_4h_9$	P	2.18E+08	1.76	-1.42	5.43E+13	2.44E+12 ^e 2.50E+12 ^f
$c=cc + h \leftrightarrow cjcc$	S	3.84E+06	1.99	1.60	2.19E+10	5.18E+10 ^g 4.80E+10 ^h
$cis-cc=cc + h \leftrightarrow ccjcc$	S	6.57E+07	1.79	1.47	2.97E+11	4.54E+11 ⁱ 5.70E+11 ^k
$tran-cc=cc + h \leftrightarrow ccjcc$	S	7.99E+08	1.49	1.60	5.44E+11	5.56E+11 ^l 6.58E+11 ^m
$c=ccc + h \leftrightarrow cjccc$	S	1.18E+06	2.21	2.05	1.12E+10	5.24E+10 ^c
$c=cc2 + h \leftrightarrow iso-c_4h_9$	T	1.51E+07	1.92	2.41	1.50E+10	1.32E+11 ^c
$c2c=cc2 + h \leftrightarrow c2cjcc2$	T	1.39E+09	1.37	1.03	1.26E+12	7.76E+11 ⁿ 5.57E+11 ^p

Note: unit of k = cm³/mol-sec, j=radical site, *a,c,e,g,i,l* and *n* are values from average or reviewed literature; *b, d, f, h, k, m* and *p* are values from average or experimental data; Source: ^a[119, 121, 129, 134], ^b[129, 135-136, 150, 170], ^c[121, 124], ^d[151-152, 171], ^e[121, 124], ^f[128, 154, 156], ^g[121, 140-141], ^h[152, 157], ⁱ[124, 141], ^k[128, 132, 172], ^l[124, 141], ^m[123, 128], ⁿ[124], ^p[132, 173]

5.3.3 Hydrogen Addition to Propene and Furthur Interaction

The kinetics and thermochemistry of intra molecular hydrogen transfer reactions ($cjcc \rightarrow ccjc$, $cjcc \rightarrow cccj$) and the beta scission elimination of a methyl (CH₃) radical ($cjcc \rightarrow c=c + ch_3$) which are reactions that result from the addition of hydrogen atom with 1 and

2 butene are also studied. High pressure-limit parameters in Table 5.8 are used in QRRK analysis for dependent rate constant and fall off analysis (Figure 4.21).

Table 5.7 High Pressure-Limit Rate Parameter for Hydrogen Elimination Reactions

Reactions	<i>E</i> Site	A	n	E _a	k at 298°K	Literature
ccj ↔ c=c + h	P	1.21E+11	0.80	37.70	4.01E-15	5.01E-15 ^a 1.78E-15 ^b
ccjc ↔ c=cc + h	P	1.79E+12	0.30	37.40	5.74E-15	5.58E-14 ^c 1.25E-14 ^d
tert-c ₄ h ₉ ↔ c=cc ₂ + h	P	3.79E+12	0.22	26.77	2.20E-14	2.73E-14 ^e 4.15E-14 ^f
cjcc ↔ c=cc + h	S	3.57E+12	0.21	36.10	5.99E-14	6.07 E-14 ^g 6.70E-16 ^h
ccjcc ↔ cis-cc=cc + h	S	5.44E+12	0.26	36.58	5.45E-14	1.30E-13 ⁱ
ccjcc ↔ tran-cc=cc + h	S	2.38E+14	-0.19	36.77	1.30E-13	5.49E-13 ⁱ
cjccc ↔ c=ccc + h	S	1.81E+12	0.27	36.07	4.33E-14	7.13E-14 ^k 4.00E-15 ^l
iso-c ₄ h ₉ ↔ c=cc ₂ + h	T	5.88E+12	0.15	34.89	5.28E-13	6.76E-12 ^k 3.60E-10 ^m
c2cjcc2 ↔ c2c=cc ₂ + h	T	1.90E+11	0.75	35.89	9.91E-14	5.14E-13 ⁿ

Note: unit of k = s⁻¹, j=radical site, *a, c, e, g,* and *k* are values from average or reviewed literature; *b, d, f, h, i, l, m,* and *n* are values from average or experimental data; Source: ^a[141, 158], ^b[160-161], ^c[121, 162], ^d[137, 151, 164], ^e[121, 137-138, 156], ^f[137, 156], ^g[121, 141], ^h[164], ⁱ[137], ^k[121], ^l[131, 137], ^m[133], ⁿ[174].

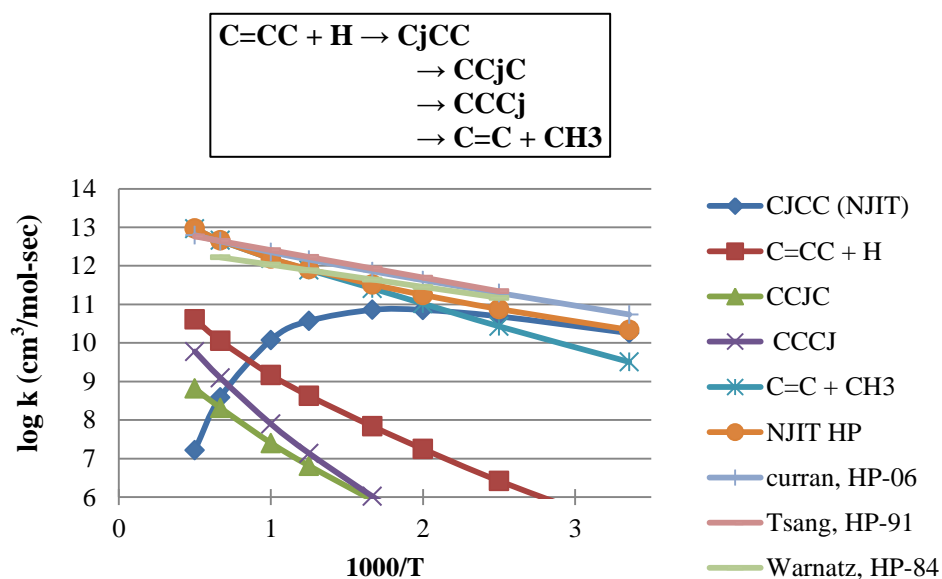
The high pressure-limit rate constant from Curran¹²¹ (Curran, HP-06), Tsang¹³⁹(Tsang,HP-91), and Warnatz¹⁴¹ (Warnatz,HP-84) are compared for hydrogen addition to butene of this work (NJIT-HP) in Table 5.8 and in Figure 5.1 and presented as log rate constant (log k) versus 1000/T. The high pressure limit rate constants in this

study show the same tendency, where rate constants increase with the increase of temperature, as in the literature data.

Table 5.8 High Pressure-Limit Rate Parameters for Hydrogen Addition to Propene

Reactions	$k = A(T)^n \exp(-Ea/RT)$		
	A	n	Ea (kcal mol ⁻¹)
c=cc + h → cjcc	3.84E+10	1.84	1.60
cjcc → c=cc + h	3.48E+08	1.34	34.68
cjcc → ccjc	1.79E+11	0.11	38.52
cjcc → cccj	1.72E+10	1.35	39.55
cjcc → c=c + ch3	9.5E+14	0.00	31.65

Note: j = radical site



Figures 5.1 Rate constants (log k) vs. 1000/T at 1 atm for c=cc + h.

The n-propyl radical formation is the dominant product at low temperature. The channel starts to falloff above 500 K while the ethene plus methyl radical channel becomes more important.

5.3.4 Hydrogen Addition to Isobutene and Further Interaction

High pressure-limit rate constants for hydrogen addition reactions to the isobutene are shown in Table 5.9. There are two different sites here a primary site which is addition to a CH₂ carbon and a tertiary site which is addition to a CH₃C carbon. The rate constant parameters of intramolecular hydrogen transfer (iso-c4h9 → tert-c4h9) and beta scission elimination reactions (iso-c4h9 → c=cc + ch₃ and iso-c4h9 → c=cc₂ + h) are also presented.

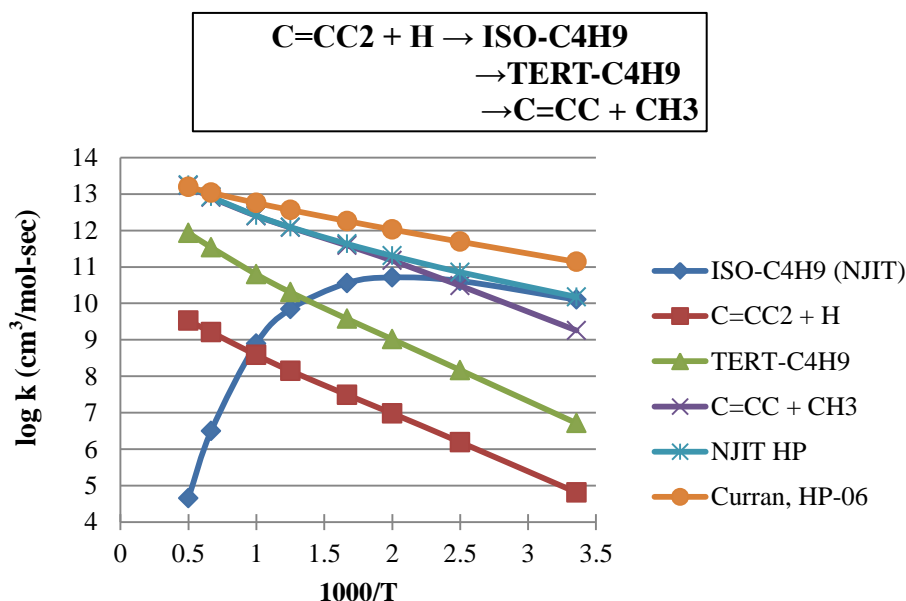
Table 5.9 High Pressure-Limit Rate Parameters for Hydrogen Addition to isobutene

Reactions	$k = A(T)^n \exp(-Ea/RT)$		
	<i>A</i>	<i>n</i>	<i>Ea</i> (kcal mol ⁻¹)
c=cc ₂ + h → iso-c4h9	1.51E+07	1.92	2.41
iso-c4h9 → tert-c4h9	5.36E+12	0.88	34.60
iso-c4h9 → c=cc + ch ₃	7.71E+13	0.77	30.71
iso-c4h9 → c=cc ₂ + h	5.88E+12	0.15	34.86

Note: j = radical site

Figure 5.2 shows rate constant as a function of temperature at pressure 1 atm. for this H atom plus isobutene and compares the (NJIT-HP) data to work of Curran(Curran, HP-06)¹²¹ – this includes comparisons falloff analysis. The high pressure-limit rate constant from this study shows a lower value at low temperature when compared to Curran's work, with the calculation data being similar at higher temperatures about 1500-2000K. Iso-c4h9 is the most important species at low temperature and begins to falloff at about 500K, showing a decreasing rate constant with increasing of temperature range.

The rate of $\text{c=cc} + \text{ch}_3$ methyl group elimination reaction increases with temperature and is dominant at the high temperatures.



Figures 5.2 Rate constants ($\log k$) vs. $1000/T$ at 1 atm for $\text{c=cc}_2 + \text{h}$.

5.4 Summary

Activation energies (E_a), thermochemistry and reaction kinetics for hydrogen atom addition to primary (P), secondary (S), tertiary (T), vinylic (olefin) carbons to form an alkyl radical are evaluated along with the reverse, beta scission reactions were studied by use of computational chemistry. Calculations used the Density Functional Theory (DFT) methods: (M06-2X/6-31g(d,p) and M06-2X/6-311+g(d,P) and the *ab initio* complete basis set methods (CBS-QB3- and CBS-APNO).

In addition the CBS-QB3 method was modified to incorporate the M06-2X (CBS//M06-2X). Activation energies and rate constants for forward and reverse paths of

hydrogen atom addition to Primary, Secondary, Tertiary carbons of Ethylene, Propene, 1-Butene, E-2-Butene, Z-2-Butene, Isobutene, and tetra-methyl ethylene are reported and compared with literature.

One objective of this study was to use the data from experiments on H atom addition to small olefins to identify calculation methods that reproduce the experimental results and therefore can be recommended for use in calculating energy barriers and structure for systems where data is not available. The higher level calculations - M06-2x modified CBS-QB3 method and the CBS-APNO show the closest agreement to the experimental data with CBS-QB3 next. Among the Density functional Methods the M06-2X/6-311+G(d,p) method showed the best agreement, where the barriers for H addition and for beta scission were high by about 3 kcal mol⁻¹ on average. In general, the DFT level calculations result in higher barriers. Falloff in the stabilization channels occurs the higher temperatures studied hydrogen addition to olefins.

CHAPTER 6

THERMOCHEMICAL AND KINETICS OF THE CHEMICAL ACTIVATION REACTIONS OF OH RADICAL ADDITION (INITIATION) WITH TRIFLUOROETHENE (1,1,2 TRIFLUOROETHENE)

6.1 Overview

The oxidation reaction of an unsaturated fluorinated hydrocarbon in the atmosphere and in combustion processes is studied to understand the overall flammability and final reaction products: the focus is on Trifluoroethylene ($\text{CHF}=\text{CF}_2$) because it is being considered as a possible heat transfer fluid in air conditioning and refrigeration applications. Fluoro- halocarbons are widely used as refrigerants and heat transfer fluids; the partially oxidized products of these chemicals are now being routinely found in environmental waters, soils and in the atmosphere. There is also a concern that they will amplify global warming and they may be harmful to health. This fluorocarbon is also used as the monomer in the preparation process in fluorocarbon industry¹⁷⁵; the atmospheric and combustion chemistry reactions have not been evaluated. Thermochemical properties and reaction kinetic paths as a function of temperature and pressure will aid in the understanding the reactions and products of fluorocarbons in combustion and in the atmospheric, aqueous and terrestrial environments.

Trifluoroethene ($\text{CF}_2=\text{CHF}$) reaction in atmospheric and combustion environments is initiated by addition of the OH radical to the unsaturated π bond (double bond) system.

This study starts with the initiation reaction of OH addition to each of the two different carbon sites of trifluorethylene and then considers the unimolecular reactions of each carbon site radical (adducts). Unimolecular reactions of each adduct include

Hydrogen Atom Transfer (HAT), Fluoride atom transfer, Hydrogen Fluoride (HF) molecular elimination, F atom elimination, H atom elimination. The reaction kinetic modeling also considers all of the reverse reaction paths.

Thermochemical properties are calculated for parent molecules and all intermediate radicals, new products and transition states. Kinetic parameters are developed and reaction modeling is performed.

One channel, hydrogen fluoride (HF) elimination is currently not reported in any previous kinetic study on the OH adduct intermediates to the best of our knowledge. The HF moiety is a highly reactive and toxic gas that can cause severe respiratory damage in humans. It is hoped the understanding of the reaction processes and products will be helpful to evaluating the safety of using the trifluoroethene as a refrigerant and heat transfer fluid.

6.2 Thermochemical Properties

Target molecules and their corresponding abbreviated nomenclature are presented in Figure 6.1. The standard enthalpies of formation at 298 K for reference species used in these reactions are summarized in Table 6.1. The enthalpies of formation of the target molecules obtained from the use of the reaction schemes are shown in Table 6.2. The reaction of $\text{OH} + \text{CHF}=\text{CF}_2$ results in the following active radical intermediates:

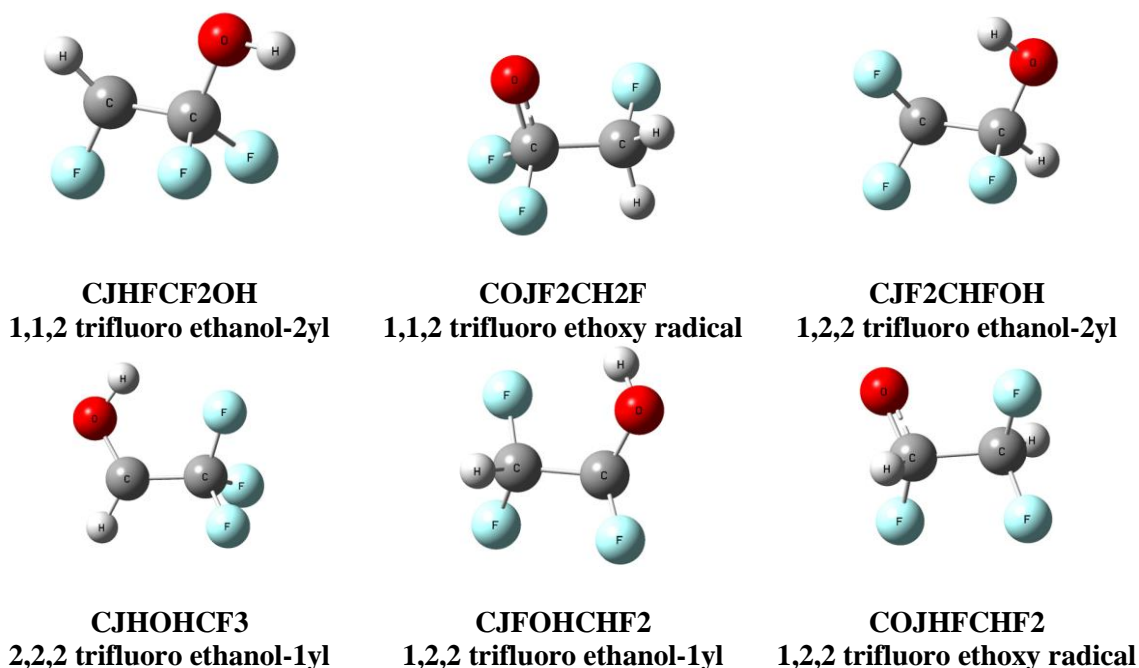


Figure 6.1 Geometries of lowest energy conformer of target molecules in the trifluoroethene + OH system.

The master equation analysis considers a Boltzmann distribution of energy levels of each adduct and uses an exponential-down model for the energy transfer function with ($\Delta E^\circ_{\text{down}}$) 900 cal mol⁻¹ for N₂ as the third body. Rate constants, $k(E)$, were evaluated using 1.0 kcal mol⁻¹ energy increments up to 65 kcal mol⁻¹ above the highest barrier. Lennard-Jones parameters, σ (Å), and ϵ/k (K) are obtained from tabulations and from an estimation method based on molar volumes and compressibility; $\sigma = 5.07$ Å and $\epsilon/k_b = 399$ K. Table 6.3 presents high-pressure-limit elementary rate parameters used as input data to the QRRK calculations.

Table 6.1 Standard Enthalpies of Formation at 298 K for Reference Species

Species	$\Delta_f H^0_{298}$ kcal mol ⁻¹	Species	$\Delta_f H^0_{298}$ kcal mol ⁻¹
ch3ch2f	-65.18 ^a	chfcf2	-117.21 ± 0.6 ⁷⁸
cis-chfdchf	-73.8 ¹⁷⁶	cjhfcf3	-18.2 ¹⁷⁶
ch2fch2oh	-100 ^a	cjhfcf2	-110.6 ¹⁷⁶
ch3chfoh	-113.7 ^a	ch2fchf2	-161.1 ¹⁷⁶
ch3f	-56.5 ¹⁷⁶	ccoj	-3.61 ⁹⁵
ch2foh	-102.1 ^a	ccjdo	-2.3 ± 0.1 ¹¹⁰
tran-chfdchf	-74.5 ¹⁷⁶	cccdof	-44.36 ± 0.2 ⁷⁸
cf2dchf	-117.21 ± 2.0 ⁷⁸	cjccdo	6.6 ± 0.9 ¹¹⁰
cf2dch2	-80.06 ± 1.08 ⁷⁸	chf2cdof	-190.7 ¹⁷⁶
ccc	-25.02 ± 0.12 ⁷⁸	cjh2ch2f	-14.1 ¹⁷⁶
cf3ch2ch3	-184.76 ^a	chf2cdoh	-130.4 ¹⁷⁶
ccdo	-39.7 ± 0.12 ⁷⁸	cc	-20.03 ± 0.1 ⁷⁸
ch3cf3	-179.79 ^a	chf2chf2	-211.17 ^a
ch4	-17.78 ± 0.1 ⁷⁸	ccj	28.4 ± 0.5 ⁷⁹
chf3	-165.99 ^a	ccoh	-56.21 ± 0.09 ⁷⁸
cf2hch2ch3	-125.34 ^a	cjcoh	-5.9 ± 0.4 ¹¹⁰
ccdof	-106.4 ± 0.5 ⁹⁹	ccjoh	-13.34 ± 0.3 ¹⁰¹
ch3chf2	-120.39 ^a	coh	-48 ¹⁷⁷
cf2h2	-107.59 ^a	coj	5.02 ⁹⁵
cjhfoh	-55.7 ^a	cccjdo	-6.9 ± 0.9 ¹¹⁰
cjf2ch3	-71.9 ¹⁷⁶	cccch	-60.97 ± 0.1 ⁷⁸
cf3ch2oh	-213.63 ^b	cccjoh	-7.91 ⁹⁷
ch2fcdof	-143.6 ¹⁷⁶	cjcdof	3.51 ¹⁷⁸

Note: j=radical site, d=double bond, ^aWang and Bozzelli (personal communication, May 2015), ^bthis work

Table 6.2 Evaluated Enthalpies of Formation At 298 K for Trifluoroethene + OH Reaction System Intermediates and Products

Work Reactions	$\Delta_f H^\circ_{298} \text{ kcal mol}^{-1}$			
	B2P ^a	M06 ^b	M06 ^c //CBS	CBS-QB3
cjhfcf2oh				
cjhfcf2oh + ch2foh \rightarrow ch2fcf2oh + cjhfoh	-163.27	-163.29	-163.09	-163.82
cjhfcf2oh + ch2fch2oh \rightarrow ch2fcf2oh + cjhch2oh	-163.34	-163.92	-161.94	-163.55
cjhfcf2oh + ch3ch2f \rightarrow cjhch3 + ch2fcf2oh	-163.67	-163.96	-160.38	-163.76
Average	-163.43 ± 0.22	-163.72 ± 0.37	-161.80 ± 1.34	-163.71 $\pm 0.14^d$
cojf2ch2f				
cojf2ch2f + coh \rightarrow coj + ch2fcf2oh	-148.83	-149.62	-148.31	-149.44
cojf2ch2f + ccoh \rightarrow ccoj + ch2fcf2oh	-148.47	-149.78	-148.09	-149.77
cojf2ch2f + cccoh \rightarrow cccoj + ch2fcf2oh	-148.5	-149.18	-148.07	-149.24
Average	-148.60 ± 0.20	-149.53 ± 0.31	-148.16 ± 0.13	-149.48 ± 0.73
cjf2chfoh				
cjf2chfoh + ch2foh \rightarrow chf2chfoh + cjhfoh	-156.43	-156.12	-155.22	-156.52
cjf2chfoh + ch2fch2oh \rightarrow chf2chfoh + cjh2chfoh	-156.27	-155.56	-153.93	-155.45
cjf2chfoh + ch3chf2 \rightarrow chf2chfoh + cjf2ch3	-156.98	-156.62	-155.55	-156.85
Average	-156.56 ± 0.38	-156.10 ± 0.53	-154.90 ± 0.86	-156.27 ± 0.73
cjhohcf3				
cjhohcf3 + ch2foh \rightarrow cf3ch2oh + cjhfoh	-168.03	-168.60	-167.24	-168.96
cjhohcf3 + ch2fch2oh \rightarrow cf3ch2oh + cjh2chfoh	-167.87	-168.04	-165.94	-167.89
cjhohcf3 + ch3chfoh \rightarrow cf3ch2oh + cjh2chfoh	-168.35	-169.80	-166.72	-168.64
Average	-168.08 ± 0.24	-168.82 ± 0.90	-166.63 ± 0.65	-168.50 ± 0.54
cjfohchf2				
cjfohchf2 + ch2foh \rightarrow chf2chfoh + cjhfoh	-158.75	-158.62	-158.32	-159.65
cjfohchf2 + ch2fch2oh \rightarrow chf2chfoh + cjh2chfoh	-158.6	-158.05	-157.02	-158.58
cjfohchf2 + ch3chfoh \rightarrow chf2chfoh + cjfohch3	-159.07	-159.33	-158.59	-159.91
Average	-158.81 ± 0.25	-158.67 ± 0.64	-156.75 ± 0.84	-159.38 ± 0.70
cojhfchf2				
cojhfchf2 + coh \rightarrow chf2chfoh + coj	-150.68	-150.85	-149.86	-151.19
cojhfchf2 + ccoh \rightarrow chf2chfoh + ccoj	-150.32	-151.01	-149.65	-151.52
cojhfchf2 + cccoh \rightarrow chf2chfoh + cccoj	-150.35	-150.40	-149.63	-150.99
Average	-150.45 ± 0.20	-151.23 ± 0.31	-149.71 ± 0.13	-151.23 ± 0.26

Note: d = double bond, j = radical, ^aB2PLYP/6-311+G(2d,d,p), ^bM062X/6-31G(d,p), ^cM062X/311+G(d,p)//CBS-QB3, ^dStandard deviation is for the work reaction sets.

6.3 Reactions and Kinetics

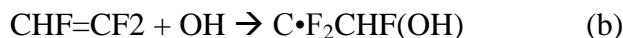
Table 6.3 High-Pressure-Limit Elementary Rate Parameters for Reactions in The Trifluoroethene + OH Reaction System

Reaction			$k = A(T/K)^n \exp(-E_a/RT)$		
			A	n	E_a (kcal mol ⁻¹)
Overall: CHF=CF ₂ + OH → C(OH)F ₂ C•HF → Products			Reaction System		
CHF=CF ₂ + OH	=>	CJHFCF ₂ OH	1.82E+04	2.3	-3.45
CJHFCF ₂ OH	=>	CHF=CF ₂ + OH	1.20E+08	2.5	54.02
CJHFCF ₂ OH	=>	COJF ₂ CH ₂ F	2.44E+07	2.2	37.47
CJHFCF ₂ OH	=>	CHFDCFOH + F	4.30E+08	2.1	64.22
CJHFCF ₂ OH	=>	CJHFCDOF + HF	2.26E+07	2.4	35.05
COJF ₂ CH ₂ F	=>	CJHFCF ₂ OH	6.86E+09	1.3	26.72
COJF ₂ CH ₂ F	=>	CF ₂ DO + CJH ₂ F	1.83E+11	1.1	7.66
Overall: CHF=CF ₂ + OH → C•F ₂ CHF(OH) → Products			Reaction System		
CHF=CF ₂ + OH	=>	CJF ₂ CHFOH	3.52E+04	2.3	-2.51
CJF ₂ CHFOH	=>	CHF=CF ₂ + OH	3.11E+07	2.8	46.80
CJF ₂ CHFOH	=>	CJHOHCF ₃	9.65E+06	2.4	35.20
CJF ₂ CHFOH	=>	CJFOHCF ₂ H	6.85E+08	1.7	57.11
CJF ₂ CHFOH	=>	COJHFCHF ₂	5.35E+05	2.8	37.93
CJF ₂ CHFOH	=>	CF ₂ DCFOH + H	8.61E+04	3.3	49.25
CJF ₂ CHFOH	=>	CJF ₂ CDOH + HF	1.15E+07	2.6	36.50
CJHOHCF ₃	=>	CJF ₂ CHFOH	1.73E+08	2.2	49.97
CJHOHCF ₃	=>	CF ₃ CDOH + H	8.86E+08	2	44.51
CJHOHCF ₃	=>	CJF ₂ CDOH + HF	6.34E+07	2.2	36.47
CJFOHCF ₂ H	=>	CJF ₂ CHFOH	8.02E+08	1.7	59.6
CJFOHCF ₂ H	=>	CF ₂ HCDOF + H	1.62E+08	2	32.91
CJFOHCF ₂ H	=>	CF ₂ DCFOH + H	1.27E+05	3.4	52.41
CJFOHCF ₂ H	=>	CJDOCF ₂ H + HF	1.42E+09	1.6	43.29
CJFOHCF ₂ H	=>	CJHFCDOF + HF	2.09E+06	2.6	27.64
CJFOHCF ₂ H	=>	CHFDCFOH + F	1.60E+08	2.5	59.54
COJHFCHF ₂	=>	CJF ₂ CHFOH	1.01E+09	1.6	35.71
COJHFCHF ₂	=>	CHFDO + CJF ₂ H	7.77E+11	1.1	9.84

Note: d = double bond, J = radical.

6.3.1 C₂F₃H + OH Reaction System

Hydrofluoro-olefins Hydrofluoro-olefins are primarily removed in the troposphere by reaction with the OH radical.



Reaction (a) and reaction (b) proceed via OH radical addition to the π bond (double bond) of the olefin to form energized hydroxylfluoroalkyl radicals (HO)CF₂C•HF* and C•F₂CHF(OH)* adducts (* indicates an energetically excited adduct). The bond strengths for the OH-Olefin adducts formed in reactions (a) and (b) are 55.4 and 47.8 kcal mol⁻¹, respectively.

Potential energy diagrams for the chemical activation calculation of the C₂F₃H + OH to products via the C(OH)F₂C•HF adduct are shown in Figures 6.2a and Figure 6.2b for reaction system via C•F₂CHF(OH) (2,2 difluoro ethanol – 2yl) adduct. The enthalpy values for intermediates and products are from the calculations as listed in Table 6.2. The formation of reactant complexes when OH addition to each of the carbon sites forming energized (HO)CF₂C•HF* and C•F₂CHF(OH)* adducts (* indicates an energized adduct resulting from the new bond formed).

Reactions of the C•F₂CHF(OH) (2,2 difluoro ethanol – 2yl) adduct

The C(OH)F₂C•HF* adduct shown in Figure 6.2a can dissociate back to reactants, stabilize to C(OH)F₂C•HF adduct, or undergo intramolecular H-transfer via four-member ring transition state with 35.8 kcal mol⁻¹ barrier forming fluorohydroxy radical; CF₂O•CFH₂. The energized adduct can also proceed to Fluorine atom (F) elimination with an endothermicity of 11.6 kcal mol⁻¹ above the entrance channel, which

makes this dissociation reaction un-important in these system. The negative energy of activation due to a hydrogen bonding intermediate on the path is, however very interesting. The HF elimination reaction occurs from the $(\text{C}(\text{OH})\text{F}_2\text{C}\cdot\text{HF})$ adduct (both chemically activated and stabilized) and reacts to $\text{C}\cdot\text{HFC}(\text{=O})\text{F} + \text{HF}$], has an energy barrier $35.9 \text{ kcal mol}^{-1}$ relative to the stabilized adduct.

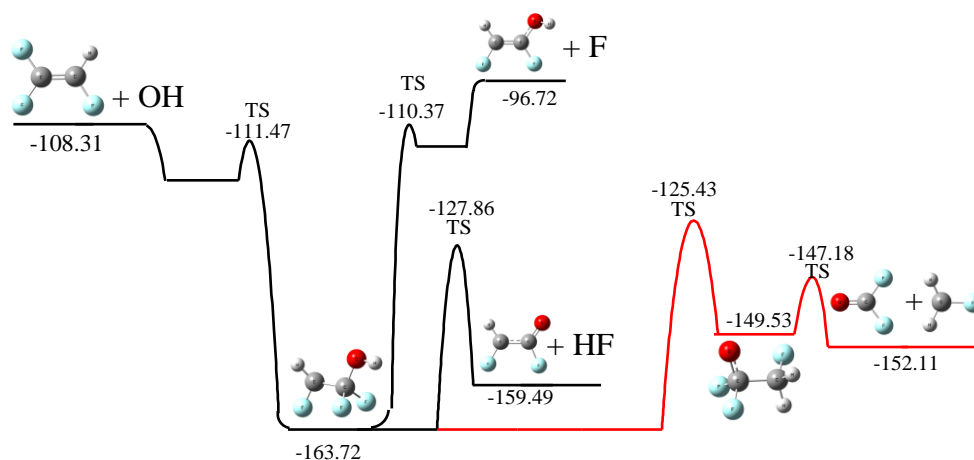


Figure 6.2a Potential energy diagram for the $\text{CHF}=\text{CF}_2 + \text{OH} \rightarrow \text{C}(\text{OH})\text{F}_2\text{C}\cdot\text{HF} \rightarrow$ products system.

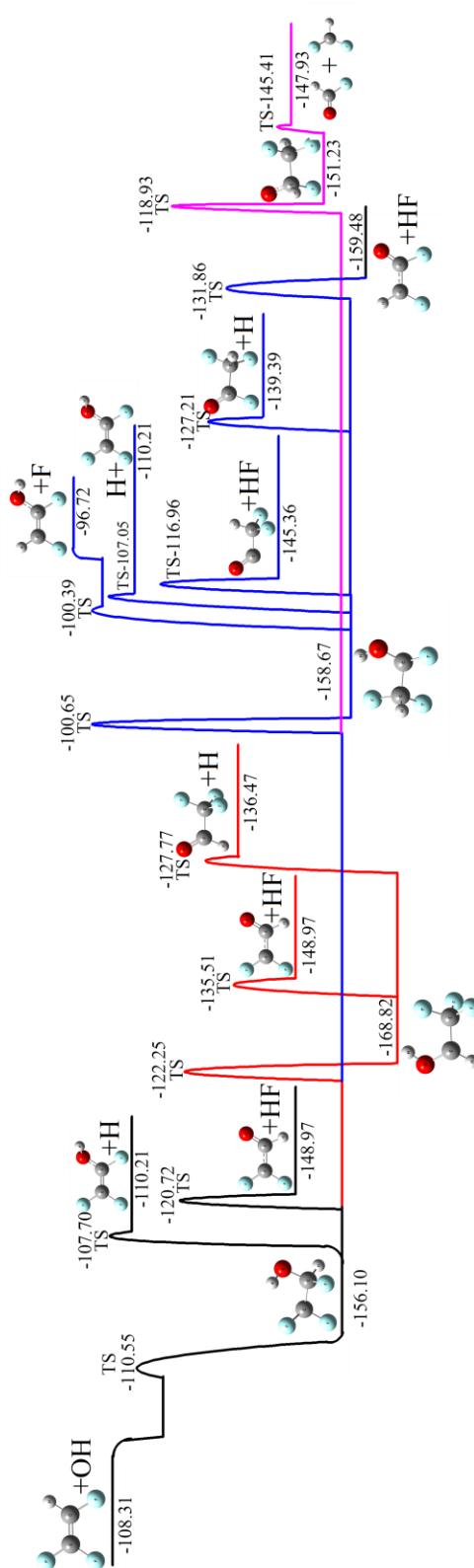


Figure 6.2b Potential energy diagrams for the $\text{CHF}=\text{CF}_2 + \text{OH} \rightarrow \text{C}\cdot\text{F}_2\text{CHF}(\text{OH}) \rightarrow \text{product system}$.

Reactions of $\text{C}\cdot\text{F}_2\text{CHF}(\text{OH})$ * adduct

Figure 6.2b below shows the reaction paths of $\text{C}\cdot\text{F}_2\text{CHF}(\text{OH})$ adduct which are similar to the $\text{C}(\text{OH})\text{F}_2\text{C}\cdot\text{HF}$ and include: dissociation back to reactants, stabilization to the $\text{C}\cdot\text{F}_2\text{CHF}(\text{OH})$ adduct, intramolecular H and F atom transfer reactions, and H atom and HF elimination reactions. Isomerization of $\text{C}\cdot\text{F}_2\text{CHF}(\text{OH})$ adduct yields two hydrofluoroalkyl radicals with a $33.9 \text{ kcal mol}^{-1}$ barrier for F atom-transfer forming $\text{CF}_3\text{C}\cdot\text{H}(\text{OH})$, and a $55.5 \text{ kcal mol}^{-1}$ barrier for H-transfer forming the $\text{CHF}_2\text{C}\cdot(\text{OH})\text{H}$ adduct. A second H-atom transfer is from the hydroxyl group forming 1,2, trifluoro ethoxy radical with a $37.2 \text{ kcal mol}^{-1}$ barrier. There are two HF elimination reaction paths, and both of them yield 2,2 difluoroethene – oxy radical + HF. This radical is a resonance isomer of 2,2 difluoro acetaldehyde ($\text{C}\cdot\text{F}_2\text{-CH(=O)} + \text{HF}$). These reactions are shown to be important reaction paths at several conditions studied in this system. The activation energy for reaction to the difluoroethene – oxy radical from $\text{C}\cdot\text{F}_2\text{CHF}(\text{OH})$ adduct is $35.4 \text{ kcal mol}^{-1}$. The second reaction path involves a F atom transfer prior to the HF elimination, see Figure 6.2b, and has a barrier and $35.3 \text{ kcal mol}^{-1}$ from the fluorine atom transfer isomer $\text{CF}_3\text{C}\cdot\text{H}(\text{OH})$.

6.3.2 Chemical Activation Results for Kinetics of $\text{CF}_2\text{CHF} + \text{OH} \rightarrow (\text{HO})\text{CF}_2\text{C}\cdot\text{HF}$ to Products System

The $\text{CF}_2\text{CHF} + \text{OH}$ The $\text{CF}_2\text{CHF} + \text{OH}$ chemical activation reaction kinetics show product distributions versus temperature for the $\text{C}_2\text{F}_3\text{H} + \text{OH} \rightarrow (\text{HO})\text{CF}_2\text{C}\cdot\text{HF}$ reaction systems at 1.0 atm and 100.0 atm in Figures 6.3a and 6.3b, respectively. At atmospheric pressure, the HF molecular elimination channel is dominant above 300 K with the $(\text{HO})\text{CF}_2\text{C}\cdot\text{HF}$ stabilization adduct dominant at lower temperature. A second important

reaction channel is the dissociation reaction to form carbonyl fluoride and alkyl radical $[\text{CF}_2\text{O} + \text{C}\cdot\text{F}_2\text{H}]$. The reverse dissociation back to $\text{C}_2\text{F}_3\text{H} + \text{OH}$ increases at higher temperature but is not as important as the HF elimination or dissociation reaction path $[(\text{HO})\text{CF}_2\text{C}\cdot\text{HF} \rightarrow \text{CF}_2(=\text{O}) + \text{C}\cdot\text{H}_2\text{F}]$ (difluoromethanal [commonly named difluorocarbonyl] plus fluoro-methyl radical. At high pressure; 100.0 atm, the major reaction channels follow the same trend as observed for the 1.0 atm reaction condition. The $(\text{HO})\text{CF}_2\text{C}\cdot\text{HF}$ stabilization adduct is the dominant path up to a higher temperature than at 1.0 atm. The Stabilized adduct becomes important below 600 K at 100.0 atm. compare to 300 K from 1.0 atm.

Plots of calculated rate constants for $\text{C}_2\text{F}_3\text{H} + \text{OH} \rightarrow (\text{HO})\text{CF}_2\text{C}\cdot\text{HF} \rightarrow \text{products}$ system versus log pressure (atm) at 298 K and 2000 K are shown in Figure 6.4a and 6.4b, respectively. At 298 K, the $(\text{HO})\text{CF}_2\text{C}\cdot\text{HF}$ stabilization adduct is the dominant path above 1.0 atm. The HF elimination channel is an important one above 1.0 atm. The reverse reaction back to $\text{C}_2\text{F}_3\text{H} + \text{OH}$ is lower by 4 orders of magnitude. Dissociation to $(\text{HO})\text{CF}=\text{CHF} + \text{F}$ has an endothermicity of $11.6 \text{ kcal mol}^{-1}$ above the reactant channel and the rate constant at low temperature is not significant compared to the other reaction channels in the system.

At high temperature; 1000 K, the HF elimination channel dominates all of the pressure studied followed by dissociation reaction to Carbonyl fluoride ($\text{C}(=\text{O})\text{F}_2$) and fluoromethyl radical ($\text{C}\cdot\text{H}_2\text{F}$). Both reaction channels are independent to the pressure at this high temperature.

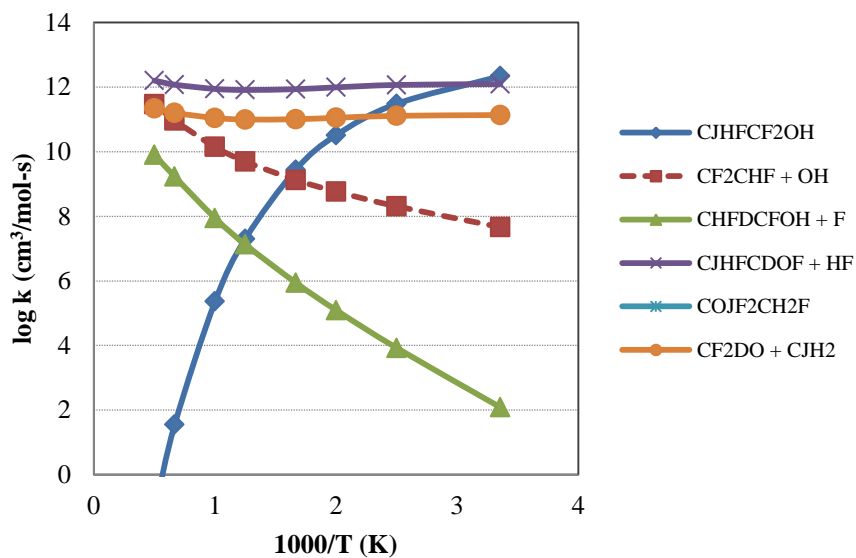


Figure 6.3a Rate constants versus $1000/T$ (K) at 1.0 atm for the chemical activation reaction of $C_2F_3H + OH \rightarrow (HO)CF_2C \cdot HF^* \rightarrow$ products system.

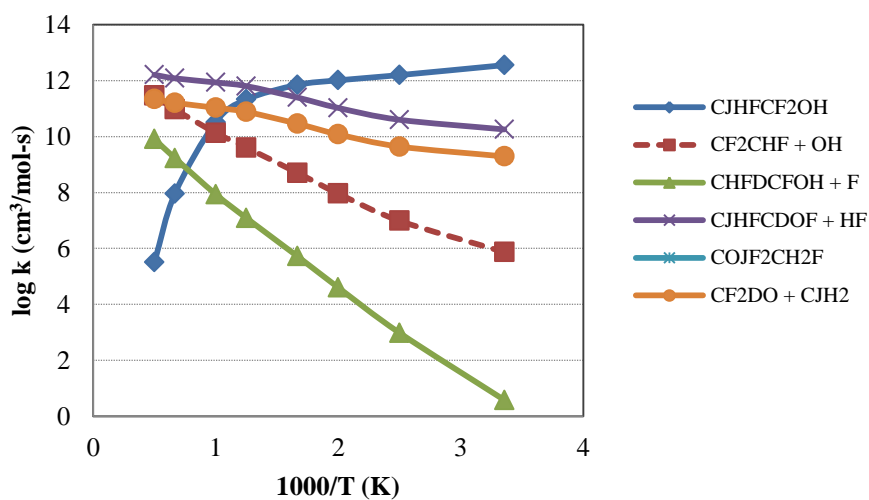


Figure 6.3b Rate constants versus $1000/T$ (K) at 100.0 atm for the chemical activation reaction of $C_2F_3H + OH \rightarrow (HO)CF_2C \cdot HF^* \rightarrow$ products system.

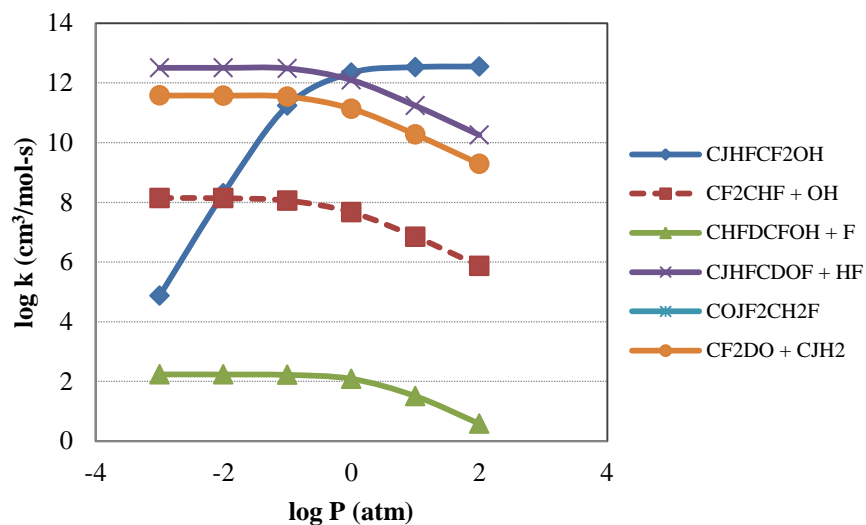


Figure 6.4a Rate constants versus log pressure (atm) at 298 K for chemical activation reactions of $\text{C}_2\text{F}_3\text{H} + \text{OH} \rightarrow (\text{HO})\text{CF}_2\text{C}\cdot\text{HF}^* \rightarrow \text{products}$ system.

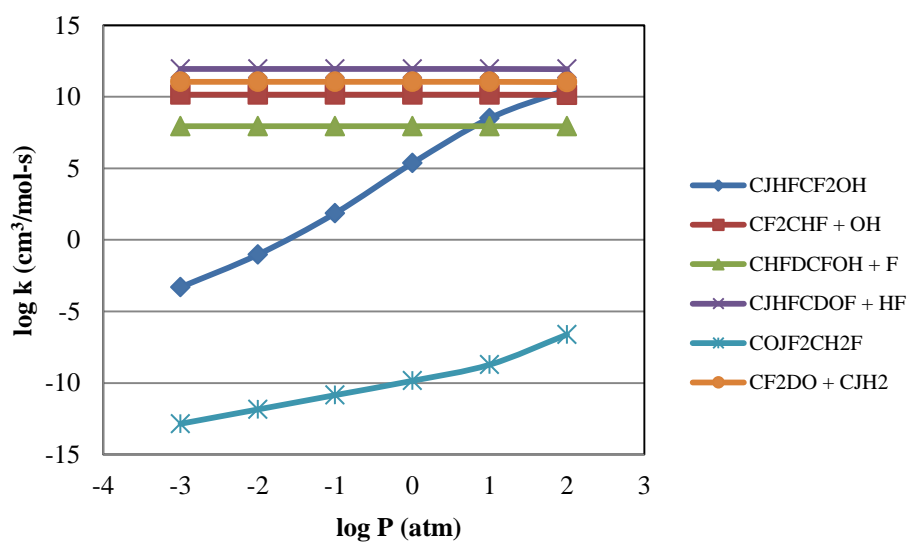


Figure 6.4b Rate constants versus log pressure (atm) at 1000 K for chemical activation reaction of $\text{C}_2\text{F}_3\text{H} + \text{OH} \rightarrow (\text{HO})\text{CF}_2\text{C}\cdot\text{HF}^* \rightarrow \text{products}$ system.

6.3.3 Unimolecular Dissociation of the (HO)CF₂C•HF Stabilization Adduct

Figures 6.5a and 6.5b show plots of the (HO)CF₂C•HF stabilized adduct dissociation at 298 K and 500 K, respectively. Plots of unimolecular dissociation rate constants for the (HO)CF₂C•HF stabilization adduct versus 1000/T (K) at 1 atm are shown in Figure 6.6. Results show the important forward reactions are HF molecular elimination. This product channel is important over the range temperature and pressure studied, the next important path is isomerization to CO•F₂-CH₂F from H atom intramolecular transfer reaction. Both reaction channels are independent of the pressure at room temperature. The F elimination reaction channels are the least important in this system due to the strong C—F bonding.

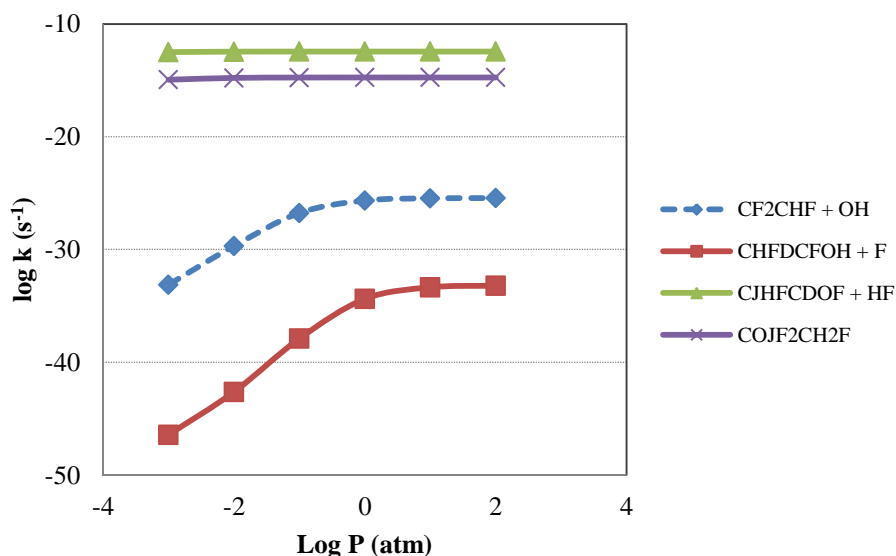


Figure 6.5a Rate constants versus log pressure (atm) at 298 K for the chemical dissociation reaction of (HO)CF₂C•HF* → C₂F₃H + OH, and → products system.

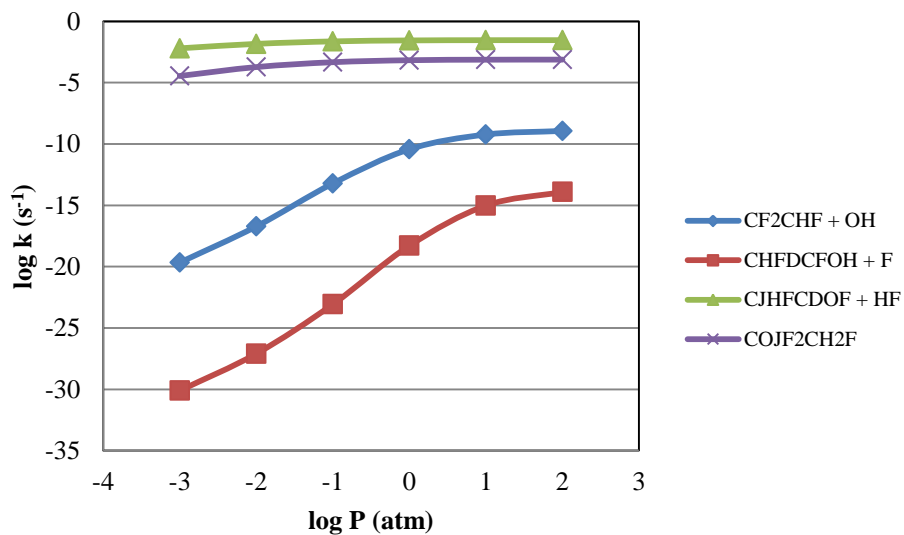


Figure 6.5b Rate constants versus log pressure (atm) at 500 K for the chemical dissociation reaction of $(\text{HO})\text{CF}_2\text{C}\cdot\text{HF}^* \rightarrow \text{C}_2\text{F}_3\text{H} + \text{OH}$, and \rightarrow products system.

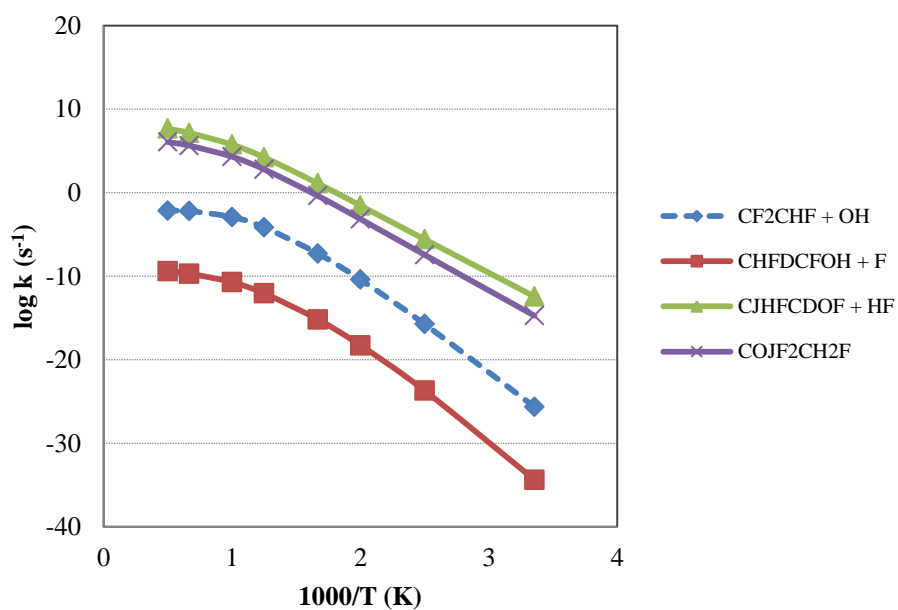


Figure 6.6 Rate constants versus 1000/T at 1.0 atm for the chemical dissociation reaction of $(\text{HO})\text{CF}_2\text{C}\cdot\text{HF}^* \rightarrow \text{C}_2\text{F}_3\text{H} + \text{OH}$, and \rightarrow products system.

6.3.4 Chemical Activation Results for Kinetics of $\text{C}_2\text{F}_3\text{H} + \text{OH} \rightarrow \text{C}\cdot\text{F}_2\text{-CHF(OH)}$ to Products System

Plots of calculated rate constants versus $1000/T$ (K) from chemical activation for $\text{C}_2\text{F}_3\text{H} + \text{OH} \rightarrow \text{C}\cdot\text{F}_2\text{-CHF(OH)} \rightarrow \text{products}$ at 1 atm and 100 atm are shown in Figure 6.7a and 6.7b, respectively. Stabilization to adduct $\text{C}\cdot\text{F}_2\text{CHFOH}$ channel is the most important reaction path at low temperature fluorocarbon oxidation; below 400 K. As temperature is increased, the rate through other channels also increases, while the stabilization rate decreases. At the higher temperatures, there is sufficient reaction of the energized adducts over the barriers and dissociate before stabilization. Important forward reactions go to HF molecular elimination; $\text{C}\cdot\text{F}_2\text{CH(=O)} + \text{HF}$. Other important product channels are H-elimination; $\text{F}_2\text{C=CH(OH)} + \text{H}$ and beta scission; $\text{CHF(=O)} + \text{C}\cdot\text{HF}_2$, reaction channels. At high pressure; 100.0 atm, the major reaction channels follow the same trend as at 1.0 atm.

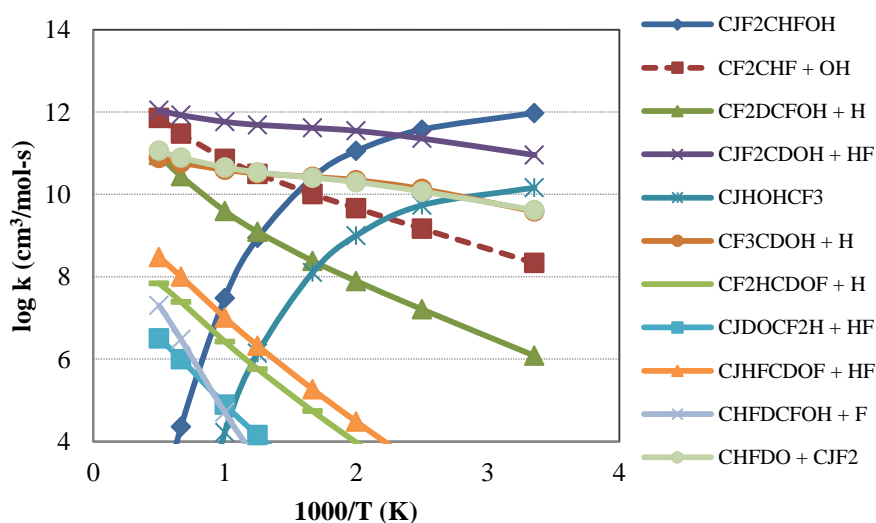


Figure 6.7a Rate constants versus $1000/T$ (K) at 1.0 atm for the chemical activation reaction of $\text{C}_2\text{F}_3\text{H} + \text{OH} \rightarrow \text{C}\cdot\text{F}_2\text{CHF(OH)}^* \rightarrow \text{products}$ system.

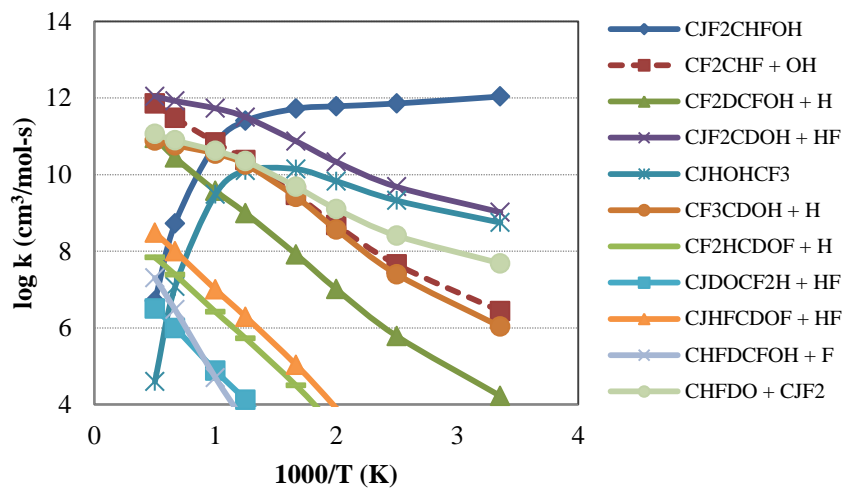


Figure 6.7b Rate constants versus $1000/T$ (K) at 100.0 atm for the chemical activation reaction of $C_2F_3H + OH \rightarrow C \cdot F_2CHF(OH)^* \rightarrow$ products system.

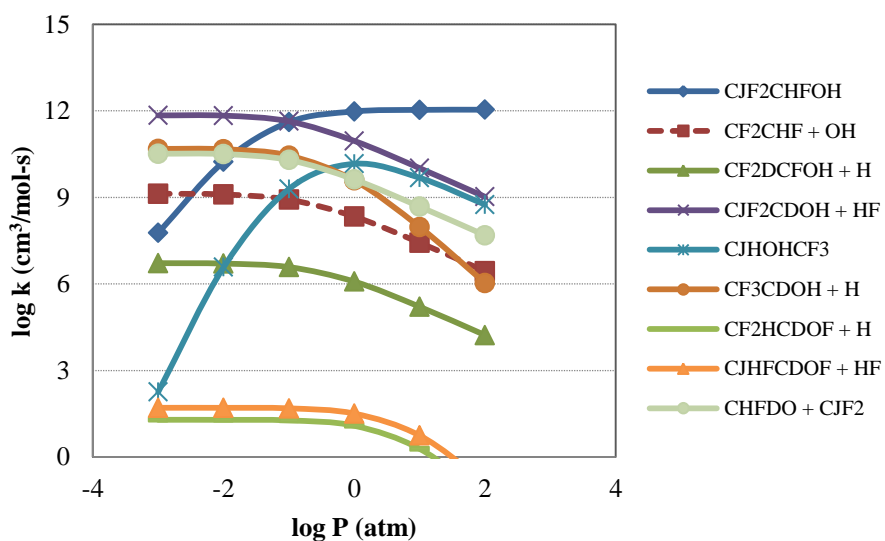


Figure 6.8a Rate constants versus log pressure (atm) at 298 K for the chemical activation reaction of $C_2F_3H + OH \rightarrow C \cdot F_2CHF(OH)^* \rightarrow$ products system.

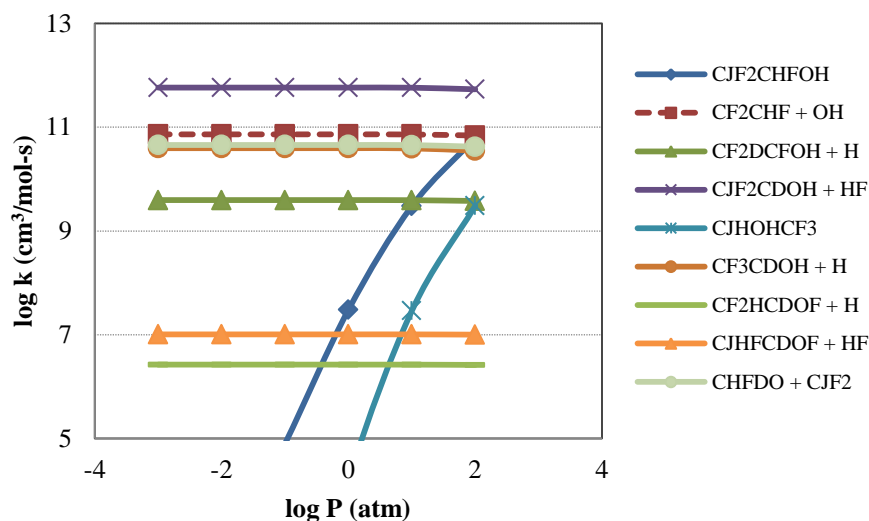


Figure 6.8b Rate constants versus log pressure (atm) at 1000 K for the chemical activation reaction of $\text{C}_2\text{F}_3\text{H} + \text{OH} \rightarrow \text{C}\cdot\text{F}_2\text{CHF}(\text{OH})^* \rightarrow \text{products}$ system.

Plots of calculated rate constants versus log pressure from chemical activation reaction of $\text{C}_2\text{F}_3\text{H} + \text{OH} \rightarrow \text{C}\cdot\text{F}_2\text{-CHF}(\text{OH})$ to products at 298 K and 1000 K are shown in Figure 6.8a and Figure 6.8b, respectively. At atmospheric temperatures $\text{C}\cdot\text{F}_2\text{CHFOH}$ stabilization adduct is the dominant path above 1.0 atm while HF molecular elimination reactions to form $\text{C}\cdot\text{F}_2\text{CH}(\text{=O}) + \text{HF}$ is important below 1.0 atm. At low pressures, some of the energized $\text{C}\cdot\text{F}_2\text{CHFOH}$ adduct can isomerize to form mono-fluoro methanal (monofluorocarbonyl) plus a difluoro methyl radical ($\text{C}(\text{=O})\text{HF} + \text{C}\cdot\text{HF}_2$) prior to stabilization but the rate of stabilization of energized alkyl radical in the atm pressure environment is slower than the rates of H atom and HF molecular elimination channels. The overall rate of stabilized adducts is low at higher temperatures. At temperatures; above 1000 K, most reactions are independent of pressure except the isomerization to the alkyl radical, which decreases as pressure decrease. Important forward reactions are the two HF molecular elimination; $\text{C}\cdot\text{F}_2\text{CH}(\text{=O}) + \text{HF}$ reaction channels.

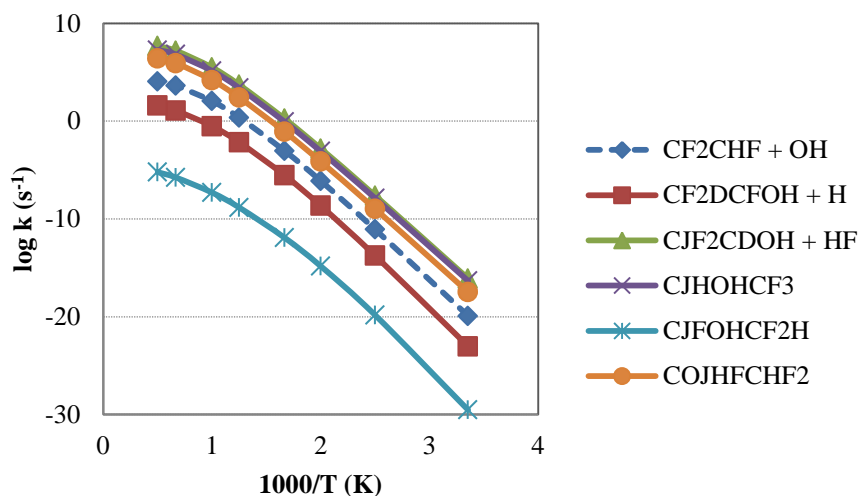


Figure 6.9 Rate constants versus $1000/T$ at 1.0 atm for the chemical dissociation reaction of $\text{C}\cdot\text{F}_2\text{CHF}(\text{OH})^* \rightarrow \text{C}_2\text{F}_3\text{H} + \text{OH}$, and \rightarrow products system.

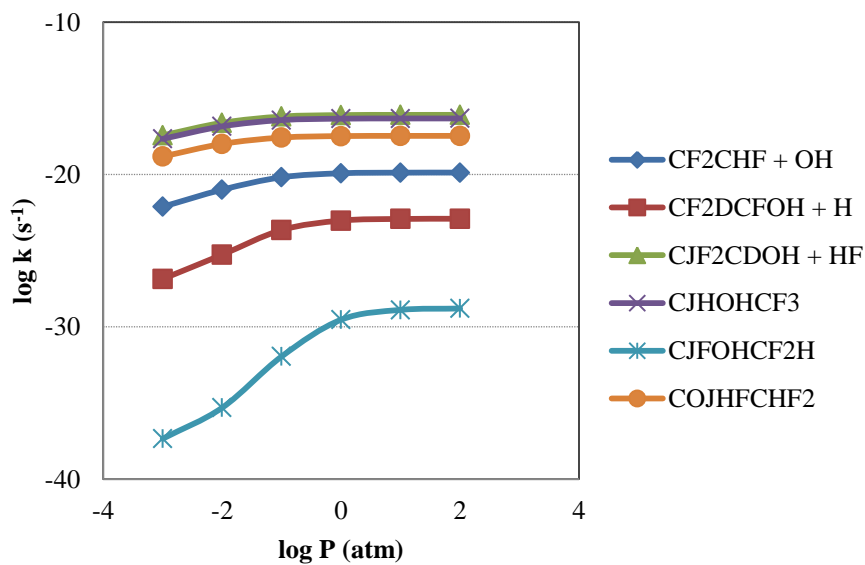


Figure 6.10a Rate constants versus $\log P$ (atm) at 298 K for the chemical dissociation reaction of $\text{C}\cdot\text{F}_2\text{CHF}(\text{OH})^* \rightarrow \text{C}_2\text{F}_3\text{H} + \text{OH}$, and \rightarrow products system.

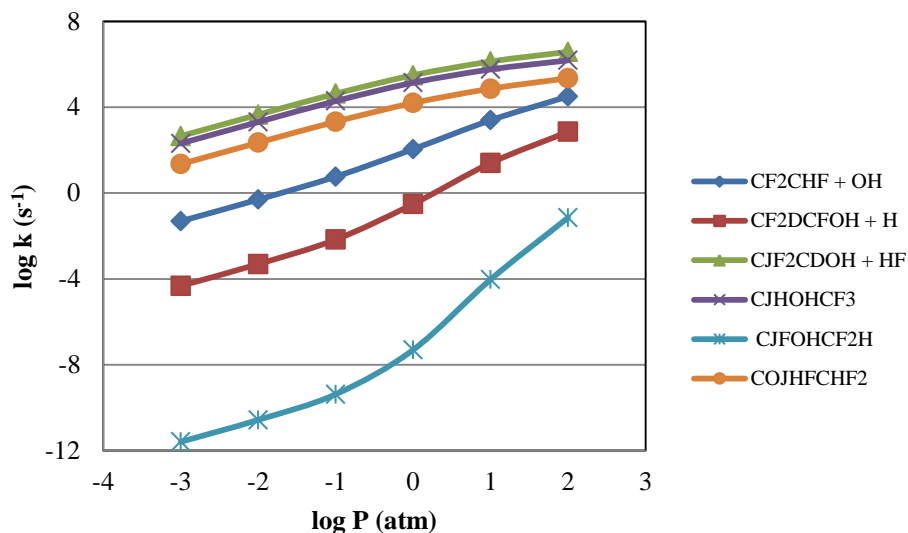


Figure 6.10b Rate constants versus log pressure (atm) at 1000 K for the chemical dissociation reaction of $\text{C}\cdot\text{F}_2\text{CHF}(\text{OH})^* \rightarrow \text{C}_2\text{F}_3\text{H} + \text{OH}$, and \rightarrow products system.

6.3.5 Unimolecular Dissociation of the $\text{C}\cdot\text{F}_2\text{CHFOH}$ Stabilization Adduct

Rate constants for reactions of the $\text{C}\cdot\text{F}_2\text{CHFOH}$ stabilized adduct dissociation at 1 atm pressure versus $1000/T$ are illustrated in Figure 6.9. Plots of rate constants versus log pressure at 298 K and 1000 K are illustrated in Figures 6.10a and Figure 6.10b, respectively. Important dissociation reactions are HF molecular elimination to $\text{C}\cdot\text{F}_2\text{CH}(\text{=O}) + \text{HF}$ and isomerization to the $\text{C}\cdot\text{H}(\text{OH})\text{CF}_3$ (trifluoro ethanl-1yl radical) channel. This F atom transfer (isomerization) to $\text{C}\cdot\text{H}(\text{OH})\text{CF}_3$ has the lowest activation energy, $33.9 \text{ kcal mol}^{-1}$, relative to other isomerization and dissociation reaction paths and this reaction path is important over all temperature and pressures studied. The rate constants do not show any strong dependence on pressure under temperature and pressure ranges of atmospheric chemistry, The reaction rates increase with pressure at high temperatures, over 2000K.

6.4 Summary

Thermochemical properties of intermediate radicals and transition state structures for the $\text{C}_2\text{F}_3\text{H} + \text{OH}$ reaction systems are calculated using density functional and ab initio methods with enthalpies of formation ($\Delta H_f^\circ(298)$) for several hydrofluoroalkyl radicals are determined. Well depths for $\text{C}_2\text{F}_3\text{H} + \text{OH}$ forming $\text{C}(\text{OH})\text{F}_2\text{C}\cdot\text{HF}$ adduct is $55.4 \text{ kcal mol}^{-1}$ and $47.8 \text{ kcal mol}^{-1}$ for forming $\text{C}\cdot\text{F}_2\text{CHF}(\text{OH})$ adduct. The values are important for the determination of the kinetic properties, since small changes in the activation energies will cause larger changes in the rate constants especially at the lower temperatures.

Under conditions of atmospheric pressure and temperature, both of the addition paths for the $\text{C}_2\text{F}_3\text{H} + \text{OH}$ reactions proceed primarily to stabilization adduct at low temperature. The major new products are from HF elimination reactions path which yield 2,2 difluoroethanol-2yl + HF from the $\text{C}\cdot\text{F}_2\text{CHF}(\text{OH})$ adduct and yield 1,2 difluoroethoxy radical from the $\text{C}(\text{OH})\text{F}_2\text{C}\cdot\text{HF}$ adduct system. The major dissociation reaction path is HF elimination reactions.

APPENDIX A

ERROR ANALYSIS: UNCERTAINTY

The comparisons of experimental $\Delta_{\text{rxn}}H^\circ_{298}$ with values determined using CBS-QB3 and B3LYP/6-31G(d,p) in this study (kcal mol^{-1}) for standard enthalpies of formation at 298 K of reference species.

Table A.1 Root Mean Square for B3LYP and CBS-QB3 Methods

Reactions							Exp.	CBS-QB3	B3LYP
coh	+	ccc	-->	ccoh	+	cc	-3.07	-2.96	-3.86
ccoh	+	ccc	-->	ccco	+	cc	0.22	-0.01	-0.15
ccco	+	cc	-->	ccoh	+	ccc	-0.22	0.01	0.15
cdcc	+	cc	-->	cdc	+	ccc	2.78	2.72	3.89
cj	+	cdcc	-->	i-c4h9			-22.88	-22.21	-21.34
cdej	+	cj	-->	cdcc			-101.32	-101.32	-102.05
y(c4h4o)	+	cdccdc	-->	y(c5h6)	+	y(c3h4do)	18.2	18.77	18.55
y(c6h5)oh	+	cc	-->	y(c6h6)	+	ccoh	6.66	6.18	8.2
y(c6h5)oh	+	ccj	-->	y(c6h5)j	+	ccoh	19.42	19.92	19.09
cdcc	+	cdcd	-->	cdc	+	y(c3h4do)	22.91	23.67	23.86
y(c6h6)	+	ccco	-->	y(c6h5)oh	+	ccc	-6.88	-6.17	-8.05
cdco	+	y(c6h6)	-->	y(c6h5)oh	+	cdc	-0.49	0.05	0.7
							RMS	0.48	0.97

The uncertainty calculation for computational method

$$Uncertainty = \bar{X} \pm [t * (\frac{s}{\sqrt{n}})]$$

Where;

\bar{X} = mean of sample, n = number of sample; here n = number of work reactions for each molecule at 95% confidential limit, t = Degree of Freedom for $n-1$, s = RMS for each method

Table A.2 95% Confidential Limit for Each of the Work Reaction Sets

Number of Work Reactions	CBS-QB3	B3LYP/6-31G(d,p)
7	0.44	0.9
5	0.59	1.21
4	0.76	1.54
3	1.18	2.42

Example calculation for 95% confidential Limit for 7 work reactions

Where; t (degree of freedom for n -1) = 2.447 with CBS-QB3 method (RMS = 0.48)

$$= [(2.447*0.48) / (7)^{0.5}]$$

$$= \mathbf{0.44}$$

APPENDIX B

RESULTING RATE CONSTANTS IN QRRK CALCULATION OF CYCLO-PENTADIENONE-2-YL AND CYCLO-PENTADIENONE-3-YL RADICAL SYSTEM

Tables B.1 and B.2 were the result from QRRK calculations for O₂ addition to cyclopentadienone-2-yl and cyclopentadienone-3-yl reactions.

Table B.1 Calculated Reaction Parameters, $K = A(T/K)^N \text{Exp}(-E_a/RT)$ ($300 \leq T/K \leq 2000$), for Cyclo-Pentadienone-2-yl Radical System

Reactions	A	n	E _a (cal/mol)	Pressure (atm)
Y(C5H3DO)J2 + O2 => Y(C5H3DO)OOJ2	1.36E+51	-17.92	5858	0.001
Y(C5H3DO)J2 + O2 => Y(C5H3DO)OOJ2	8.02E+75	-24.57	11441	0.01
Y(C5H3DO)J2 + O2 => Y(C5H3DO)OOJ2	5.14E+91	-27.98	16772	0.1
Y(C5H3DO)J2 + O2 => Y(C5H3DO)OOJ2	1.42E+97	-28.21	21948	1
Y(C5H3DO)J2 + O2 => Y(C5H3DO)OOJ2	4.25E+88	-24.57	22569	10
Y(C5H3DO)J2 + O2 => Y(C5H3DO)OOJ2	2.77E+76	-20.35	20211	50
Y(C5H3DO)J2 + O2 => Y(C5H3DO)OOJ2	2.06E+70	-18.32	18721	100
Y(C5H3DO)J2 + O2 => Y(C5H3DO)J2 + O2	2.29E-01	3.92	3647	0.001
Y(C5H3DO)J2 + O2 => Y(C5H3DO)J2 + O2	2.62E-01	3.91	3680	0.01
Y(C5H3DO)J2 + O2 => Y(C5H3DO)J2 + O2	8.30E-01	3.76	3967	0.1
Y(C5H3DO)J2 + O2 => Y(C5H3DO)J2 + O2	2.04E+02	3.08	5417	1
Y(C5H3DO)J2 + O2 => Y(C5H3DO)J2 + O2	1.61E+05	2.28	7856	10
Y(C5H3DO)J2 + O2 => Y(C5H3DO)J2 + O2	2.03E+04	2.6	8731	50
Y(C5H3DO)J2 + O2 => Y(C5H3DO)J2 + O2	7.59E+02	3.05	8723	100
Y(C5H3DO)J2 + O2 => Y(C5H3DO)OJ2 + O	1.64E+06	2.1	186	0.001
Y(C5H3DO)J2 + O2 => Y(C5H3DO)OJ2 + O	1.69E+06	2.1	193	0.01
Y(C5H3DO)J2 + O2 => Y(C5H3DO)OJ2 + O	2.90E+06	2.03	326	0.1
Y(C5H3DO)J2 + O2 => Y(C5H3DO)OJ2 + O	1.03E+09	1.3	1856	1
Y(C5H3DO)J2 + O2 => Y(C5H3DO)OJ2 + O	1.79E+11	0.71	4174	10
Y(C5H3DO)J2 + O2 => Y(C5H3DO)OJ2 + O	1.34E+09	1.39	4613	50
Y(C5H3DO)J2 + O2 => Y(C5H3DO)OJ2 + O	1.45E+07	1.99	4399	100
Y(C5H3DO)J2 + O2 => Y(C5H3DO)Q2-3J	2.04E-04	4.55	445	0.001
Y(C5H3DO)J2 + O2 => Y(C5H3DO)Q2-3J	2.32E-04	4.53	477	0.01
Y(C5H3DO)J2 + O2 => Y(C5H3DO)Q2-3J	8.26E-04	4.37	795	0.1
Y(C5H3DO)J2 + O2 => Y(C5H3DO)Q2-3J	4.10E-01	3.6	2463	1
Y(C5H3DO)J2 + O2 => Y(C5H3DO)Q2-3J	9.36E+01	2.97	4811	10
Y(C5H3DO)J2 + O2 => Y(C5H3DO)Q2-3J	1.81E+00	3.53	5399	50
Y(C5H3DO)J2 + O2 => Y(C5H3DO)Q2-3J	3.18E-02	4.07	5265	100

Table B.1 Calculated Reaction Parameters, $K = A(T/K)^N \text{Exp}(-E_a/RT)$ ($300 \leq T/K \leq 2000$), for Cyclo-Pentadienone-2-yl Radical System (Continued)

Reactions	A	n	E_a (cal/mol)	Pressure (atm)
Y(C5H3DO)J2 + O2 => YCPDO-4,5-Y(COOC)	3.01E-02	3.72	302	0.001
Y(C5H3DO)J2 + O2 => YCPDO-4,5-Y(COOC)	3.38E-02	3.71	331	0.01
Y(C5H3DO)J2 + O2 => YCPDO-4,5-Y(COOC)	1.10E-01	3.56	629	0.1
Y(C5H3DO)J2 + O2 => YCPDO-4,5-Y(COOC)	5.20E+01	2.8	2286	1
Y(C5H3DO)J2 + O2 => YCPDO-4,5-Y(COOC)	1.03E+04	2.18	4616	10
Y(C5H3DO)J2 + O2 => YCPDO-4,5-Y(COOC)	1.64E+02	2.77	5173	50
Y(C5H3DO)J2 + O2 => YCPDO-4,5-Y(COOC)	2.65E+00	3.32	5024	100
Y(C5H3DO)J2 + O2 => YCPDO-2-Y(OO)	2.41E+09	1.01	426	0.001
Y(C5H3DO)J2 + O2 => YCPDO-2-Y(OO)	2.38E+09	1.01	423	0.01
Y(C5H3DO)J2 + O2 => YCPDO-2-Y(OO)	2.78E+09	0.99	453	0.1
Y(C5H3DO)J2 + O2 => YCPDO-2-Y(OO)	9.36E+11	0.27	1906	1
Y(C5H3DO)J2 + O2 => YCPDO-2-Y(OO)	2.69E+14	-0.39	4299	10
Y(C5H3DO)J2 + O2 => YCPDO-2-Y(OO)	1.95E+12	0.3	4741	50
Y(C5H3DO)J2 + O2 => YCPDO-2-Y(OO)	1.92E+10	0.91	4512	100
Y(C5H3DO)OOJ2 => Y(C5H3DO)J2 + O2	2.09E+41	-14.03	50782	0.001
Y(C5H3DO)OOJ2 => Y(C5H3DO)J2 + O2	5.82E+54	-17.14	52674	0.01
Y(C5H3DO)OOJ2 => Y(C5H3DO)J2 + O2	1.77E+71	-20.78	58118	0.1
Y(C5H3DO)OOJ2 => Y(C5H3DO)J2 + O2	5.77E+72	-19.83	61817	1
Y(C5H3DO)OOJ2 => Y(C5H3DO)J2 + O2	1.76E+66	-16.87	62859	10
Y(C5H3DO)OOJ2 => Y(C5H3DO)J2 + O2	1.20E+56	-13.32	61011	50
Y(C5H3DO)OOJ2 => Y(C5H3DO)J2 + O2	9.82E+50	-11.62	59803	100
Y(C5H3DO)OOJ2 => Y(C5H3DO)OJ2 + O	1.25E+47	-12.13	33353	0.001
Y(C5H3DO)OOJ2 => Y(C5H3DO)OJ2 + O	3.15E+50	-12.66	36079	0.01
Y(C5H3DO)OOJ2 => Y(C5H3DO)OJ2 + O	8.68E+49	-12.05	37461	0.1
Y(C5H3DO)OOJ2 => Y(C5H3DO)OJ2 + O	6.98E+41	-9.22	36015	1
Y(C5H3DO)OOJ2 => Y(C5H3DO)OJ2 + O	8.75E+34	-6.88	34571	10
Y(C5H3DO)OOJ2 => Y(C5H3DO)OJ2 + O	1.87E+29	-5.02	33091	50
Y(C5H3DO)OOJ2 => Y(C5H3DO)OJ2 + O	6.01E+26	-4.21	32396	100
Y(C5H3DO)OOJ2 => Y(C5H3DO)Q2-3J	1.11E+41	-12.68	41394	0.001
Y(C5H3DO)OOJ2 => Y(C5H3DO)Q2-3J	6.30E+53	-15.58	45469	0.01
Y(C5H3DO)OOJ2 => Y(C5H3DO)Q2-3J	8.48E+60	-16.72	50072	0.1
Y(C5H3DO)OOJ2 => Y(C5H3DO)Q2-3J	1.72E+55	-14.15	50823	1
Y(C5H3DO)OOJ2 => Y(C5H3DO)Q2-3J	7.56E+46	-11.06	49956	10
Y(C5H3DO)OOJ2 => Y(C5H3DO)Q2-3J	2.55E+38	-8.22	48017	50
Y(C5H3DO)OOJ2 => Y(C5H3DO)Q2-3J	3.17E+34	-6.94	46999	100

Table B.1 Calculated Reaction Parameters, $K = A(T/K)^N \text{Exp}(-E_a/RT)$ ($300 \leq T/K \leq 2000$), for Cyclo-Pentadienone-2-yl Radical System (Continued)

Reactions	A	n	E_a (cal/mol)	Pressure (atm)
Y(C5H3DO)OOJ2 \Rightarrow YCPDO-4,5-Y(COOC)	1.35E+43	-13.24	39946	0.001
Y(C5H3DO)OOJ2 \Rightarrow YCPDO-4,5-Y(COOC)	1.08E+55	-15.9	44339	0.01
Y(C5H3DO)OOJ2 \Rightarrow YCPDO-4,5-Y(COOC)	5.63E+60	-16.7	48585	0.1
Y(C5H3DO)OOJ2 \Rightarrow YCPDO-4,5-Y(COOC)	2.70E+54	-14.01	48950	1
Y(C5H3DO)OOJ2 \Rightarrow YCPDO-4,5-Y(COOC)	1.19E+46	-10.98	47914	10
Y(C5H3DO)OOJ2 \Rightarrow YCPDO-4,5-Y(COOC)	8.64E+37	-8.25	46009	50
Y(C5H3DO)OOJ2 \Rightarrow YCPDO-4,5-Y(COOC)	1.65E+34	-7.04	45029	100
Y(C5H3DO)OOJ2 \Rightarrow YCPDO-2-Y(OO)	3.97E+43	-10.7	29288	0.001
Y(C5H3DO)OOJ2 \Rightarrow YCPDO-2-Y(OO)	5.18E+44	-10.73	30796	0.01
Y(C5H3DO)OOJ2 \Rightarrow YCPDO-2-Y(OO)	7.27E+42	-9.89	31206	0.1
Y(C5H3DO)OOJ2 \Rightarrow YCPDO-2-Y(OO)	2.24E+35	-7.35	29537	1
Y(C5H3DO)OOJ2 \Rightarrow YCPDO-2-Y(OO)	4.90E+29	-5.46	28228	10
Y(C5H3DO)OOJ2 \Rightarrow YCPDO-2-Y(OO)	1.63E+25	-4	27019	50
Y(C5H3DO)OOJ2 \Rightarrow YCPDO-2-Y(OO)	1.82E+23	-3.37	26465	100

Table B.2 Calculated Reaction Parameters, $K = A(T/K)^N \text{Exp}(-E_a/RT)$ ($300 \leq T/K \leq 2000$), for Cyclo-Pentadienone-3-yl Radical System

Reactions	A	n	E_a (cal/mol)	Pressure (atm)
Y(C5H3DO)J3 + O2 \Rightarrow Y(C5H3DO)OOJ22	5.08E+65	-22.11	9089	0.001
Y(C5H3DO)J3 + O2 \Rightarrow Y(C5H3DO)OOJ22	4.52E+83	-26.44	13292	0.01
Y(C5H3DO)J3 + O2 \Rightarrow Y(C5H3DO)OOJ22	1.38E+97	-29.07	19847	0.1
Y(C5H3DO)J3 + O2 \Rightarrow Y(C5H3DO)OOJ22	1.27E+96	-27.51	23199	1
Y(C5H3DO)J3 + O2 \Rightarrow Y(C5H3DO)OOJ22	9.34E+83	-22.98	22030	10
Y(C5H3DO)J3 + O2 \Rightarrow Y(C5H3DO)OOJ22	4.86E+71	-18.84	19284	50
Y(C5H3DO)J3 + O2 \Rightarrow Y(C5H3DO)OOJ22	7.34E+65	-16.92	17791	100
Y(C5H3DO)J3 + O2 \Rightarrow Y(C5H3DO)J3 + O2	1.02E-02	4.23	2959	0.001
Y(C5H3DO)J3 + O2 \Rightarrow Y(C5H3DO)J3 + O2	1.54E-02	4.18	3060	0.01
Y(C5H3DO)J3 + O2 \Rightarrow Y(C5H3DO)J3 + O2	2.83E-01	3.82	3778	0.1
Y(C5H3DO)J3 + O2 \Rightarrow Y(C5H3DO)J3 + O2	1.12E+03	2.79	6034	1
Y(C5H3DO)J3 + O2 \Rightarrow Y(C5H3DO)J3 + O2	2.23E+05	2.18	8479	10
Y(C5H3DO)J3 + O2 \Rightarrow Y(C5H3DO)J3 + O2	5.00E+03	2.73	9117	50
Y(C5H3DO)J3 + O2 \Rightarrow Y(C5H3DO)J3 + O2	1.15E+02	3.23	9036	100

Table B.2 Calculated Reaction Parameters, $K = A(T/K)^N \text{Exp}(-E_a/RT)$ ($300 \leq T/K \leq 2000$), for Cyclo-Pentadienone-3-yl Radical System (Continued)

Reactions	A	n	E_a (cal/mol)	Pressure (atm)
Y(C5H3DO)J3 + O2 => Y(C5H3DO)OJ3 + O	1.47E+05	2.39	241	0.001
Y(C5H3DO)J3 + O2 => Y(C5H3DO)OJ3 + O	1.73E+05	2.37	281	0.01
Y(C5H3DO)J3 + O2 => Y(C5H3DO)OJ3 + O	2.49E+06	2.04	938	0.1
Y(C5H3DO)J3 + O2 => Y(C5H3DO)OJ3 + O	1.10E+10	1.01	3356	1
Y(C5H3DO)J3 + O2 => Y(C5H3DO)OJ3 + O	4.96E+10	0.89	5295	10
Y(C5H3DO)J3 + O2 => Y(C5H3DO)OJ3 + O	3.45E+07	1.88	5365	50
Y(C5H3DO)J3 + O2 => Y(C5H3DO)OJ3 + O	2.06E+05	2.56	5051	100
Y(C5H3DO)J3 + O2 => Y(C5H3DO)Q3-2J	1.86E-07	5.26	1114	0.001
Y(C5H3DO)J3 + O2 => Y(C5H3DO)Q3-2J	2.99E-07	5.2	1229	0.01
Y(C5H3DO)J3 + O2 => Y(C5H3DO)Q3-2J	8.74E-06	4.78	2069	0.1
Y(C5H3DO)J3 + O2 => Y(C5H3DO)Q3-2J	4.70E-02	3.72	4474	1
Y(C5H3DO)J3 + O2 => Y(C5H3DO)Q3-2J	2.58E+00	3.28	6765	10
Y(C5H3DO)J3 + O2 => Y(C5H3DO)Q3-2J	1.85E-02	3.97	7220	50
Y(C5H3DO)J3 + O2 => Y(C5H3DO)Q3-2J	2.78E-04	4.53	7067	100
Y(C5H3DO)J3 + O2 => Y(C5H3DO)Q3-4J	3.82E-08	5.41	1326	0.001
Y(C5H3DO)J3 + O2 => Y(C5H3DO)Q3-4J	6.23E-08	5.35	1445	0.01
Y(C5H3DO)J3 + O2 => Y(C5H3DO)Q3-4J	1.82E-06	4.93	2284	0.1
Y(C5H3DO)J3 + O2 => Y(C5H3DO)Q3-4J	9.81E-03	3.87	4678	1
Y(C5H3DO)J3 + O2 => Y(C5H3DO)Q3-4J	6.67E-01	3.4	6996	10
Y(C5H3DO)J3 + O2 => Y(C5H3DO)Q3-4J	5.73E-03	4.07	7481	50
Y(C5H3DO)J3 + O2 => Y(C5H3DO)Q3-4J	9.23E-05	4.62	7340	100
Y(C5H3DO)J3 + O2 => YCPDO-4,5-Y(COOC)	1.22E-04	4.34	311	0.001
Y(C5H3DO)J3 + O2 => YCPDO-4,5-Y(COOC)	1.88E-04	4.29	417	0.01
Y(C5H3DO)J3 + O2 => YCPDO-4,5-Y(COOC)	5.55E-03	3.87	1264	0.1
Y(C5H3DO)J3 + O2 => YCPDO-4,5-Y(COOC)	2.81E+01	2.82	3702	1
Y(C5H3DO)J3 + O2 => YCPDO-4,5-Y(COOC)	5.55E+02	2.51	5855	10
Y(C5H3DO)J3 + O2 => YCPDO-4,5-Y(COOC)	1.66E+00	3.31	6168	50
Y(C5H3DO)J3 + O2 => YCPDO-4,5-Y(COOC)	1.80E-02	3.91	5958	100
Y(C5H3DO)J3 + O2 => YCPDO-3,4-Y(COOC)	5.38E-06	4.69	543	0.001
Y(C5H3DO)J3 + O2 => YCPDO-3,4-Y(COOC)	8.44E-06	4.63	654	0.01
Y(C5H3DO)J3 + O2 => YCPDO-3,4-Y(COOC)	2.54E-04	4.21	1504	0.1
Y(C5H3DO)J3 + O2 => YCPDO-3,4-Y(COOC)	1.33E+00	3.15	3936	1
Y(C5H3DO)J3 + O2 => YCPDO-3,4-Y(COOC)	3.79E+01	2.8	6139	10
Y(C5H3DO)J3 + O2 => YCPDO-3,4-Y(COOC)	1.55E-01	3.56	6503	50
Y(C5H3DO)J3 + O2 => YCPDO-3,4-Y(COOC)	1.89E-03	4.15	6314	100

Table B.2 Calculated Reaction Parameters, $K = A(T/K)^N \exp(-E_a/RT)$ ($300 \leq T/K \leq 2000$), for Cyclo-Pentadienone-3-yl Radical System (Continued)

Reactions			A	n	E_a (cal/mol)	Pressure (atm)
Y(C5H3DO)J3 + O2	=>	YCPDO-3-Y(OO)	1.44E+10	0.68	798	0.001
Y(C5H3DO)J3 + O2	=>	YCPDO-3-Y(OO)	1.37E+10	0.69	784	0.01
Y(C5H3DO)J3 + O2	=>	YCPDO-3-Y(OO)	9.53E+10	0.45	1229	0.1
Y(C5H3DO)J3 + O2	=>	YCPDO-3-Y(OO)	6.14E+14	-0.64	3668	1
Y(C5H3DO)J3 + O2	=>	YCPDO-3-Y(OO)	2.13E+15	-0.72	5575	10
Y(C5H3DO)J3 + O2	=>	YCPDO-3-Y(OO)	7.64E+11	0.36	5536	50
Y(C5H3DO)J3 + O2	=>	YCPDO-3-Y(OO)	3.26E+09	1.08	5166	100
Y(C5H3DO)OOJ22	=>	Y(C5H3DO)J3 + O2	9.51E+47	-15.73	51362	0.001
Y(C5H3DO)OOJ22	=>	Y(C5H3DO)J3 + O2	2.00E+64	-19.53	55122	0.01
Y(C5H3DO)OOJ22	=>	Y(C5H3DO)J3 + O2	4.74E+79	-22.78	62194	0.1
Y(C5H3DO)OOJ22	=>	Y(C5H3DO)J3 + O2	5.22E+74	-20.04	64069	1
Y(C5H3DO)OOJ22	=>	Y(C5H3DO)J3 + O2	9.08E+64	-16.3	63447	10
Y(C5H3DO)OOJ22	=>	Y(C5H3DO)J3 + O2	1.00E+55	-12.92	61316	50
Y(C5H3DO)OOJ22	=>	Y(C5H3DO)J3 + O2	1.93E+50	-11.36	60128	100
Y(C5H3DO)OOJ22	=>	Y(C5H3DO)OJ3 + O	3.79E+53	-14.22	38607	0.001
Y(C5H3DO)OOJ22	=>	Y(C5H3DO)OJ3 + O	3.46E+56	-14.45	41642	0.01
Y(C5H3DO)OOJ22	=>	Y(C5H3DO)OJ3 + O	2.26E+55	-13.59	43042	0.1
Y(C5H3DO)OOJ22	=>	Y(C5H3DO)OJ3 + O	2.97E+45	-10.18	41098	1
Y(C5H3DO)OOJ22	=>	Y(C5H3DO)OJ3 + O	3.81E+37	-7.52	39327	10
Y(C5H3DO)OOJ22	=>	Y(C5H3DO)OJ3 + O	3.59E+31	-5.56	37718	50
Y(C5H3DO)OOJ22	=>	Y(C5H3DO)OJ3 + O	8.72E+28	-4.72	36981	100
Y(C5H3DO)OOJ22	=>	Y(C5H3DO)Q3-2J	1.50E+45	-14.57	47684	0.001
Y(C5H3DO)OOJ22	=>	Y(C5H3DO)Q3-2J	9.28E+60	-18.21	52563	0.01
Y(C5H3DO)OOJ22	=>	Y(C5H3DO)Q3-2J	5.10E+70	-19.92	58469	0.1
Y(C5H3DO)OOJ22	=>	Y(C5H3DO)Q3-2J	9.38E+62	-16.6	58916	1
Y(C5H3DO)OOJ22	=>	Y(C5H3DO)Q3-2J	9.66E+52	-12.97	57652	10
Y(C5H3DO)OOJ22	=>	Y(C5H3DO)Q3-2J	7.62E+43	-9.92	55542	50
Y(C5H3DO)OOJ22	=>	Y(C5H3DO)Q3-2J	4.86E+39	-8.55	54443	100
Y(C5H3DO)OOJ22	=>	Y(C5H3DO)Q3-4J	1.25E+44	-14.43	47738	0.001
Y(C5H3DO)OOJ22	=>	Y(C5H3DO)Q3-4J	1.23E+60	-18.12	52650	0.01
Y(C5H3DO)OOJ22	=>	Y(C5H3DO)Q3-4J	2.88E+70	-20	58803	0.1
Y(C5H3DO)OOJ22	=>	Y(C5H3DO)Q3-4J	1.32E+63	-16.75	59513	1
Y(C5H3DO)OOJ22	=>	Y(C5H3DO)Q3-4J	1.34E+53	-13.09	58345	10
Y(C5H3DO)OOJ22	=>	Y(C5H3DO)Q3-4J	7.35E+43	-9.98	56224	50
Y(C5H3DO)OOJ22	=>	Y(C5H3DO)Q3-4J	3.80E+39	-8.58	55109	100

Table B.2 Calculated Reaction Parameters, $K = A(T/K)^N \text{Exp}(-E_a/RT)$ ($300 \leq T/K \leq 2000$), for Cyclo-Pentadienone-3-yl Radical System (Continued)

Reactions			A	n	E_a (cal/mol)	Pressure (atm)
Y(C5H3DO)OOJ22	=>	YCPDO-4,5-Y(COOC)	4.14E+48	-15.01	44095	0.001
Y(C5H3DO)OOJ22	=>	YCPDO-4,5-Y(COOC)	2.97E+61	-17.8	49598	0.01
Y(C5H3DO)OOJ22	=>	YCPDO-4,5-Y(COOC)	1.66E+66	-18.24	54001	0.1
Y(C5H3DO)OOJ22	=>	YCPDO-4,5-Y(COOC)	9.13E+56	-14.67	53416	1
Y(C5H3DO)OOJ22	=>	YCPDO-4,5-Y(COOC)	1.74E+47	-11.25	51796	10
Y(C5H3DO)OOJ22	=>	YCPDO-4,5-Y(COOC)	1.04E+39	-8.52	49781	50
Y(C5H3DO)OOJ22	=>	YCPDO-4,5-Y(COOC)	2.00E+35	-7.31	48782	100
Y(C5H3DO)OOJ22	=>	YCPDO-3,4-Y(COOC)	7.65E+46	-14.81	45615	0.001
Y(C5H3DO)OOJ22	=>	YCPDO-3,4-Y(COOC)	5.35E+61	-18.17	51074	0.01
Y(C5H3DO)OOJ22	=>	YCPDO-3,4-Y(COOC)	2.28E+68	-19.08	56046	0.1
Y(C5H3DO)OOJ22	=>	YCPDO-3,4-Y(COOC)	3.58E+59	-15.57	55798	1
Y(C5H3DO)OOJ22	=>	YCPDO-3,4-Y(COOC)	4.78E+49	-12.06	54285	10
Y(C5H3DO)OOJ22	=>	YCPDO-3,4-Y(COOC)	1.30E+41	-9.21	52227	50
Y(C5H3DO)OOJ22	=>	YCPDO-3,4-Y(COOC)	1.65E+37	-7.94	51188	100
Y(C5H3DO)OOJ22	=>	YCPDO-3-Y(OO)	1.78E+46	-11.44	31952	0.001
Y(C5H3DO)OOJ22	=>	YCPDO-3-Y(OO)	5.82E+45	-10.96	33058	0.01
Y(C5H3DO)OOJ22	=>	YCPDO-3-Y(OO)	1.69E+43	-9.92	33201	0.1
Y(C5H3DO)OOJ22	=>	YCPDO-3-Y(OO)	6.32E+34	-7.12	31152	1
Y(C5H3DO)OOJ22	=>	YCPDO-3-Y(OO)	6.56E+28	-5.15	29657	10
Y(C5H3DO)OOJ22	=>	YCPDO-3-Y(OO)	2.87E+24	-3.74	28444	50
Y(C5H3DO)OOJ22	=>	YCPDO-3-Y(OO)	4.08E+22	-3.14	27911	100

APPENDIX C

POTENTIAL ENERGY PROFILES FOR INTERNAL ROTATIONS OF CYCLO-PENTADIENONE-2-YL AND CYCLO-PENTADIENONE-3-YL RADICAL SYSTEM

Potential energy surface for clopentadienone and related radical species are investigated in this study.

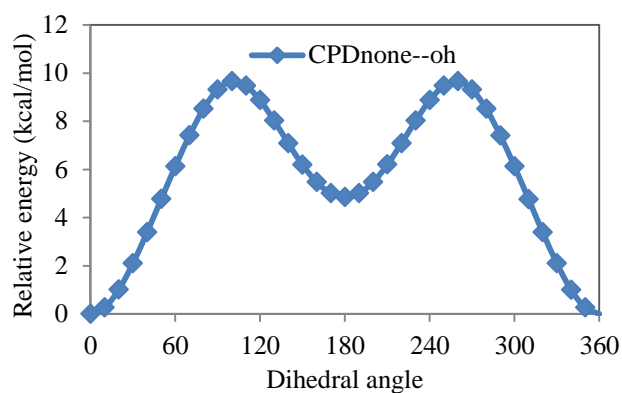


Figure C.1 Potential energy profiles for internal rotations in y(c5h3do)oh2.

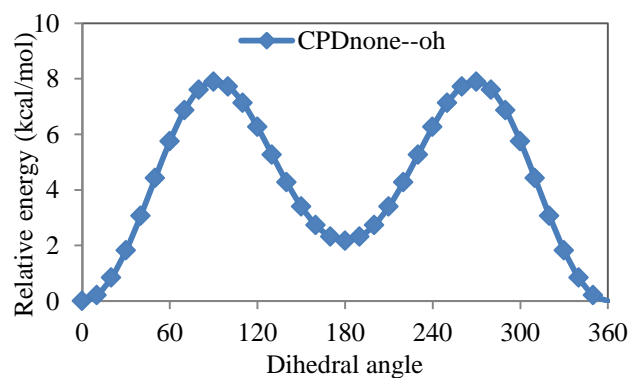


Figure C.2 Potential energy profiles for internal rotations in y(c5h3do)oh3.

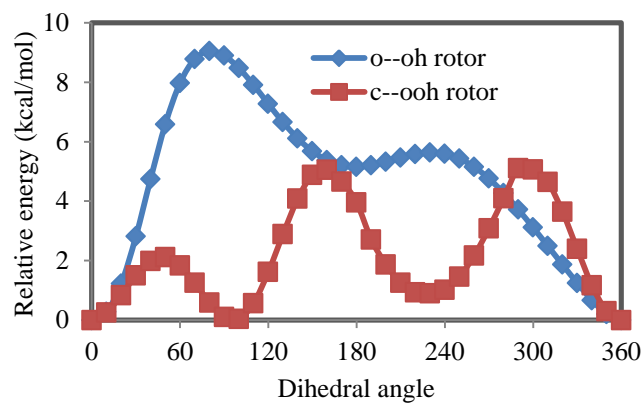


Figure C.3 Potential energy profiles for internal rotations in y(c5h3do)oooh2.

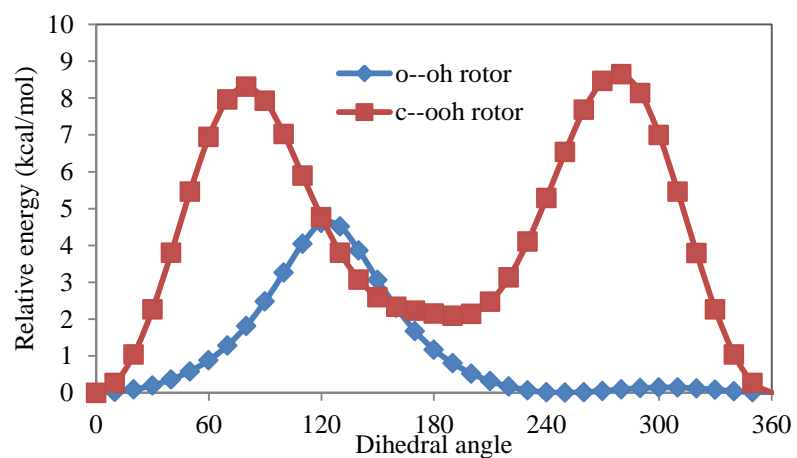


Figure C.4 Potential energy profiles for internal rotations in y(c5h3do)oooh3.

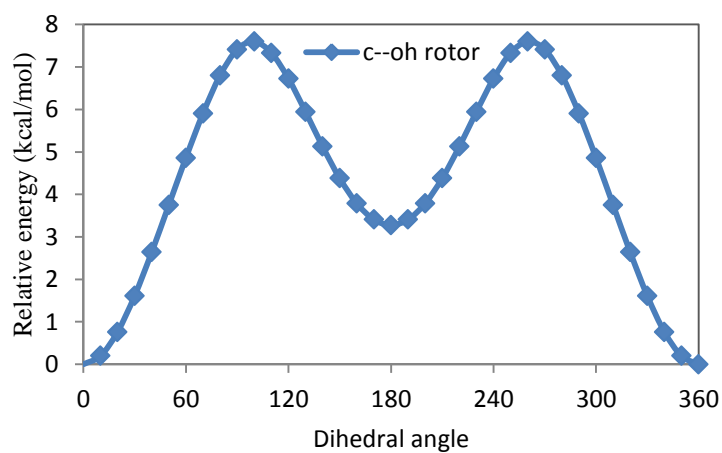


Figure C.5 Potential energy profiles for internal rotations in y(c5h3do)oh2-3j.

(Note: other potential energy profiles of -oh rotor in y(c5h3do)oh2-4j and y(c5h3do)oh2-5j also have the same trend. The highest barrier energy for y(c5h3do)oh2-4j and y(c5h3do)oh2-5j are 9.0 and 8.19 kcal/mol, respectively).

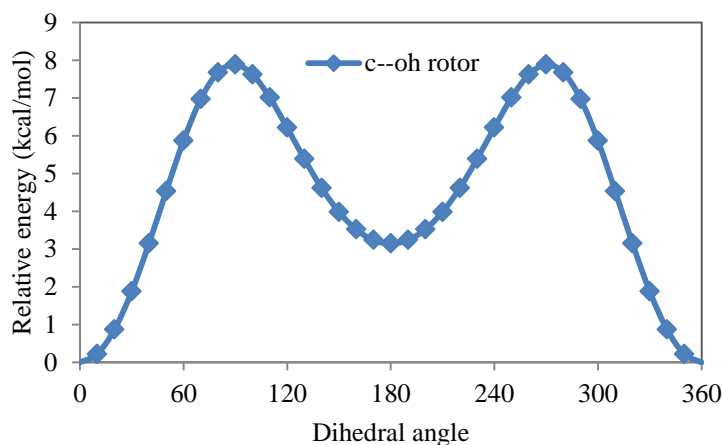


Figure C.6 Potential energy profiles for internal rotations in y(c5h3do)oh3-2j .

(Note: other potential energy profiles of -oh rotor in y(c5h3do)oh3-4j and y(c5h3do)oh3-5j also have the same trend. The highest barrier energy for y(c5h3do)oh3-4j and y(c5h3do)oh3-5j are 7.49 and 7.39 kcal/mol, respectively).

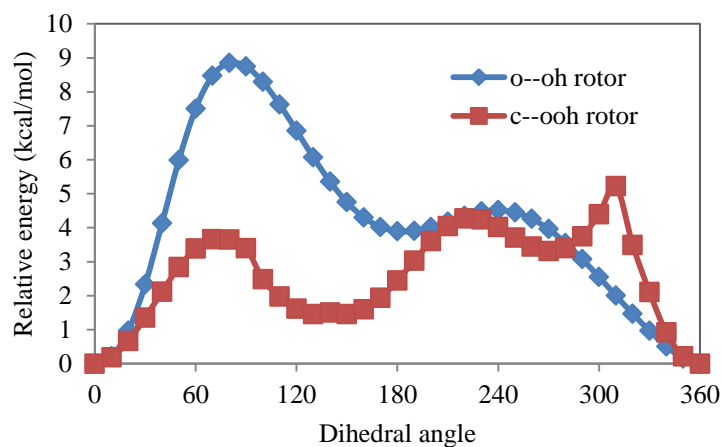


Figure C.7 Potential energy profiles for internal rotations in y(c5h3do)ooh2-3j .

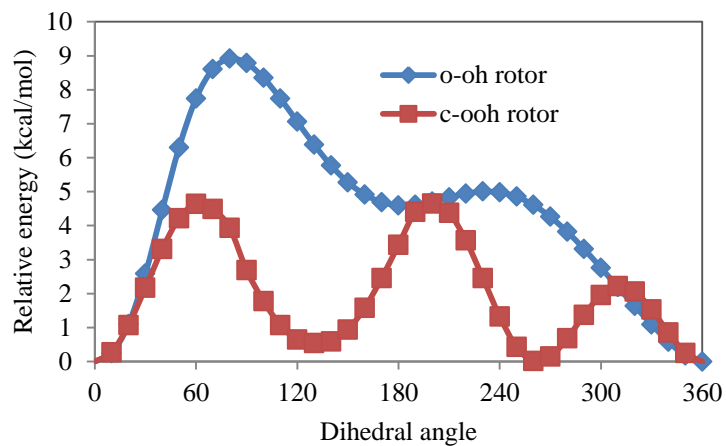


Figure C.8 Potential energy profiles for internal rotations in y(c5h3do)ooH2-4j.

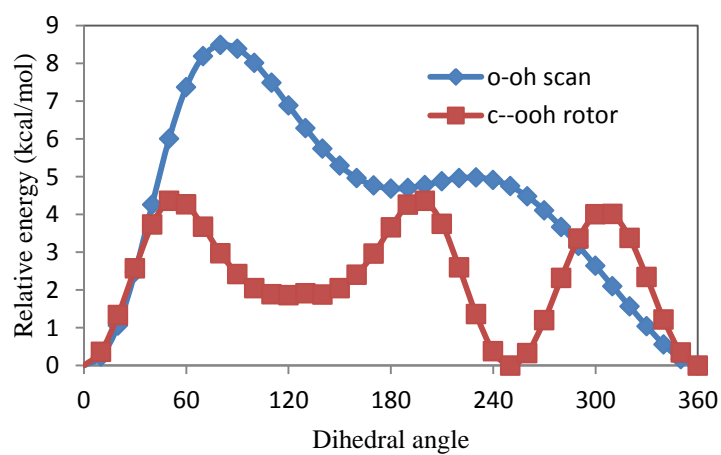


Figure C.9 Potential energy profiles for internal rotations in y(c5h3do)ooH2-5j.

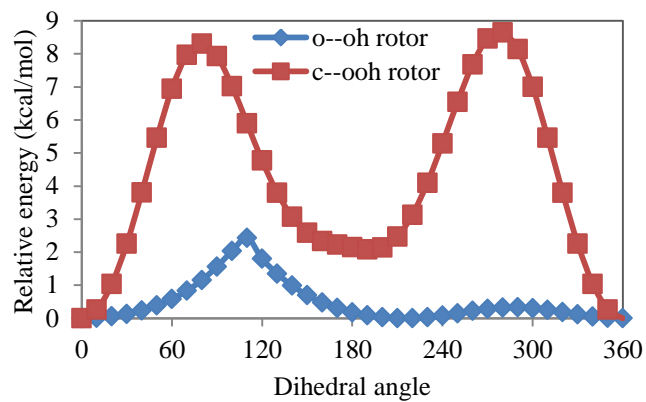


Figure C.10 Potential energy profiles for internal rotations in y(c5h3do)ooh3-2j.

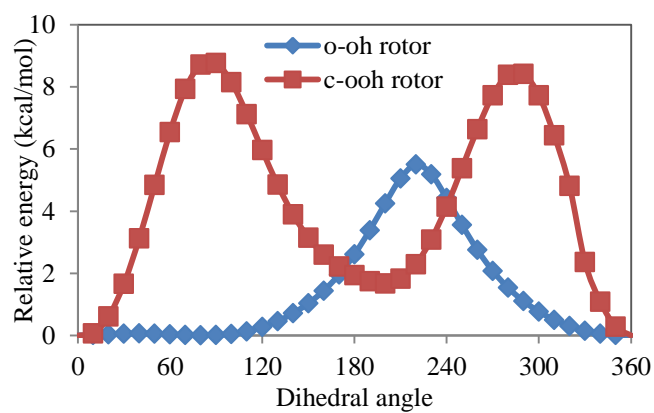


Figure C.11 Potential energy profiles for internal rotations in y(c5h3do)ooh3-4j.

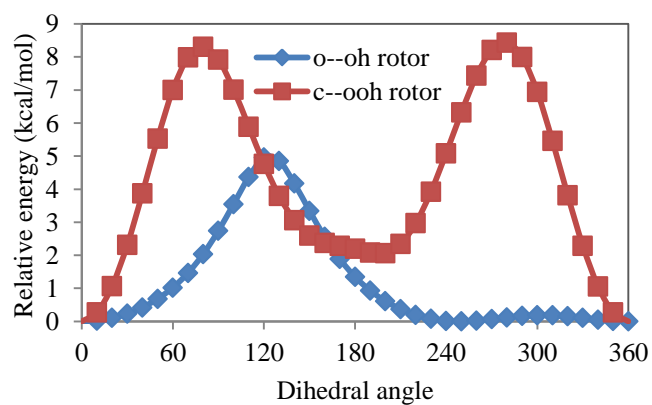


Figure C.12 Potential energy profiles for internal rotations in y(c5h3do)ooh3-5j.

APPENDIX D

GEOMETRY COORDINATES AT CBS-QB3 COMPOSITE, VIZ B3LYP/CBSB7 LEVEL

Numbering of atoms follows figure above each table presenting the z-matrix according to the cyclopentadienone and related radical species.

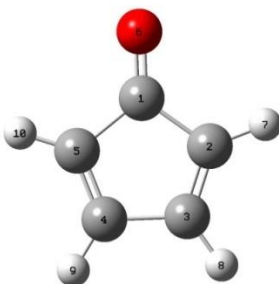


Table D.1 Geometry Parameters of $y(c_5h_4do)$

Bond Distances, angstrom (Å)		Angles, degree (°)		Dihedral Angles, degree (°)	
R(1,2)	1.51	A(2,1,5)	105.63	D(5,1,2,3)	-0.01
R(1,5)	1.51	A(2,1,6)	127.18	D(5,1,2,7)	180.00
R(1,6)	1.21	A(5,1,6)	127.18	D(6,1,2,3)	-179.99
R(2,3)	1.34	A(1,2,3)	107.40	D(6,1,2,7)	0.01
R(2,7)	1.08	A(1,2,7)	123.49	D(2,1,5,4)	0.01
R(3,4)	1.50	A(3,2,7)	129.11	D(2,1,5,10)	-180.00
R(3,8)	1.08	A(2,3,4)	109.79	D(6,1,5,4)	179.99
R(4,5)	1.34	A(2,3,8)	126.93	D(6,1,5,10)	-0.01
R(4,9)	1.08	A(4,3,8)	123.28	D(1,2,3,4)	0.00
R(5,10)	1.08	A(3,4,5)	109.79	D(1,2,3,8)	-180.00
		A(3,4,9)	123.28	D(7,2,3,4)	-180.00
		A(5,4,9)	126.93	D(7,2,3,8)	0.00
		A(1,5,4)	107.40	D(2,3,4,5)	0.00
		A(1,5,10)	123.49	D(2,3,4,9)	180.00
		A(4,5,10)	129.11	D(8,3,4,5)	-180.00
				D(8,3,4,9)	0.00
				D(3,4,5,1)	-0.01
				D(3,4,5,10)	180.00
				D(9,4,5,1)	180.00
				D(9,4,5,10)	0.00

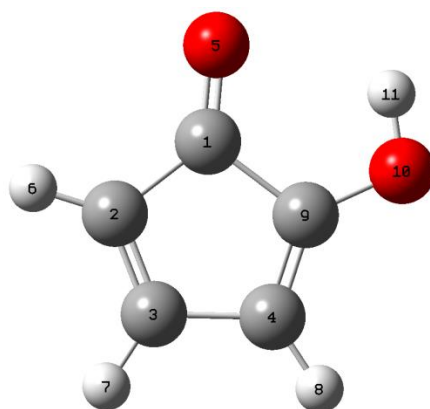


Table D.2 Geometry Parameters of $\gamma(\text{c}_5\text{h}_3\text{do})\text{oh}_2$

Bond Distances, angstrom (Å)		Angles, degree (°)		Dihedral Angles, degree (°)	
R(1,2)	1.48	A(2,1,5)	132.44	D(5,1,2,3)	-179.98
R(1,5)	1.21	A(2,1,9)	105.77	D(5,1,2,6)	0.03
R(1,9)	1.54	A(5,1,9)	121.80	D(9,1,2,3)	-0.02
R(2,3)	1.35	A(1,2,3)	106.01	D(9,1,2,6)	179.99
R(2,6)	1.08	A(1,2,6)	125.17	D(2,1,9,4)	0.02
R(3,4)	1.49	A(3,2,6)	128.82	D(2,1,9,10)	180.01
R(3,7)	1.08	A(2,3,4)	112.90	D(5,1,9,4)	-180.02
R(4,8)	1.08	A(2,3,7)	125.08	D(5,1,9,10)	-0.02
R(4,9)	1.34	A(4,3,7)	122.02	D(1,2,3,4)	0.01
R(9,10)	1.33	A(3,4,8)	124.89	D(1,2,3,7)	180.01
R(10,11)	0.97	A(3,4,9)	106.72	D(6,2,3,4)	-179.99
		A(8,4,9)	128.39	D(6,2,3,7)	0.00
		A(1,9,4)	108.60	D(2,3,4,8)	-180.01
		A(1,9,10)	118.91	D(2,3,4,9)	0.00
		A(4,9,10)	132.49	D(7,3,4,8)	0.00
		A(9,10,11)	106.31	D(7,3,4,9)	-180.00
				D(3,4,9,1)	-0.01
				D(3,4,9,10)	180.00
				D(8,4,9,1)	180.00
				D(8,4,9,10)	0.00
				D(1,9,10,11)	0.00
				D(4,9,10,11)	-180.01

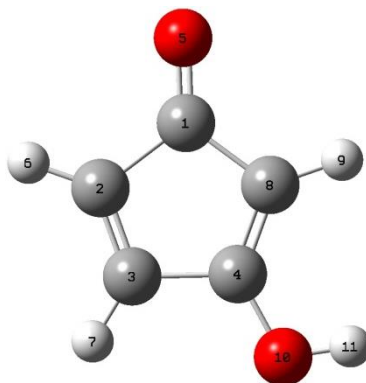


Table D.3 Geometry Parameters of $\gamma(\text{C}_5\text{H}_3\text{DO})\text{OH}_3$

Bond Distances,		Angles,		Dihedral Angles,	
angstrom (Å)		degree (°)		degree (°)	
R(1,2)	1.53	A(2,1,5)	125.43	D(5,1,2,3)	-180.00
R(1,5)	1.21	A(2,1,8)	106.23	D(5,1,2,6)	0.00
R(1,8)	1.48	A(5,1,8)	128.34	D(8,1,2,3)	0.00
R(2,3)	1.33	A(1,2,3)	107.67	D(8,1,2,6)	180.00
R(2,6)	1.08	A(1,2,6)	123.25	D(2,1,8,4)	0.00
R(3,4)	1.50	A(3,2,6)	129.08	D(2,1,8,9)	-180.00
R(3,7)	1.08	A(2,3,4)	108.43	D(5,1,8,4)	179.99
R(4,8)	1.35	A(2,3,7)	129.10	D(5,1,8,9)	0.00
R(4,10)	1.34	A(4,3,7)	122.47	D(1,2,3,4)	0.00
R(8,9)	1.08	A(3,4,8)	111.21	D(1,2,3,7)	180.00
R(10,11)	0.97	A(3,4,10)	117.36	D(6,2,3,4)	-180.00
		A(8,4,10)	131.43	D(6,2,3,7)	0.00
		A(1,8,4)	106.46	D(2,3,4,8)	-0.01
		A(1,8,9)	124.28	D(2,3,4,10)	-180.00
		A(4,8,9)	129.26	D(7,3,4,8)	180.00
		A(4,10,11)	109.67	D(7,3,4,10)	0.00
				D(3,4,8,1)	0.01
				D(3,4,8,9)	180.00
				D(10,4,8,1)	180.00
				D(10,4,8,9)	0.00
				D(3,4,10,11)	180.00
				D(8,4,10,11)	0.00

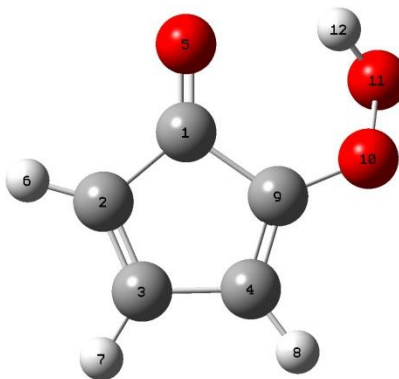


Table D.4 Geometry Parameters of $y(c_5h_3do)q_2$

Bond Distances, angstrom (Å)		Angles, degree (°)		Dihedral Angles, degree (°)	
R(1,2)	1.49	A(2,1,5)	129.85	D(5,1,2,3)	-175.69
R(1,5)	1.21	A(2,1,9)	105.14	D(5,1,2,6)	6.65
R(1,9)	1.54	A(5,1,9)	124.95	D(9,1,2,3)	1.66
R(2,3)	1.34	A(1,2,3)	106.92	D(9,1,2,6)	-175.99
R(2,6)	1.08	A(1,2,6)	124.16	D(2,1,9,4)	-2.47
R(3,4)	1.49	A(3,2,6)	128.87	D(2,1,9,10)	-171.69
R(3,7)	1.08	A(2,3,4)	111.84	D(5,1,9,4)	175.06
R(4,8)	1.08	A(2,3,7)	125.79	D(5,1,9,10)	5.83
R(4,9)	1.34	A(4,3,7)	122.36	D(1,2,3,4)	-0.40
R(9,10)	1.34	A(3,4,8)	125.06	D(1,2,3,7)	-179.27
R(10,11)	1.47	A(3,4,9)	107.73	D(6,2,3,4)	177.11
R(11,12)	0.97	A(8,4,9)	127.18	D(6,2,3,7)	-1.76
		A(1,9,4)	108.30	D(2,3,4,8)	177.10
		A(1,9,10)	122.48	D(2,3,4,9)	-1.22
		A(4,9,10)	128.18	D(7,3,4,8)	-3.99
		A(9,10,11)	109.37	D(7,3,4,9)	177.69
		A(10,11,12)	100.62	D(3,4,9,1)	2.22
				D(3,4,9,10)	170.65
				D(8,4,9,1)	-176.05
				D(8,4,9,10)	-7.63
				D(1,9,10,11)	-50.35
				D(4,9,10,11)	142.71
				D(9,10,11,12)	73.01

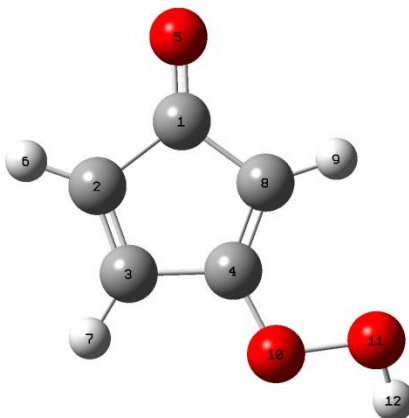


Table D.5 Geometry Parameters of $y(c_5h_3do)q_3$

Bond Distances, angstrom (Å)		Angles, degree (°)		Dihedral Angles, degree (°)	
R(1,2)	1.53	A(2,1,5)	125.28	D(5,1,2,3)	179.93
R(1,5)	1.21	A(2,1,8)	106.46	D(5,1,2,6)	-0.05
R(1,8)	1.48	A(5,1,8)	128.26	D(8,1,2,3)	0.00
R(2,3)	1.33	A(1,2,3)	107.84	D(8,1,2,6)	-179.98
R(2,6)	1.08	A(1,2,6)	123.41	D(2,1,8,4)	0.11
R(3,4)	1.50	A(3,2,6)	128.75	D(2,1,8,9)	-179.69
R(3,7)	1.08	A(2,3,4)	107.77	D(5,1,8,4)	-179.81
R(4,8)	1.34	A(2,3,7)	129.18	D(5,1,8,9)	0.39
R(4,10)	1.34	A(4,3,7)	123.04	D(1,2,3,4)	-0.10
R(8,9)	1.08	A(3,4,8)	112.08	D(1,2,3,7)	179.94
R(10,11)	1.45	A(3,4,10)	115.38	D(6,2,3,4)	179.87
R(11,12)	0.97	A(8,4,10)	132.53	D(6,2,3,7)	-0.08
		A(1,8,4)	105.84	D(2,3,4,8)	0.19
		A(1,8,9)	125.35	D(2,3,4,10)	179.93
		A(4,8,9)	128.80	D(7,3,4,8)	-179.85
		A(4,10,11)	109.37	D(7,3,4,10)	-0.12
		A(10,11,12)	98.73	D(3,4,8,1)	-0.18
				D(3,4,8,9)	179.61
				D(10,4,8,1)	-179.86
				D(10,4,8,9)	-0.06
				D(3,4,10,11)	-177.63
				D(8,4,10,11)	2.04
				D(4,10,11,12)	-155.85

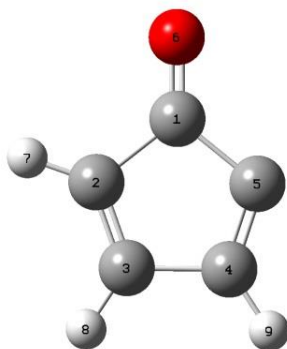


Table D.6 Geometry Parameters of $y(c_5h_3do)j_2$

Bond Distances, angstrom (Å)		Angles, degree (°)		Dihedral Angles, degree (°)	
R(1,2)	1.52	A(2,1,5)	103.05	D(5,1,2,3)	0.00
R(1,5)	1.52	A(2,1,6)	127.46	D(5,1,2,7)	-180.00
R(1,6)	1.20	A(5,1,6)	129.49	D(6,1,2,3)	180.00
R(2,3)	1.34	A(1,2,3)	108.34	D(6,1,2,7)	0.00
R(2,7)	1.08	A(1,2,7)	122.63	D(2,1,5,4)	0.00
R(3,4)	1.51	A(3,2,7)	129.03	D(6,1,5,4)	180.00
R(3,8)	1.08	A(2,3,4)	110.43	D(1,2,3,4)	0.00
R(4,5)	1.32	A(2,3,8)	126.78	D(1,2,3,8)	-180.00
R(4,9)	1.08	A(4,3,8)	122.79	D(7,2,3,4)	180.00
		A(3,4,5)	107.43	D(7,2,3,8)	0.00
		A(3,4,9)	123.92	D(2,3,4,5)	-0.01
		A(5,4,9)	128.65	D(2,3,4,9)	180.00
		A(1,5,4)	110.75	D(8,3,4,5)	180.00
				D(8,3,4,9)	0.00
				D(3,4,5,1)	0.01
				D(9,4,5,1)	-180.00

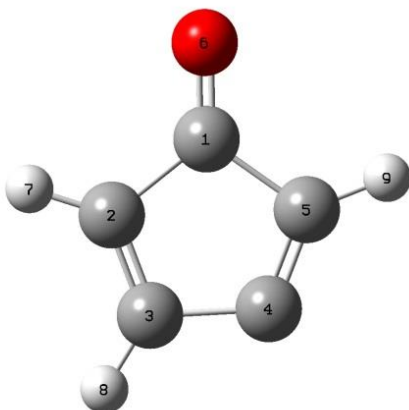


Table D.7 Geometry Parameters of $y(c_5h_3do)_3$

Bond Distances, angstrom (Å)		Angles, degree (°)		Dihedral Angles, degree (°)	
R(1,2)	1.51	A(2,1,5)	106.19	D(5,1,2,3)	0.00
R(1,5)	1.54	A(2,1,6)	127.38	D(5,1,2,7)	180.00
R(1,6)	1.20	A(5,1,6)	126.42	D(6,1,2,3)	180.00
R(2,3)	1.34	A(1,2,3)	107.64	D(6,1,2,7)	0.00
R(2,7)	1.08	A(1,2,7)	123.68	D(2,1,5,4)	0.00
R(3,4)	1.49	A(3,2,7)	128.68	D(2,1,5,9)	180.00
R(3,8)	1.08	A(2,3,4)	107.99	D(6,1,5,4)	180.00
R(4,5)	1.32	A(2,3,8)	127.36	D(6,1,5,9)	0.00
R(5,9)	1.08	A(4,3,8)	124.65	D(1,2,3,4)	0.00
		A(3,4,5)	113.94	D(1,2,3,8)	180.00
		A(1,5,4)	104.24	D(7,2,3,4)	-180.00
		A(1,5,9)	123.35	D(7,2,3,8)	0.00
		A(4,5,9)	132.41	D(2,3,4,5)	0.00
				D(8,3,4,5)	180.00
				D(3,4,5,1)	0.00
				D(3,4,5,9)	180.00

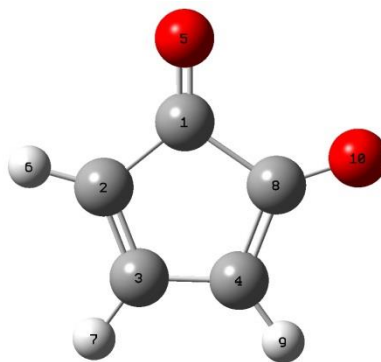


Table D.8 Geometry Parameters of *y(c₅h₃do)oj2*

Bond Distances, angstrom (Å)		Angles, degree (°)		Dihedral Angles, degree (°)	
R(1,2)	1.47	A(2,1,5)	129.44	D(5,1,2,3)	-179.97
R(1,5)	1.21	A(2,1,8)	104.79	D(5,1,2,6)	0.03
R(1,8)	1.57	A(5,1,8)	125.77	D(8,1,2,3)	0.00
R(2,3)	1.40	A(1,2,3)	108.97	D(8,1,2,6)	-180.01
R(2,6)	1.08	A(1,2,6)	124.48	D(2,1,8,4)	-0.01
R(3,4)	1.40	A(3,2,6)	126.56	D(2,1,8,10)	180.05
R(3,7)	1.08	A(2,3,4)	112.49	D(5,1,8,4)	179.96
R(4,8)	1.47	A(2,3,7)	123.76	D(5,1,8,10)	0.01
R(4,9)	1.08	A(4,3,7)	123.76	D(1,2,3,4)	0.02
R(8,10)	1.21	A(3,4,8)	108.97	D(1,2,3,7)	180.00
		A(3,4,9)	126.56	D(6,2,3,4)	-179.98
		A(8,4,9)	124.48	D(6,2,3,7)	0.00
		A(1,8,4)	104.79	D(2,3,4,8)	-0.02
		A(1,8,10)	125.77	D(2,3,4,9)	-180.02
		A(4,8,10)	129.44	D(7,3,4,8)	180.00
				D(7,3,4,9)	0.00
				D(3,4,8,1)	0.02
				D(3,4,8,10)	-180.04
				D(9,4,8,1)	-179.99
				D(9,4,8,10)	-0.04

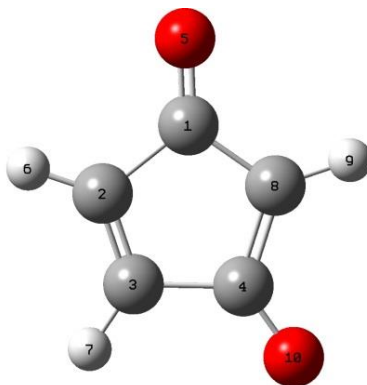


Table D.9 Geometry Parameters of $y(c_5h_3do)oj_3$

Bond Distances, angstrom (Å)		Angles, degree (°)		Dihedral Angles, degree (°)	
R(1,2)	1.51	A(2,1,5)	126.38	D(5,1,2,3)	-180.01
R(1,5)	1.22	A(2,1,8)	105.64	D(5,1,2,6)	-0.02
R(1,8)	1.47	A(5,1,8)	127.97	D(8,1,2,3)	0.01
R(2,3)	1.34	A(1,2,3)	110.18	D(8,1,2,6)	-179.99
R(2,6)	1.08	A(1,2,6)	121.95	D(2,1,8,4)	-0.02
R(3,4)	1.51	A(3,2,6)	127.88	D(2,1,8,9)	179.99
R(3,7)	1.08	A(2,3,4)	110.18	D(5,1,8,4)	180.01
R(4,8)	1.47	A(2,3,7)	127.88	D(5,1,8,9)	0.02
R(4,10)	1.22	A(4,3,7)	121.94	D(1,2,3,4)	0.00
R(8,9)	1.08	A(3,4,8)	105.64	D(1,2,3,7)	-180.00
		A(3,4,10)	126.38	D(6,2,3,4)	180.00
		A(8,4,10)	127.98	D(6,2,3,7)	0.00
		A(1,8,4)	108.36	D(2,3,4,8)	-0.01
		A(1,8,9)	125.81	D(2,3,4,10)	180.01
		A(4,8,9)	125.83	D(7,3,4,8)	179.99
				D(7,3,4,10)	0.01
				D(3,4,8,1)	0.02
				D(3,4,8,9)	-179.99
				D(10,4,8,1)	-180.00
				D(10,4,8,9)	-0.01

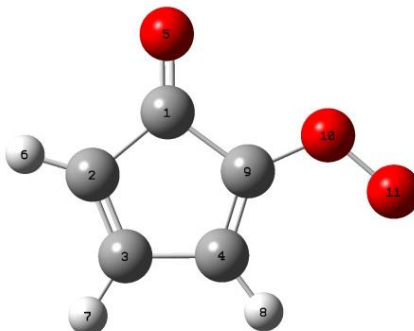


Table D.10 Geometry Parameters of y(c₅h₃do)ooj2

Bond Distances, angstrom (Å)		Angles, degree (°)		Dihedral Angles, degree (°)	
R(1,2)	1.50	A(2,1,5)	129.18	D(5,1,2,3)	180.02
R(1,5)	1.20	A(2,1,9)	103.89	D(5,1,2,6)	0.02
R(1,9)	1.53	A(5,1,9)	126.93	D(9,1,2,3)	0.00
R(2,3)	1.35	A(1,2,3)	107.84	D(9,1,2,6)	180.00
R(2,6)	1.08	A(1,2,6)	123.43	D(2,1,9,4)	0.01
R(3,4)	1.48	A(3,2,6)	128.73	D(2,1,9,10)	180.01
R(3,7)	1.08	A(2,3,4)	111.40	D(5,1,9,4)	-180.01
R(4,8)	1.08	A(2,3,7)	126.05	D(5,1,9,10)	-0.01
R(4,9)	1.35	A(4,3,7)	122.54	D(1,2,3,4)	0.00
R(9,10)	1.35	A(3,4,8)	125.90	D(1,2,3,7)	180.00
R(10,11)	1.33	A(3,4,9)	107.63	D(6,2,3,4)	-180.00
		A(8,4,9)	126.48	D(6,2,3,7)	0.00
		A(1,9,4)	109.24	D(2,3,4,8)	-180.00
		A(1,9,10)	119.43	D(2,3,4,9)	0.01
		A(4,9,10)	131.33	D(7,3,4,8)	-0.01
		A(9,10,11)	115.14	D(7,3,4,9)	-180.00
				D(3,4,9,1)	-0.01
				D(3,4,9,10)	-180.01
				D(8,4,9,1)	180.00
				D(8,4,9,10)	0.00
				D(1,9,10,11)	180.00
				D(4,9,10,11)	0.00

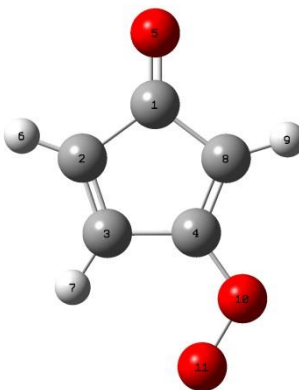


Table D.11 Geometry Parameters of $y(c_5h_3do)ooj_3$

Bond Distances, angstrom (Å)		Angles, degree (°)		Dihedral Angles, degree (°)	
R(1,2)	1.517	A(2,1,5)	126.6794	D(5,1,2,3)	180.0016
R(1,5)	1.2065	A(2,1,8)	106.054	D(5,1,2,6)	0.0014
R(1,8)	1.4986	A(5,1,8)	127.2666	D(8,1,2,3)	0.0003
R(2,3)	1.3361	A(1,2,3)	108.3226	D(8,1,2,6)	180.0001
R(2,6)	1.0799	A(1,2,6)	123.214	D(2,1,8,4)	0.0018
R(3,4)	1.4926	A(3,2,6)	128.4634	D(2,1,8,9)	180.0008
R(3,7)	1.0781	A(2,3,4)	107.8215	D(5,1,8,4)	180.0005
R(4,8)	1.3474	A(2,3,7)	129.2935	D(5,1,8,9)	-0.0005
R(4,10)	1.357	A(4,3,7)	122.8851	D(1,2,3,4)	-0.0021
R(8,9)	1.0778	A(3,4,8)	112.1278	D(1,2,3,7)	179.9997
R(10,11)	1.3326	A(3,4,10)	124.4717	D(6,2,3,4)	179.9981
		A(8,4,10)	123.4005	D(6,2,3,7)	-0.0001
		A(1,8,4)	105.6741	D(2,3,4,8)	0.0035
		A(1,8,9)	125.4569	D(2,3,4,10)	-179.999
		A(4,8,9)	128.869	D(7,3,4,8)	-179.998
		A(4,10,11)	114.7546	D(7,3,4,10)	-0.0007
				D(3,4,8,1)	-0.0031
				D(3,4,8,9)	-180.002
				D(10,4,8,1)	179.9994
				D(10,4,8,9)	0.0004
				D(3,4,10,11)	0.0015
				D(8,4,10,11)	-180.001

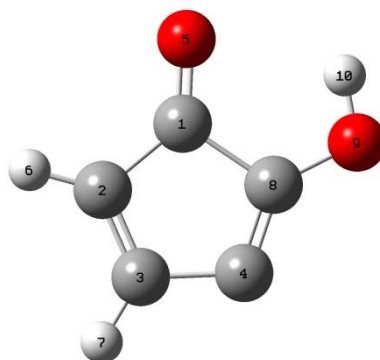


Table D.12 Geometry Parameters of $y(c_5h_3do)oh_2-3j$

Bond Distances,		Angles,		Dihedral Angles,	
angstrom (Å)		degree (°)		degree (°)	
R(1,2)	1.48	A(2,1,5)	132.29	D(5,1,2,3)	180.00
R(1,5)	1.21	A(2,1,8)	106.48	D(5,1,2,6)	0.00
R(1,8)	1.56	A(5,1,8)	121.23	D(8,1,2,3)	0.00
R(2,3)	1.35	A(1,2,3)	106.14	D(8,1,2,6)	180.00
R(2,6)	1.08	A(1,2,6)	125.18	D(2,1,8,4)	0.00
R(3,4)	1.47	A(3,2,6)	128.68	D(2,1,8,9)	180.00
R(3,7)	1.08	A(2,3,4)	111.20	D(5,1,8,4)	-180.00
R(4,8)	1.33	A(2,3,7)	125.52	D(5,1,8,9)	0.00
R(8,9)	1.33	A(4,3,7)	123.28	D(1,2,3,4)	0.00
R(9,10)	0.97	A(3,4,8)	110.89	D(1,2,3,7)	180.00
		A(1,8,4)	105.28	D(6,2,3,4)	180.00
		A(1,8,9)	119.26	D(6,2,3,7)	0.00
		A(4,8,9)	135.46	D(2,3,4,8)	0.00
		A(8,9,10)	106.56	D(7,3,4,8)	-180.00
				D(3,4,8,1)	0.00
				D(3,4,8,9)	180.00
				D(1,8,9,10)	0.00
				D(4,8,9,10)	180.00

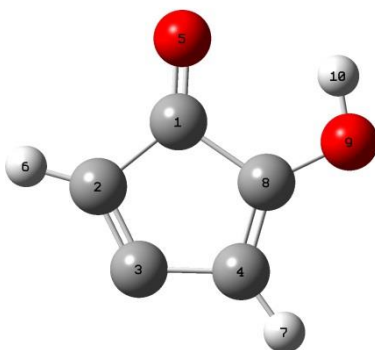


Table D.13 Geometry Parameters of y(c₅h₃do)oh₂-4j

Bond Distances, angstrom (Å)		Angles, degree (°)		Dihedral Angles, degree (°)	
R(1,2)	1.49	A(2,1,5)	131.79	D(5,1,2,3)	-180.01
R(1,5)	1.21	A(2,1,8)	106.21	D(5,1,2,6)	-0.01
R(1,8)	1.54	A(5,1,8)	122.01	D(8,1,2,3)	0.02
R(2,3)	1.34	A(1,2,3)	103.02	D(8,1,2,6)	-179.99
R(2,6)	1.08	A(1,2,6)	125.29	D(2,1,8,4)	-0.02
R(3,4)	1.47	A(3,2,6)	131.69	D(2,1,8,9)	-180.02
R(4,7)	1.08	A(2,3,4)	117.36	D(5,1,8,4)	180.00
R(4,8)	1.35	A(3,4,7)	126.61	D(5,1,8,9)	0.00
R(8,9)	1.33	A(3,4,8)	104.47	D(1,2,3,4)	-0.01
R(9,10)	0.97	A(7,4,8)	128.93	D(6,2,3,4)	180.00
		A(1,8,4)	108.94	D(2,3,4,7)	180.01
		A(1,8,9)	119.24	D(2,3,4,8)	0.00
		A(4,8,9)	131.82	D(3,4,8,1)	0.01
		A(8,9,10)	106.64	D(3,4,8,9)	180.01
				D(7,4,8,1)	-180.00
				D(7,4,8,9)	0.00
				D(1,8,9,10)	0.00
				D(4,8,9,10)	180.00

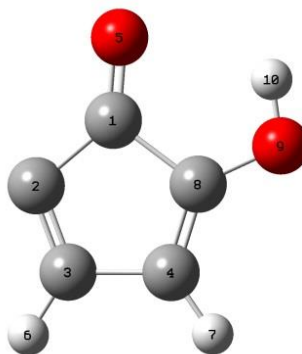


Table D.14 Geometry Parameters of y(c₅h₃do)oh₂-5j

Bond Distances, angstrom (Å)		Angles, degree (°)		Dihedral Angles, degree (°)	
R(1,2)	1.48	A(2,1,5)	134.51	D(5,1,2,3)	-179.98
R(1,5)	1.20	A(2,1,8)	103.32	D(8,1,2,3)	0.03
R(1,8)	1.55	A(5,1,8)	122.17	D(2,1,8,4)	-0.01
R(2,3)	1.33	A(1,2,3)	109.56	D(2,1,8,9)	179.98
R(3,4)	1.51	A(2,3,4)	110.59	D(5,1,8,4)	179.99
R(3,6)	1.08	A(2,3,6)	126.83	D(5,1,8,9)	-0.01
R(4,7)	1.08	A(4,3,6)	122.59	D(1,2,3,4)	-0.04
R(4,8)	1.34	A(3,4,7)	124.51	D(1,2,3,6)	180.03
R(8,9)	1.33	A(3,4,8)	107.17	D(2,3,4,7)	-179.97
R(9,10)	0.97	A(7,4,8)	128.32	D(2,3,4,8)	0.03
		A(1,8,4)	109.36	D(6,3,4,7)	-0.03
		A(1,8,9)	118.64	D(6,3,4,8)	-180.03
		A(4,8,9)	132.00	D(3,4,8,1)	-0.01
		A(8,9,10)	106.86	D(3,4,8,9)	-180.00
				D(7,4,8,1)	179.99
				D(7,4,8,9)	0.00
				D(1,8,9,10)	0.01
				D(4,8,9,10)	-180.00

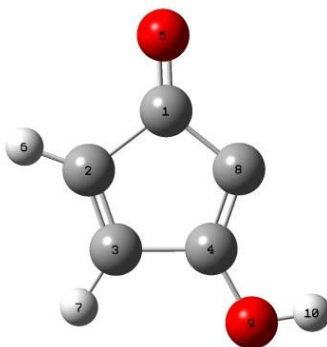


Table D.15 Geometry Parameters of $\gamma(\text{C}_5\text{H}_3\text{DO})\text{OH}_3\cdot 2\text{H}_2\text{O}$

Bond Distances, angstrom (Å)		Angles, degree (°)		Dihedral Angles, degree (°)	
R(1,2)	1.54	A(2,1,5)	125.20	D(5,1,2,3)	180.00
R(1,5)	1.20	A(2,1,8)	103.49	D(5,1,2,6)	0.00
R(1,8)	1.48	A(5,1,8)	131.31	D(8,1,2,3)	0.01
R(2,3)	1.33	A(1,2,3)	108.74	D(8,1,2,6)	180.01
R(2,6)	1.08	A(1,2,6)	122.07	D(2,1,8,4)	-0.01
R(3,4)	1.51	A(3,2,6)	129.19	D(5,1,8,4)	-180.00
R(3,7)	1.08	A(2,3,4)	108.73	D(1,2,3,4)	0.00
R(4,8)	1.34	A(2,3,7)	128.94	D(1,2,3,7)	-180.00
R(4,9)	1.34	A(4,3,7)	122.32	D(6,2,3,4)	180.00
R(9,10)	0.97	A(3,4,8)	108.98	D(6,2,3,7)	0.00
		A(3,4,9)	118.45	D(2,3,4,8)	0.00
		A(8,4,9)	132.57	D(2,3,4,9)	-180.00
		A(1,8,4)	110.07	D(7,3,4,8)	-180.01
		A(4,9,10)	109.26	D(7,3,4,9)	0.00
				D(3,4,8,1)	0.01
				D(9,4,8,1)	180.01
				D(3,4,9,10)	-180.00
				D(8,4,9,10)	0.00

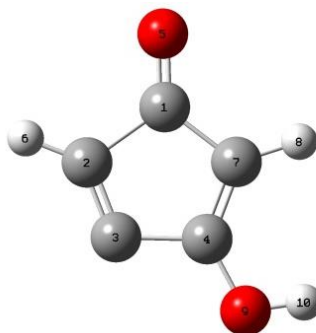


Table D.16 Geometry Parameters of y(c₅h₃do)oh₃-4j

Bond Distances,		Angles,		Dihedral Angles,	
angstrom (Å)		degree (°)		degree (°)	
R(1,2)	1.56	A(2,1,5)	124.15	D(5,1,2,3)	179.99
R(1,5)	1.20	A(2,1,7)	106.76	D(5,1,2,6)	-0.01
R(1,7)	1.48	A(5,1,7)	129.09	D(7,1,2,3)	0.01
R(2,3)	1.32	A(1,2,3)	104.59	D(7,1,2,6)	-180.00
R(2,6)	1.08	A(1,2,6)	122.68	D(2,1,7,4)	-0.01
R(3,4)	1.49	A(3,2,6)	132.73	D(2,1,7,8)	-180.00
R(4,7)	1.36	A(2,3,4)	112.31	D(5,1,7,4)	-179.99
R(4,9)	1.33	A(3,4,7)	109.43	D(5,1,7,8)	0.01
R(7,8)	1.08	A(3,4,9)	119.27	D(1,2,3,4)	0.00
R(9,10)	0.97	A(7,4,9)	131.30	D(6,2,3,4)	180.00
		A(1,7,4)	106.91	D(2,3,4,7)	0.00
		A(1,7,8)	124.43	D(2,3,4,9)	180.00
		A(4,7,8)	128.66	D(3,4,7,1)	0.00
		A(4,9,10)	109.67	D(3,4,7,8)	180.00
				D(9,4,7,1)	-180.00
				D(9,4,7,8)	0.00
				D(3,4,9,10)	-180.00
				D(7,4,9,10)	0.00

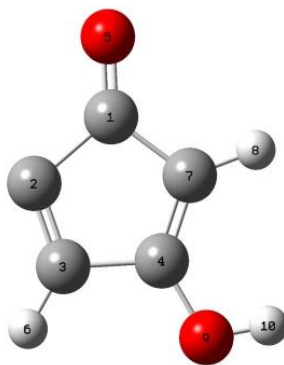


Table D.17 Geometry Parameters of $y(c_5h_3do)oh_3-5j$

Bond Distances, angstrom (Å)		Angles, degree (°)		Dihedral Angles, degree (°)	
R(1,2)	1.54	A(2,1,5)	128.12	D(5,1,2,3)	-179.99
R(1,5)	1.20	A(2,1,7)	103.42	D(7,1,2,3)	-0.01
R(1,7)	1.49	A(5,1,7)	128.46	D(2,1,7,4)	0.01
R(2,3)	1.32	A(1,2,3)	110.90	D(2,1,7,8)	-179.99
R(3,4)	1.51	A(2,3,4)	106.23	D(5,1,7,4)	179.99
R(3,6)	1.08	A(2,3,6)	130.64	D(5,1,7,8)	-0.01
R(4,7)	1.35	A(4,3,6)	123.13	D(1,2,3,4)	0.01
R(4,9)	1.34	A(3,4,7)	111.76	D(1,2,3,6)	180.00
R(7,8)	1.08	A(3,4,9)	117.30	D(2,3,4,7)	0.00
R(9,10)	0.97	A(7,4,9)	130.94	D(2,3,4,9)	-180.00
		A(1,7,4)	107.69	D(6,3,4,7)	-180.00
		A(1,7,8)	123.15	D(6,3,4,9)	0.00
		A(4,7,8)	129.16	D(3,4,7,1)	0.00
		A(4,9,10)	109.83	D(3,4,7,8)	180.00
				D(9,4,7,1)	180.00
				D(9,4,7,8)	0.00
				D(3,4,9,10)	-180.00
				D(7,4,9,10)	0.00

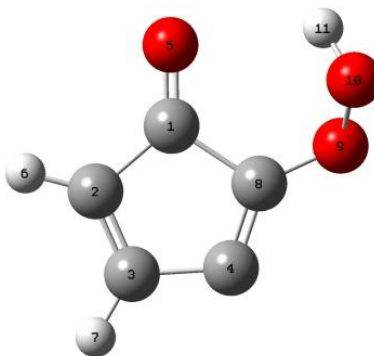


Table D.18 Geometry Parameters of $y(c_5h_3do)q_2-3j$

Bond Distances, angstrom (Å)		Angles, degree (°)		Dihedral Angles, degree (°)	
R(1,2)	1.49	A(2,1,5)	129.87	D(5,1,2,3)	175.35
R(1,5)	1.20	A(2,1,8)	105.91	D(5,1,2,6)	-7.68
R(1,8)	1.56	A(5,1,8)	124.14	D(8,1,2,3)	-1.48
R(2,3)	1.35	A(1,2,3)	107.03	D(8,1,2,6)	175.49
R(2,6)	1.08	A(1,2,6)	124.38	D(2,1,8,4)	1.51
R(3,4)	1.48	A(3,2,6)	128.51	D(2,1,8,9)	170.51
R(3,7)	1.08	A(2,3,4)	110.16	D(5,1,8,4)	-175.55
R(4,8)	1.33	A(2,3,7)	126.20	D(5,1,8,9)	-6.55
R(8,9)	1.34	A(4,3,7)	123.60	D(1,2,3,4)	0.93
R(9,10)	1.48	A(3,4,8)	111.93	D(1,2,3,7)	178.57
R(10,11)	0.97	A(1,8,4)	104.94	D(6,2,3,4)	-175.87
		A(1,8,9)	121.86	D(6,2,3,7)	1.76
		A(4,8,9)	132.02	D(2,3,4,8)	0.08
		A(8,9,10)	108.65	D(7,3,4,8)	-177.63
		A(9,10,11)	100.23	D(3,4,8,1)	-1.00
				D(3,4,8,9)	-168.40
				D(1,8,9,10)	56.40
				D(4,8,9,10)	-137.97
				D(8,9,10,11)	-83.18

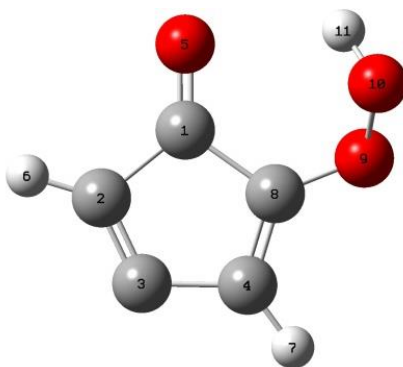


Table D.19 Geometry Parameters of y(c₅h₃do)q₂-4j

Bond Distances, angstrom (Å)		Angles, degree (°)		Dihedral Angles, degree (°)	
R(1,2)	1.51	A(2,1,5)	129.04	D(5,1,2,3)	175.65
R(1,5)	1.21	A(2,1,8)	105.47	D(5,1,2,6)	-5.75
R(1,8)	1.54	A(5,1,8)	125.43	D(8,1,2,3)	-1.60
R(2,3)	1.33	A(1,2,3)	104.00	D(8,1,2,6)	176.99
R(2,6)	1.08	A(1,2,6)	123.98	D(2,1,8,4)	1.96
R(3,4)	1.48	A(3,2,6)	132.00	D(2,1,8,9)	172.27
R(4,7)	1.08	A(2,3,4)	116.08	D(5,1,8,4)	-175.42
R(4,8)	1.35	A(3,4,7)	126.68	D(5,1,8,9)	-5.12
R(8,9)	1.34	A(3,4,8)	105.74	D(1,2,3,4)	0.82
R(9,10)	1.47	A(7,4,8)	127.56	D(6,2,3,4)	-177.62
R(10,11)	0.97	A(1,8,4)	108.67	D(2,3,4,7)	-178.12
		A(1,8,9)	122.72	D(2,3,4,8)	0.43
		A(4,8,9)	127.78	D(3,4,8,1)	-1.46
		A(8,9,10)	109.06	D(3,4,8,9)	-171.13
		A(9,10,11)	100.53	D(7,4,8,1)	177.08
				D(7,4,8,9)	7.41
				D(1,8,9,10)	51.69
				D(4,8,9,10)	-139.96
				D(8,9,10,11)	-77.89

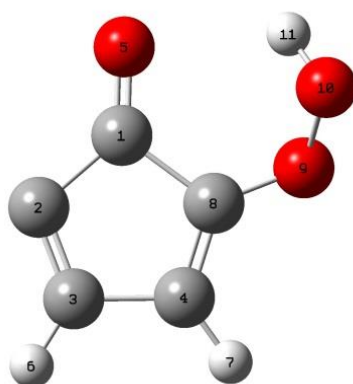


Table D.20 Geometry Parameters of $y(c_5h_3do)q2-5j$

Bond Distances, angstrom (Å)		Angles, degree (°)		Dihedral Angles, degree (°)	
R(1,2)	1.49	A(2,1,5)	132.44	D(5,1,2,3)	-179.53
R(1,5)	1.20	A(2,1,8)	102.61	D(8,1,2,3)	3.48
R(1,8)	1.55	A(5,1,8)	124.88	D(2,1,8,4)	0.47
R(2,3)	1.33	A(1,2,3)	110.04	D(2,1,8,9)	166.28
R(3,4)	1.50	A(2,3,4)	109.89	D(5,1,8,4)	-176.83
R(3,6)	1.08	A(2,3,6)	127.26	D(5,1,8,9)	-11.01
R(4,7)	1.08	A(4,3,6)	122.83	D(1,2,3,4)	-5.88
R(4,8)	1.34	A(3,4,7)	124.97	D(1,2,3,6)	172.48
R(8,9)	1.34	A(3,4,8)	108.00	D(2,3,4,7)	-170.93
R(9,10)	1.48	A(7,4,8)	126.96	D(2,3,4,8)	6.21
R(10,11)	0.97	A(1,8,4)	109.09	D(6,3,4,7)	10.62
		A(1,8,9)	121.33	D(6,3,4,8)	-172.24
		A(4,8,9)	127.78	D(3,4,8,1)	-3.76
		A(8,9,10)	108.97	D(3,4,8,9)	-168.40
		A(9,10,11)	100.38	D(7,4,8,1)	173.31
				D(7,4,8,9)	8.67
				D(1,8,9,10)	56.84
				D(4,8,9,10)	-140.20
				D(8,9,10,11)	-78.27

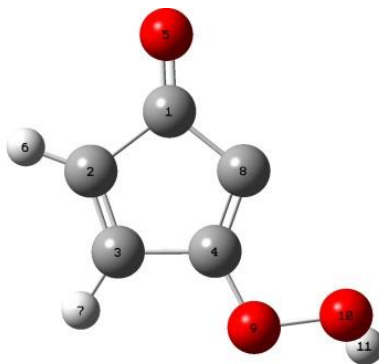


Table D.21 Geometry Parameters of y(c₅h₃do)q₃-2j

Bond Distances, angstrom (Å)		Angles, degree (°)		Dihedral Angles, degree (°)	
R(1,2)	1.54	A(2,1,5)	125.12	D(5,1,2,3)	-179.27
R(1,5)	1.20	A(2,1,8)	103.84	D(5,1,2,6)	1.40
R(1,8)	1.48	A(5,1,8)	131.05	D(8,1,2,3)	0.97
R(2,3)	1.33	A(1,2,3)	108.88	D(8,1,2,6)	-178.36
R(2,6)	1.08	A(1,2,6)	122.23	D(2,1,8,4)	-1.69
R(3,4)	1.51	A(3,2,6)	128.89	D(5,1,8,4)	178.57
R(3,7)	1.08	A(2,3,4)	108.10	D(1,2,3,4)	0.02
R(4,8)	1.34	A(2,3,7)	129.03	D(1,2,3,7)	-179.70
R(4,9)	1.34	A(4,3,7)	122.88	D(6,2,3,4)	179.29
R(9,10)	1.45	A(3,4,8)	109.95	D(6,2,3,7)	-0.43
R(10,11)	0.97	A(3,4,9)	116.60	D(2,3,4,8)	-1.15
		A(8,4,9)	133.45	D(2,3,4,9)	178.81
		A(1,8,4)	109.21	D(7,3,4,8)	178.60
		A(4,9,10)	109.37	D(7,3,4,9)	-1.45
		A(9,10,11)	99.68	D(3,4,8,1)	1.78
				D(9,4,8,1)	-178.17
				D(3,4,9,10)	-174.73
				D(8,4,9,10)	5.21
				D(4,9,10,11)	-123.48

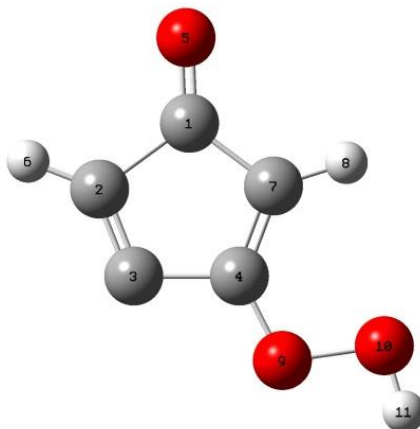


Table D.22 Geometry Parameters of y(c₅h₃do)q₃-4j

Bond Distances, angstrom (Å)		Angles, degree (°)		Dihedral Angles, degree (°)	
R(1,2)	1.57	A(2,1,5)	123.75	D(5,1,2,3)	180.00
R(1,5)	1.20	A(2,1,7)	107.03	D(5,1,2,6)	0.00
R(1,7)	1.48	A(5,1,7)	129.22	D(7,1,2,3)	0.00
R(2,3)	1.31	A(1,2,3)	104.65	D(7,1,2,6)	180.00
R(2,6)	1.08	A(1,2,6)	122.57	D(2,1,7,4)	0.00
R(3,4)	1.49	A(3,2,6)	132.78	D(2,1,7,8)	-180.00
R(4,7)	1.35	A(2,3,4)	111.60	D(5,1,7,4)	-180.00
R(4,9)	1.33	A(3,4,7)	110.63	D(5,1,7,8)	0.00
R(7,8)	1.08	A(3,4,9)	117.07	D(1,2,3,4)	0.00
R(9,10)	1.45	A(7,4,9)	132.30	D(6,2,3,4)	-180.00
R(10,11)	0.97	A(1,7,8)	106.09	D(2,3,4,7)	0.00
		A(1,7,8)	125.58	D(2,3,4,9)	-180.00
		A(4,7,8)	128.33	D(3,4,7,1)	0.00
		A(4,9,10)	108.86	D(3,4,7,8)	180.00
		A(9,10,11)	98.50	D(9,4,7,1)	180.00
				D(9,4,7,8)	0.00
				D(3,4,9,10)	-180.00
				D(7,4,9,10)	0.00
				D(4,9,10,11)	-179.96

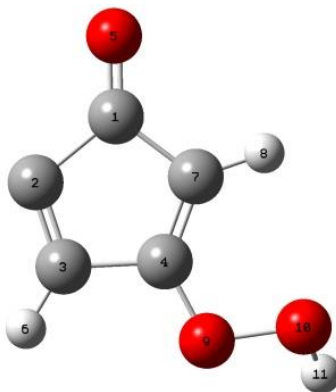


Table D.23 Geometry Parameters of $y(c_5h_3do)q_3-5j$

Bond Distances, angstrom (Å)		Angles, degree (°)		Dihedral Angles, degree (°)	
R(1,2)	1.54	A(2,1,5)	128.00	D(5,1,2,3)	179.78
R(1,5)	1.20	A(2,1,7)	103.58	D(7,1,2,3)	-0.12
R(1,7)	1.49	A(5,1,7)	128.42	D(2,1,7,4)	0.19
R(2,3)	1.32	A(1,2,3)	111.10	D(2,1,7,8)	-179.37
R(3,4)	1.51	A(2,3,4)	105.55	D(5,1,7,4)	-179.71
R(3,6)	1.08	A(2,3,6)	130.71	D(5,1,7,8)	0.73
R(4,7)	1.35	A(4,3,6)	123.74	D(1,2,3,4)	0.01
R(4,9)	1.34	A(3,4,7)	112.62	D(1,2,3,6)	-179.96
R(7,8)	1.08	A(3,4,9)	115.23	D(2,3,4,7)	0.12
R(9,10)	1.45	A(7,4,9)	132.14	D(2,3,4,9)	179.77
R(10,11)	0.97	A(1,7,4)	107.14	D(6,3,4,7)	-179.90
		A(1,7,8)	124.11	D(6,3,4,9)	-0.26
		A(4,7,8)	128.75	D(3,4,7,1)	-0.20
		A(4,9,10)	109.67	D(3,4,7,8)	179.34
		A(9,10,11)	98.95	D(9,4,7,1)	-179.77
				D(9,4,7,8)	-0.23
				D(3,4,9,10)	-176.94
				D(7,4,9,10)	2.62
				D(4,9,10,11)	-143.70

APPENDIX E

INPUT FILE FOR MODIFIED COMPUTATIONAL METHOD M062X/6-311+G(D,P)//CBS-QB3

The input file example for modified method [M062X/6-311+G(d,p)//CBS-QB3] are separated in two sections as following pattern.

```
%nprocshared=4
%chk=m2cdc
# M062X/6-311+g(d,p) opt freq

Molecule name or note

0 1
C
C      1      B1
H      2      B2  1      A1
H      2      B3  1      A2  3      D1  0
H      1      B4  2      A3  3      D2  0
H      1      B5  2      A4  3      D3  0

B1      1.32567400
B2      1.08417073
B3      1.08417073
B4      1.08417126
B5      1.08417073
A1      121.60780692
A2      121.60780692
A3      121.60785192
A4      121.60780692
D1      180.00000000
D2      0.00000000
D3      180.00000000

1 2 2.0 5 1.0 6 1.0
2 3 1.0 4 1.0
3
4
5
6

--link1--
%chk=m2cdc
# guess=read geom=allcheck CBS-QB3 iop(1/7=1000000)
```

APPENDIX F

RESULTING RATE CONSTANTS IN QRRK CALCULATION OF OH RADICAL ADDITION (INITIATION) WITH TRIFLUOROETHENE (1,1,2 TRIFLUOROETHENE)

The kinetic analysis in Tables F.1 and F.2 were results from QRRK calculation for OH addition to trifluoroethene system.

Table F.1 Calculated Reaction Parameters, $k = A(T/K)^n \exp(-E_a/RT)$ ($300 \leq T/K \leq 2000$), for $\text{CHF}=\text{CF}_2 + \text{OH} \rightarrow \text{C}(\text{OH})\text{F}_2\text{C}\cdot\text{HF} \rightarrow \text{Products}$ System

Reactions			A	n	E_a (cal/mol)	Pressure (atm)
CF ₂ CHF + OH	=>	CJHFCF ₂ OH	2.97E+40	-14.67	-912	0.001
CF ₂ CHF + OH	=>	CJHFCF ₂ OH	2.04E+48	-16.54	-1247	0.01
CF ₂ CHF + OH	=>	CJHFCF ₂ OH	7.09E+66	-21.36	3634	0.1
CF ₂ CHF + OH	=>	CJHFCF ₂ OH	3.93E+90	-27.34	14483	1
CF ₂ CHF + OH	=>	CJHFCF ₂ OH	6.44E+89	-25.84	18543	10
CF ₂ CHF + OH	=>	CJHFCF ₂ OH	7.15E+70	-19.16	15378	100
CF ₂ CHF + OH	=>	CF ₂ CHF + OH	7.97E-07	5.29	-1510	0.001
CF ₂ CHF + OH	=>	CF ₂ CHF + OH	9.35E-07	5.27	-1473	0.01
CF ₂ CHF + OH	=>	CF ₂ CHF + OH	3.67E-06	5.1	-1150	0.1
CF ₂ CHF + OH	=>	CF ₂ CHF + OH	2.50E-03	4.28	443	1
CF ₂ CHF + OH	=>	CF ₂ CHF + OH	9.59E+01	2.98	3431	10
CF ₂ CHF + OH	=>	CF ₂ CHF + OH	1.22E+03	2.74	5587	100
CF ₂ CHF + OH	=>	CHFDCFOH + F	7.50E-05	4.48	6501	0.001
CF ₂ CHF + OH	=>	CHFDCFOH + F	7.69E-05	4.48	6507	0.01
CF ₂ CHF + OH	=>	CHFDCFOH + F	9.80E-05	4.45	6566	0.1
CF ₂ CHF + OH	=>	CHFDCFOH + F	9.28E-04	4.17	7107	1
CF ₂ CHF + OH	=>	CHFDCFOH + F	6.23E+00	3.07	9373	10
CF ₂ CHF + OH	=>	CHFDCFOH + F	7.46E+03	2.24	12094	100
CF ₂ CHF + OH	=>	CJHFCDOF + HF	9.04E+04	2.09	-3228	0.001
CF ₂ CHF + OH	=>	CJHFCDOF + HF	9.01E+04	2.09	-3229	0.01
CF ₂ CHF + OH	=>	CJHFCDOF + HF	1.31E+05	2.05	-3145	0.1
CF ₂ CHF + OH	=>	CJHFCDOF + HF	1.16E+08	1.2	-1529	1
CF ₂ CHF + OH	=>	CJHFCDOF + HF	3.85E+12	-0.08	1553	10
CF ₂ CHF + OH	=>	CJHFCDOF + HF	1.87E+12	0.1	3238	100
CF ₂ CHF + OH	=>	COJF ₂ CH ₂ F	8.52E-13	-0.47	-2505	0.001
CF ₂ CHF + OH	=>	COJF ₂ CH ₂ F	1.33E-17	1.21	-5596	0.01
CF ₂ CHF + OH	=>	COJF ₂ CH ₂ F	5.20E-28	4.44	12985	0.1

Table F.1 Calculated Reaction Parameters, $k = A(T/K)^n \exp(-E_a/RT)$ ($300 \leq T/K \leq 2000$), for $\text{CHF}=\text{CF}_2 + \text{OH} \rightarrow \text{C}(\text{OH})\text{F}_2\text{C}\cdot\text{HF} \rightarrow \text{Products}$ System (Continued)

Reactions			A	n	E_a (cal/mol)	Pressure (atm)
CF ₂ CHF + OH	=>	COJF ₂ CH ₂ F	9.73E-14	0.44	-9263	1
CF ₂ CHF + OH	=>	COJF ₂ CH ₂ F	1.09E+02	-3.69	-4150	10
CF ₂ CHF + OH	=>	COJF ₂ CH ₂ F	4.87E+10	-6	-3936	100
CF ₂ CHF + OH	=>	CF ₂ DO + CJH ₂ F	2.39E+03	2.3	-3391	0.001
CF ₂ CHF + OH	=>	CF ₂ DO + CJH ₂ F	2.45E+03	2.3	-3385	0.01
CF ₂ CHF + OH	=>	CF ₂ DO + CJH ₂ F	4.53E+03	2.22	-3242	0.1
CF ₂ CHF + OH	=>	CF ₂ DO + CJH ₂ F	4.59E+06	1.36	-1573	1
CF ₂ CHF + OH	=>	CF ₂ DO + CJH ₂ F	1.25E+11	0.11	1480	10
CF ₂ CHF + OH	=>	CF ₂ DO + CJH ₂ F	6.30E+10	0.28	3167	100
CJHFCF ₂ OH	=>	CF ₂ CHF + OH	1.02E+36	-11.91	53991	0.001
CJHFCF ₂ OH	=>	CF ₂ CHF + OH	1.09E+44	-13.84	53718	0.01
CJHFCF ₂ OH	=>	CF ₂ CHF + OH	7.59E+62	-18.75	58716	0.1
CJHFCF ₂ OH	=>	CF ₂ CHF + OH	1.50E+84	-23.96	68817	1
CJHFCF ₂ OH	=>	CF ₂ CHF + OH	4.47E+82	-22.23	72658	10
CJHFCF ₂ OH	=>	CF ₂ CHF + OH	1.30E+65	-16	69896	100
CJHFCF ₂ OH	=>	CHFDCFOH + F	1.55E+30	-12.04	63785	0.001
CJHFCF ₂ OH	=>	CHFDCFOH + F	1.07E+36	-13.34	62171	0.01
CJHFCF ₂ OH	=>	CHFDCFOH + F	5.62E+46	-15.97	61392	0.1
CJHFCF ₂ OH	=>	CHFDCFOH + F	9.96E+75	-23.66	70290	1
CJHFCF ₂ OH	=>	CHFDCFOH + F	3.52+104	-30.59	84802	10
CJHFCF ₂ OH	=>	CHFDCFOH + F	6.15E+93	-25.74	86758	100
CJHFCF ₂ OH	=>	CJHFCDOF + HF	1.57E+51	-12.66	44108	0.001
CJHFCF ₂ OH	=>	CJHFCDOF + HF	3.10E+51	-12.41	45368	0.01
CJHFCF ₂ OH	=>	CJHFCDOF + HF	4.33E+49	-11.53	45886	0.1
CJHFCF ₂ OH	=>	CJHFCDOF + HF	1.17E+43	-9.23	44752	1
CJHFCF ₂ OH	=>	CJHFCDOF + HF	5.92E+35	-6.76	43164	10
CJHFCF ₂ OH	=>	CJHFCDOF + HF	8.94E+28	-4.51	41461	100
CJHFCF ₂ OH	=>	COJF ₂ CH ₂ F	8.58E+55	-14.91	46264	0.001
CJHFCF ₂ OH	=>	COJF ₂ CH ₂ F	1.09E+58	-15.01	48647	0.01
CJHFCF ₂ OH	=>	COJF ₂ CH ₂ F	8.40E+55	-13.91	49568	0.1
CJHFCF ₂ OH	=>	COJF ₂ CH ₂ F	4.18E+48	-11.28	48536	1
CJHFCF ₂ OH	=>	COJF ₂ CH ₂ F	3.48E+40	-8.51	46921	10
CJHFCF ₂ OH	=>	COJF ₂ CH ₂ F	3.95E+32	-5.87	44999	100
COJF ₂ CH ₂ F	=>	CF ₂ DO + CJH ₂ F	2.44E+23	-4.94	13351	0.001
COJF ₂ CH ₂ F	=>	CF ₂ DO + CJH ₂ F	2.44E+24	-4.94	13351	0.01
COJF ₂ CH ₂ F	=>	CF ₂ DO + CJH ₂ F	2.45E+25	-4.94	13352	0.1
COJF ₂ CH ₂ F	=>	CF ₂ DO + CJH ₂ F	2.50E+26	-4.95	13359	1
COJF ₂ CH ₂ F	=>	CF ₂ DO + CJH ₂ F	3.08E+27	-4.97	13421	10

Table F.1 Calculated Reaction Parameters, $k = A(T/K)^n \exp(-E_a/RT)$ ($300 \leq T/K \leq 2000$), for $\text{CHF}=\text{CF}_2 + \text{OH} \rightarrow \text{C}(\text{OH})\text{F}_2\text{C}\cdot\text{HF} \rightarrow \text{Products}$ System (Continued)

Reactions			A	n	E_a (cal/mol)	Pressure (atm)
COJF2CH2F	=>	CF2DO + CJH2F	1.21E+29	-5.14	13869	100
COJF2CH2F	=>	CJHFCF2OH	1.12E+11	-4.27	26348	0.001
COJF2CH2F	=>	CJHFCF2OH	1.12E+12	-4.27	26347	0.01
COJF2CH2F	=>	CJHFCF2OH	1.09E+13	-4.26	26339	0.1
COJF2CH2F	=>	CJHFCF2OH	8.44E+13	-4.23	26259	1
COJF2CH2F	=>	CJHFCF2OH	8.81E+13	-3.96	25528	10
COJF2CH2F	=>	CJHFCF2OH	1.27E+11	-2.9	21773	100

Table F.2 Calculated Reaction Parameters, $k = A(T/K)^n \exp(-E_a/RT)$ ($300 \leq T/K \leq 2000$), for $\text{CHF}=\text{CF}_2 + \text{OH} \rightarrow \text{C}\cdot\text{F}_2\text{CHF}(\text{OH}) \rightarrow \text{Products}$ System

Reactions			A	n	E_a (cal/mol)	Pressure (atm)
CF2CHF + OH	=>	CJF2CHFOH	5.03E+43	-14.39	505	0.001
CF2CHF + OH	=>	CJF2CHFOH	3.19E+52	-16.53	1821	0.01
CF2CHF + OH	=>	CJF2CHFOH	3.40E+70	-21.21	8716	0.1
CF2CHF + OH	=>	CJF2CHFOH	1.26E+81	-23.45	15269	1
CF2CHF + OH	=>	CJF2CHFOH	3.06E+74	-20.6	16029	10
CF2CHF + OH	=>	CJF2CHFOH	3.78E+60	-15.76	13467	100
CF2CHF + OH	=>	CF2CHF + OH	1.25E-01	3.86	-582	0.001
CF2CHF + OH	=>	CF2CHF + OH	1.98E-01	3.8	-475	0.01
CF2CHF + OH	=>	CF2CHF + OH	4.54E+00	3.41	269	0.1
CF2CHF + OH	=>	CF2CHF + OH	5.56E+04	2.24	2625	1
CF2CHF + OH	=>	CF2CHF + OH	1.23E+09	1.02	5724	10
CF2CHF + OH	=>	CF2CHF + OH	1.77E+09	1.06	7579	100
CF2CHF + OH	=>	CF2DCFOH + H	2.26E-04	4.47	1014	0.001
CF2CHF + OH	=>	CF2DCFOH + H	2.92E-04	4.44	1074	0.01
CF2CHF + OH	=>	CF2DCFOH + H	2.47E-03	4.17	1580	0.1
CF2CHF + OH	=>	CF2DCFOH + H	9.36E+00	3.14	3611	1
CF2CHF + OH	=>	CF2DCFOH + H	3.58E+05	1.85	6714	10
CF2CHF + OH	=>	CF2DCFOH + H	2.19E+06	1.7	8783	100
CF2CHF + OH	=>	CJF2CDOH + HF	1.10E+06	1.76	-1959	0.001
CF2CHF + OH	=>	CJF2CDOH + HF	1.28E+06	1.74	-1923	0.01
CF2CHF + OH	=>	CJF2CDOH + HF	4.38E+07	1.3	-1100	0.1
CF2CHF + OH	=>	CJF2CDOH + HF	1.74E+12	-0.02	1610	1
CF2CHF + OH	=>	CJF2CDOH + HF	4.29E+15	-0.95	4490	10
CF2CHF + OH	=>	CJF2CDOH + HF	1.13E+14	-0.4	5727	100

Table F.2 Calculated Reaction Parameters, $k = A(T/K)^n \exp(-E_a/RT)$ ($300 \leq T/K \leq 2000$), for $\text{CHF}=\text{CF}_2 + \text{OH} \rightarrow \text{C}\cdot\text{F}_2\text{CHF}(\text{OH}) \rightarrow \text{Products}$ System (Continued)

Reactions			A	n	E_a (cal/mol)	Pressure (atm)
CF ₂ CHF + OH	=>	CJHOHCF ₃	6.97E+27	-11.94	-5381	0.001
CF ₂ CHF + OH	=>	CJHOHCF ₃	2.90E+47	-17.35	-2979	0.01
CF ₂ CHF + OH	=>	CJHOHCF ₃	6.01E+83	-27.19	9681	0.1
CF ₂ CHF + OH	=>	CJHOHCF ₃	1.10+102	-31.16	20296	1
CF ₂ CHF + OH	=>	CJHOHCF ₃	7.80E+96	-28.13	24399	10
CF ₂ CHF + OH	=>	CJHOHCF ₃	2.99E+77	-21.18	22899	100
CF ₂ CHF + OH	=>	CF ₃ CDOH + H	2.86E+04	1.89	-2106	0.001
CF ₂ CHF + OH	=>	CF ₃ CDOH + H	3.70E+04	1.85	-2045	0.01
CF ₂ CHF + OH	=>	CF ₃ CDOH + H	1.78E+06	1.37	-1133	0.1
CF ₂ CHF + OH	=>	CF ₃ CDOH + H	1.42E+12	-0.32	2305	1
CF ₂ CHF + OH	=>	CF ₃ CDOH + H	6.78E+19	-2.48	7771	10
CF ₂ CHF + OH	=>	CF ₃ CDOH + H	7.36E+20	-2.63	11618	100
CF ₂ CHF + OH	=>	CJF ₂ CDOH + HF	9.08E+07	0.94	-1656	0.001
CF ₂ CHF + OH	=>	CJF ₂ CDOH + HF	9.32E+07	0.93	-1652	0.01
CF ₂ CHF + OH	=>	CJF ₂ CDOH + HF	2.89E+09	0.5	-861	0.1
CF ₂ CHF + OH	=>	CJF ₂ CDOH + HF	1.80E+15	-1.16	2479	1
CF ₂ CHF + OH	=>	CJF ₂ CDOH + HF	8.62E+22	-3.32	7939	10
CF ₂ CHF + OH	=>	CJF ₂ CDOH + HF	3.81E+23	-3.35	11656	100
CF ₂ CHF + OH	=>	CJFOHCF ₂ H	6.96E-21	1.53	-2213	0.001
CF ₂ CHF + OH	=>	CJFOHCF ₂ H	4.32E-22	1.99	-7141	0.01
CF ₂ CHF + OH	=>	CJFOHCF ₂ H	2.09E-12	-0.82	10075	0.1
CF ₂ CHF + OH	=>	CJFOHCF ₂ H	2.41E+27	-12.23	-2302	1
CF ₂ CHF + OH	=>	CJFOHCF ₂ H	1.20+102	-33.61	24884	10
CF ₂ CHF + OH	=>	CJFOHCF ₂ H	1.48+134	-41.33	43982	100
CF ₂ CHF + OH	=>	CF ₂ HCDOF + H	1.67E+01	2.28	7637	0.001
CF ₂ CHF + OH	=>	CF ₂ HCDOF + H	1.72E+01	2.27	7645	0.01
CF ₂ CHF + OH	=>	CF ₂ HCDOF + H	2.40E+01	2.23	7724	0.1
CF ₂ CHF + OH	=>	CF ₂ HCDOF + H	5.97E+02	1.83	8490	1
CF ₂ CHF + OH	=>	CF ₂ HCDOF + H	1.81E+08	0.26	11675	10
CF ₂ CHF + OH	=>	CF ₂ HCDOF + H	1.19E+16	-1.94	17216	100
CF ₂ CHF + OH	=>	CF ₂ DCFOH + H	2.25E-12	6.17	7810	0.001
CF ₂ CHF + OH	=>	CF ₂ DCFOH + H	2.32E-12	6.17	7818	0.01
CF ₂ CHF + OH	=>	CF ₂ DCFOH + H	3.21E-12	6.13	7894	0.1
CF ₂ CHF + OH	=>	CF ₂ DCFOH + H	7.95E-11	5.73	8654	1
CF ₂ CHF + OH	=>	CF ₂ DCFOH + H	1.17E-04	3.96	12161	10
CF ₂ CHF + OH	=>	CF ₂ DCFOH + H	3.60E+04	1.57	18000	100

Table F.2 Calculated Reaction Parameters, $k = A(T/K)^n \exp(-E_a/RT)$ ($300 \leq T/K \leq 2000$), for $\text{CHF}=\text{CF}_2 + \text{OH} \rightarrow \text{C}\cdot\text{F}_2\text{CHF}(\text{OH}) \rightarrow \text{Products}$ System (Continued)

Reactions			A	n	E_a (cal/mol)	Pressure (atm)
CF ₂ CHF + OH	=>	CJDOCF ₂ H + HF	1.22E-03	3.12	7345	0.001
CF ₂ CHF + OH	=>	CJDOCF ₂ H + HF	1.26E-03	3.12	7353	0.01
CF ₂ CHF + OH	=>	CJDOCF ₂ H + HF	1.77E-03	3.07	7433	0.1
CF ₂ CHF + OH	=>	CJDOCF ₂ H + HF	4.95E-02	2.66	8225	1
CF ₂ CHF + OH	=>	CJDOCF ₂ H + HF	4.76E+04	0.94	11672	10
CF ₂ CHF + OH	=>	CJDOCF ₂ H + HF	5.11E+12	-1.32	17353	100
CF ₂ CHF + OH	=>	CJHFCDOF + HF	3.78E+01	2.37	7865	0.001
CF ₂ CHF + OH	=>	CJHFCDOF + HF	3.90E+01	2.36	7872	0.01
CF ₂ CHF + OH	=>	CJHFCDOF + HF	5.41E+01	2.32	7950	0.1
CF ₂ CHF + OH	=>	CJHFCDOF + HF	1.24E+03	1.93	8698	1
CF ₂ CHF + OH	=>	CJHFCDOF + HF	1.78E+08	0.45	11708	10
CF ₂ CHF + OH	=>	CJHFCDOF + HF	1.15E+16	-1.74	17195	100
CF ₂ CHF + OH	=>	CHFDCFOH + F	2.53E-11	5.79	9891	0.001
CF ₂ CHF + OH	=>	CHFDCFOH + F	2.59E-11	5.79	9897	0.01
CF ₂ CHF + OH	=>	CHFDCFOH + F	3.25E-11	5.76	9950	0.1
CF ₂ CHF + OH	=>	CHFDCFOH + F	3.45E-10	5.46	10507	1
CF ₂ CHF + OH	=>	CHFDCFOH + F	1.33E-04	3.86	13639	10
CF ₂ CHF + OH	=>	CHFDCFOH + F	1.15E+05	1.33	19521	100
CF ₂ CHF + OH	=>	COJHFCHF ₂	2.14E-22	2.17	-5725	0.001
CF ₂ CHF + OH	=>	COJHFCHF ₂	3.84E-23	2.67	-6670	0.01
CF ₂ CHF + OH	=>	COJHFCHF ₂	4.00E-22	2.65	-7014	0.1
CF ₂ CHF + OH	=>	COJHFCHF ₂	2.05E-14	0.69	-3926	1
CF ₂ CHF + OH	=>	COJHFCHF ₂	4.35E-13	0.6	-3838	10
CF ₂ CHF + OH	=>	COJHFCHF ₂	1.19E-14	1.22	-8244	100
CF ₂ CHF + OH	=>	CHFDO + CJF ₂ H	3.70E+03	2.21	-1990	0.001
CF ₂ CHF + OH	=>	CHFDO + CJF ₂ H	4.72E+03	2.18	-1933	0.01
CF ₂ CHF + OH	=>	CHFDO + CJF ₂ H	1.76E+05	1.73	-1083	0.1
CF ₂ CHF + OH	=>	CHFDO + CJF ₂ H	6.24E+09	0.42	1604	1
CF ₂ CHF + OH	=>	CHFDO + CJF ₂ H	1.82E+13	-0.53	4501	10
CF ₂ CHF + OH	=>	CHFDO + CJF ₂ H	6.84E+11	-0.02	5795	100
CJF ₂ CHFOH	=>	CF ₂ CHF + OH	4.52E+42	-10.91	51532	0.001
CJF ₂ CHFOH	=>	CF ₂ CHF + OH	2.76E+43	-10.86	51248	0.01
CJF ₂ CHFOH	=>	CF ₂ CHF + OH	8.59E+48	-12.18	53104	0.1
CJF ₂ CHFOH	=>	CF ₂ CHF + OH	1.53E+58	-14.51	57539	1
CJF ₂ CHFOH	=>	CF ₂ CHF + OH	8.44E+59	-14.51	60042	10
CJF ₂ CHFOH	=>	CF ₂ CHF + OH	1.89E+52	-11.72	59168	100

Table F.2 Calculated Reaction Parameters, $k = A(T/K)^n \exp(-E_a/RT)$ ($300 \leq T/K \leq 2000$), for $\text{CHF}=\text{CF}_2 + \text{OH} \rightarrow \text{C}\cdot\text{F}_2\text{CHF}(\text{OH}) \rightarrow \text{Products}$ System (Continued)

Reactions			A	n	E_a (cal/mol)	Pressure (atm)
CJF2CHFOH	=>	CF2DCFOH + H	1.18E+38	-10.2	54163	0.001
CJF2CHFOH	=>	CF2DCFOH + H	1.78E+36	-9.41	52208	0.01
CJF2CHFOH	=>	CF2DCFOH + H	4.06E+41	-10.74	52631	0.1
CJF2CHFOH	=>	CF2DCFOH + H	2.95E+59	-15.6	59761	1
CJF2CHFOH	=>	CF2DCFOH + H	9.54E+65	-16.86	64496	10
CJF2CHFOH	=>	CF2DCFOH + H	5.88E+56	-13.44	63639	100
CJF2CHFOH	=>	CJF2CDOH + HF	2.38E+48	-11.55	50784	0.001
CJF2CHFOH	=>	CJF2CDOH + HF	2.59E+50	-11.85	51421	0.01
CJF2CHFOH	=>	CJF2CDOH + HF	5.28E+53	-12.49	53192	0.1
CJF2CHFOH	=>	CJF2CDOH + HF	2.51E+54	-12.35	54536	1
CJF2CHFOH	=>	CJF2CDOH + HF	1.38E+51	-11.08	54424	10
CJF2CHFOH	=>	CJF2CDOH + HF	1.06E+46	-9.32	53412	100
CJF2CHFOH	=>	CJHOHCF3	4.76E+48	-11.77	50785	0.001
CJF2CHFOH	=>	CJHOHCF3	5.22E+50	-12.06	51426	0.01
CJF2CHFOH	=>	CJHOHCF3	9.96E+53	-12.7	53192	0.1
CJF2CHFOH	=>	CJHOHCF3	3.33E+54	-12.51	54480	1
CJF2CHFOH	=>	CJHOHCF3	1.26E+51	-11.2	54287	10
CJF2CHFOH	=>	CJHOHCF3	1.21E+46	-9.48	53268	100
CJF2CHFOH	=>	CJFOHCF2H	1.00E+37	-11.7	61952	0.001
CJF2CHFOH	=>	CJFOHCF2H	3.12E+32	-10.14	58370	0.01
CJF2CHFOH	=>	CJFOHCF2H	2.83E+30	-9.39	53333	0.1
CJF2CHFOH	=>	CJFOHCF2H	1.03E+58	-17.23	60884	1
CJF2CHFOH	=>	CJFOHCF2H	3.08E+88	-25.38	74387	10
CJF2CHFOH	=>	CJFOHCF2H	1.24E+84	-22.9	77048	100
CJF2CHFOH	=>	COJHFCHF2	3.95E+46	-11.39	50782	0.001
CJF2CHFOH	=>	COJHFCHF2	4.27E+48	-11.69	51416	0.01
CJF2CHFOH	=>	COJHFCHF2	9.34E+51	-12.34	53192	0.1
CJF2CHFOH	=>	COJHFCHF2	6.74E+52	-12.25	54603	1
CJF2CHFOH	=>	COJHFCHF2	6.57E+49	-11.05	54609	10
CJF2CHFOH	=>	COJHFCHF2	3.77E+44	-9.24	53613	100
CJHOHCF3	=>	CF3CDOH + H	1.66E+50	-14.22	48044	0.001
CJHOHCF3	=>	CF3CDOH + H	3.11E+64	-17.82	53846	0.01
CJHOHCF3	=>	CF3CDOH + H	3.18E+70	-18.82	58418	0.1
CJHOHCF3	=>	CF3CDOH + H	1.08E+60	-14.88	57425	1
CJHOHCF3	=>	CF3CDOH + H	5.18E+51	-11.87	56364	10
CJHOHCF3	=>	CF3CDOH + H	8.98E+40	-8.26	53903	100

REFERENCES

1. Stewart, J. J. P., Optimization of parameters for semiempirical methods V: Modification of NDDO approximations and application to 70 elements. *J. Mol. Model.* **2007**, *13* (12), 1173-1213.
2. Becke, A. D., A new mixing of Hartree-Fock and local density-functional theories. *J. Chem. Phys.* **1993**, *98* (3), 1372-1377.
3. Lee, C.; Yang, W.; Parr, R. G., Development of the Colic-Salvetti correlation-energy formula into a functional of the electron density. *Phys. Rev. B* **1988**, *37*, 785-789.
4. Montgomery, J. A., Jr.; Frisch, M. J.; Ochterski, J. W.; Petersson, G. A., A Complete Basis Set Model Chemistry. VI. Use of Density Functional Geometries and Frequencies. *J. Chem. Phys.* **1999**, *110*, 2822-2827.
5. Zhao, Y.; Truhlar, D., The M06 suite of density functionals for main group thermochemistry, thermochemical kinetics, noncovalent interactions, excited states, and transition elements: two new functionals and systematic testing of four M06-class functionals and 12 other functionals. *Theor. Chem. Account.* **2008**, *120* (1-3), 215-241.
6. Chai, J.-D.; Head-Gordon, M., Systematic optimization of long-range corrected hybrid density functionals. *J. Chem. Phys.* **2008**, *128* (8), 084106.
7. Ochterski, J. W.; Petersson, G. A.; Montgomery, J. A., A complete basis set model chemistry. V. Extensions to six or more heavy atoms. *J. Chem. Phys.* **1996**, *104* (7), 2598-2619.
8. Shankar, R., *Principles of Quantum Mechanics*. Kluwer Academic/Plenum Publishers: New York, NY., 1994.
9. Hehre, W.; Random, L.; Schleyer, P. R.; Pople, J. A., *Ab Initio Molecular Orbital Theory* John Wiley & Son: New York, NY., 1986.
10. Møller, C.; Plesset, M. S., Note on an approximation treatment for many-electron systems. *Phys. Rev.* **1934**, *46* (7), 618-622.
11. Boese, A. D.; Martin, J. M. L., Development of density functionals for thermochemical kinetics. *J. Chem. Phys.* **2004**, *121* (8), 3405-3416.
12. Chai, J. D.; Head-Gordon, M., Systematic optimization of long-range corrected hybrid density functionals. *J. Chem. Phys.* **2008**, *128* (8), 40-55.
13. Grimme, S., Semiempirical hybrid density functional with perturbative second-order correlation. *J. Chem. Phys.* **2006**, *124* (3), 67-83.
14. Frisch, M. J.; Trucks, G. W.; Schlegel, H. B.; Scuseria, G. E.; Robb, M. A.; Cheeseman, J. R.; Montgomery, J. A., Jr.; Vreven, T.; Kudin, K. N.; Burant, J. C.; Millam, J. M.; Iyengar, S. S.; Tomasi, J.; Barone, V.; Mennucci, B.; Cossi, M.; Scalmani, G.; Rega, N.; Petersson, G. A.; Nakatsuji, H.; Hada, M.; Ehara, M.; Toyota, K.; Fukuda, R.; Hasegawa, J.; Ishida, M.; Nakajima, T.;

- Honda, Y.; Kitao, O.; Nakai, H.; Klene, M.; Li, X.; Knox, J. E.; Hratchian, H. P.; Cross, J. B.; Adamo, C.; Jaramillo, J.; Gomperts, R.; Stratmann, R. E.; Yazyev, O.; Austin, A. J.; Cammi, R.; Pomelli, C.; Ochterski, J. W.; Ayala, P. Y.; Morokuma, K.; Voth, G. A.; Salvador, P.; Dannenberg, J. J.; Zakrzewski, V. G.; Dapprich, S.; Daniels, A. D.; Strain, M. C.; Farkas, O.; Malick, D. K.; Rabuck, A. D.; Raghavachari, K.; Foresman, J. B.; Ortiz, J. V.; Cui, Q.; Baboul, A. G.; Clifford, S.; Cioslowski, J.; Stefanov, B. B.; Liu, G.; Liashenko, A.; Piskorz, P.; Komaromi, I.; Martin, R. L. *Gaussian03*, Gaussian, Inc.: Wallingford, CT., 2003.
15. Frisch, M. J.; Trucks, G. W.; Schlegel, H. B.; Scuseria, G. E.; Robb, M. A.; Cheeseman, J. R.; Scalmani, G.; Barone, V.; Mennucci, B.; Petersson, G. A.; Nakatsuji, H.; Caricato, M.; Li, X.; Hratchian, H. P.; Izmaylov, A. F.; Bloino, J.; Zheng, G.; Sonnenberg, J. L.; Hada, M.; Ehara, M.; Toyota, K.; Fukuda, R.; Hasegawa, J.; Ishida, M.; Nakajima, T.; Honda, Y.; Kitao, O.; Nakai, H.; Vreven, T.; Montgomery, J., J.A.; Peralta, J. E.; Ogliaro, F.; Bearpark, M.; Heyd, J. J.; Brothers, E.; Kudin, K. N.; Staroverov, V. N.; Kobayashi, R.; Normand, J.; Raghavachari, K.; Rendell, A.; Burant, J. C.; Iyengar, S. S.; Tomasi, J.; Cossi, M.; Rega, N.; Millam, J. M.; Klene, M.; Knox, J. E.; Cross, J. B.; Bakken, V.; Adamo, C.; Jaramillo, J.; Gomperts, R.; Stratmann, R. E.; Yazyev, O.; Austin, A. J.; Cammi, R.; Pomelli, C.; Ochterski, J. W.; Martin, R. L.; Morokuma, K.; Zakrzewski, V. G.; Voth, G. A.; Salvador, P.; Dannenberg, J. J.; Dapprich, S.; Daniels, A. D.; Farkas, Ö.; Foresman, J. B.; Ortiz, J. V.; Cioslowski, J.; Fox, D. J. *Gaussian 09, Revision A.1*, Wallingford, CT., 2009.
 16. Asatryan, R.; Bozzelli, J. W.; Simmie, J., Thermochemistry of methyl and ethyl Nitro, RNO₂, and nitrite, RONO, organic compounds. *J. Phys. Chem. A* **2008**, *112* (14), 3172-3185.
 17. Hehre, W.; Radom, L.; Schleyer, P. R.; Pople, J. A., *Ab Initio Molecular Orbital Theory* John Wiley & Sons: New York, NY., 1986.
 18. Scott, A. P.; Radom, L., Harmonic vibrational frequencies: an evaluation of hartree-fock, moller-plesset, quadratic configuration interaction, density functional theory and semiempirical scale factors. *J. Phys. Chem.* **1996**, *100*, 16502-16513.
 19. Minkin, V. I., Glossary of terms used in theoretical organic chemistry. *Pure Appl. Chem.* **1999**, *71*, 1919-1981.
 20. Burcat, A.; Ruscic, B. *Third Millennium Ideal Gas and Condensed Phase Thermochemical Database for Combustion with Updates from Active Thermochemical Table*; Technion Aerospace Engineering: Haifa, Israel, 2005.
 21. Baulch, D. L.; Bowman, C. T.; Cobos, C. J.; Cox, R. A.; Just, T.; Kerr, J. A.; Pilling, M. J.; Stocker, D.; Troe, J.; Tsang, W.; Walker, R. W.; Warnatz, J., Evaluated kinetic data for combustion modeling: supplement II. *J. Phys. Chem. Ref. Data* **2005**, *24*, 757-1397.

22. Ruscic, B.; Pinzon, R. E.; Morton, M. L.; Srinivasan, N. K.; Su, M.; Sutherland, J. W.; Michael, J. V., Active Thermochemical Tables: Accurate Enthalpy of Formation of Hydroperoxyl Radical, HO₂. *J. Phys. Chem. A* **2006**, *110*, 6592-6601.
23. Sheng, C. Elementary, pressure dependent model for combustion of C₁, C₂ and nitrogen containing hydrocarbons : operation of a pilot scale incinerator and model comparison. New Jersey Institute of Technology, 2002.
24. Benson, S. W.; Buss, J. H., Additivity rules for the estimate for the molecular properties, thermodynamic properties. *J. Chem. Phys.* **1958**, *29*, 546-573.
25. Lay, T. H.; Bozzelli, J. W.; Dean, A. M.; Ritter, E. R., Hydrogen atom bond increments for calculation of thermodynamic properties of hydrocarbon radical species. *J. Phys. Chem.* **1995**, *99* (39), 14514-14527.
26. Lay, T. H.; Krasnoperov, L. N.; Venanzi, C. A.; Bozzelli, J. W.; Shokhirev, N. V., Ab initio study of α -chlorinated ethyl hydroperoxides CH₃CH₂OOH, CH₃CHClOOH, and CH₃CCl₂OOH: conformational analysis, internal rotation barriers, vibrational frequencies, and thermodynamic properties. *J. Phys. Chem.* **1996**, *100* (20), 8240-8249.
27. Lay, T. H.; Tsai, P. L.; Yamada, T.; Bozzelli, J. W., Thermodynamic parameters and group additivity ring corrections for three-to-six-membered oxygen heterocyclic hydrocarbons. *J. Phys. Chem. A* **1997**, *101* (13), 2471-2477.
28. Truhlar, D. G.; Garrett, B. C., Variational transition state theory. *Ann. Rev. Phys. Chem.* **1984**, *35* (1), 159-189.
29. Sheng, C. Y.; Bozzelli, J. W.; Dean, A. M.; Chang, A. Y., Detailed kinetics and thermochemistry of C₂H₅ + O₂: reaction kinetics of the chemically-activated and stabilized CH₃CH₂OO• adduct. *J. Phys. Chem. A* **2002**, *106* (32), 7276-7293.
30. Chang, A. Y.; Bozzelli, J. W.; Dean, A. M., Kinetic analysis of complex chemical activation and unimolecular dissociation reactions using QRRK theory and the modified strong collision approximation. *Z. Phys. Chem.* **2000**, *214*, 1533-1568.
31. Dean, A. M.; Westmoreland, P. R., Bimolecular QRRK analysis of methyl radical reactions. *Int. J. Chem. Kinet.* **1987**, *19* (3), 207-228.
32. Westmoreland, P. R.; Howard, J. B.; Longwell, J. P.; Dean, A. M., Prediction of rate constants for combustion and pyrolysis reactions by bimolecular QRRK. *AIChE J.* **1986**, *32* (12), 1971-1979.
33. Gilbert, R. G.; Luther, K.; Troe, J., Theory of Thermal Unimolecular Reactions in the Fall-Off Range. II. Weak Collision Rate Constants. *Ber. Bunsen-Ges. Phys. Chem.* **1983**, *87*, 169-177.
34. Gilbert, R. G.; Smith, S. C., *Theory of unimolecular and recombination reactions*. Blackwell Scientific Publications: Oxford, UK., 1990.

35. Gilbert, R. G.; Smith, S. C.; Jordan, M. J. T. *UNIMOL program suite (calculation of fall off curves for unimolecular and recombination reactions)*, Sydney University: Sydney, AU., 1993.
36. Bozzelli, J. W.; Chang, A. Y.; Dean, A. M., Molecular density of states from estimated vapor phase heat capacities. *Int. J. Chem. Kinet.* **1997**, 29, 161-170.
37. Ritter, E. R., Therm: a computer code for estimating thermodynamic properties for species important to combustion and reaction modeling. *J. Chem. Inf. Comput. Sci.* **1991**, 31, 400-408.
38. Stout, J. M.; Dykstra, C. E., Static Dipole Polarizabilities of Organic Molecules. Ab Initio Calculations and a Predictive Model. *J. Am. Chem. Soc.* **1995**, 117 (18), 5127-5132.
39. Maroulis, G.; Begue, D.; Pouchan, C., Accurate dipole polarizabilities of small silicon clusters from ab initio and density functional theory calculations. *J. Chem. Phys.* **2003**, 119 (2), 794-797.
40. Das, G. P.; Dudis, D. S., An approximate ab initio study of the polarizability and hyperpolarizabilities of organic molecules. *Chem. Phys. Lett.* **1991**, 1 (2), 151-158.
41. Hickey, A. L.; Rowley, C. N., Benchmarking quantum chemical methods for the calculation of molecular dipole moments and polarizability. *J. Phys. Chem. A* **2014**, 118, 3678-3687.
42. Muller, K.; Mokrushina, L., Second-order group contribution method for the determination of the dipole moment. *J. Chem. Eng. Data* **2012**, 57, 1231-1236.
43. Halpern, A. M.; Glendening, E. D., Estimating molecular collision diameters using computational methods. *J. Mol. Struct. THEOCHEM* **1996**, 365, 9-12.
44. Hirschfelder, J. O.; Curtiss, C. F.; Bird, R. B., *Molecular theory of gases and liquids*. John Wiley and Sons, Inc.: New York, NY., 1954.
45. Joback, K. G.; Reid, R. C., Estimation of pure-component properties from group-contributions. *Chem. Eng. Commun.* **1987**, 57 (1-6), 233-243.
46. Alparone, A.; Librando, V.; Minniti, Z., Validation of semiempirical PM6 method for the prediction of molecular properties of polycyclic aromatic hydrocarbons and fullerenes. *Chem. Phys. Lett.* **2008**, 460 (1-3), 151-154.
47. Puzyn, T.; Suzuki, N.; Haranczyk, M.; Rak, J., Calculation of quantum-mechanical descriptors for QSPR at the DFT Level: Is it necessary? *J. Chem. Inf. Model.* **2008**, 48 (6), 1174-1180.
48. Staikova, M.; Wania, F.; Donaldson, D. J., Molecular polarizability as a single-parameter predictor of vapor pressures and octanol-air partitioning coefficients of non-polar compounds: a-priori approach and results. *Atmos. Env.* **2004**, 38, 213-225.

49. Computational Chemistry Comparison and Benchmark DataBase. August 2013 ed.; National Institute of Standards and Technology (NIST), Standard Reference Database 101, (accessed on Apr, 2015).
50. Nelson, R. D.; Lide, D. R.; Maryott, A. A. *Selected values of electric dipole moments for molecules in the gas phase*; National Bureau of Standards (NBS): Washington, D.C., 1967.
51. Atkins, P.; de Paula, J.; Friedman, R., *Quanta, matter, and change: a molecular approach to physical chemistry*. Oxford University Press: Cary, NC., 2009.
52. Denbigh, K. G., The polarisabilities of bonds-I. *Trans. Faraday Soc.* **1940**, *36*, 936-948.
53. Batsanov, S. S., *Refractometry and Chemical Structure*. Consultants Bureau: New York, NY., 1961.
54. Landolt-Börnstein, *Atom und Molekularphysik*. Springer-Verlag: West Berlin, Germany, 1951; Vol. 1, p 511-513.
55. Applequist, J.; Carl, J. R.; Fung, K.-K., Atom dipole interaction model for molecular polarizability. Application to polyatomic molecules and determination of atom polarizabilities. *J. Am. Chem. Soc.* **1972**, *94* (9), 2952-2960.
56. Svehla, R. A. *Estimated Viscosities and Thermal Conductivities of Gases at High Temperatures*. NASA Tech. Rep. R-132; Washington D.C., 1962.
57. Ben-Amotz, D.; Herschbach, D. R., Estimation of effective diameters for molecular fluids. *J. Phys. Chem.* **1990**, *94* (3), 1038-1047.
58. Mourits, F. M.; Rummens, F. H. A., A Critical evaluation of Lennard-Jones and Stockmayer potential parameters and of some correlation methods. *Can. J. Chem.* **1977**, *55*, 3007-3020.
59. Jasper, A. W.; Miller, J. A., Lennard-Jones parameters for combustion and chemical kinetics modeling from full-dimensional intermolecular potentials. *Combust Flame* **2014**, *161* (1), 101-110.
60. Da Costa, I.; Fournet, R.; Billaud, F.; Battin-Leclerc, F., Experimental and modeling study of the oxidation of benzene. *Int. J. Chem. Kinet.* **2003**, *35*, 503-524.
61. Wang, H.; Brezinsky, K., Computational study on the thermochemistry of cyclopentadiene derivatives and kinetics of cyclopentadienone thermal decomposition. *J. Phys. Chem. A* **1998**, *102*, 1530-1541.
62. Robichaud, D. J.; Scheer, A. M.; Mukarakate, C.; Ormond, T. K.; Buckingham, G. T.; Ellison, G. B.; Nimlos, M. R., Unimolecular thermal decomposition of dimethoxybenzenes. *J. Chem. Phys.* **2014**, *140* (23), 234302.
63. Scheer, A. M. Thermal Decomposition Mechanisms of Lignin Model Compounds: From Phenol to Vanillin. University of Colorado, Boulder, CO., 2001.

64. Scheer, A. M.; Mukarakate, C.; Robichaud, D. J.; Nimlos, M. R.; Ellison, G. B., Thermal decomposition mechanisms of the methoxyphenols: formation of phenol, cyclopentadienone, vinylacetylene, and acetylene. *J. Phys. Chem. A* **2011**, *115*, 13381-13389.
65. Shin, E. J.; Nimlos, M. R.; Evans, R. J., A study of the mechanisms of vanillin pyrolysis by mass spectrometry and multivariate analysis. *Fuel* **2001**, *80* (12), 1689-1696.
66. Butler, G. R.; Glassman, I., Cyclopentadiene combustion in a plug flow reactor near 1150 K. *Proc. Combust. Inst.* **2009**, *32*, 395-402.
67. Alzueta, M. U.; Glarborg, P.; Dam-Johansen, K., Experimental and kinetic modeling study of the oxidation of benzene. *Int. J. Chem. Kinet.* **2000**, *21*, 498-522.
68. Sharma, S.; Raman, S.; Green, W. H., Intramolecular hydrogen migration in alkylperoxy and hydroperoxyalkylperoxy radicals: accurate treatment of hindered rotors. *J. Phys. Chem. A* **2010**, *114*, 5689-5701.
69. De Jongh, D. C.; Van Fossen, R. Y.; Bourgeois, C. F., Comparative studies of electron-impact and thermolytic fragmentation. II. View the MathML source-phenylene sulfite. *Tetrahedron Letters* **1967**, *8* (3), 271-276.
70. Sebbar, N.; Bockhorn, H.; Bozzelli, J. W., Thermodynamic properties of the species resulting from the phenyl radical with O₂ reaction system. *Int. J. Chem. Kinet.* **2008**, *40* (9), 583-604.
71. Kirk, B. B.; Harman, D. G.; Kenttamaa, H. I.; Trevitt, A. J.; Blanksby, S. J., Isolation and characterization of charge-tagged phenylperoxyl radicals in the gas phase: direct evidence for products and pathways in low temperature benzene oxidation. *Phys. Chem. Chem. Phys.* **2012**, *14*, 16719-16730.
72. Emdee, J. L.; Brezinsky, K.; Glassman, I., A kinetic model for the oxidation of toluene near 1200 K. *J. Phys. Chem.* **1992**, *96*, 2151-2161.
73. Ormond, T. K.; Scheer, A. M.; Nimlos, M. R.; Robichaud, D. J.; Daily, J. W.; Stanton, J. F.; Ellison, G. B., Polarized matrix infrared spectra of cyclopentadienone: observations, calculations, and assignment for an important intermediate in combustion and biomass pyrolysis. *J. Phys. Chem. A* **2014**, *118*, 708-718.
74. Sirjean, B.; Ruiz-Lopez, M. F.; Glaude, P. A.; Battin-Leclerc, F.; Fournet, R. In *Theoretical study of the thermal decomposition mechanism of phenylperoxy radical*, Proc. Euro. Combust. Meet., Louvain-la-Neuve, Belgium, Louvain-la-Neuve, Belgium, 2005.
75. Battin-Leclerc, F., Detailed chemical kinetic models for the low-temperature combustion of hydrocarbons with application to gasoline and diesel fuel surrogates. *Prog. Energ. Combust.* **2008**, *34*, 440-498.
76. Zhong, X.; Bozzelli, J. W., Thermochemical and kinetic analysis of the H, OH, HO₂, O, and O₂ association reactions with cyclopentadienyl radical. *J. Phys. Chem. A* **1998**, *102*, 3537-3555.

77. Robinson, R. K.; Lindstedt, R. P., On the chemical kinetics of cyclopentadiene oxidation. *Combust. Flame* **2011**, *158*, 666-686.
78. Pedley, J. B.; Naylor, R. D.; Kirby, S. P., *Thermochemical Data and Structures of Organic Compounds*. Chapman and Hall: London, UK., 1986.
79. Tsang, W., *Heats of Formation of Organic Free Radicals by Kinetic Methods in Energetics of Organic Free Radicals*. Blackie Academic and Professional: London, UK., 1996; p 22-58.
80. Asatryan, R.; Da Silva, G.; Bozzelli, J. W., Quantum chemical study of the acrolein (CH_2CHCHO) + OH + O₂ reactions. *J. Phys. Chem. A* **2010**, *114*, 8302-8311.
81. Sebbar, N.; Bockhorn, H.; Bozzelli, J. W., Structures, thermochemical properties (enthalpy, entropy and heat capacity), rotation barriers, and peroxide bond energies of vinyl, allyl, ethynyl and phenyl hydroperoxides. *Phys. Chem. Chem. Phys.* **2002**, *4*, 3691-3703.
82. Prosen, E. J.; Maron, F. W.; Rossini, F. D., Heats of combustion, formation, and isomerization of ten C₄ hydrocarbons. *J. Res. NBS* **1951**, *46*, 106-112.
83. Guthrie, G. B.; Scott, D. W.; Hubbard, W. N.; Katz, C.; McCullough, J. P.; Gross, M. E.; Williamson, K. D.; Waddington, G., Thermodynamic properties of furan. *J. Am. Chem. Soc.* **1952**, *74*, 4662-46.
84. Guthrie, J. P., Equilibrium constants for a series of simple aldol condensations, and linear free energy relations with other carbonyl addition reactions. *Can. J. Chem.* **1978**, *56*, 962-973.
85. Simmie, M. J.; Curran, H. J., Formation enthalpies and bond dissociation energies of alkylfurans. The strongest CsX bonds known? *J. Phys. Chem. A* **2009**, *113*, 5128-5137.
86. Steele, W. V.; Chirico, R. D.; Nguyen, A.; Hossenlopp, I. A.; Smith, N. K., Determination of some pure compound ideal-gas enthalpies of formation. *AIChE Symp. Ser.* **1989**, *85*, 140-162.
87. Zhu, L.; Bozzelli, J. W., Kinetics and thermochemistry for the gas-phase keto-enol tautomerism of phenol T 2,4-cyclohexadienone. *J. Phys. Chem. A* **2003**, *107*, 3696-3703.
88. Rutz, L. K.; Da Silva, G.; Bozzelli, J. W.; Bockhorn, H., Reaction of the i-C₄H₅ ($\text{CH}_2\text{CCHCH}_2$) radical with O₂. *J. Phys. Chem. A* **2011**, *115*, 1018-1026.
89. Prosen, E. J.; Johnson, W. H.; Rossini, F. D., Heats of formation and combustion of the normal alkylcyclopentanes and cyclohexanes and the increment per CH₂ group for several homologous series of hydrocarbons. *J. Res. NBS* **1946**, *37*, 51-56.
90. Wiberg, K. B.; Crocker, L. S.; Morgan, K. M., Thermochemical studies of carbonyl compounds. 5. Enthalpies of reduction of carbonyl groups. *J. Am. Chem. Soc.* **1991**, *113*, 3447-3450.

91. Wang, H.; Frenklach, M., Calculations of rate coefficients for the chemically activated reactions of acetylene with vinylic and aromatic radicals. *J. Phys. Chem.* **1994**, *98*, 11465-11489.
92. Lias, S. G.; Bartmess, J. E.; Liebman, J. F.; Holmes, J. L.; Levin, R. D.; Mallard, W. G., Gas-phase ion and neutral thermochemistry. *J. Phys. Chem. Ref. Data, Suppl. 1* **1988**, *17*, 1-861.
93. Morales, G.; Martinez, R., Thermochemical properties and contribution groups for ketene dimers and related structures from theoretical calculations. *J. Phys. Chem. A* **2009**, *113*, 8683-8703.
94. Steele, W. V.; Chirico, R. D.; Knipmeyer, S. E.; Nguyen, A.; Smith, N. K.; Tasker, I. R., Thermodynamic properties and ideal-gas enthalpies of formation for cyclohexene, phthalan (2,5-dihydrobenzo-3,4-furan), isoxazole, octylamine, dioctylamine, trioctylamine, phenyl isocyanate, and 1,4,5,6-tetrahydropyrimidine. *J. Chem. Eng. Data* **1996**, *41*, 1269-1284.
95. Ruscic, B.; Boggs, J. E.; Burcat, A.; Csazar, A. G.; Demaison, J.; Janoschek, R.; Martin, J. M. L.; Morton, M. L.; Rossi, M. J.; Stanton, J. F.; Szalay, P. G.; Westmoreland, P. R.; Zabel, F.; Berces, T., IUPAC Critical evaluation of thermochemical properties of selected radicals. *J. Phys. Chem. Ref. Data* **2005**, *34*, 573-656.
96. Holmes, J. L.; Lossing, F. P., Heats of formation of the ionic and neutral enols of acetaldehyde and acetone. *J. Am. Chem. Soc.* **1982**, *104*, 2648-2649.
97. Simmie, J. M.; Black, G.; Curran, H. J.; Hinde, J. P., Enthalpies of formation and bond dissociation energies of lower alkyl hydroperoxides and related hydroperoxy and alkoxy radicals. *J. Phys. Chem. A* **2008**, *112* (22), 5010-5016.
98. Roux, M. V.; Temprado, M.; Chickos, J. S.; Nagano, Y., Critically evaluated thermochemical properties of polycyclic aromatic hydrocarbons. *J. Phys. Chem. Ref. Data* **2008**, *37* (4), 1855-1996.
99. Cox, J. D., The heats of combustion of phenol and the three cresols. *Pure Appl. Chem.* **1961**, *2*, 125-128.
100. Turecek, F. H., Z., Thermochemistry of unstable enols: the O-(Cd)(H) group equivalent. *J. Org. Chem.* **1986**, *51*, 4066-4067.
101. Sun, H.; Bozzelli, J. W., Thermochemical and kinetic analysis on the reactions of neopentyl and hydroperoxy-neopentyl radicals with oxygen: Part I. OH and Initial Stable HC Product Formation. *J. Phys. Chem. A* **2004**, *108*, 1694-1711.
102. Sebbar, N.; Bozzelli, J. W.; Bockhorn, H., Thermochemical properties, rotation Barriers, bond energies, and group additivity for vinyl, phenyl, ethynyl, and allyl peroxides. *J. Phys. Chem. A* **2004**, *108*, 8353-8366.

103. Bozzelli, J. W.; Chad, W., Thermochemistry, reaction paths, and kinetics on the hydroperoxy-ethyl Radical reaction with O₂: New chain branching reactions in hydrocarbon oxidation. *J. Phys. Chem. A* **2002**, *106*, 1113-1121.
104. Blanksby, S. J.; Ramond, T. M.; G.E., D.; Nimols, M. R.; Kato, S.; Bierbaum, V. M.; Lineberger, W. C.; Ellison, G. B.; Okumura, M., **2001**, *J. Am. Chem. Soc.* (123), 9585-9596.
105. Pittam, D. A.; Pilcher, G., Measurements of heats of combustion by flame calorimetry. Part 8.-Methane, ethane, propane, n-butane and 2-methylpropane. *J. Chem. Soc. Faraday Trans.1* **1972**, *68*, 2224-2229.
106. Guthrie, G. B.; Scott, D. W.; Hubbard, W. N.; Katz, C.; McCullough, J. P.; Gross, M. E.; Williamson, K. D.; Waddington, G., Thermodynamic properties of furan. *J. Am. Chem. Soc.* **1952**, *74* (18), 4662-4669.
107. Rodriguez, H. J.; Chang, J.-C.; Thomas, T. F., Thermal, photochemical, and photophysical processes in cyclopropanone vapor. *J. Am. Chem. Soc.* **1976**, *98* (8), 2027-2034.
108. Lee, J.; Bozzelli, J. W., Thermochemical and kinetic analysis Of The allyl radical with O₂ reaction system. *Prepr. Pap.-Am. Chem. Soc. Div. Fuel Chem.* **2004**, *49* (1), 439.
109. Catoire, L.; Swihart, M. T.; Gail, S.; Dagaut, P., Anharmonic thermochemistry of cyclopentadiene derivatives. *Int. J. Chem. Kinet.* **2003**, *35*, 453-463.
110. Goldsmith, C. F.; Magoon, G. R.; Green, W. H., Database of small molecule thermochemistry for combustion. *J. Phys. Chem. A* **2012**, *116* (36), 9033-9057.
111. Jian, R. Thermochemical properties of c3 to c5 unsaturated carbonyl alkenes: enthalpies of formation, entropy, heat capacity, bond enthalpy. New Jersey Institute of Technology, 2014.
112. Hudzik, J. M.; Bozzelli, J. W., Structure and thermochemical properties of 2-methoxyfuran, 3-methoxyfuran, and their carbon-centered radicals using computational chemistry. *J. Phys. Chem. A* **2010**, *114* (30), 7984-7995.
113. Auzmendi-Murua, I.; Bozzelli, J. W., Thermochemical properties and bond dissociation energies of C3 - C5 cycloalkyl hydroperoxides and peroxy radicals: cycloalkyl radical + 3O₂ reaction thermochemistry. *J. Phys. Chem. A* **2012**, *116* (28), 7550-7563.
114. Lee, J.; Bozzelli, J. W., Thermochemical and kinetic analysis of the formyl methyl radical + O₂ reaction system. *J. Phys. Chem. A* **2003**, *107*, 3778-3791.
115. Zhang, H. R.; Eddings, E. G.; Sarofim, A. F., Olefin chemistry in a premixed n-heptane flame. *Energy and Fuels* **2007**, *21* (2), 677-685.

116. Miller, J. A.; Klippenstein, S. J., The $\text{H} + \text{C}_2\text{H}_2 (+\text{M}) \rightarrow \text{C}_2\text{H}_3 (+\text{M})$ and $\text{H} + \text{C}_2\text{H}_2 (+\text{M}) \rightarrow \text{C}_2\text{H}_5 (+\text{M})$ reactions: Electronic structure, variational transition-state theory, and solutions to a two-dimensional master equation. *Phys. Chem. Chem. Phys.* **2004**, 6 (6), 1192-1202.
117. Turányi, T.; Zalotai, L.; Dóbbé, S.; Bérces, T., Effect of the uncertainty of kinetic and thermodynamic data on methane flame simulation results. *Phys. Chem. Chem. Phys.* **2002**, 4, 2568-2578.
118. Allinger, N. L.; Dodziuk, H.; Rogers, D. W.; Naik, S. N., Heats of hydrogenation and formation of some 5-membered ring compounds by molecular mechanics calculations and direct measurements. *Tetrahedron* **1982**, 38, 1593-1597.
119. Baulch, D. L.; Cobos, C. J.; Cox, R. A.; Frank, P.; Hayman, G.; Just, T.; Kerr, J. A.; Murrells, T.; Pilling, M. J.; Troe, J.; Walker, R. W.; Warnatz, J., Evaluated kinetic data for combustion modelling. Supplement I. *J. Phys. Chem. Ref. Data* **1994**, 23, 847-1033.
120. Canosa, C. E.; Marshall, R. M.; Sheppard, A., The rate constant for $\text{H} + \text{i-C}_4\text{H}_8 \rightarrow \text{t-C}_4\text{H}_9$ in the range of 298-563 K. *Int. J. Chem. Kinet.* **1981**, 13, 295-301.
121. Curran, H. J., Rate constant estimation for C1 to C4 alkyl and alkoxy radical decomposition. *Int. J. Chem. Kinet.* **2006**, 38 (4), 250-275.
122. Furuyama, S.; Golden, D. M.; Benson, S. W., Thermochemistry of the gas phase equilibria $\text{i-C}_3\text{H}_7\text{I} = \text{C}_3\text{H}_6 + \text{HI}$, $\text{n-C}_3\text{H}_7\text{I} = \text{i-C}_3\text{H}_7\text{I}$, and $\text{C}_3\text{H}_6 + 2\text{HI} = \text{C}_3\text{H}_8 + \text{I}_2$. *J. Chem. Thermodyn.* **1969**, 1, 363-375.
123. Harris, G. W.; Pitts, J. N., Jr., Absolute rate constants and temperature dependences for the gas phase reactions of H atoms with propene and the butenes in the temperature range 298 to 445 K. *J. Chem. Phys.* **1982**, 77.
124. Kerr, J. A.; Parsonage, M. J., *Evaluated Kinetic Data on Gas Phase Addition Reactions. Reactions of Atoms and Radicals with Alkenes, Alkynes and Aromatic Compounds*. Butterworths: London, UK., 1972.
125. Kerr, J. A.; Trotman-Dickenson, A. F., The reactions of alkyl radicals. Part 2. s-Propyl radicals from the photolysis of isobutyraldehyde. *Trans. Faraday Soc.* **1959**, 55, 921-928.
126. Kerr, J. A.; Trotman-Dickenson, A. F., The reactions of alkyl radicals. Part 1.-n-propyl radicals from the photolysis of n-butyraldehyde. *Trans. Faraday Soc.* **1959**, 55, 572-580.
127. Kurylo, M. J.; Peterson, N. C.; Braun, W., Temperature and pressure effects in the addition of H atoms to propylene. *J. Chem. Phys.* **1971**, 54, 4662-4666.
128. Kyogoku, T.; Watanabe, T.; Tsunashima, S.; Sato, S., Arrhenius parameters for the reactions of hydrogen and deuterium atoms with four butenes. *Bull. Chem. Soc. Jpn.* **1983**, 56, 19-21.
129. Lightfoot, P. D.; Pilling, M. J., Temperature and pressure dependence of the rate constant for the addition of H to C_2H_4 . *J. Phys. Chem.* **1987**, 91, 3373-3379.

130. Lin, M. C.; Back, M. H., The thermal decomposition of ethane. Part II. The unimolecular decomposition of the ethane molecule and the ethyl radical. *Can. J. Chem.* **1966**, *44*, 2357-2367.
131. Lin, M. C.; Laidler, K. J., Thermal decomposition of the sec-butyl radical. *Can. J. Chem.* **1967**, *45*.
132. Melville, H. W.; Robb, J. C., The kinetics of the interaction of atomic hydrogen with olefines. V. Results obtained for a further series of compounds. *Proc. R. Soc. London A* **1950**, 202.
133. Metcalfe, E. L.; Trotman-Dickenson, A. F., The reactions of alkyl radicals. Part VIII. Isobutyl radicals from the photolysis of isovaleraldehyde. *J. Chem. Soc.* **1960**, 5072-5077.
134. Michael, J. V.; Su, M. C.; Sutherland, J. W.; Harding, L. B.; Wagner, A. F., Rate constants for $D + C_2H_4 \rightarrow C_2H_3D + H$ at high temperature: implications to the high pressure rate constant for $H + C_2H_4 \rightarrow C_2H_5$. *Proc. Combust. Inst.* **2005**, *30*, 965-973.
135. Sugawara, K.; Okazaki, K.; Sato, S., Temperature dependence of the rate constants of H and D-atom additions to C_2H_4 , C_2H_3D , C_2D_4 , C_2H_2 , and C_2D_2 . *Bull. Chem. Soc. Jpn.* **1981**, *54*.
136. Sugawara, K.; Okazaki, K.; Sato, S., Kinetic isotope effects in the reaction $H + C_2H_4 \rightarrow C_2H_5$. *Chem. Phys. Lett.* **1981**, 78.
137. Tsang, W., The stability of alkyl radicals. *J. Am. Chem. Soc.* **1985**, *107*, 2872-2880.
138. Tsang, W., Chemical kinetic data base for combustion chemistry. Part 4. Isobutane. *J. Phys. Chem. Ref. Data* **1990**, *19*, 1-68.
139. Tsang, W., Chemical kinetic data base for combustion chemistry. Part V. Propene. *J. Phys. Chem. Ref. Data* **1991**, *20*, 221-273.
140. Tsang, W., Chemical kinetic data base for hydrocarbon pyrolysis. *Ind. Eng. Chem.* **1992**, *31*, 3-8.
141. Warnatz, J., *Rate coefficients in the C/H/O system Combustion Chemistry*. Springer-Verlag, New York, NY., 1984.
142. Zhao, Y.; Truhlar, D., The M06 suite of density functionals for main group thermochemistry, thermochemical kinetics, noncovalent interactions, excited states, and transition elements: two new functionals and systematic testing of four M06-class functionals and 12 other functionals. *Theor Chem Account* **2008**, *120* (1-3), 215-241.
143. Stevens, W. R.; Ruscic, B.; Baer, T., Heats of formation of $C_6H_5^\bullet$, $C_6H_5^+$, and C_6H_5NO by threshold photoelectron photoion coincidence and active thermochemical tables analysis. *J. Phys. Chem. A* **2010**, *114* (50), 13134-13145.

144. Seetula, J. A.; Slagle, I. R., Kinetics and thermochemistry of the $R+HBr \rightleftharpoons RH+Br$ ($R=n\text{-C}_3\text{H}_7$, isoC_3H_7 , $n\text{-C}_4\text{H}_9$, isoC_4H_9 , $\text{sec-C}_4\text{H}_9$ or $\text{tert-C}_4\text{H}_9$) equilibrium. *J. Chem. Soc., Faraday Trans.* **1997**, 93 (9), 1709-1719.
145. Dean, A. M.; Westmoreland, P. R., Bimolecular QRRK analysis of methyl radical reactions. *International Journal of Chemical Kinetics* **1987**, 19 (3), 207-228.
146. Westmoreland, P. R.; Howard, J. B.; Longwell, J. P.; Dean, A. M., Prediction of rate constants for combustion and pyrolysis reactions by bimolecular QRRK. *AIChE Journal* **1986**, 32 (12), 1971-1979.
147. Bozzelli, J. W.; Chang, A. Y.; Dean, A. M., Molecular density of states from estimated vapor phase heat capacities. *Int. J. Chem. Kinet.* **1997**, 29 (3), 161-170.
148. Tsang, W.; Hampson, R. F., Chemical kinetic data base for combustion chemistry. Part I. Methane and related compounds. *J. Phys. Chem. Ref. Data* **1986**, 15, 1087-1222.
149. Dodonov, A. F.; Lavrovskaya, G. K.; Talroze, V. L., Mass-spectroscopic determination of rate constants for elementary reactions. III. The reactions $H + C_2H_4$, $H + C_3H_6$, and $H + n\text{-C}_4H_8$. *Kinet. Catal.* **1969**, 10, 573.
150. Lee, J. H.; Michael, J. V.; Payne, W. A.; Stief, L. J., Absolute rate of the reaction of atomic hydrogen with ethylene from 198 to 320 K at High Pressure. *J. Chem. Phys.* **1978**, 68, 1817-1820.
151. Seakins, P. W.; Robertson, S. H.; Pilling, M. J.; Slagle, I. R.; Gmurczyk, G. W.; Bencsura, A.; Gutman, D.; Tsang, W., Kinetics of the unimolecular decomposition of $\text{iso-C}_3\text{H}_7$: weak collision effects in helium, argon, and nitrogen. *J. Phys. Chem.* **1993**, 97, 4450-4458.
152. Wagner, H. G.; Zellner, R., Reaktionen von Wasserstoffatomen mit ungesättigten C₃-Kohlenwasserstoffen. I. Die Reaktion von H-Atomen mit Propylen. *Ber. Bunsenges. Phys. Chem.* **1972**, 76.
153. Bradley, J. N.; West, K. O., Single-pulse shock tube studies of hydrocarbon pyrolysis. part 5. pyrolysis of neopentane. *J. Chem. Soc. Faraday Trans. 1* **1976**, 72, 8-19.
154. Bryukov, M. G.; Slagle, I. R.; Knyazev, V. D., Kinetics of reactions of H atoms with methane and chlorinated methanes. *J. Phys. Chem. A* **2001**, 105, 3107-3122.
155. Dalgleish, D. G.; Knox, J. H., The reactions of hydrogen atoms with isobutane and isobutene. *J. Chem. Soc. Chem. Commun.* **1966**, 917-918.
156. Knyazev, V. D.; Dubinsky, I. A.; Slagle, I. R.; Gutman, D., Unimolecular decomposition of $t\text{-C}_4\text{H}_9$ radical. *J. Phys. Chem.* **1994**, 98, 5279-5289.
157. Manion, J. A.; Awan, I. A., Evaluated kinetics of terminal and non-terminal addition of hydrogen atoms to 1-alkenes: a shock tube study of $H + 1\text{-butene}$. *J. Phys. Chem. A* **2014**, 119 (3), 429-441.

158. Feng, Y.; Niiranen, J. T.; Bencsura, A.; Knyazev, V. D.; Gutman, D.; Tsang, W., Weak collision effects in the reaction $\text{C}_2\text{H}_5 = \text{C}_2\text{H}_4 + \text{H}$. *J. Phys. Chem.* **1993**, *97*, 871-880.
159. Loucks, L. F.; Laidler, K. J., Thermal decomposition of the ethyl radical. *Can. J. Chem.* **1967**, *45*, 2795-2803.
160. Simon, Y.; Foucaut, J. F.; Scacchi, G., Etude experimentale et modelisation theorique de la decomposition du radical ethyle. *Can. J. Chem.* **1988**, *66*.
161. Trenwith, A. B., The pyrolysis of ethane. A study of the dissociation reaction $\text{C}_2\text{H}_5 \rightarrow \text{C}_2\text{H}_4 + \text{H}$. *J. Chem. Soc. Faraday Trans. 2* **1986**, *82*.
162. Tsang, W., Chemical kinetic data base for combustion chemistry. Part 3. Propane. *J. Phys. Chem. Ref. Data* **1988**, *17*.
163. Camilleri, P.; Marshall, R. M.; Purnell, H., Arrhenius parameters for the unimolecular decompositions of azomethane and n-propyl and isopropyl radicals and for methyl radical attack on propane. *J. Chem. Soc. Faraday Trans. 1* **1975**, *71*, 1491-1502.
164. Dean, A. M., Predictions of pressure and temperature effects upon radical addition and recombination reactions. *J. Phys. Chem.* **1985**, *89*, 4600-4608.
165. Dombi, A.; Huhn, P., Effect of olefins on the thermal decomposition of propane. Part I. The model reaction. *Int. J. Chem. Kinet.* **1986**, *18*, 227-239.
166. Leathard, D. A.; Purnell, J. H., Propyl radical isomerization and heterogeneous effects in the pyrolysis of propane below 500°C. *Proc. R. Soc. London A* **1968**, *306*, 553-567.
167. Papic, M. M.; Laidler, K. J., Kinetics of the mercury-photosensitized decomposition of propane. part II. reactions of the propyl radicals. *Can. J. Chem.* **1971**, *49*, 549-554.
168. Birrell, R. N. T.-D., A.F., The reactions of alkyl radicals. part VII. t-butyl radicals from the photolysis of pivalaldehyde. *J. Chem. Soc.* **1960**, 4218-4224.
169. Mintz, K. J.; Le Roy, D. J., Kinetics of radical reactions in sodium diffusion flames. *Can. J. Chem.* **1978**, *56*, 941-949.
170. Teng, L.; Jones, W. E., Kinetics of the reactions of hydrogen atoms with ethylene and vinyl fluoride. *J. Chem. Soc. Faraday Trans. 1* **1972**, *68*, 1267-1277.
171. Munk, J.; Pagsberg, P.; Ratajczak, E.; Sillesen, A., Spectrokinetic studies of i-C₃H₇ and i-C₃H₇O₂ radicals. *Chem. Phys. Lett.* **1986**, *132*, 417-421.
172. Daby, E. E.; Niki, H., Mass-spectrometric study of rate constants for addition reactions of H and D atoms with cis- and trans-butenes in discharge-flow system at 300°K. *J. Chem. Phys.* **1969**, *51*, 1255-1256.
173. Daby, E. E.; Niki, H.; Weinstock, B., Mass Spectrometric Studies of Rate Constants for Addition Reactions of Hydrogen and of Deuterium Atoms with Olefins in a Discharge-Flow System at 300 oK. *J. Phys. Chem.* **1971**, *75*.

174. Baldwin, R. R.; Drewery, G. R.; Walker, R. W., Decomposition of 2,3-dimethylbutane in the presence of oxygen. Part 2.-Elementary reactions involved in the formation of products. *J. Chem. Soc. Faraday Trans. 1* **1984**, *80*, 3195-3207.
175. Chanda, M.; Roy, S. K., *Industrial Polymers, Specialty Polymers, and Their Applications*. CRC Press: Boca Raton, FL., 2008.
176. Haworth, N. L.; Smith, M. H.; Bacskey, G. B.; Mackie, J. C., Heats of formation of hydrofluorocarbons obtained by gaussian-3 and related quantum chemical computations. *J. Phys. Chem. A* **2000**, *104* (32), 7600-7611.
177. Chen, C.; Bozzelli, J. W., Analysis of tertiary butyl radical + O₂, isobutene + HO₂, isobutene + OH, and isobutene-OH adducts + O₂: a detailed tertiary butyl oxidation mechanism. *J. Phys. Chem. A* **1999**, *103*, 9731-9769.
178. El-Nahas, A. M.; Bozzelli, J. W.; Simmie, J. M.; Navarro, M. V.; Black, G.; Curran, H. J., Thermochemistry of acetonyl and related radicals. *J. Phys. Chem. A* **2006**, *110* (50), 13618-13623.